École Doctorale Sciences Pour l'Ingénieur

Thèse de doctorat

Présentée en vue d'obtenir le grade de

Docteur

Dans le domaine de

Génie informatique, automatique et traitement du signal

Par

Shahood uz ZAMAN

THE DEVELOPMENT OF RELIABLE AND WASHABLE INTELLIGENT TEXTILES; NORMS AND CHARACTERIZATION

CONTRIBUTION AU DEVELOPPEMENT DES TEXTILES INTELLIGENTS FIABLES ET LAVABLES; STANDARDS ET CARACTERISATION

Soutenue publiquement le 16 juin, 2021 devant le jury formé de :

Prof. Mireille Bayart Merchez	Université de Lille	**Présidente**
Prof. Henry Yi Li	University of Manchester	**Rapporteur**
Prof. Marie-Ange Bueno	ENSISA, Université de Haute Alsace	**Rapporteur**
Prof. Ahmed Rachid	Université de Picardie Jules Verne	**Examinateur**
Assoc. Prof. Senem Kurşun Bahadir	Istanbul Technical University	**Examinatrice**
Prof. Vladan Koncar	ENSAIT, GEMTEX Laboratoire	**Directeur de thèse**
Assoc. Prof. Xuyuan Tao	ENSAIT, GEMTEX Laboratoire	**Encadrant de thèse**
Assoc. Prof. Cédric Cochrane	ENSAIT, GEMTEX Laboratoire	**Co-Directeur de thèse**

“No two things have been combined together better than knowledge and patience.”

“hadith”

Acknowledgement

First of all, thanks to Almighty, who gave me the opportunity and enabled me to accomplish my Ph.D. thesis. It was a great experience to work in the GEMTEX laboratory located in the ENSAIT School. I was very comfortable and happy to be a part of it during my thesis. All the staff members were very welcoming and supportive for all these years.

Then, all my gratitude and warm thanks to my supervisor and co-supervisors, ***Prof. Vladan Koncar***, ***Dr. Cedric Cochrane***, and ***Dr. Xuyuan Tao***, who helped me and enabled me to complete my research. Special appreciation for their time, guidance, knowledge, and experience, which empowered me to improve my skills. I was lucky to have such a supportive team that was always available to guide me throughout these years.

I want to present my deep regards to ***Prof. Vladan Koncar,*** who managed to accept me for the thesis research in GEMTEX laboratory and trusted me for this opportunity. He was very kind and encouraging, and his valuable advice always helped to enrich my scientific abilities. I am very thankful to him for giving me opportunities and confidence to present my research work at various conferences.

I extend my thanks to ***Prof. Henry Yi Li*** from the University of Manchester and ***Prof. Marie-Ange Beuno*** for ENSISA, Université de Haut Alsace, who accepted the request to be the reviewer of my thesis report. I am very thankful for their time evaluating my work and giving me valuable comments to enrich my knowledge. I want to give special thanks to ***Prof. Mireille Bayart Merchez***, Université de Lille, ***Prof. Ahmed Rachid***, Université de Picardie Jules Verne, and Associate professor ***Senem Kurşun Bahadir***, Istanbul Technical University, to show interest in my work and honored me by becoming the examiner of my thesis report. I am thankful for their valuable time to study my work.

I present my regards to the laboratory staff who helped me during my experiments. I want to say special thanks to *Francois Dassonville* and *Christian Catel*, who are always available with some solutions whenever I was stuck during my experiments. I am thankful for their help through the research work. I want to say thanks to Miss. *Hayriye Gidik,* Assistant professor, who helped me to perform experiments in HEI, Lille. I am thankful to my colleagues and other doctoral researchers who provided me with a good research atmosphere and helped me complete these research activities. I am also thankful to *Muzzamal Hussain*, *Ezgi Ismar*, *Baptiste Garnier*, and *Amale Ankhili*. I am grateful to *Dr. Yasir Nawab*, who motivated me to pursue my doctoral research and supported me throughout this journey.

I am thankful to National Textile University, Pakistan, for financial support and funding for my Ph.D. work.

Finally, I want to pay my gratitude to my parents, wife, and family members, who supported me throughout these years, and without them, it was impossible to reach this level.

Table of Contents

List of Figures

List of Tables

1. Introduction

We are living in an era where modernization and digitalization are increasing rapidly, and industries are attracting their customers with novel techniques and customized product ranges. This competition increased the development of new and hybrid fields for customers satisfactions. In recent decades we have many modern innovative notations that ancient peoples can't even imagine [1]. One typical example is the telephone and internet industry. From posted letters and then lined telephone, it is converted to electronic mails and video calls that just 20-30 years before anyone can't even imagine [2,3]. It is now considered a fundamental and essential requirement for the modern generation. Now mobile phones are converted more than calls and messaging instruments. Today they cover all our needs related to computer activities and different daily life gadgets, including banking services, fitness, and health monitoring activities. These wireless activities even could not be imagined in the recent past [4,5].

Similarly, the usage of textiles and textiles as the wearing element has a vast history in human evolution since ancient times. The wearing cloth concept started as the replacement of leaf used for covering of body parts, but now day's textile wearable have multiple included options along with wearing requirements [6–9]. In the current era of competition and to attract more customers, we can see many value-added and user-defined additions along with normal textile wearing habits of these products [10]. Initially, these concepts started from the medical industry to use the integrated sensors in the undergarments but, these are not limited to this field only. Nowadays, these user-defined textile wearable are being used in various fields ranging from medical, sports, military, and different defense-related projects [11–13]. These new add-ons completely changed the way to use and develop wearable textiles. That's why now textile has not remained an independent industry, but a mixture of different industries working together subject to the integrated user-defined functionalities. Multipurpose and improved functionality textiles may comprise one or several textile or non-textile smart components that were woven, embroidered, sewed, integrated, or attached using different available techniques [5]. Based on requirements, these components can include sensors, actuators, antennas, processing units, energy storage, production and harvesting, and power transmitting devices [14,15]. These advanced wearable textiles are usually named smart textiles, wearable electronics, e-textiles, smart clothing, textronic, etc. [8,16]. They are enlightened further in the following explanations.

1.1 Smart textiles

The word smart material was first introduced in Japan in 1989. The first textile material in history that, in retroaction, was stated as a 'smart textile' was silk yarn having a shape memory capacity. However, the discovery of shape-memory materials in the 60s and intelligent polymeric gels in the 70s was generally accepted as the birth of real smart materials. Although intelligent materials were first introduced in textiles in the late 90s, the first textile electronic semiconductive components have been recognized in the early 2000s [17].

Smart textiles can be defined as textiles that can sense and respond to simulation from the external environment. They may be divided into two classes: passive and active smart textiles. Passive smart textiles can change their properties according to environmental stimulation. Shape memory materials, hydrophobic or hydrophilic textiles, etc. make part of this category [16,18,19].

Active smart textiles generally contain sensors and actuators to connect internal parameters to the transmitted message. They can detect different signals from the outer environment (temperature, light intensity, pollution, etc.), choose how to react, and finally act using various textile-based, flexible, or miniaturized actuators (textile displays, micro vibrating devices, LED, etc.). This "decision" can be taken locally, e.g., electronic devices (textile electronics) embedded in smart textile structures or perhaps remotely, if the smart textile is wirelessly connected to external clouds containing the database. These servers may be connected with artificial intelligence software, etc., and could be a part of the Internet of Things (IoT) concept [20].

1.2 E-textile system

Categorically we can state that all e-textiles will be smart textiles, but not all smart textiles need to be e-textiles. E-textile can be defined as “A textile structure (fiber, yarn, fabric or finished product) permanently integrated, sewn or attached, etc. with electrical and/or electronic functionality” (Figure 1.1).

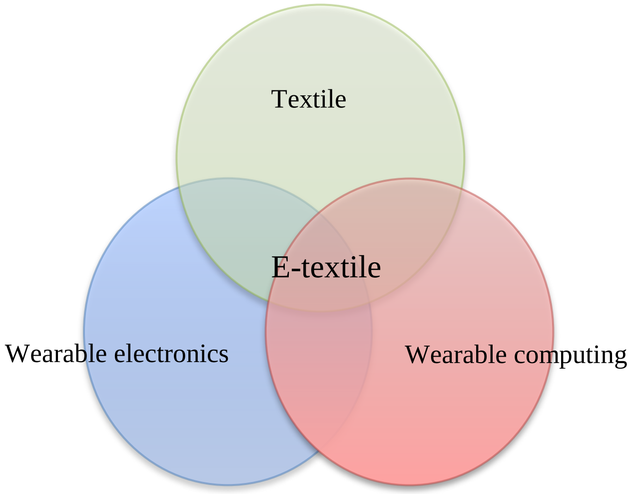

Figure 1.1. E-textile system

Any electronic behavior added to normal textiles converts them into e-textile systems. These electronic components can be textile-based, e.g., flexible textile sensors and antennas, or they can be non-textile-based, e.g., flexible PCBs and LEDs. These electronic components may be fabricated with the textile structure as a substrate or even entirely textile-based using various available textile manufacturing techniques, including weaving, sewing, embedding, embroidering, soldering, crimping, flip-chip, and magnetic, etc. [21–24]. The use of conductive fibers, which have energy and data transmission capacity, for detecting, sensing, monitoring, or communicating the external stimuli response based on specific requirements, is the basic element of a textile integrated electronic system. Depending on the usage and fabrication techniques, these textile integrated electronic systems can be classified as integrated electronic textiles, fabricated electronic devices [25], or normal electronic devices embedded in textile substrates [6,26,27]. Figure 1.2 highlights the dedicated example of an e-textile connected t-shirt prepared by “Caree Technologies Inc.”.

Figure 1.2. E-textile example (“Astroskin” shirt by Carre Technologies Inc. (Hexoskin))

1.3 E-textile types

E-textile products may be divided into two categories (wearable and non-wearable e-textile systems) depending on end-user types.

1.3.1 Wearable e-textile

Daily life wearable textiles having integrated or attached functional components are known as wearable e-textile. These wearable textiles perform some additional functionality along with everyday wearing purposes. They may include sensing, detecting, reacting to specific stimuli, or transmitting some specific data to external clouds. Many wearable e-textile products are available in the market, mainly in medical and personal protection equipment (PPE) fields [28].

The usage of health monitoring sensors in the undergarments for sensitive patients is an example of e-textile wearable systems. The integrated sensors may transmit real-time health monitoring data to external clouds for 24/7 patients nursing [29–31]. Similarly, heat and temperature sensors are attached to fire-fighters uniforms. These sensors help to monitor the outdoor and inner-body temperature of fire-fighters working on fire emergency sites. Hence, the life of workers can be protected in the case of a rapid increase in inner temperature or heartbeats rate [32,33].

1.3.2 Non-wearable e-textiles

Non-wearable e-textiles are used in our routine life for non-wearable purposes with additional functionalities in them. They include bed sheets, curtains, seat covering for household furniture and automobiles, textile usages in geotextile and construction industries, etc. Electronic functionalities may be introduced into these textiles to convert them into non-wearable e-textiles systems. For example, smart pressure sensors can be added to bedsheets to analyze the sleep cycle for customers. Similarly, seat warming technologies and textile color-changing dashboards are widely used in automobile industries [34,35]. Smart textile pressure and temperature sensors can be used in construction industries to analyze and detect any defects in sky-high buildings or underground constructions [36,37]. Photovoltaic and color-changing textiles are also being used in disco and dancing clubs [38].

1.4 E-textile Market

The smart textile market is flourishing day by day. Change in human habits and demand for user-defined facilities has increased the importance of the e-textile systems in the normal textile market. Just five to seven years back, the healthcare sector was a major contributor to the smart and wearable electronics market. Since then, the e-textile market is significantly improving with many applications in fitness monitoring, wireless communications, and defense purposes [4,17,39]. The progressive development and applications increased consumer awareness in this newly emerging field which witnessed the growing investment in e-textile and its associated industries. This progress ultimately reduced the manufacturing cost and easy access to these emerging e-textile systems to customers [40]. However, it’s too early to state that e-textile systems are comprehensively integrated into the “Internet of things (IoT)” infrastructure. There is still room for improvements in terms of security, safety, and reliability to guarantee the IoT nodes for wearable e-textile products. As we are progressing in infrastructures and standardizations, we can see more and more products in the market and ultimately a handy growth rate [41].

A survey conducted by "Ameri research corporation" [42] claims that the global smart textile market will reach up to 9 billion US dollars in 2024 (Figure 1.3). In the wearable electronic market, still, a large portion is captured by wearable gadgets, but smart clothing and e-textile medical systems are gaining rapid acceptance in customers.

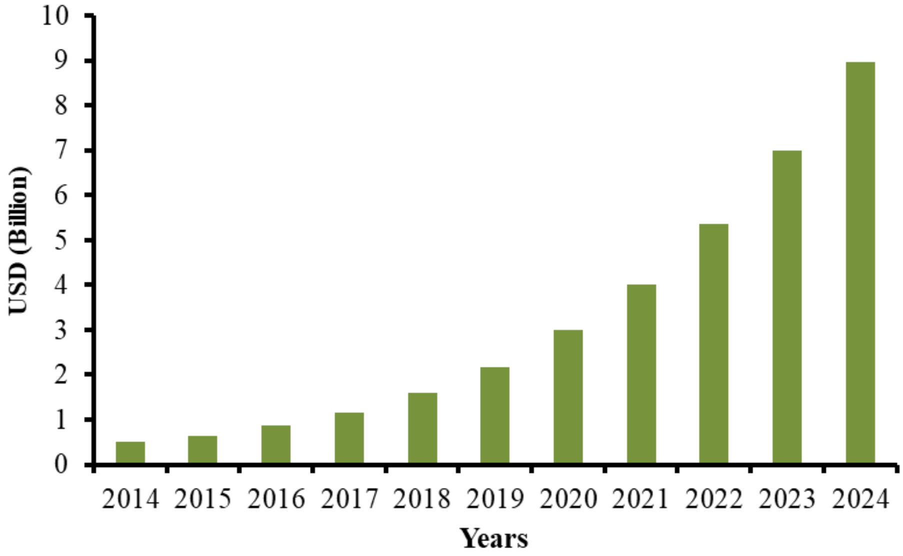

Figure 1.3. Global Smart textile market forecast (Ameri Research Inc.)

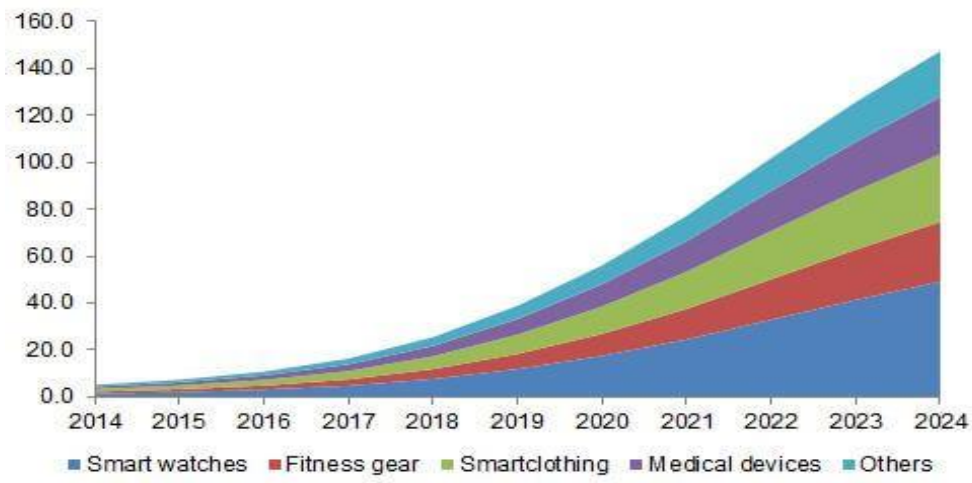

Figure 1.4. Global electronic market by product category (Ameri Research Inc.) [42]

In another survey conducted by "IDTechEx", it is claimed that annual revenue from wearable technology products will reach 80 billion US dollars in 2020 (Figure 1.5). Wearable device's yearly sales volume is predicted to reach 2.5 billion US dollars in 2025 [43].

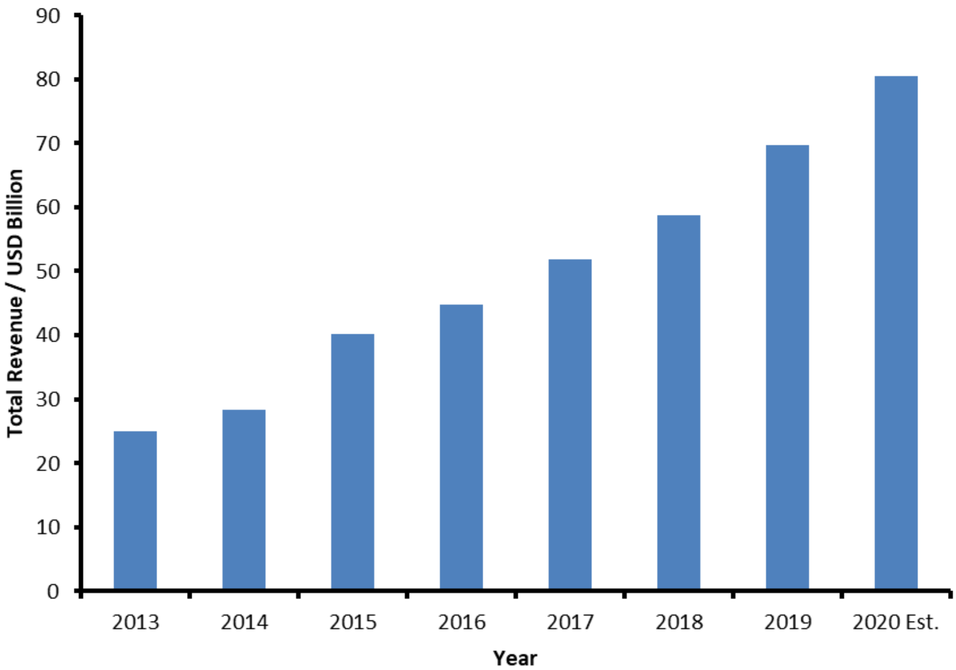

Figure 1.5. Wearable technology revenue IDTechEX survey

1.5 Reliability and washability

The E-textile market is developing continuously, and a lot of new products in the market can be expected. These products often lack reliability and user confidence. Recent surveys predicted valuable growth in this sector, but this is attached with the adoption of e-textile systems to our daily life. E-textile is a hybrid product obtained with a combination of mainly textile and electronic industries [13,44–46]. Figure 1.6 describes the e-textile systems manufacturing process and the purpose of new standardized testing requirements. Both industries are well developed and already have standard protocols for their reliability. We have standards available for the washability of textile products. On the other side, electronic items usually are not considered for washing reliability. When these products or components are combined with textiles ones to create the e-textile system, their reliability and washability will be changed entirely.

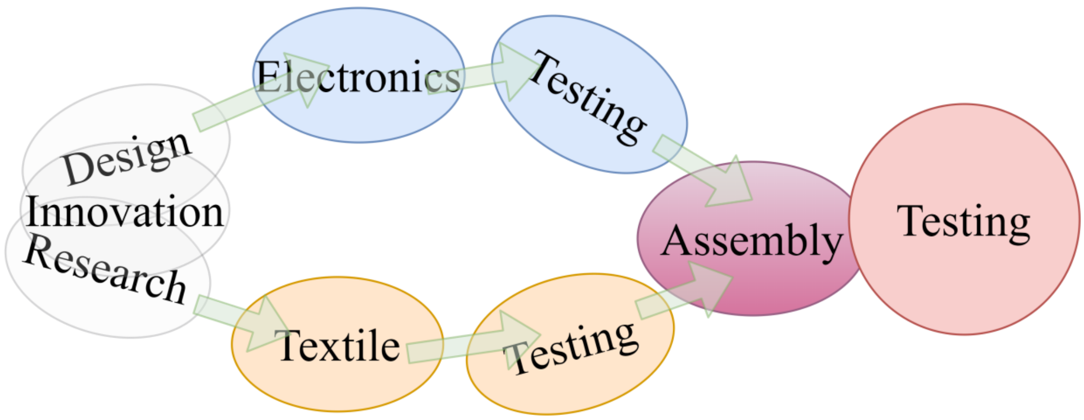

Figure 1.6. E-textile manufacturing layout

When we purchase electronic components and electronic gadgets, we don't consider their washing reliability because we will not put them in the washing machine. But when these electronic systems or their components are attached to the textiles, they should be protected against wash damages. There should be some standardized protocols suitable for both electronic and textile components of e-textile systems [47,48]. The existing and available textile reliability and washability standards cannot be used for them as they are not intended for taking care of electronic components in the e-textile products. Similarly, available electronic protocols don't deal with washing durability and reliability standards. The reliability and durability of the e-textile systems are attached with the proper functionality of all the components, either permanently attached or detachable. Their functionality behavior is different from traditional textile behavior, and the required protocols are not available in the textile standardized test methods. To overcome these problems, new standards related to reliability and washing durability of e-textile systems, in terms of the proper functioning of all components attached to the system, should be developed.

1.6 Recent achievements in standardization

Reliability and durability are critical factors for the new hybrid field to get user confidence; otherwise, it will vanish from the market. Several researchers groups are working on e-textile standardization protocols. Some of them focus on developing new standards, while others are targeting to modify and combine available test methods to make them suitable for e-textile systems. American Association of Textile Chemists and Colorists (AATCC) is currently working on different drafts related to electronically integrated textiles. They published an evaluation procedure for electrical resistance as the outcome functionality of e-textile systems. In another initial draft, "AATCC RA 111", electronically integrated textile test methods are discussed. ASTM international standard organization is working on the durability of smart textile electrodes after laundering (ASTM WK-61480). This initial draft covers the determination of electrical resistivity of textile materials that are generally categorized as good or moderately conductive materials. International organization for standardization (ISO) published a standard document report covering smart textile definitions, applications, and the need for standardization (ISO/TR 23383:2020 [49]). Another organization specialized in electronics and leading source of standards for the electronic industry, Association Connecting Electronics Industries (IPC), is also working on different initial drafts related to washability and reliability of wearable electronics. Recently they published the draft report IPC-8921 [50] related to definitions of e-textile components. This report covers the requirements for woven and knitted electronic textiles (E-textiles) integrated with conductive fibers, conductive yarns, and/or wires. A working group under this organization is working on quality and reliability for e-textiles wearable, and the initial draft IPC-8981 is due to be finalized in June 2021. The European sub-group (D-75a-EU, E-textiles wearables standard task group in Europe) of this committee is working on washability problems related to wearable e-textiles, classifications of the products in terms of standard requirements, and transition of available standards into e-textile standards with required modification and addition. All these efforts are under process to streamline this new and emerging field in terms of reliability and durability. Different organizations and research groups are progressing in these achievements, and some initial drafts are available in the market. This is a collective effort, and it can't be quantified quickly. These developments surely confirm the pathway in the right direction, and it may be expected the e-textile reliability and washability protocols will be developed in the coming years.

1.7 Objectives and target output

My research is planned to investigate and highlight the difficulties the e-textile market is facing in terms of reliability and washability. These problems directly impact the market acceptance, user-confidence, and ultimately the success of the e-textile systems. The main objectives of this study are highlighted below.

Objective 1

Investigation of washability and reliability issues related to e-textiles and their importance in this field. Study of different available washing options and highlight the differences among them to better understand how to select the most suitable washing option for e-textile systems. Identification of washing stresses during the different washing phases and their damage intensity on the e-textile systems.

Objective 2

Categorization of different e-textile components, including detachable and permanently fixed ones, for the investigation of the washing stresses separately on each of the components in terms of their functionality. Use of the accelerometer device for stress analysis in washing drum to highlight the available mechanical standardized test protocols that can be used as the simulation of comparable damages, without the washing process.

Objective 3

Presentation of a washing simulation model based on the experimental analyses, which can be exercised for wash damages and reliability predictions without actually washing the e-textile systems. Shortlist the available test protocols that may be adapted, with some modifications, to claim e-textile system reliability. Finally, preparation of standard protocol draft claiming washability and functionality for wearable e-textile systems.

Different e-textile components are investigated separately in these experiments and the impact of damages is studied. These details are further explained in the coming chapters. Chapter 2 presents some recent developments in the standardization of e-textile reliability along with a literature review of current e-textile developments. E-textile wearable products available in markets are discussed along with their functionality and washing instructions. Chapter 3 contains a detailed explanation of tests and materials used in this research work. The experiment flow is explained in this chapter with all required information of instruments and apparatus used for this investigation. Chapter 4 contains the outcomes from these experiments and an in-depth discussion of the results. Proposed standards based on these results and discussions are covered in chapter 5 and 6.

References

1. Ankhili, A.; Tao, X.; Cochrane, C.; Coulon, D.; Koncar, V. Washable and Reliable Textile Electrodes Embedded into Underwear Fabric for Electrocardiography (ECG) Monitoring. Materials 2018, 11, 256, doi:10.3390/ma11020256.

2. Wu, H.; Huang, Y.; Xu, F.; Duan, Y.; Yin, Z. Energy Harvesters for Wearable and Stretchable Electronics: From Flexibility to Stretchability. Adv. Mater. 2016, 28, 9881–9919, doi:10.1002/adma.201602251.

3. Waqar, S.; Wang, L.; John, S. Piezoelectric energy harvesting from intelligent textiles. In Electronic Textiles; Elsevier, 2015; pp. 173–197 ISBN 978-0-08-100201-8.

4. Bahru, R.; Hamzah, A.A.; Mohamed, M.A. Thermal Management of Wearable and Implantable Electronic Healthcare Devices: Perspective and Measurement Approach. Int J Energy Res 2020, er.6031, doi:10.1002/er.6031.

5. Hussain, M.M.; El-Atab, N. Handbook of Flexible and Stretchable Electronics. 551.

6. Wang, L.; Fu, X.; He, J.; Shi, X.; Chen, T.; Chen, P.; Wang, B.; Peng, H. Application Challenges in Fiber and Textile Electronics. Adv. Mater. 2020, 32, 1901971, doi:10.1002/adma.201901971.

7. Mecnika, V.; Scheulen, K.; Anderson, C.F.; Hörr, M.; Breckenfelder, C. Joining technologies for electronic textiles. In Electronic Textiles; Elsevier, 2015; pp. 133–153 ISBN 978-0-08-100201-8.

8. Zaman, S. uz; Tao, X.; Cochrane, C.; Koncar, V. Understanding the Washing Damage to Textile ECG Dry Skin Electrodes, Embroidered and Fabric-Based; Set up of Equivalent Laboratory Tests. Sensors 2020, 20, 1272, doi:10.3390/s20051272.

9. Tseghai, G.B.; Malengier, B.; Fante, K.A.; Nigusse, A.B.; Langenhove, L.V. Integration of Conductive Materials with Textile Structures, an Overview. 2020, 28.

10. Pang, Y.; Yang, Z.; Yang, Y.; Ren, T. Wearable Electronics Based on 2D Materials for Human Physiological Information Detection. Small 2020, 16, 1901124, doi:10.1002/smll.201901124.

11. Ismar, E.; Tao, X.; Rault, F.; Dassonville, F.; Cochrane, C. Towards Embroidered Circuit Board From Conductive Yarns for E-Textiles. 2020, 8, 9.

12. Valentine, L.; Ballie, J.; Bletcher, J.; Robertson, S.; Stevenson, F. Design Thinking for Textiles: Let’s Make It Meaningful. The Design Journal 2017, 20, S964–S976, doi:10.1080/14606925.2017.1353041.

13. Scataglini, S.; Andreoni, G.; Gallant, J. A Review of Smart Clothing in Military. In

Proceedings of the Proceedings of the 2015 workshop on Wearable Systems and Applications - WearSys ’15; ACM Press: Florence, Italy, 2015; pp. 53–54.

14. Abed, A.; Cochrane, C.; Boussu, F.; Cherkaoui, O.; Elmoznine, R. Design and Development of a Piezo-Resistive Sensor Based on PEDOT: PSS Applied to Sisal’s Natural Fiber for Monitoring of 3D Warp Interlock Fabric. IOP Conf. Ser.: Mater. Sci. Eng. 2020, 827, 012019, doi:10.1088/1757-899X/827/1/012019.

15. Kim, G.; Vu, C.C.; Kim, J. Single-Layer Pressure Textile Sensors with Woven Conductive Yarn Circuit. Applied Sciences 2020, 10, 2877, doi:10.3390/app10082877.

16. Park, S.; Jayaraman, S. Smart Textiles: Wearable Electronic Systems. MRS Bulletin 2003, 28, 585–591, doi:10.1557/mrs2003.170.

17. Sungmee Park; Jayaraman, S. Enhancing the Quality of Life through Wearable Technology. IEEE Engineering in Medicine and Biology Magazine 2003, 22, 41–48, doi:10.1109/MEMB.2003.1213625.

18. Tao, X. Smart technology for textiles and clothing – introduction and overview. In Smart Fibres, Fabrics and Clothing; Elsevier, 2001; pp. 1–6 ISBN 978-1-85573-546-0.

19. Koncar, V. Introduction to smart textiles and their applications. In Smart Textiles and their Applications; Elsevier, 2016; pp. 1–8 ISBN 978-0-08-100574-3.

20. Koncar, V. Smart textiles for monitoring and measurement applications. In Smart Textiles for In Situ Monitoring of Composites; Elsevier, 2019; pp. 1–151 ISBN 978-0-08-102308-2.

21. Linz, T.; Kallmayer, C.; Aschenbrenner, R.; Reichl, H. Embroidering Electrical Interconnects with Conductive Yarn for The Integration of Flexible Electronic Modules into Fabric. In Proceedings of the Ninth IEEE International Symposium on Wearable Computers (ISWC’05); IEEE: Osaka, Japan, 2005; pp. 86–91.

22. Linz, T.; von Krshiwoblozki, M.; Walter, H. Novel Packaging Technology for Body Sensor Networks Based on Adhesive Bonding A Low Cost, Mass Producible and High Reliability Solution. In Proceedings of the 2010 International Conference on Body Sensor Networks; IEEE: Singapore, Singapore, June 2010; pp. 308–314.

23. Linz, T.; von Krshiwoblozki, M.; Walter, H.; Foerster, P. Contacting Electronics to Fabric Circuits with Nonconductive Adhesive Bonding. Journal of The Textile Institute 2012, 103, 1139–1150, doi:10.1080/00405000.2012.664867.

24. Capineri, L. Resistive Sensors with Smart Textiles for Wearable Technology: From Fabrication Processes to Integration with Electronics. Procedia Engineering 2014, 87, 724–727, doi:10.1016/j.proeng.2014.11.748.

25. Garnier, B.; Mariage, P.; Rault, F.; Cochrane, C.; Koncar, V. Textile NFC Antenna for Power and Data Transmission across Clothes. Smart Mater. Struct. 2020, 29, 085017, doi:10.1088/1361-665X/ab8a6d.

26. Ismar, E.; Kurşun Bahadir, S.; Kalaoglu, F.; Koncar, V. Futuristic Clothes: Electronic Textiles and Wearable Technologies. Global Challenges 2020, 4, 1900092, doi:10.1002/gch2.201900092.

27. Jansen, K.M.B. How to Shape the Future of Smart Clothing. In Proceedings of the Proceedings of the 2019 ACM International Joint Conference on Pervasive and Ubiquitous Computing and Proceedings of the 2019 ACM International Symposium on Wearable Computers - UbiComp/ISWC '19; ACM Press: London, United Kingdom, 2019; pp. 1037–1039.

28. Ferraro, V.; Pasold, A. Emerging Materials et Technologies: New Approaches in Design Teaching Methods on Four Exemplified Areas 2020.

29. Bystricky, T.; Moravcova, D.; Kaspar, P.; Soukup, R.; Hamacek, A. A Comparison of Embroidered and Woven Textile Electrodes for Continuous Measurement of ECG. In Proceedings of the 2016 39th International Spring Seminar on Electronics Technology (ISSE); IEEE: Pilsen, Czech Republic, May 2016; pp. 7–11.

30. Jin, H.; Matsuhisa, N.; Lee, S.; Abbas, M.; Yokota, T.; Someya, T. Enhancing the Performance of Stretchable Conductors for E-Textiles by Controlled Ink Permeation. Adv. Mater. 2017, 29, 1605848, doi:10.1002/adma.201605848.

31. Ankhili, A.; Zaman, S.U.; Tao, X.; Cochrane, C.; Koncar, V.; Coulon, D. How to Connect Conductive Flexible Textile Tracks to Skin Electrocardiography Electrodes and Protect Them Against Washing. IEEE Sensors Journal 2019, 19, 11995–12002, doi:10.1109/JSEN.2019.2938333.

32. Sandulescu, V.; Dobrescu, R. Wearable System for Stress Monitoring of Firefighters in Special Missions. In Proceedings of the 2015 E-Health and Bioengineering Conference (EHB); IEEE: Iasi, Romania, November 2015; pp. 1–4.

33. Caya, M.V.C.; Casaje, J.S.; Catapang, G.B.; Dandan, R.A.V.; Linsangan, N.B. Warning System for Firefighters Using E-Textile. In Proceedings of the 2018 3rd International Conference on Computer and Communication Systems (ICCCS); IEEE: Nagoya, April 2018; pp. 362–366.

34. Nanjappan, V.; Shi, R.; Liang, H.-N.; Lau, K.K.-T.; Yue, Y.; Atkinson, K. Towards a Taxonomy for In-Vehicle Interactions Using Wearable Smart Textiles: Insights from a User-Elicitation Study. MTI 2019, 3, 33, doi:10.3390/mti3020033.

35. Textile Advances in the Automotive Industry; Shishoo, R.L., Textile Institute, Eds.; Woodhead publishing in textiles; CRC Press [u.a.]: Boca Raton, Fla., 2008; ISBN 978-1-84569-331-2.

36. Zangani, D.; Fuggini, C.; Loriga, G. Electronic textiles for geotechnical and civil engineering. In Electronic Textiles; Elsevier, 2015; pp. 275–300 ISBN 978-0-08-100201-8.

37. Rowley, E. Lighting Up Your Garments: An Investigation into Methods of Making Fabrics Glow. 5.

38. Stylios, G.K.; Yang, D.Y. The Concept of Mood Changing Garments Made from Luminescent Woven Fabrics and Flexible Photovoltaics "MoodWear." AST 2012, 80, 22–29, doi:10.4028/www.scientific.net/AST.80.22.

39. Smart Textiles and Their Applications | Request PDF;

40. Gopalsamy, C.; Park, S.; Rajamanickam, R.; Jayaraman, S. (ARTS) MedicalApplications. 17.

41. Tao, X.; Huang, T.-H.; Shen, C.-L.; Ko, Y.-C.; Jou, G.-T.; Koncar, V. Bluetooth Low Energy-Based Washable Wearable Activity Motion and Electrocardiogram Textronic Monitoring and Communicating System. Advanced Materials Technologies 2018, 3, 1700309, doi:10.1002/admt.201700309.

42. Smart Textiles Market To 2024 Available online: https://www.ameriresearch.com/product/smart-textiles-market/.

43. James Hayward E-Textiles and Smart Clothing 2020-2030: Technologies, Markets and Players Available online: https://www.idtechex.com/en/research-report/e-textiles-and-smart-clothing-2020-2030-technologies-markets-and-players/735.

44. Flexible, Wearable, and Stretchable Electronics. 373.

45. Li, R.-W.; Liu, G. Flexible and Stretchable Electronics. 409.

46. Ojstršek, A.; Gorgieva, S. Tailoring of Durable Conductive and UV-Shielding Properties on Cotton and Polyester Fabrics by PEDOT:PSS Screen-Printing. Polymers 2020, 12, 2356, doi:10.3390/polym12102356.

47. Guibert, M.; Massicart, A.; Chen, X.; He, H.; Torres, J.; Ukkonen, L.; Virkki, J. Washing Reliability of Painted, Embroidered, and Electro-Textile Wearable RFID Tags. In Proceedings of the 2017 Progress in Electromagnetics Research Symposium - Fall (PIERS - FALL); IEEE: Singapore, November 2017; pp. 828–831.

48. Li, Y.; Yong, S.; Hillier, N.; Arumugam, S.; Beeby, S. Screen Printed Flexible Water Activated Battery on Woven Cotton Textile as a Power Supply for E-Textile Applications. IEEE Access 2020, 8, 206958–206965, doi:10.1109/ACCESS.2020.3038157.

49. ISO/TR 23383:2020 Available online: https://www.iso.org/cms/render/live/en/sites/isoorg/contents/data/standard/07/53/75383.html (accessed on 21 December 2020).
50. IPC-8921: Requirements for Woven and Knitted Electronic Textiles (E-Textiles) Integrated with Conductive Fibers, Conductive Yarns and/or Wires Available online: https://shop.ipc.org/IPC-8921-English-D (accessed on 21 December 2020).

2. Literature review

The reliability and durability of smart textile structures are key factors for market acceptance and success to this new emerging portion of the textile industry. The electronic textile structures are supposed to be in good functioning “as the whole” against various stresses faced during the life span of this specific system [1]. These stresses depend on different elements, including multiple types of the smart textile system, end-use, life cycle, etc. [2]. Among the stresses, washability is the major issue that most wearable electronic smart textiles face during their life cycles. Various products are available in the market, and somehow, they are successful in meeting the user requirements, but these products lack in terms of washability and washing reliability. Different standards are available for textile washing protocols, but these cannot work in the case of e-textile systems. These standards are specially designed for textile structures and can’t be used for the electronics portion attached or embedded in the e-textile system. Similarly, the standardized test protocols are available for the electronic industry, but they are not designed to deal with textile wearable structures. We don’t test the electronic functionality of wearable clothing or the washability behavior of electronic gadgets. Special precautions should be adopted for these hybrid structures to claim durability and washing reliability. Different available standards in the textile and electronic industry along with recent work on the standardization of electronic wearable textiles, are highlighted in detail.

2.1 Standards related to textile wearable

Many standards are available for textile washing protocols. International organization for standardization (ISO) is a leading organization, particularly in Europe, working on several standardization methods, including textiles. Several well-organized standards for textile and textile washing are being practiced in the market. The most commonly used textile washing standard is ISO 6330 [3], which highlights various requirements regarding washing load, washing time, speed, and temperature. Washing machine types, top-loading, and front-loading are described in detail, separately based on different specifications. These standards recommend that washing temperature should be 30°C - 40°C for delicate washing cycles and go maximum up to 90°C for cotton fabrics. Commonly, these temperatures do not have exact values, and there is always a tolerance limit that varies in different machines. Washing load/ ballast is divided into three categories, including cotton, polyester, and a mixture of both. Multiple drying options, including line dry, drip line dry, flat dry, drip flat dry, flat presses, and tumble drying, are described.

Similarly, the tumbling temperature goes a maximum of 60°C for delicate and 80°C for normal clothes. Many detergent types, their chemical compositions, and dosage for washing cycles are explained. Washing procedures and water hardness properties are also highlighted in detail. Standardized drum volume range and water pressure, used in each phase of the washing procedure, are also discussed in this standard.

Textile testing conditions and laboratory atmosphere standards are explained in ISO 139 [4]. Tolerance limits and uncertainty of measured values are described in this standard document. Pre-testing conditions, rapid or accelerated conditioning, and details regarding alternate standard atmosphere requirements are summarized in ISO 139/A1. ISO 3759 [5] highlights textile sample preparations, measurement specifications, and bulk samples identification methods. Dimensional changes undergo due to external stresses, and the test types to be performed are also covered in it.

ISO 105 is the standard test protocol regarding the color-fastness properties of textile after the laundering process. It is a complete series of standards that explain every possible way of damage textile can undergo due to washing, water damage, chemical, light and weathering, atmosphere etc. ISO 105-A series regulate general principle and different scale assessment levels. ISO 105-A05 [6] and C06 [7] explain the colorfastness problems for domestic and commercial laundering machines. Further explanations are provided in a series of separate modules. For example, ISO 105-C12 [8] discuss complications related to industrial laundering. ISO 105-C09 [9] and ISO 105-C10 [10] highlight the complaints due to the bleaching response created by non-phosphate detergent and soap or soap and soda, respectively. ISO 105-E series discuss problems created by water, acids, alkalis, chlorinated water, hot water, steaming, etc. ISO 105-N series explains different bleaching agents.

ISO 3175-2 [11] provides a standardized test procedure for dry-cleaning and wet-cleaning. Assessments of performance and testing protocols are described, and the cleaning and finishing of textiles using tetrachloroethene, hydrocarbon solvents, and simulated wet-cleaning are covered in this standard protocol.

ISO 811 [12] is a standard test method for hydrostatic tests and resistance to water penetration for textile fabrics. Testing procedure, water grade, water pressure, mechanism of measuring the increase in pressure, testing atmosphere, and sample conditioning are explained in it.

AATCC 135 [13] is another washing standard prepared by the American Association of Textile Chemists and Colorists (AATCC). It defines the number of washing cycles for different textile materials being washed in the washing machine. Dimensional changing problems after washing are also discussed in this test standard. AATCC-6-2016 [14] monograph explains standardization test conditions for domestic laundry machines. They divided the machine setting based on the wash temperature, starting from 16°C for cold wash setting to 54°C for extra hot washing setting. Water temperatures, machine speed and time, spin speed and time, and water levels are discussed for different types of front-load and top-load washing machines. AATCC 1993 [15] defines other standard reference detergents, and laundry detergents in general, used for the washing process. They provided a comparison of detergents in terms of soil removal efficiency at different water hardness levels. AATCC 2003 specifically explained liquid detergents most commonly used in the current washing machines. The impact of color fastness testing on fabric in the presence of standard liquid detergent is discussed in it.

2.2 Standards for electronic functionality

Standards related to electronics functionality are well developed and covers the fundamental requirements for this industry. Some standards that can be used or modified to be adopted for this new hybrid e-textile system are discussed briefly. IEC 60601-2 [16] standard protocol describes practical requirements and essential medical electrical equipment performance. Similarly, IEC 60601-1 [17] and 60601-4-1 [18] cover the general requirements for basic safety features concerned with medical equipment. Laboratory testing requirements, classifications of equipment and systems, equipment parameters, accuracy allowance, protection against electric shock, warning set-up, and equipment identification systems are standardized in this document. IEC 61340-4-1 [19] is another specific test protocol that is being adopted in the electronic textile industry. This test protocol covers the requirements related to electrical resistance and data transmission through sensors and antennas. IEC 62631-3-1 [20] describes the dielectric and resistive properties. This specific standard is related to volume resistance and volume resistivity through the "DC method." The surface resistance and surface resistivity are covered in IEC 62631-3-2 [21]. There are certain methods to test electronic devices against water, such as Ingress Protection numbers against solid and liquids, e.g., IP67, IP68, [22]. However, none of them include the washing process commonly used for textile products such as underwear, clothing, home textile, etc.

IPC, a trade association, is working on the standardization of electronic equipment and assemblies especially printed electronics. They have well-developed standards related to rigid circuit boards. After some modifications, these standards may be used in flexible textile motherboards or even in electronic textiles. IPC-A-610D [23] is a general acceptability standard for electronic assemblies. IPC-A-600J [24] defines the acceptability standard for printed circuits.

Similarly, IPC-9204 [25] gives a detailed guideline on flexibility and stretchability testing related to printed electronics. On the other side, IPC-6903 [26] covers the terms and definitions of printed electronics design and manufacturing methods. IPC-9252B [27] explains the electrical functionality testing of simplified printed boards. Testing protocols and processes for accessing the electrochemical performance of electronics are covered in IPC-9202 [28].

2.3 Standards related to textile mechanical properties

Mechanical properties are the typical requirements for any product's reliability in textile, electronic, or hybrid electronic smart textile categories. Each product undergoes wear and tear during its life span. These mechanical stresses may be due to environmental exposure on the surface or their routine usage and handling [29]. Different types of mechanical properties have several well-developed standards available for diverse types of product and their usages. Textile products have standard protocols based on their types and uses. Abrasion resistance is one of the common properties of textile material. ISO 12947-1 to 4 [30–33] is a standard protocol for determining abrasion of the fabric by Martindale test methods. It is the complete standard divided into different portions. Parts 1 and 2 describe test specimens and testing apparatus. The appearance change and the way to calculate mass loss due to the abrasion test are explained in Part 3 and 4. ISO 12945 [34–37] highlights the surface pilling and fuzzing properties of fabric surfaces. Part 1 of this method covers the pilling properties observed by the Pilling box test method. Part 2 explains the Martindale abrasion test in terms of surface pilling, fuzzing, or matting properties. Similarly, in part 3, the random tumble pilling technique is standardized. Part 4 is a test protocol related to pilling, fuzzing, or matting assessment by visual analysis.

ISO EN-388 [38] and the addition of ISO 13997 [39] in 2016 regulate the mechanical risks related to protective textiles. This protocol covers the mechanical problems attached to abrasion, cuts, tears, and perforations. The obsolete cutting method in ISO 388 used the cut-off method for evaluating the cut resistance of the protective textiles. It involved the back-and-forth movements of the circular blade under the specific load. ISO 13997 is the addition to this standard which replaced the cut-off method by Tomodynamometer (TDM). The impact test protocols for high-grade textiles are also added in the new test protocol. Cut resistance of samples is described as the cut force required for the standardized blade to pass through the material from a fixed 20 mm stroke.

ISO EN 6945 [40] is another test protocol explaining the abrasion resistance of the outer covering for rubber and plastic hosing. It is not a standard protocol in the textile family but may be modified for some semi-rigid electronics components attached to e-textile systems.

ISO 20253 [41] is a standard protocol for textile covering and concerns the blade test specifications for the flocked surfaces. It is not an essential requirement for typical e-textile applications but can be considered in e-textile products being used in the fashion and leisure fields.

ASTM developed multiple standard protocol documents covering abrasion resistance and measured by various techniques. ASTM D4157 [42] is the standard test protocol prepared for abrasion resistance of textile fabrics with the help of the Oscillatory cylinder method. D3884 [43] covers the abrasion resistance evaluated using the rotary platform, double head method.

D3885 [44] discusses the flexing and abrasion method for this functionality. D3886 [45] uses the inflated diaphragm apparatus to calculate the abrasion resistance of textile fabrics. D4158 [46] standardized the abrasion resistance for textile fabrics using uniform abrasion methods. ASTM D4966 [47] is one of the most commonly used standard procedures for abrasion resistance testing. This standard test method measures the abrasion resistance of textile fabrics using the Martindale abrasion tester method. AATCC 93 [48] is another test standard for abrasion resistance of textile fabrics. This protocol discusses the accelerometer method for this measurement.

ASTM F392 [49] is the standard practice used for flex durability of flexible materials. This test method summarizes various test conditions, including full flex for one-hour, full flex for 20 minutes, full flex for 6 minutes, full flex for 20 cycles, and partial flex for 20 cycles. Conditions suitable for the prototype may be decided based on the requirement. This test method can be easily modified to adapt for e-textile prototypes by adjusting the cycle speed and testing duration.

ISO 7854 [50] is a standard test method originally developed for measuring the flex resistance of coated fabrics by the flexing method. Rubber and plastic-coated fabrics are discussed in this document. ISO 2062 [51] is a standard protocol developed for measuring the single-end breaking force and elongation at break using a constant rate of the extension test method. This standard covers the textile yarns taken from ready-to-use packages by four different methods. They are based on the way specimens taken from the packages. In the most commonly used test method, specimens are taken directly from conditioned packages. It is also used for stretching and stretch cycle measurement of textile fabrics.

ISO 13934 [52,53] is a detailed test protocol developed to measure the tensile properties. It is generally used for woven fabrics and fabrics with elastomeric fibers. It does not apply to geotextiles, nonwovens, coated fabrics, textile-glass woven fabrics, and fabrics made from carbon fibers or polyolefin tape yarns. The method identifies the specimens in equilibrium with the standard atmosphere for testing and test specimens in the wet state. It is restricted to the use of a constant rate of extension (CRE) testing machines. This procedure is divided into two parts. Part 1 covers the tensile properties in maximum force and elongation at maximum textile fabrics force using a strip method. Part 2 determines the maximum force of textile fabrics through the Grab test procedure.

ASTM D 5034 [54] also explains the standard protocol for the tensile properties of textiles. This method covers the breaking strength and elongation determined by the "Grab procedure." It applies to woven, nonwoven, and felted fabrics and is not recommended for glass or knit fabrics. ASTM D 5035 [55] uses the strip method to measure the breaking strength and tensile properties. This test method describes procedures for carrying out fabric tensile tests using four types of specimens and three alternative types of testing machines.

Another test protocol, ASTM D5587 [56], covers the tearing strength of fabrics using the TRAPEZOID procedure. It applies to most types of woven, non-woven, and knit fabrics. Tear strength, as determined in this test method, requires the tear to be initiated before testing. It may be reported either as the single-peak force or the average of the five highest peaks.

ISO 14704 [57] is a standard test protocol used to measure the flexural strength of fine ceramic or ceramic-based composites having a grain size of less than 200 µm. This test protocol is not related to the textile industry, but it can be used or modified for semi-flexible electronic components attached to e-textile systems.

IPC 9204 [25] is a standard test protocol for flexibility and stretchability testing of printed electronics used for stretchable electronics or wearable applications. This test method can be used, with required modifications, for e-textile systems having semi-flexible / flexible electronic circuits attached to them.

ASTM D 2594 [58] is a test protocol designed for a knitted fabric having low power properties. This standard covers the measurement of fabric stretch and fabric growth of knitted fabrics proposed for applications requiring low-power stretch properties. It includes procedures for fabric growth and stretch and may be used individually when required by individual specifications. Fabric growth usually is expressed as a percentage of the change in length of the specimen after the tension application. It is a crucial test protocol because most of the wearable textile clothing is made by knitting techniques, and the e-textile system developed by these textiles can take guidelines from the existing standard.

ASTM D3107 [59] test protocol covers the tensile properties of woven textile fabrics. This test method standardizes the fabric stretch procedure and material's dimensional change after a specified extension and is held for a specified time. This standard, along with D2594 [58] for knitted fabrics, entertains the almost complete range of textile garments or fabrics that may be used in wearable e-textile systems.

2.4 Standards related to conductive functionality measurement

In the previous discussion, important test procedures related to or can be modified to adopt in e-textile systems are highlighted. These test protocols should be discussed, and necessary modifications may be planned for their use in the reliability development of e-textile systems. Along with mechanical or washability test standards, protocols for conductive functionality testing related to the acceptable performance of these e-textile systems, based on new requirements, should also be developed. In the following discussion, some initially developed drafts or previous standards that are being adopted to verify the e-textile functionality after mechanical or washing stresses are discussed.

AATCC EP 13 [60] is a test procedure evaluating the electrical resistance of electronically integrated textiles. E-textile fabrics or end products with incorporated conductive paths/tracks may be assessed. This method is not for the evaluation of yarns or fibers. Electrical resistance may be measured as received or after treatment, such as stretch or laundering, etc. The change in resistance due to treatment may also be calculated. Electrical resistance is measured using surface probes along with a digital multi-meter. It is the primary and most commonly used method for e-textile systems electrical resistance measurements.

AATCC TM 76 [61] is the standard test protocol for surface resistivity measurement of textile fabric. The surface resistivity is calculated using the measured electrical resistance, between superficially positioned parallel plates or concentric rings and their spacing. Results are reported as ohm per square. This is an effective test method for resistance measurement for the flow of current between two electrodes. Concentric ring electrodes with a constant distance from each other are generally used in this experiment. This test method is usually not preferred for sensitive resistive fabrics.

CEN EN 16812 [62] is under publication test protocol. It explains a test method for determining the linear electric resistance of conductive tracks for textile structures or intended for application in/to textiles, e.g., yarns, printed or coated tracks, ropes, ribbons, and webbing. Conductive behavior is calculated using Ohm’s law, and electrical resistance is expressed in ohm / m. A detailed explanation regarding specimen preparation and pretension for non-elastic fabrics is provided. Two different types of test set-up are covered in this protocol. Four electrode-four wire method is a preferred test method, but two electrodes-four wire method may also be used where the other method is not possible to use due to the specifications of the tracks.

ISO/CD 24584 [63] is under development test protocol dedicated for sheet resistance of conductive textiles using non-contact type procedures. This standard is in its initial development stage, and no further details are available.

ISO/TR 23383 [64] is also a new test protocol related to smart textile, and its initial draft is published recently under the supervision of the ISO/TC 38 technical committee. This standard highlights the smart textile definitions, their categorizations, and applications. Smart textiles are mainly divided into functional textile products and interactive textile products. Based on their categorization and application, requirements of new standards are pointed out in this standard document.

IEC 61482 [65,66] is a test protocol currently under work for modifications. This standard discusses the protective clothing against thermal hazards of an electric arc. This procedure is more related to electrical properties instead of textile properties. But in the case of e-textile systems, electronics components are attached with textiles, and there are chances for them to be in direct contact with the body. In this case, thermal hazard properties will also be important for an e-textile system.

2.5 Progress on e-textile standardization

Different available standards that can be used or modified are mentioned in the above discussion. These standards are being adopted as the replacement, because standards especially designed for e-textile systems are still not available in the market. Many groups are working on it, and some initial drafts regarding definitions and classifications are available in the market.

ASTM WK61480 [67] is a standard test draft related to the durability of textile electrodes after laundering. AATCC RA111 [68] explains electrically integrated textiles after home laundering. IEC 63203 [69] is under process working draft for wearable electronic devices in the supervision of sub-committee TC124 in "International Electrotechnical Commission (IEC)." It is a series of documents covering different portions related to wearable e-textile. Part 204-1 is a working draft that describes the washability and durability of leisure and sports-related wearable e-textile systems. Washing test conditions, pre-treatments, post washing treatments, and test results protocols are discussed in it. However still, no explanation related to different behavior for various e-textile components is added in this draft. Part 101-1 covers the norms and terminologies related to wearable e-textile systems. Similarly, part 201-3 discusses textile-based electrically conductive tracks in terms of their linear electrical resistances and microclimate testing for fabric samples. On the other side, parts 401 and 402 explain device and system functionality evaluation tests for textile-based sensors.

A guideline on connection yarns in e-textile systems (IPC-8941) is being developed by IPC (www.ipc.org) under the D-71 committee, e-textiles joining and interconnection techniques sub-committee. This industry guideline will provide key considerations and best practices for connecting e-textiles components. These components can be attached to e-textiles to augment their performance. It will help users and manufacturers to work together to make the best decisions for selecting connector types, connection materials, and connection processes based on the e-textile technology to be used and the component to which the e-textile will be connected.

IPC 8921 [70], published in 2019, is another effort to develop the requirements for woven and knitted electronic textiles integrated with conductive fibers, yarns, and wires. This standard highlights the guideline for critical characteristics and durability of woven and knitted e-textiles integrated with conductive fibers, conductive yarns, and/or wires. It also explains the classifications for knitted and woven e-textiles and their definitions.

Another task group in IPC, D-73a, e-textiles printed electronics design standard task group, is working on e-textile printing electronics designs. This standard will establish specific requirements for the design of printed electronic applications; and types of component mounting and interconnecting structures on coated or treated textile substrates. As pertains to this standard, the textile substrate could be a bare textile or an integrated e-textile (e.g., woven or knitted e-textile). Coated or treated textile substrates are textile that has or will have a coating or treatment localized or across the full substrate. Target standard draft will be finalized in late 2021 under the standard nom IPC-8952.

Currently, we are working with IPC on the new e-textile classifications and standards sub-committee (D-75a-EU) dedicated to the companies producing electronic circuits and components to be involved in e-textiles product development and manufacturing. This protocol will establish the required testing and reliability expectations for e-textiles wearable systems. An e-textiles wearable will be any wearable product that is a complete system utilizing non-electrical textiles and e-textiles (woven, knitted, printed, etc.) with attached/connected functional components, sensors, devices, etc. This working group's initial target is to define an e-textiles wearable and other e-textiles structures that could be part of this system (e.g., wires on textile, laminated, conductive polymers, sensors, actuators, etc.). Our group will also cover the e-textile functionality testing requirements and specifications required for conductive textiles (fibers, yarns, wires) for a specific application. The initial draft is expected to be available in 2021 under IPC-8981, quality and reliability of e-textiles wearable document [71].

2.6 Wearable e-textile applications

Wearable e-textiles are being used in our daily life in different shapes and applications. These applications range from light-emitting T-shirts for fashion to ECG monitoring shirts for special emergency patients, motion monitoring bands to foot pressure monitoring soles, and video recording jackets to day and night color-changing jackets [72,73]. Some examples are highlighted in Figure 2.1. They include foot pressure monitoring insole [74,75], motion monitoring bands [76,77], medicated socks [78], medical analyzing textiles [79–81], heat, and temperature-controlled dresses [82], specifically IoT equipped undergarments [83,84], and real-time data recording jackets for personal protection equipment [85,86].

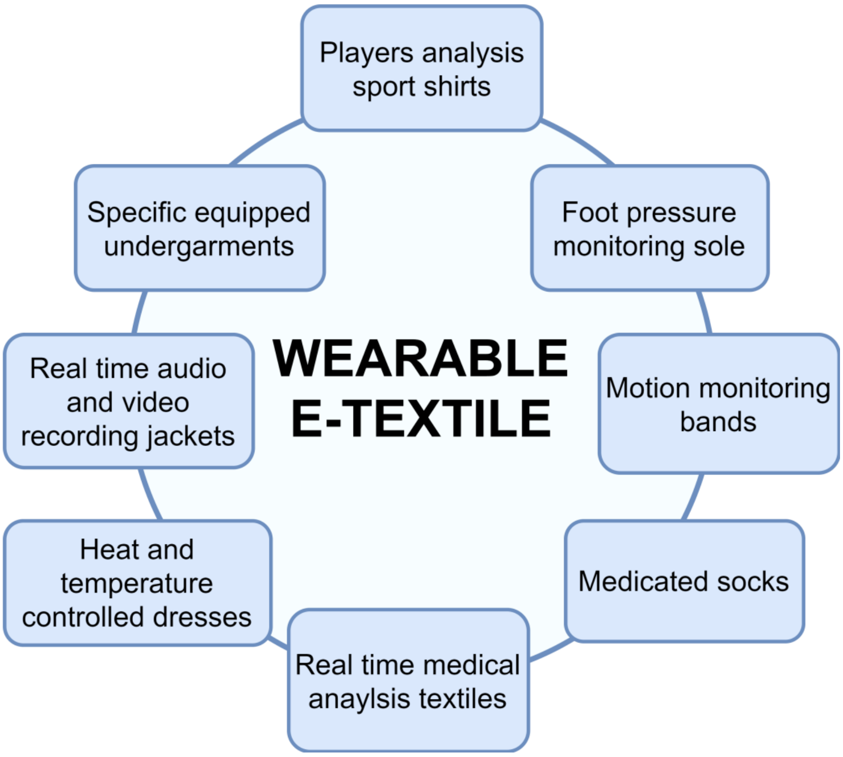

Figure 2.1. Wearable e-textile application

E-textile systems are being widely used in different applications, and their usage depends on customers' requirements. Based on applications, wearable e-textile can be divided into five different categories, including healthcare e-textiles, personal protection (PPE) e-textiles, military e-textiles, sports and leisure e-textiles, and e-textile applications in the aesthetic and fashion category (Figure 2.2) [2].

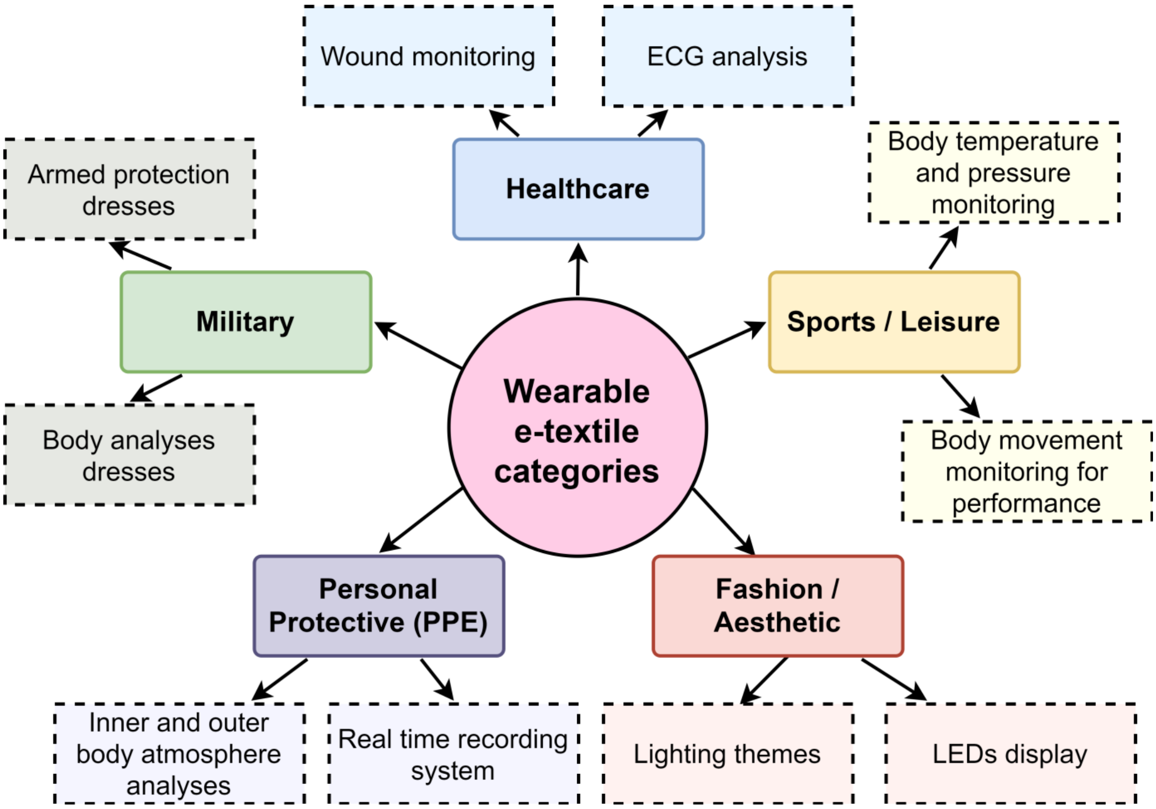

Figure 2.2. Wearable e-textile categories

2.6.1 E-textile wearable in medical

The use of e-textile in the medical field is one of the first fields where e-textile started integration initially. Nowadays, we can see many products related to medical fields that are using "electronic structures." One typical example is the use of ECG sensors in undergarments [87–89]. Textile-based flexible sensors are integrated with undergarments, and hospitals can use these garments in real-time measurements for sensitive patients. This data can be forwarded to the central database in case any urgent action is required. Fiber optic sensors (FOSs), appropriate for monitoring biological parameters (e.g., respiratory and heartbeat monitoring), during magnetic resonance techniques and procedures, are being used in the medical industry [72,90,91]. The wearable e-textile systems are also being used in lung ventilation treatment and cardiac functions related to it [92]. Light-emitting wearable e-textile systems are prepared with the help of optical fibers and they are being used normally for photodynamic therapy [93,94]. Similarly, chemical sensors integrated into wearable textiles are used for metabolic disorder investigations [95]. Smart textiles are also being used for phototherapy. “NeoMedLight” [96] prepared a revolutionary “The BiliCocoon” Nest and Bag system. The Nest system consists of a pad that allows wrapping and is used for kangaroo care and incubator. The Bag system is adapted for cuddling and breastfeeding the baby.

Figure 2.3. The BiliCocoon phototherapy system [96]

The smart textile company “Kymira” [97] has developed the prototype of the cardiac monitoring t-shirt to detect the risk of heart attack for athletes. It will transmit the heart rhythm to the mobile phone via Bluetooth, and hence an unusual rhythm that leads to sudden cardiac arrest can be detected.

Xiaomi Mijia [98] cardiogram t-shirt has integrated ECG sensors to monitor the patient’s physical state. These shirts have a joint lightening system that can create an alert in the case of dangerous heart rate values by changing the color according to the heart stroke intensity. The resulting cardiogram can also be downloaded via Bluetooth.

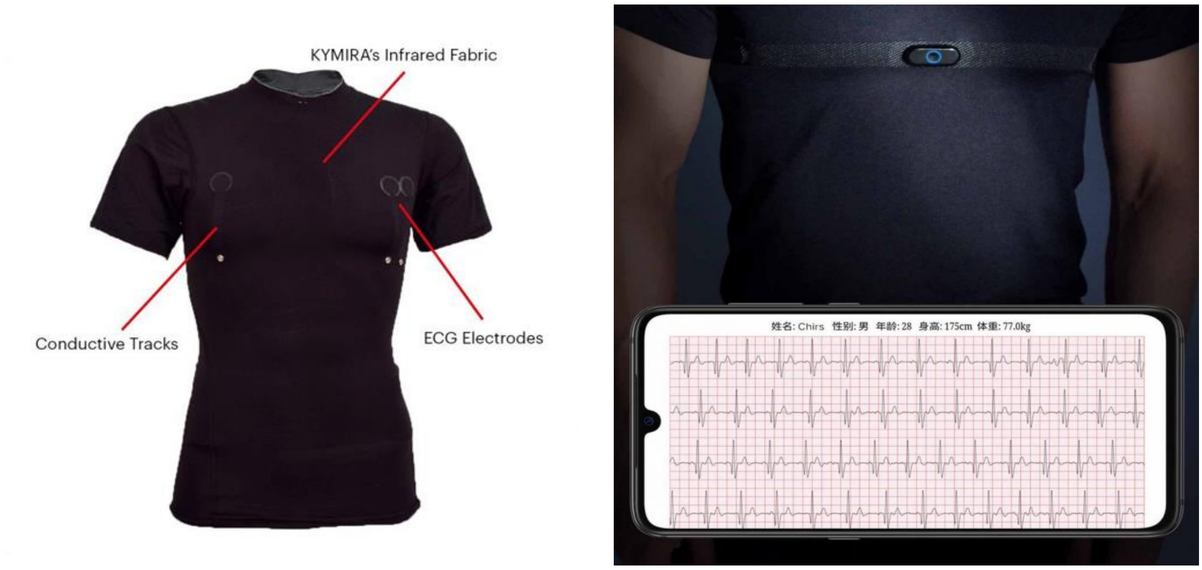

(a) (b)

Figure 2.4. Cardiac monitoring t-shirt, (a) Kymira [97] (b) Xiaomi Mijia [98]

"HealthWatch" [99] launched a 15-lead ECG-sensing shirt that allowed doctors and health workers to track heart conditions remotely. It is prepared with specially designed electrocardiogram sensors weaved in synthetic or cotton t-shirt. These sensors can read vital signs and then transmit them to a monitoring device through Bluetooth.

Figure 2.5. HealthWatch ECG t-shirt [99]

AiQ Smart Clothing [100] prepared different variants, including vests, t-shirts, and sports bra, with five types of electrode structures suitable in various applications. They can be used for heart monitoring for Fitness Enthusiasts, heart monitoring compression vest for marathons and cycling, elderly care units as 1-3 lead ECG monitoring vests physically or remotely, and cardiac rehabilitation & Fitness.

EMGLARE t-shirt [101] is another example of a smart t-shirt with integrated ECG and heart rate monitoring sensors attached to a mobile application for data recording and transferring to the medical experts.

Figure 2.6. AiQ sports Bra [100]

Figure 2.7. EMGLARE smart t-shirt [101]

2.6.2 E-textile wearable in the military and protective clothing

Different application-based e-textile systems are attached in uniforms designed for armed forces (military and police) and firefighter staff [102]. Specially designed outer clothing for armed forces can monitor the surroundings of the surveillance area in real-time. It can transmit data to the central system to monitor and change the strategy quickly if required [72,103]. On the other side, these systems can be attached to lifesaving firefighter's uniforms to monitor their health conditions during rescue work. Body temperature, heartbeat, stress level, and outer atmosphere can be recorded using multiple sensors and actuators

[85,104,105]. Scataglini *et al.* [106] prepared outer clothing for Army soldiers. Wearable electrodes, along with data connections, were placed at appropriate positions in the garment. Different wearing designs and the best possible positions suitable for sensors, considering security equipment to be installed on it, are discussed in this study.

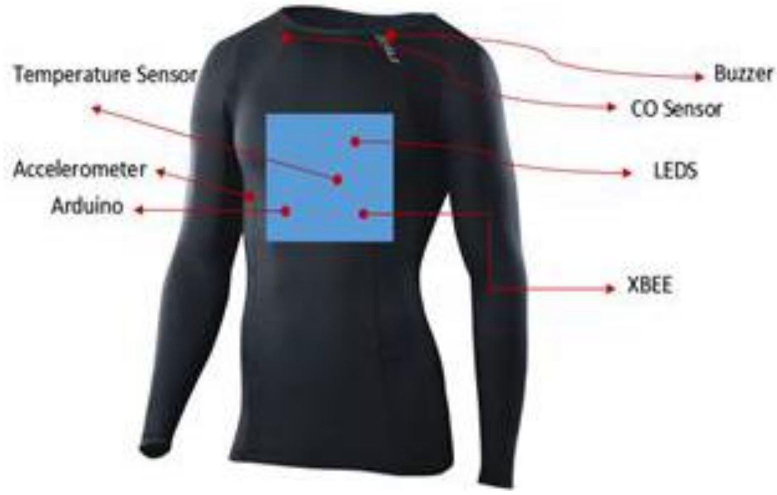

Figure 2.8. Warning system for fire fighter [86]

"Cityzen Sciences", a French company already developed the D-shirt for sports and cyclist, displayed the prototype for big data platform beyond the sports performance [107]. They prepared the "D-shirt" with a built-in GPS, accelerometer, and altimeter that can be linked to the smartphone via Bluetooth. They revealed their plans to add carbon fiber contact points in the shirt for accurate electrocardiogram monitoring.

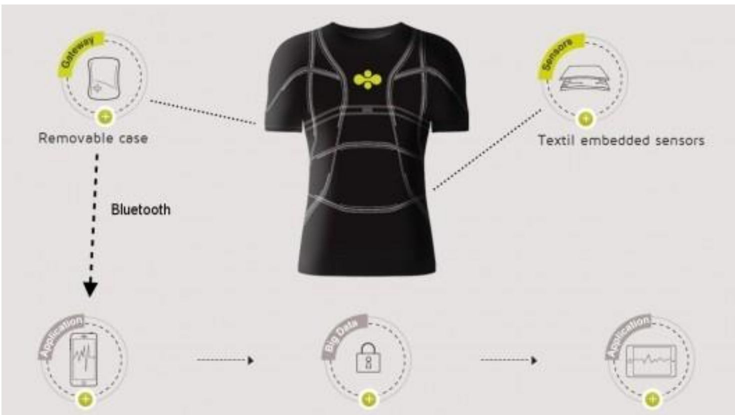

Figure 2.9. Cityzen Sciences D-shirt

Another US company called "Sensatex" prepared the smart t-shirt for military usages. The movement of the soldiers and clusters derived from accelerometer data can be used for better arranging the task groups in the field.

Figure 2.10. The Smart Shirt by Sensatex, Inc., USA

2.6.3 E-textile wearable in sports and leisure

The use of e-textile systems in sports is also gaining much attraction nowadays. E-textile shirts are used to monitor the health condition and heart rates of players during practice. Textile pressure sensors integrated with gloves and shoe soles are used to monitor the activity. Hence, body analysis can be used to enhance or improve the player performance on a précised technical basis [91,108]. These systems can also be used for real-time live recording during the matches to avoid cheating or misbehave between players. These devices will be attached to players, and it will be difficult for the players to hide anything from these devices. Google's advanced technologies project "Jacquard," in collaboration with Levi's smart jacket, has prepared sports garments, especially for cyclists. It can be used by simply touching the fabric to check the time and distance, play music, etc. They are also preparing smart shoes in collaboration with "adidas," which will help the football players calculate the speed, distance, shot, and kick power and synchronize the data in real-time to better understand the football moves [109].

Nike Adapt BB [110], a breakthrough lacing system, was launched in early 2019. It electronically adjusts the lace' pressure with your foot shape and according to different footstep requirements in various games. This system works wirelessly through a smart device application, which can personalize your shoes with available fit modes and a possibility to change shoelace colors.

Figure 2.11. Nike adapt lacing system

Another example is Sensoria fitness products [111,112]. A smart sock is prepared with high-tech fabrics instrumented with textile sensors. Sensoria care microelectronics is attached externally with a snap button. These socks are attached with Bluetooth smart cool that counts the footsteps, calories burnt, altitude, and distance tracking. It can also detect injury-prone running patterns to reduce harm. Sensoria fitness smart t-shirt provides consistent heart rate reading without any additional strap wearing. The information can be stored in mobile applications through Bluetooth data transfer. It also provides antimicrobial and moisture evaporation properties.

Figure 2.12. Sensoria fitness products

2.6.4 E-textile wearable in aesthetic and fashion

The use of e-textile systems for aesthetic purposes is gaining much attention from the general public especially young people. As this field does not require a high level of standards than the medical and PPE, many products are already available in the market. LED displays in disco dresses and different aesthetic products in the fashion industry are typical examples of e-textile usages [113]. We can find light-emitting wearable bands in the market. Some products are presented in this section.

The "CuteCircuit" company prepared the dress with "Graphene" in collaboration with the University of Manchester. This dress can change the color according to the wearer's breathing pattern. This company has developed another product called "SoundShirt", which has 28 high-resolution actuators. It will help deaf and hearing audiences to experience the music deeply, and real-time sensation will enhance virtual reality. Their other projects include "TshirtOS" (a shirt that can allow you to share your status, tweet, or play songs), "Twirkle t-shirt" (built-in LEDs will change the color when someone is close to you), "Hug Shirt," and pilots and cabin-crew suits that will help to identify them in case of any emergency [114].

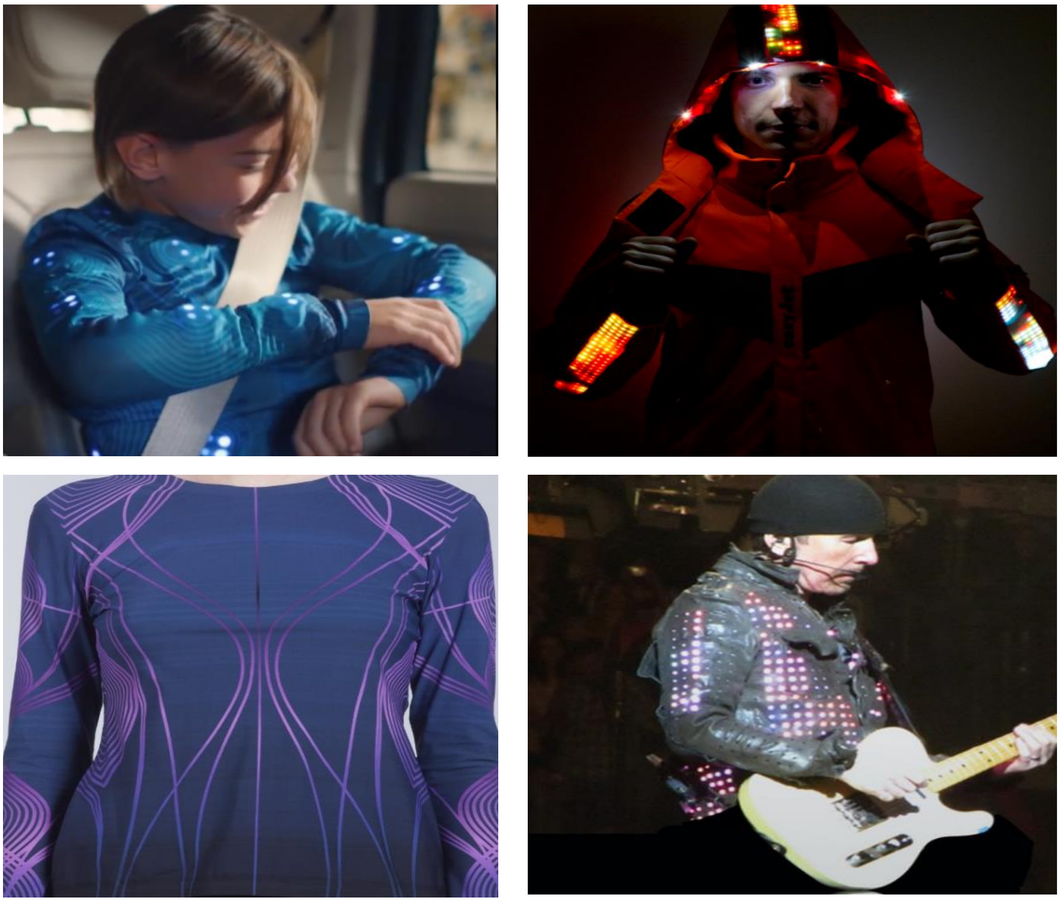

Figure 2.13. CuteCircuit smart textile projects

"Wearable Solar" is another project preparing wearable solar dresses and wearable solar coats. These shirts are seamlessly incorporated with about 120 thin-film solar cells combined in functional modules and can become the natural electricity source. These additional parts of solar cells may be revealed in daylight or folded in the nighttime. It is claimed that if worn for one hour under full sunlight, it can produce electricity enough to charge the smartphone up to 50% [115].

Teslasuit is another example of a smart shirt that gives touch and force feedback to define actions and develop reflexes. Ten internal motion sensors are attached for better motion tracking activities [116].

Table 2.1 highlights different instructions provided by these products for their washability. Certain companies explained detailed guidelines for their product washing settings and maximum temperatures and in other cases, this information is not available in product manuals.

Table 2.1. E-textile product washing instructions

Brand	Max. Temp.	Instructions	Machine wash	Product availability (Price)
Kymira heart monitoring t-shirt	30°C	Do not tumble dry	Yes	Not available
Xiaomi Mijia smart t-shirt	30°C	Gentle wash	No	Available (US $ 69)
Sensoria fitness smart t-shirt		Remove sensors before washing	Yes	Available (US $ 129)
EMGLARE smart shirt	30°C	Minimal washing	Yes	Pre-order (US $ 249)
AiQ Sports Bra		Machine washable	Yes	Not available
HealthWatch ECG t-shirt		Home machine washable	Yes	Demo
CuteCircuit smart shirt		Washable	No	Pre-order (£550)

2.7 E-textile components

2.7.1 Flexible sensors and electrodes

The uses of textile-based sensors in daily life are increasing based on different applications, including physical and biochemical sensing [117]. One common example is the flexible/stretchable stress-strain sensors. The impact of stress on textile fabric or the amount of recovery against it can be detected and recorded using these sensors. Conductive coated knitted fabrics are commonly available in the market [118]. Graphene-coated fabrics and carbon nano-tubes (CNT) based fabrics are also available in the market. Pressure sensors are another form of textile-based sensors. They can be resistive pressure sensors or capacitive pressure sensors [119]. Temperature sensors are also being used widely in the smart textile industry. These sensors can be integrated into the system or may be used independently for some specific applications. These sensing mechanisms may be piezoelectric, piezoresistive, or capacitive sensing [120]. Kim *et al.* [75] prepared a single-layer pressure sensor by interweaving conductive wool yarn and non-conductive yarn. They performed mechanical testing on these sensors integrated smart gloves in terms of loading and unloading cycles and tensile testing machines.

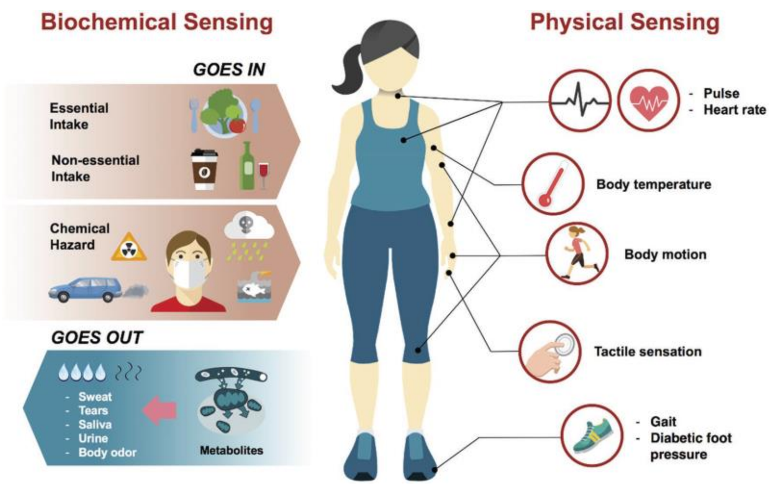

Figure 2.14. Flexible wearable sensors [117]

Humidity sensors are also being developed with conductive textile fabrics. They have a limited range of detection, and many more improvements are required. Metal wires are used during the weaving process to prepare temperature sensors. They are used to detect the body temperature of wearers. The use of metal wires creates flexibility problems in the sensors. Recently CNT based temperature sensors are also developed, but still, they have some limitations in performance. Chemical sensors are also one example of textile sensors that limit the danger of chemical exposure. These chemical sensors can be resistive, electrochemical, and semiconductor-based chemical sensors. Depending on usage, one or more sensors can be used simultaneously, keeping in mind unintentional interferences. Communication modules are used to collect and store data [119,121,122].

Real-time tracking of electrocardiogram (ECG) can be used to alert the patient a while before the fetal mishap such as a stroke or a heart attack, and thus life can be saved. Textile sensors can be fabricated/encapsulated in undergarments at different positions [123,124]. These electrodes can record sensitive pulse movements and ECG signals. The generated data can further be used to detect and indicate different medical diseases [91,125]. Meghrazi *et al.* [126] prepared the textile electrodes and placed them at different waist positions for ECG signal detections. Signals were recorded at different body positions, including sitting, standing, jogging, etc. [127]. Arquilla *et al.* [128] developed textile-based ECG skin electrodes by zigzag pattern sewing of silver-plated conductive yarns on normal fabrics. ECG data acquisition was carried out by three lead positioning systems and compared with normal gel electrodes. Wang *et al.* [129] reported textiles-based flexible sensors for ECG and breathing monitoring. Weft-knitted sensors were embedded at different positions in undergarments. Conductive silver platted nylon filament yarn was used for sensor preparations. Shathi *et al.* [108] worked on graphene-based washable textile electrodes using the pad-dry-cure method. To verify their samples, they performed different tests for the electrodes, including tensile strength, water contact angle, and colorfastness to rubbing. ECG responses at different body positions were monitored and claimed to be acceptable. Shahariar *et al.* [130] researched on printed electronic material by direct-write printing process on different types of substrates for healthcare applications. They used three different types of laminates, including polyethylene terephthalate (PET) nonwoven textiles, thermoplastic polyurethane (TPU), and nylon-PET nonwoven textiles. The durability of these types of sensors was directly related to ink-fiber micro structure attachment and penetration into the surface. Bystrickt *et al.* [88] investigated the ECG textile sensors and compared the knitted and embroidered-based sensors in terms of performance. In both cases, they found problems in dry (without gel) measurement, such as movement of electrodes due to muscular activity and false peaks generation due to the lack of moisture on the electrodes. However, these electrodes were good enough to detect P wave, QRS complex, and heart monitoring. Saleh *et al.* [131] produced textiles-based flexible ECG sensors with graphene oxide, and then a reduction process was carried out to obtain reduced graphene oxide cotton electrodes (rGOC). These samples were used for ECG signal detection. Rymarczyk *et al.* [92] proposed a system that records lung ventilation and cardiac function through a wearable garment. Different algorithms and image analyzing techniques were used to observe the changes during measurements. Tang *et al.* [132] developed textile electrodes for the replacement of ECG acquisition through capacitive electrodes. They proposed a controlled electrodes humidification system that can better perform in different ambient conditions. Fu *et al.* [133] discussed different types of ECG electrodes and their performance. They explained the importance and convenience of dry textile electrodes for long-term monitoring. These electrodes can be adapted to different shapes easily and according to body position.

Wang *et al.* [134] prepared Nano-mesh organic electrochemical transistors for medical and fitness sensing applications. They claimed to achieve simultaneous local amplifications of ECG signals on human skin with a high signal-to-noise ratio of 25.89 dB.

Nigusse *et al.* [135] developed washable silver printed textile electrodes that can be used for long-term ECG monitoring. They claimed that these electrodes had a surface resistance of 1.64 Ω/sq. They stated that these electrodes' signal quality was parallel to the standard Ag/AgCl electrodes, even after 10 washing cycles. Kim *et al.* [136] prepared textile-based electrodes for electrocardiogram measurements. They investigated the impact of electrode size and textile pressure on signal quality.

Figure 2.15. Textile based ECG sensors [128]

Similarly, chemical sensors integrated into the textile substrate can be used to investigate metabolic disorders. Shi *et al.* [105] and Grancaric´ *et al.* [95] worked on glucose-sensing electrodes integrated into the textile substrate along with pH, Sodium, and calcium-sensing electrodes. These electrodes justified a comprehensive datasheet about sweating. Gaubert *et al.* [84] developed urine leakage sensing underwear for children having Enuresis problems coupled with the bladder content sensor based on the bioimpedance real-time measurement device. Leakage sensors detect the conductivity of urine liquid, and signals were processed using electronic modules. They prepared two different types of sensors using stainless steel and silver-plated conductive yarns.

Pressure sensors can be used to investigate sleep analysis. These sensors can be integrated into a sleeping mattress, and body movement during sleep can be recorded. On the other hand, these sensors can be attached to wrist bands, and heart rate data can be collected precisely based on muscular pressure sensing. This data further can be used to predict sleep quality and other diseases. These sensors can also be integrated into sportswear. They can be installed into the inner footwear sole. Foot posture during jogging can be monitored and used to improve performance. Similarly, real-time heart monitoring of players can be useful to investigate their performances in different sports activities. Shathi *et al.* [108] prepared pressure sensors to investigate minor pulse rate changes by applying them on the wrist. Atakan *et al.* [76] produced the smart chest band. Accelerometers and gyroscope sensors were integrated into this chest band with a normal sewing method. The bands were then used for mobility and fall detection during sports activities. Cao *et al.* [137] experimented with electronic textile sensors with screen printing. They used carbon nanotubes (CNT) for screen printing ink and prepared the three-layers pressure sensors with the help of a hot press machine. They used different fabrics types, including silk, nylon, flax, cotton, wool, and leather. These sensors were then fixed in gloves, and finger movements were analyzed based on the pressure change in sensors. Sliz *et al.* [138] prepared roll-to-roll printed flexible electrodes for multi-purpose e-textile applications. Qureshi *et al.* [139] developed flexible strain sensors using Ny-6 (polyamide 6.6) yarn with silver nanoparticles plated on it. Silver nanoparticles were deposited on yarn using an electroless plating process.

Zhao *et al.* [140] prepared multifunctional strain sensors. PET-based Ag sensors were used for static and dynamic strain mapping. Different human body motions, pressure/strain distribution are recognized in various body positions. This low-cost sensor array can be helpful for next-generation human-machine interfaces.

Zhang *et al.* [141] prepared silver/silver chloride woven electrode, with uniform micro-convex shape, for different health monitoring applications. These electrodes enhanced the impedance reliability with the skin for long-term monitoring. Monitoring performance was analyzed with a different set of Ag/AgCl electrodes in terms of skin-electrode interface impedance and electrode resistance.

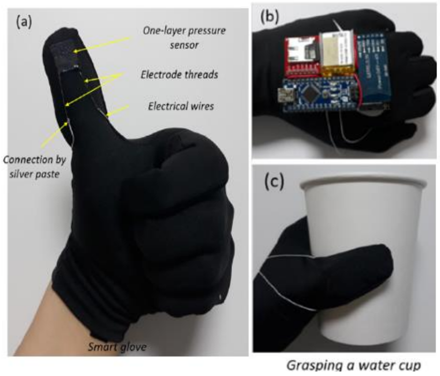

Figure 2.16. Pressure Sensor [75]

2.7.2 Actuators

These are kinds of devices that create a mechanical response to external stimuli. Textile flexible shape actuators are much more flexible and lightweight as compared to traditional shape actuators. These are widely used in intelligent robotics and medical treatments. Depending on usage, these actuators can be divided into humidity actuators, thermal and electrochemical actuators, and pneumatic actuators [105,142].

Figure 2.17. Smart textile jacket [143]

Jin *et al.* [144] prepared four-channel electromyogram (EMG) monitoring garment by the printing process. They developed electrically and mechanically stabled wiring structures by monitoring ink permeation in textiles using butyl carbitol acetate. They claimed sheet resistance as low as 0.06 Ω/sq. and 70 times increase after 450 % strain. This stretchable and mechanically stable conductive ink can be used on different textile substrates for multiple e-textile applications, especially health monitoring sensors. Mordon *et al.* [83] produced the light-emitting fabrics used for photodynamic therapy. They were used in vitro (CELL-LEF) and in vivo (VIVO-LEF). As the transmit range for optical fiber is 400 to 1200 nm, these fabrics can be used in almost all photosensitizers currently being used in the medical field.

Ryan *et al.* [145] and Yu *et al.* [146] prepared PEDOT: PSS coated fibers that can change shape on external stimuli. Logothetis *et al.* [147] reported silver-plated e-textiles electrodes for bioelectrical impedance analysis. The electrodes contain three different materials, including silver plated thread, PES thread, and substrate. Cotton and polyester substrate with different weaving techniques were used. The e-textiles were tested under different ambient conditions, and a change in resistance was calculated.

Koo *et al.* [148] prepared an innovative tactile display device based on soft actuator technology with the help of electroactive polymers. They claimed high flexibility, simple manufacturing, and better simulation with human skin as the important advantages for this device. But an extra protective layer is required for the safety of the actuator unit.

Likewise, motion sensors can be integrated into the textile substrate. Motion and strain sensing gloves are available in the markets. These gloves can precisely detect the motion of arms and fingers. LED displays can further be attached to these motion sensors, and thus different motions can be highlighted with different colors on the textiles. One good example can be traffic control officers. They can use their arm positions to blink different colors on their jackets, and these signals can be seen from a distance. These sensors can also be used in hospitals to detect patient movement either through their hospital gowns or through centralized display in nurse restrooms. Kim *et al.* [75] produced single-layer pressure sensors with conductive wool yarn. Gloves with encapsulated sensors at different finger positions were prepared. Change in resistance with finger movements was recorded. Afroj *et al.* [149] investigated graphene-based electronic textiles that can be used in ultra-flexible supercapacitor and skin-mounted strain sensors. Graphene was encapsulated on textiles with a scalable pad-dry-cure method and claimed surface resistance was 11.9 Ω /sq. Danova *et al.* [150] worked on piezo-resistive elastic sensors for human breath analysis. They prepared a commercially available t-shirt integrated with piezo-resistive elastic sensors prepared by purified multiwall carbon nanotubes (MWCNTs) network synthesized with the help of a chemical vapor deposition method and encapsulated by elastic silicon. Abed *et al.* [74] prepared a piezoelectric sensor based on natural sisal fiber. The conductive layer on these fibers is obtained by PEDOT: PSS coating on it. These sensors can be helpful in 3D interlock fabric for monitoring the stress and elongation into the structure.

2.7.3 Antennas

Currently, wireless communication is gaining much interest. Antennas are important components of wireless communication devices. For electronic wearable textiles, the antennas should also be flexible and properly integrated into wearable textiles [151,152]. Different types of antennas are being developed for wearable and stretchable applications. They include organic paper-based antennas, flexible optically transparent antennas, Printed magnetic conductive antennas, circularly polarized wearable antennas, and textile-based Rectennas [153]. Apart from communication, antennas can also be used for energy harvesting and energy transfer. Shi *et al.* [105] developed the antennas having a triple band feature. They are suitable for communication systems and military usages, but they face problems in terms of proximity to the human body. Garnier *et al.* [154] prepared NFC textile antennas with highly conductive yarn. These antennas can be used with mobile NFC powers to transmit the data or energy to the source (Figure 2.18).

Lee *et al.* [155] prepared textile antennas with screen printing using flat yarn PET fabric as the substrate. They claimed to achieve sheet resistance in the range of 16 mΩ/sq. These antennas were designed to work at 2.4 GHz, largely used for local area networks. The textile antennas were analyzed with different printing layers and the impact of the layer's uniformity.

Guibert *et al.* [156] developed flexible textile antennas for wearable RFID applications. They used different techniques, including embroidery, painted, and electro-textile for antenna manufacturing. Reliability of RFID tags was performed with moisture testing by dipping the samples in the tap water for an hour and then washing them in the domestic washing machine.

Kazani *et al.* [157] used conductive-based ink for screen printing in textile antennas. They prepared antennas based on the 2.5-D EM field simulator Momentum of Agilent's Advanced Design System (ADS) by using Acheson and Dupont inks. Two types of substrates, 100 % polyester and (20/80 %) cotton/polyester, were used in these experiments. Then, the antennas were covered with a TPU layer to protect them during washing. They washed all these samples at 40^{o}C for five washing cycles, and finally, the reflection coefficient and the radiation efficiency were measured. They claimed that all antennas showed stable performance after five washing cycles.

Figure 2.18. Textile based NFC antenna [154]

2.7.4 Energy harvesting, stockage, and transfer

Devices that can convert environmental energy into electrical energy are called energy harvesting devices. The energy sources are critical for complete e-textile systems. Wearable textiles can be converted into energy harvesting devices by coating or filming energy-active materials on the textile surface [103]. The active materials generate piezoelectric or triboelectric effects. The triboelectric effect is generated due to the collision of dissimilar materials, which causes the flow of electrons. The piezoelectric effect is obtained by applying some external mechanical stress to the material. Thermoelectric and photovoltaic effects are also achieved by different types of active materials [158]. The use of smart devices also increased the need for modified energy sources for more efficient charging. E-textile can be used as the source of energy by converting mechanical and solar energy into electrical energy. Piezoelectric devices integrated into textiles can convert mechanical energy into electrical energy. Similarly, organic solar cells can be integrated into textiles to generate and store solar energy. CNT-based stretchable materials can be used for energy harvesting purposes. Currently, nanowires prepared using Ag particles are also gaining attention due to higher conductivity. The textile-based energy sources can be used for power supply portable devices as well as the e-textile system itself [159,160]. Wau *et al.* [161] discussed current progress on energy harvesting in the wearable. They discussed different types of manufacturing techniques to enhance the flexibility of materials. Ag nanowires harvesters, ZnO nanowires harvesters, PZT energy harvesters, $BiTo_3$ energy harvesters, and other piezoelectric materials for energy harvesting such as GaN, $ZnSnO_3$, and NaNbO3 are explained in details. Current progress on highly stretchable and flexible energy harvesters is compiled in this study. Zopf *et al*. [162] experimented with different army-rated textiles for screen printing, and energy harvesting capacity for various samples were highlighted. Li *et al.* [163] prepared the screen-printed flexible battery that can be used as a power source for e-textile systems. They claimed that this battery could easily be integrated with woven cotton textiles and easy to use, flexible, and lightweight, but these batteries need to be encapsulated for better performance.

Recently, a German research team led by The Fraunhofer Institute for Reliability and Micro-integration developed a battery that can be printed on the textile substrate. These batteries were fabricated by screen printing using a silver-oxide thick base layer and a final 120µm thick AgO-ZN battery layer [164].

Electrochemically storage devices, including super-capacitors and lithium-ion batteries, can also be integrated into e-textile systems. The flexible smart textile materials, when properly developed, can be used for multiple power source applications. Recent research conducted by IDTechEx [165] estimated that the flexible, printed, and thin-film batteries market can reach up to 109 M US dollars in 2025 (Figure 2.19). They claimed that recent innovations in health, fitness, cosmetics, wearable, medical, and smart devices opened the doors for new kinds of smart power solutions.

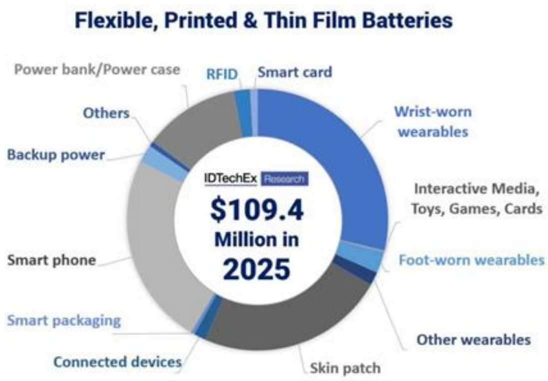

Figure 2.19. Flexible batteries market share [165]

2.7.5 Flexible circuits

For electronic textiles, circuits have gained much importance because they provide mechanical support and electrical connections for the entire network. The circuit boards should be reliable and comfortable for wearable applications [72]. Flexibility is key propriety for them. These circuits can be printed on textiles using inkjet printing, screen printing, aerosol jet printing, gravure printing, and offset printing. They can also be prepared by using fabrication techniques, including embroidery and weaving [105,166]. Copper-coated thin sheets are also used to obtain the flexible circuit boards. The flexible boards are then fixed on wearable textile by different means. However, adhesion issues and flexibility mismatch with substrate create problems [105,166]. Georgia Tech Wearable Motherboard (GTWM) prepared the smart shirt in collaboration with the US navy for use in combat conditions. Optical fibers used in it help to detect bullet wounds. Additional sensors installed on the shirt can help locate and monitor the vital signs in combat conditions [167]. Chow *et al.* [168] highlighted the current progress in photo-detectors suitable for wearable systems. Organic photo-detectors suitable for next-generation wearable devices in terms of both mechanical and optoelectronic properties are outlined in this discussion. These devices can be used in various applications, including health monitoring and energy harvesting. Ma *et al.* [169] discussed various flexible electronics that can be used in many smart textile applications. A brief chronology and advancements in applications, including bioelectrical monitoring, optical monitoring, Acoustic monitoring, and body fluid testing, are explained in detail.

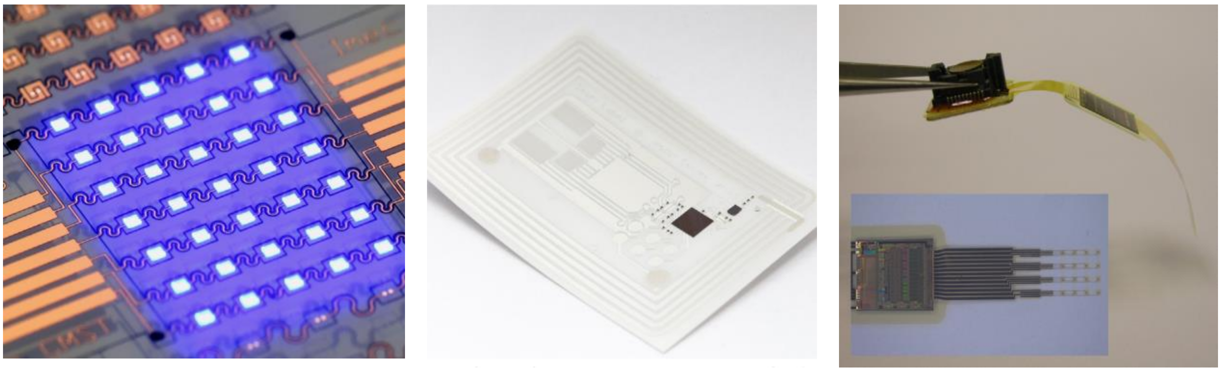

Figure 2.20. Flexible motherboards [123]

2.7.6 Component connections/ transmission lines

Wearable e-textiles can have multiple components depending on the product requirements and functionalities. These components need to be self-connected by conductive threads. They can be 100 % metallic such as aluminum, copper, or stainless steel, or a conductive polymer such as polypyrrole and PEDOT: PSS or conductive polymer composite such as carbon-based or silver-based, etc. [170]. Some examples of transmission lines are displayed in Figure 2.22.

Soldering is the most common connecting technique used for traditionally electronic connections [171]. However, soldering joints on metallic textile circuits are difficult and create durability interface integration problems [166,172,173]. Similarly, soldering connection failure is common on textile substrate LEDs joints. Conductive adhesive is another alternative that can be used for this purpose. They normally consist of conductive particles with adhesive materials for proper adhesion to the textile substrate, but they are usually affected by temperature and humidity conditions. Different protective layers are used to minimize these damages [174]. Other techniques that are being used randomly includes embroidering [175], crimping [176], flip-chip [177] and magnetic [178] etc. (Figure 2.21). Different techniques have various usage limitations for the specific type of materials. For example, techniques requiring high temperatures are not suitable for polymer-based materials, and the embroidery technique is not suitable for metallic yarns, etc.

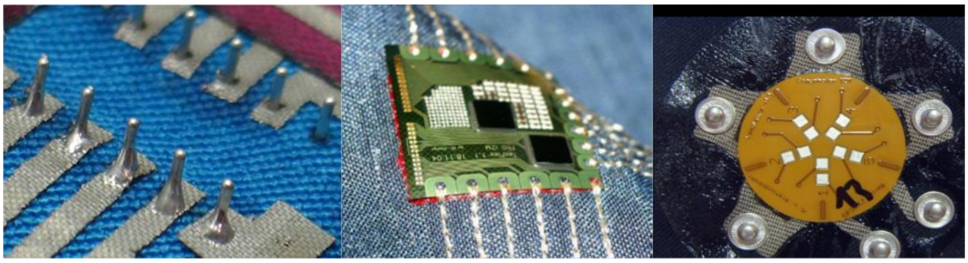

Figure 2.21. Different connection techniques, (a) soldering [171], (b) embroidering [175], (c) flip-chip [177]

Conductive wires are most commonly used to connect different components of e-textile wearable systems. Metallic yarns have better electrical properties than polymer yarns, but these yarns create discomfort with human skin and create problems in terms of flexibility. Polymer-based conductive yarns, especially silver-plated polymer yarns, are most commonly used in smart textile structures due to their flexibility and easy processing [179]. These wires can be woven into the fabric during the textile weaving process. Simple stitch or embroidery techniques can also be used to fix these wires on textile substrates. These connection wires are distributed all over the e-textile system, making them more readily available to damage. Different protection techniques are used to avoid damages. The connection wires can be protected by TPU coating, polymer adhesive coating, or protective yarns stitched over these wires [95,105,180].

De Vries *et al.* [181] developed a measurement methodology by simultaneous mechanical and electrical tests on bare conductive yarns extracted from woven fabric. The electrical and mechanical failure of the conductive fabric depends on the thickness and spacing of the textile yarns in the fabric. They prepared three different samples with varying diameters of yarns and different weft densities and measured the electrical response during tensile strength tests. They found that the mechanical failure occurred before electrical failure because even if the filament breaks randomly in the length of yarn, electrical contacts between filaments remained. However, no simulation formulas were given to reveal the relationship between mechanical stress and conductive yarns failure.

Paul *et al.* [182] examined the Durability of Screen Printed Conductive Tracks on Textiles with silver polymer paste, encapsulated with polyurethane film. They claimed that 97.1 % of the conductive tracks remained conductive after ten domestic machine washes with 1 kg load at 40^{o}C and 1000 rpm tumble drying speed. However, the authors have not developed a model that could be applied to estimate damages affecting conductivity after a certain number of washing cycles.

Zeagler *et al.* [183] washed the electronic interface in hot water. They used two types of conductive yarns Shieldtex size 33 (polyamide silver-plated conductive yarn) and Shieldtex size 40 (double ply thread). They checked the resistance after each washing and claimed that Shieldtex size 33 conductive yarns showed better results than others.

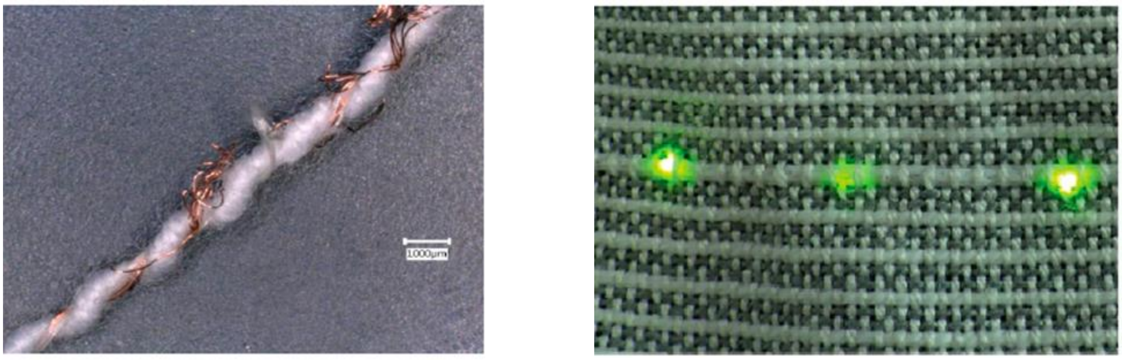

Figure 2.22. Conductive wire strand in e-textile structure [172], functional LED yarn [184]

Ryan *et al.* [145] prepared PEDOT: PSS coated silk conducted yarn and used it as the connecting thread with LEDs in e-textile structure. Lund *et al.* [185] worked on conductive yarns with different types of conjugated polymers, polymers blends, and nano-composites. They discussed different fabrication techniques, including weaving, knitting, non-woven, etc., for yarn integration into e-textile. Hardy *et al.* [172] reported four different types of conductive yarn (e-yarns). They prepared copper wire e-yarns, illuminating e-yarns, temperature sensing e-yarns, and acoustic sensing e-yarns. Laing *et al.* [186] explained different conductive yarn structures and techniques for their integration/fabrication in the fabric. Furthermore, different fabric treatments to achieve better conductivity and properties required to claim better conductive fabric sensors were also discussed in detail. Hwang *et al.* [187] fabricated machine washable and highly conductive silk coated yarn for electronic textile applications. Silk yarn was coated with a composite of Ag nanowires and PEDOT: PSS through a dip-coating process.

2.8 Washability

Washability and reliability are major issues wearable textiles are facing nowadays [188–190]. Various prototypes are available in the market, and they are much successful in meeting the user requirements, but these products lack in terms of washability and wash reliability. Wash reliability depends on the proper functioning of the complete e-textile system after the pre-described number of wash cycles. Different standards are available for textile wash protocols, but they cannot work for e-textile products. Special precautions should be adopted for electronic textile washability [191,192].

To work on electronic textile wash issues, it is important first to analyze the wash procedure and then prepare requirements that should be followed for this wash process. Almost every household has a domestic wash machine, and it is not feasible to convince customers to buy a separate machine for e-textile washing. These hybrid products should be adopted for the currently available wash machine for routine household wash process.

Several research groups are working on e-textiles prototypes, and we can see so many valuable products depending on requirements. There are no standards available for washability and reliability for e-textile products. That's why various groups used their locally available wash processes to claim washability. Similarly, different people used different temperatures and speed settings to wash their samples. Diverse research articles found claiming the washability of their products for a different number of wash cycles. Some used laboratory-based wash machines, and some preferred user-oriented wash processes.

Ryan *et al.* [145] worked with a household wash machine to wash dyed silk yarn samples. These samples were washed at 30°C and 900 rpm up to four wash cycles. Kim et al. [15] used a mini wash machine to wash textile sensors up to 50 wash cycles. Gaubert *et al.* [84] prepared urine leakage sensors encapsulated into underwear and washed these sensors in the household machine for 20 wash cycles. Cao *et al.* [137] developed electronic textile sensors with screen printing and claimed washability after immersing in water for 15 hours. Afroj *et al.* [149] investigated graphene-based electronic textiles and washed them up to 10 house-held wash cycles using AATCC 105 standards and claimed no change after these washes. Jin *et al.* [144] produced a multilayer color coated e-textile and washed them for 50 wash cycles following AATCC 135. Hardy *et al.* [172] checked the washing behavior of conductive yarns. They used a household machine for 25 wash cycles by following ISO 6330 wash standards. Shahariar *et al.* [130] prepared printed electronic material by direct-write printing process on different types of substrates. These samples were washed for 25 wash cycles according to AATCC 61-2a. Hwang *et al.* [187] claimed machine washable highly conductive silk coated yarn for electronic textile applications. They washed the prototypes for 10 wash cycles, but no further details are explained. Salavagione *et al.* [193] investigated conductive smart textiles with graphene-based coating on the textile and washed them for 10 wash cycles, but here again, no further explanation is provided. Gaubert *et al.* [93] observed the washing behavior of silver-plated nylon yarn. The effects of bleaching agents on the morphology of silver coating and loss of conductivity after certain wash cycles were discussed. These yarns were investigated in household machines according to AATCC 135 standards. 30 wash cycles, with a 60 min process for each cycle with 900 rpm speed and 30°C temperature, were used for this experiment. Sliz *et al.* [138] checked roll-to-roll printed flexible electrodes for multi-purpose e-textile applications. The mechanical behavior and wash properties of these electrodes were investigated. They were washed at 40°C for 63 minutes and up to 10 wash cycles at 1000 rpm in a normal household machine. Saleh *et al.* [131] produced textiles-based flexible ECG sensors with graphene oxide and then a reduction process was carried out to obtain reduced graphene oxide cotton electrodes (rGOC). The conductivity of these electrodes was above 70 % of the original value after 5 wash cycles. But again, no further details about the wash process were provided. Liang *et al.* [194] developed different types of textile stretch sensors. A washability test was performed for these samples in a front load washing machine for 3 washing cycles according to ISO 6330:2012 test protocols. Kellomäki *et al.* [152] developed washable RFID antennas for tagging and washed them for laundry tests. These samples were washed for 10 washing cycles with 1000 rpm spin speed and 40°C washing temperature.

Table 2.2 explains the different researchers' approaches to the wash process. As no standardized process is available, each experiment is performed based on feasibility. Hence, each claim of washable and reliable e-textile is based on different scenarios, and in some cases, no data regarding wash parameters are communicated. To obtain a centralized statement and commercially accepted washable e-textile products, they should be claimed washable and reliable based on the standardized functionality test and wash protocols.

Table 2.2. Wash details in different research articles

Author	No. of washes	Washing time (min)	Tumble speed (rpm)	Standard followed	Wash temp. (°C)	Washing type
Ryan *et al.* [145]	4	50	900	-	30	Household machine
Afroj *et al.* [149]	10	-	-	ISO 105 C06	-	Household machine
Kim *et al.* [75]	50	12	-	-	-	Mini wash machine
Gaubert *et al.* [84]	20	30	-	-	60	Household machine
Cao *et al.* [137]	-	120	-	-	-	Immersed in water
Jin *et al.* [144]	50	-	-	AATCC 135	40	Laboratory wash
Hardy *et al.* [172]	25	23	800	ISO 6330:2012	40	Household machine
Ryan *et al.* [145]	5	50	900		30	Household machine
Shahariar *et al.* [130]	25	-	-	AATCC 61-2a	-	-
Hwang *et al.*	10	-	-	-	-	-
Gaubert *et al.* [195]	30	60	400	AATCC 135	30	Household machine
Sliz *et al.* [138]	10	63	1000		40	Household machine
Saleh *et al.* [131]	5	-	-	-	-	-
Liang *et el.* [194]	3	-	800	ISO 6330:2012	40	Household machine
Kellom¨aki *et al.* [152]	10	150	1000		40	-
Guibert *et al.* [156]	5	-	-	-	40	Household machine
Ojstršek *et al.* [196]	20	30	-	ISO 105 C06	40	Laboratory wash
Nigusse *et al.* [135]	10	30		ISO 105 C06	40	-
Schwarz *et al.* [197]	25	40		ISO 6330:2012	40	Household machine

2.9 Conclusion

The textile industry is shifting its momentum from conventional textile to smart user-defined functional textiles. Today's textile became the platform for various functionalities as well as normal textile usages. These e-textile systems are lacking of standardization and functional reliability. Various available standard test protocols established for conventional textiles are shortlisted here, along with recent progress to develop new norms dedicated to e-textile systems. An overview of recent developments in wearable e-textile products and available products in different fields based on their applications (medical, sports, military, etc.) is presented in this chapter. Various e-textile system components (sensors, actuators, connection threads, etc.) are discussed in detail, with some recent research progress ongoing in these system developments.

In the later part, washability and reliability problems associated with these e-textile systems are highlighted by discussing some current research progresses using various available textile standard protocols. Various researchers claimed the washability of their prototypes using different available standards. These problems enhance the importance of new standards dedicated to wearable e-textile systems.

This research is targeted to investigate the washing problems related to e-textile systems. Because to go forward in washing standardization, first, it is important to understand the wash process and know what is going on in washing. Some basic development is under process and different organizations are already working on it. Useful fundamental understanding is already well developed in terms of definitions and categorization for basic understanding. For example, IEC 63203-204-1 recently published test method for assessing washing reliability of leisurewear and sportswear, explaining the basic definition of e-textile systems, conductive textiles, washability test conditions, and after washing protocols. However, washing analyses are not performed and it is only focused on already developed washing standards that are not designed for e-textile system washability. There is a need to investigate the washing characteristics and behavior of different e-textiles and their components separately for a better understanding of their washing predictions. Therefore, we believe that a new washing standard taking into account all the particularities of the e-textile systems should be defined to improve the already existing standards such as ISO 6330, etc. Also, the objective of our work is to better understand the types of damages provoked by washing on e-textile systems to be able to simulate them in laboratory conditions. For instance, mechanical damages could be simulated by existing textile testing apparatuses.

For the washing of smart textiles, there are two possibilities. One is a laboratory standardized washing procedure, and the other is washing in household washing machines. To be successful in smart textiles, they should be able to withstand after washing in normal washing machines as ultimately, they will be laundered at homes. For these reasons, the focus is given to commercially available washing machines. Secondly, this research is dedicated to e-textile systems developed by textile manufacturing methods. In other words, the major part of e-textile systems should be textile structure. Although they can be prepared by other techniques, they are not in the scope of this work. Only textile manufacturing methods are focused on, keeping in mind that conventional textile products prepared by these techniques are widely being replaced by e-textile systems, and there is a lot of discussion about their washability issues.

References

1. Chen, C.-Y.; Huang, S.Y.; Wan, H.-Y.; Chen, Y.-T.; Yu, S.-K.; Wu, H.-C.; Yang, T.-I. Electrospun Hydrophobic Polyaniline/Silk Fibroin Electrochromic Nanofibers with Low Electrical Resistance. *Polymers* **2020**, *12*, 2102, doi:10.3390/polym12092102.
2. Li, R.-W.; Liu, G. Flexible and Stretchable Electronics. 409.
3. ISO 6330:2012(En), Textiles — Domestic Washing and Drying Procedures for Textile Testing Available online: https://www.iso.org/obp/ui#iso:std:iso:6330:ed-3:v1:en (accessed on 11 September 2020).
4. BS EN ISO 139-2005+A1-2011--[2017-12-21--01-16-11 PM].Pdf.
5. ISO 3759:2011 Available online: https://www.iso.org/cms/render/live/en/sites/isoorg/contents/data/standard/05/73/57309.html (accessed on 21 December 2020).
6. ISO 105-A05:1996 Available online: https://www.iso.org/cms/render/live/en/sites/isoorg/contents/data/standard/00/37/3789.html (accessed on 21 December 2020).
7. ISO 105-C06:2010 Available online: https://www.iso.org/cms/render/live/en/sites/isoorg/contents/data/standard/05/12/51276.html (accessed on 21 December 2020).
8. ISO 105-C12:2004 Available online: https://www.iso.org/cms/render/live/en/sites/isoorg/contents/data/standard/03/76/37645.html (accessed on 21 December 2020).
9. ISO 105-C09:2001 Available online: https://www.iso.org/cms/render/live/en/sites/isoorg/contents/data/standard/03/32/33204.html (accessed on 21 December 2020).
10. ISO 105-C10:2006 Available online: https://www.iso.org/cms/render/live/en/sites/isoorg/contents/data/standard/03/17/31775.html (accessed on 21 December 2020).
11. ISO 3175-2:2017 Available online: https://www.iso.org/cms/render/live/en/sites/isoorg/contents/data/standard/06/51/65154.html (accessed on 21 December 2020).
12. ISO 811:2018 Available online: https://www.iso.org/cms/render/live/en/sites/isoorg/contents/data/standard/06/51/65149.html (accessed on 21 December 2020).

13. AATCC - AATCC Available online: https://members.aatcc.org/store/tm135/543/ (accessed on 11 September 2020).
14. AATCC - AATCC Available online: https://members.aatcc.org/store/lp001/2212/ (accessed on 11 September 2020).
15. AATCC 1993 Standard Reference Detergent. *AATCC*.
16. IEC 60601-2-31:2020 Available online: https://www.iso.org/cms/render/live/en/sites/isoorg/contents/data/standard/07/24/72452.html (accessed on 21 December 2020).
17. IEC 60601-1-12:2014 Available online: https://www.iso.org/cms/render/live/en/sites/isoorg/contents/data/standard/05/95/59536.html (accessed on 21 December 2020).
18. IEC/TR 60601-4-1:2017 Available online: https://www.iso.org/cms/render/live/en/sites/isoorg/contents/data/standard/07/07/70755.html (accessed on 21 December 2020).
19. IEC 61340-4-1:2003+AMD1:2015 CSV | IEC Webstore Available online: https://webstore.iec.ch/publication/22337 (accessed on 21 December 2020).
20. IEC 62631-3-1:2016 | IEC Webstore Available online: https://webstore.iec.ch/publication/24397 (accessed on 21 December 2020).
21. IEC 62631-3-2:2015 | IEC Webstore Available online: https://webstore.iec.ch/publication/23875 (accessed on 21 December 2020).
22. IP Rating Chart.Pdf.
23. IPC-A-610D WAM1: Acceptability of Electronic Assemblies | IPC Store Available online: https://shop.ipc.org/IPC-A-610D-WAM1-English-D (accessed on 21 December 2020).
24. IPC-A-600J: Acceptability of Printed Boards Available online: https://shop.ipc.org/IPC-A-600J-English-MDL (accessed on 21 December 2020).
25. IPC-9204: Guideline on Flexibility and Stretchability Testing for Printed Electronics Available online: https://shop.ipc.org/IPC-9204-English-D (accessed on 21 December 2020).
26. IPC-6903: Terms and Definitions for the Design and Manufacture of Printed Electronics (Additive Circuitry) Available online: https://shop.ipc.org/IPC-6903-English-D (accessed on 21 December 2020).

27. IPC-9252B: Requirements for Electrical Testing of Unpopulated Printed Boards Available online: https://shop.ipc.org/IPC-9252B-English-D (accessed on 21 December 2020).
28. IPC-9202: Material and Process Characterization/Qualification Test Protocol for Assessing Electrochemical Performance Available online: https://shop.ipc.org/IPC-9202-English-D (accessed on 21 December 2020).
29. Flexible, Wearable, and Stretchable Electronics.Pdf.
30. ISO 12947-1:1998 Available online: https://www.iso.org/cms/render/live/en/sites/isoorg/contents/data/standard/00/19/1931.html (accessed on 21 December 2020).
31. ISO 12947-2:2016 Available online: https://www.iso.org/cms/render/live/en/sites/isoorg/contents/data/standard/06/10/61058.html (accessed on 21 December 2020).
32. ISO 12947-3:1998 Available online: https://www.iso.org/cms/render/live/en/sites/isoorg/contents/data/standard/02/36/23620.html (accessed on 21 December 2020).
33. ISO 12947-4:1998/Cor 1:2002 Available online: https://www.iso.org/cms/render/live/en/sites/isoorg/contents/data/standard/03/73/37375.html (accessed on 21 December 2020).
34. ISO 12945-1:2020 Available online: https://www.iso.org/cms/render/live/en/sites/isoorg/contents/data/standard/07/53/75374.html (accessed on 21 December 2020).
35. ISO 12945-2:2020 Available online: https://www.iso.org/cms/render/live/en/sites/isoorg/contents/data/standard/07/53/75375.html (accessed on 21 December 2020).
36. ISO 12945-3:2020 Available online: https://www.iso.org/cms/render/live/en/sites/isoorg/contents/data/standard/07/53/75376.html (accessed on 21 December 2020).
37. ISO 12945-4:2020 Available online: https://www.iso.org/cms/render/live/en/sites/isoorg/contents/data/standard/07/53/75377.html (accessed on 21 December 2020).
38. ISO/R 388:1964 Available online: https://www.iso.org/cms/render/live/en/sites/isoorg/contents/data/standard/00/43/4372.html (accessed on 21 December 2020).

39. ISO/CD 13997 Available online: https://www.iso.org/cms/render/live/en/sites/isoorg/contents/data/standard/07/11/71111.html (accessed on 21 December 2020).
40. ISO 6945:1991/Amd 1:1998 Available online: https://www.iso.org/cms/render/live/en/sites/isoorg/contents/data/standard/02/90/29091.html (accessed on 21 December 2020).
41. ISO 20253:2016 Available online: https://www.iso.org/cms/render/live/en/sites/isoorg/contents/data/standard/06/74/67423.html (accessed on 21 December 2020).
42. D13 Committee *Test Method for Abrasion Resistance of Textile Fabrics (Oscillatory Cylinder Method)*; ASTM International;
43. D13 Committee *Guide for Abrasion Resistance of Textile Fabrics (Rotary Platform, Double-Head Method)*; ASTM International;
44. D13 Committee *Test Method for Abrasion Resistance of Textile Fabrics (Flexing and Abrasion Method)*; ASTM International;
45. D13 Committee *Test Method for Abrasion Resistance of Textile Fabrics (Inflated Diaphragm Apparatus)*; ASTM International;
46. D13 Committee *Guide for Abrasion Resistance of Textile Fabrics (Uniform Abrasion)*; ASTM International;
47. D13 Committee *Test Method for Abrasion Resistance of Textile Fabrics (Martindale Abrasion Tester Method)*; ASTM International;
48. AATCC - AATCC Available online: https://members.aatcc.org/store/tm93/508/ (accessed on 21 December 2020).
49. F02 Committee *Practice for Conditioning Flexible Barrier Materials for Flex Durability*; ASTM International;
50. ISO 7854:1995 Available online: https://www.iso.org/cms/render/live/en/sites/isoorg/contents/data/standard/01/47/14777.html (accessed on 21 December 2020).
51. ISO 2062:2009 Available online: https://www.iso.org/cms/render/live/en/sites/isoorg/contents/data/standard/04/56/45642.html (accessed on 21 December 2020).
52. ISO 13934-1:2013 Available online: https://www.iso.org/cms/render/live/en/sites/isoorg/contents/data/standard/06/06/60676.html (accessed on 21 December 2020).

53. ISO 13934-2:2014 Available online: https://www.iso.org/cms/render/live/en/sites/isoorg/contents/data/standard/06/06/60677.html (accessed on 21 December 2020).
54. D13 Committee *Test Method for Breaking Strength and Elongation of Textile Fabrics (Grab Test)*; ASTM International;
55. D13 Committee *Test Method for Breaking Force and Elongation of Textile Fabrics (Strip Method)*; ASTM International;
56. D13 Committee *Test Method for Tearing Strength of Fabrics by Trapezoid Procedure*; ASTM International;
57. ISO 14704:2016 Available online: https://www.iso.org/cms/render/live/en/sites/isoorg/contents/data/standard/06/54/65411.html (accessed on 21 December 2020).
58. D13 Committee *Test Method for Stretch Properties of Knitted Fabrics Having Low Power*; ASTM International;
59. D13 Committee *Test Methods for Stretch Properties of Fabrics Woven from Stretch Yarns*; ASTM International;
60. AATCC - AATCC.
61. AATCC - AATCC.
62. BS EN 16812:2016 - Textiles and Textile Products. Electrically Conductive Textiles. Determination of the Linear Electrical Resistance of Conductive Tracks Available online: https://shop.bsigroup.com/ProductDetail/?pid=000000000030293513 (accessed on 21 December 2020).
63. ISO/CD 24584 Available online: https://www.iso.org/cms/render/live/en/sites/isoorg/contents/data/standard/07/89/78999.html (accessed on 21 December 2020).
64. ISO/TR 23383:2020 Available online: https://www.iso.org/cms/render/live/en/sites/isoorg/contents/data/standard/07/53/75383.html (accessed on 21 December 2020).
65. IEC 61482-1-1:2019 | IEC Webstore Available online: https://webstore.iec.ch/publication/26682 (accessed on 21 December 2020).
66. IEC 61482-1-2:2014 | IEC Webstore Available online: https://webstore.iec.ch/publication/5498 (accessed on 21 December 2020).
67. WK61480 New Test Method for Durability of Smart Garment Textile Electrodes after Laundering Available online:

https://www.astm.org/DATABASE.CART/WORKITEMS/WK61480.htm (accessed on 21 December 2020).

68. RA111, Electronically Integrated Textiles Test Methods. *AATCC*.
69. IEC - TC 124 Dashboard > Projects: Work Programme, Publications, Maintenance Cycle, Project Files, TC/SC in Figures Available online: https://www.iec.ch/dyn/www/f?p=103:38:0::::FSP_ORG_ID,FSP_APEX_PAGE,FSP_PROJECT_ID:20537,109,101883 (accessed on 5 January 2021).
70. IPC-8921: Requirements for Woven and Knitted Electronic Textiles (E-Textiles) Integrated with Conductive Fibers, Conductive Yarns and/or Wires Available online: https://shop.ipc.org/IPC-8921-English-D (accessed on 21 December 2020).
71. IPC E-Textiles Initiative - Join the Effort Available online: https://www.ipc.org/ipc-e-textiles-initiative-join-effort (accessed on 21 December 2020).
72. Hussain, M.M.; El-Atab, N. Handbook of Flexible and Stretchable Electronics. 551.
73. Bahru, R.; Hamzah, A.A.; Mohamed, M.A. Thermal Management of Wearable and Implantable Electronic Healthcare Devices: Perspective and Measurement Approach. *Int J Energy Res* **2020**, er.6031, doi:10.1002/er.6031.
74. Abed, A.; Cochrane, C.; Boussu, F.; Cherkaoui, O.; Elmoznine, R. Design and Development of a Piezo-Resistive Sensor Based on PEDOT: PSS Applied to Sisal's Natural Fiber for Monitoring of 3D Warp Interlock Fabric. *IOP Conf. Ser.: Mater. Sci. Eng.* **2020**, *827*, 012019, doi:10.1088/1757-899X/827/1/012019.
75. Kim, G.; Vu, C.C.; Kim, J. Single-Layer Pressure Textile Sensors with Woven Conductive Yarn Circuit. *Applied Sciences* **2020**, *10*, 2877, doi:10.3390/app10082877.
76. Atakan, R.; Acikgoz Tufan, H.; Baskan, H.; Eryuruk, S.H.; Akalin, N.; Kose, H.; Li, Y.; Kursun Bahadir, S.; Kalaoglu, F. Design of an Electronic Chest-Band. *IOP Conf. Ser.: Mater. Sci. Eng.* **2017**, *254*, 072002, doi:10.1088/1757-899X/254/7/072002.
77. Yang, C.-M.; Wu, C.-C.; Chou, C.-M.; Yang, C.-W. Textile-Based Monitoring System for Biker. In Proceedings of the 2009 9th International Conference on Information Technology and Applications in Biomedicine; IEEE: Larnaka, Cyprus, November 2009; pp. 1–4.
78. Rachel, M.D.A. HEALTHCARE TEXTILE DYED NATURAL SOCKS. **2019**, *4*, 6.
79. Edmison, J.; Lehn, D.; Jones, M.; Martin, T. E-Textile Based Automatic Activity Diary for Medical Annotation and Analysis. In Proceedings of the International Workshop on Wearable and Implantable Body Sensor Networks (BSN'06); IEEE: Cambridge, MA, USA, 2006; pp. 131–134.

80. De jonckheere, J.; Narbonneau, F.; Jeanne, M.; Kinet, D.; Witt, J.; Krebber, K.; Paquet, B.; Depre, A.; Logier, R. OFSETH: Smart Medical Textile for Continuous Monitoring of Respiratory Motions under Magnetic Resonance Imaging. In Proceedings of the 2009 Annual International Conference of the IEEE Engineering in Medicine and Biology Society; IEEE: Minneapolis, MN, September 2009; pp. 1473–1476.
81. Witt, J.; Narbonneau, F.; Schukar, M.; Krebber, K.; De Jonckheere, J.; Jeanne, M.; Kinet, D.; Paquet, B.; Depre, A.; D'Angelo, L.T.; et al. Medical Textiles With Embedded Fiber Optic Sensors for Monitoring of Respiratory Movement. *IEEE Sensors J.* **2012**, *12*, 246–254, doi:10.1109/JSEN.2011.2158416.
82. Ferrara, M. Smart Experience in Fashion Design: A Speculative Analysis of Smart Material Systems Applications. *Arts* **2018**, *8*, 4, doi:10.3390/arts8010004.
83. Mordon, S.; Thécua, E.; Ziane, L.; Lecomte, F.; Deleporte, P.; Baert, G.; Vignion-Dewalle, A. Light Emitting Fabrics for Photodynamic Therapy: Technology, Experimental and Clinical Applications. *Translational Biophotonics* **2020**, *2*, doi:10.1002/tbio.202000005.
84. Gaubert, V.; Gidik, H.; Koncar, V. Boxer Underwear Incorporating Textile Moisture Sensor to Prevent Nocturnal Enuresis. *Sensors* **2020**, *20*, 3546, doi:10.3390/s20123546.
85. Sandulescu, V.; Dobrescu, R. Wearable System for Stress Monitoring of Firefighters in Special Missions. In Proceedings of the 2015 E-Health and Bioengineering Conference (EHB); IEEE: Iasi, Romania, November 2015; pp. 1–4.
86. Caya, M.V.C.; Casaje, J.S.; Catapang, G.B.; Dandan, R.A.V.; Linsangan, N.B. Warning System for Firefighters Using E-Textile. In Proceedings of the 2018 3rd International Conference on Computer and Communication Systems (ICCCS); IEEE: Nagoya, April 2018; pp. 362–366.
87. Zaman, S. uz; Tao, X.; Cochrane, C.; Koncar, V. Understanding the Washing Damage to Textile ECG Dry Skin Electrodes, Embroidered and Fabric-Based; Set up of Equivalent Laboratory Tests. *Sensors* **2020**, *20*, 1272, doi:10.3390/s20051272.
88. Bystricky, T.; Moravcova, D.; Kaspar, P.; Soukup, R.; Hamacek, A. A Comparison of Embroidered and Woven Textile Electrodes for Continuous Measurement of ECG. In Proceedings of the 2016 39th International Spring Seminar on Electronics Technology (ISSE); IEEE: Pilsen, Czech Republic, May 2016; pp. 7–11.
89. Ankhili, A.; Tao, X.; Cochrane, C.; Koncar, V.; Coulon, D.; Tarlet, J.-M. Ambulatory Evaluation of ECG Signals Obtained Using Washable Textile-Based Electrodes Made

with Chemically Modified PEDOT:PSS. *Sensors* **2019**, *19*, 416, doi:10.3390/s19020416.

90. Medical Smart Textile Market Scope And Challenges 2018-2027 by Players, Technology and Applications | MarketResrarchFuture.Com | Medgadget.
91. Scataglini, S.; Moorhead, A.P.; Feletti, F. A Systematic Review of Smart Clothing in Sports: Possible Applications to Extreme Sports. *Muscle Ligaments and Tendons J* **2020**, *10*, 333, doi:10.32098/mltj.02.2020.19.
92. Rymarczyk, T.; Vejar, A.; Nita, P.; Stefaniak, B.; Wos, M.; Oleszek, M. Using Electrical Tomography for Remote Monitoring Cardiopulmonary State of Patients by Complementary Investigation Techniques. In Proceedings of the 2019 19th International Symposium on Electromagnetic Fields in Mechatronics, Electrical and Electronic Engineering (ISEF); IEEE: Nancy, France, August 2019; pp. 1–2.
93. Gaubert, V.; Gidik, H.; Bodart, N.; Koncar, V. Quantification of the Silver Content of a Silver-Plated Nylon Electrode According to the Nature of the Laundering Detergent. *IOP Conf. Ser.: Mater. Sci. Eng.* **2020**, *827*, 012033, doi:10.1088/1757-899X/827/1/012033.
94. Quandt, B.M.; Scherer, L.J.; Boesel, L.F.; Wolf, M.; Bona, G.-L.; Rossi, R.M. Body-Monitoring and Health Supervision by Means of Optical Fiber-Based Sensing Systems in Medical Textiles. *Adv. Healthcare Mater.* **2015**, *4*, 330–355, doi:10.1002/adhm.201400463.
95. Grancarić, A.M.; Jerković, I.; Koncar, V.; Cochrane, C.; Kelly, F.M.; Soulat, D.; Legrand, X. Conductive Polymers for Smart Textile Applications. *Journal of Industrial Textiles* **2018**, *48*, 612–642, doi:10.1177/1528083717699368.
96. NeoMedLight Bilicocoon® Available online: https://www.neomedlight.com/bilicocoon/ (accessed on 22 December 2020).
97. Andrew Cohen Heart-Monitoring T-Shirt Available online: https://www.sporttechie.com/smart-textile-company-kymira-cardiac-monitoring-tshirt-athletes/.
98. Xiaomi Mijia Cardiogram T-Shirt: Smart T-Shirt with ECG Measurement. *Xiaomi Planet* 2020.
99. Daniely, H. A T-Shirt That Monitors Your Heart. *HealthWatch Ltd.| Healthcare Wearables* 2017.
100. Products & Services. *AiQ Smart Clothing*.

101. Inc, E. Sport T-Shirt Available online: https://emglare.com/products/sport-tshirt (accessed on 21 December 2020).
102. Bonato, P. Advances in Wearable Technology for Rehabilitation. 17.
103. Scataglini, S.; Andreoni, G.; Gallant, J. A Review of Smart Clothing in Military. In Proceedings of the Proceedings of the 2015 workshop on Wearable Systems and Applications - WearSys '15; ACM Press: Florence, Italy, 2015; pp. 53–54.
104. Nayak, R.; Wang, L.; Padhye, R. Electronic textiles for military personnel. In *Electronic Textiles*; Elsevier, 2015; pp. 239–256 ISBN 978-0-08-100201-8.
105. Shi, J.; Liu, S.; Zhang, L.; Yang, B.; Shu, L.; Yang, Y.; Ren, M.; Wang, Y.; Chen, J.; Chen, W.; et al. Smart Textile-Integrated Microelectronic Systems for Wearable Applications. *Adv. Mater.* **2020**, *32*, 1901958, doi:10.1002/adma.201901958.
106. Scataglini, S.; Andreoni, G.; Truyen, E.; Warnimont, L.; Gallant, J.; Van, D.; di Milano, P. Design of Smart Clothing for Belgian Soldiers through a Preliminary Anthropometric Approach. 6.
107. Cityzen Sciences : Champion Français Du Textile Connecté Available online: https://www.inpi.fr/fr/innovation-la-galerie/talents/citizen-sciences-champion-francais-du-textile-connecte (accessed on 22 December 2020).
108. Shathi, M.A.; Chen, M.; Khoso, N.A.; Rahman, M.T.; Bhattacharjee, B. Graphene Coated Textile Based Highly Flexible and Washable Sports Bra for Human Health Monitoring. *Materials & Design* **2020**, *193*, 108792, doi:10.1016/j.matdes.2020.108792.
109. Jacquard by Google - Adidas Available online: https://atap.google.com/jacquard/products/gmr/ (accessed on 19 March 2021).
110. Nike Adapt. Self-Lacing Shoes Available online: https://www.nike.com/adapt (accessed on 21 December 2020).
111. Sensoria Core Pair Available online: https://store.sensoriafitness.com/sensoria-core-pair/ (accessed on 21 December 2020).
112. T-Shirt Short Sleeve + HRM Available online: https://store.sensoriafitness.com/t-shirt-short-sleeve-hrm/ (accessed on 21 December 2020).
113. Deng, H.-Y.; Cui, Y.-M. The Application of Smart Textiles in the Brand Fashion Design. *MATEC Web of Conferences* **2016**, *61*, 04022, doi:10.1051/matecconf/20166104022.
114. CUTECIRCUIT | Special Projects Available online: https://cutecircuit.com/special-projects/ (accessed on 22 December 2020).

115. Wearable Solar Dress Available online: http://www.paulinevandongen.nl/project/wearable-solar/ (accessed on 22 December 2020).
116. Full Body Haptic Feedback & Motion Capture Tracking VR Suit Available online: https://teslasuit.io/ (accessed on 22 March 2021).
117. Gao, Y.; Yu, L.; Yeo, J.C.; Lim, C.T. Flexible Hybrid Sensors for Health Monitoring: Materials and Mechanisms to Render Wearability. *Adv. Mater.* **2020**, *32*, 1902133, doi:10.1002/adma.201902133.
118. Nag, A.; Mukhopadhyay, S.C.; Kosel, J. Wearable Flexible Sensors: A Review. *IEEE Sensors J.* **2017**, *17*, 3949–3960, doi:10.1109/JSEN.2017.2705700.
119. Bosowski, P.; Hoerr, M.; Mecnika, V.; Gries, T.; Jockenhövel, S. Design and manufacture of textile-based sensors. In *Electronic Textiles*; Elsevier, 2015; pp. 75–107 ISBN 978-0-08-100201-8.
120. Trung, T.Q.; Lee, N.-E. Flexible and Stretchable Physical Sensor Integrated Platforms for Wearable Human-Activity Monitoringand Personal Healthcare. *Adv. Mater.* **2016**, *28*, 4338–4372, doi:10.1002/adma.201504244.
121. Dias, T.; Ratnayake, A. Integration of micro-electronics with yarns for smart textiles. In *Electronic Textiles*; Elsevier, 2015; pp. 109–116 ISBN 978-0-08-100201-8.
122. Waqar, S.; Wang, L.; John, S. Piezoelectric energy harvesting from intelligent textiles. In *Electronic Textiles*; Elsevier, 2015; pp. 173–197 ISBN 978-0-08-100201-8.
123. van den Brand, J.; de Kok, M.; Koetse, M.; Cauwe, M.; Verplancke, R.; Bossuyt, F.; Jablonski, M.; Vanfleteren, J. Flexible and Stretchable Electronics for Wearable Health Devices. *Solid-State Electronics* **2015**, *113*, 116–120, doi:10.1016/j.sse.2015.05.024.
124. Fukuma, N.; Hasumi, E.; Fujiu, K.; Waki, K.; Toyooka, T.; Komuro, I.; Ohe, K. Feasibility of a T-Shirt-Type Wearable Electrocardiography Monitor for Detection of Covert Atrial Fibrillation in Young Healthy Adults. *Sci Rep* **2019**, *9*, 11768, doi:10.1038/s41598-019-48267-1.
125. Hong, Y.J.; Jeong, H.; Cho, K.W.; Lu, N.; Kim, D. Wearable and Implantable Devices for Cardiovascular Healthcare: From Monitoring to Therapy Based on Flexible and Stretchable Electronics. *Adv. Funct. Mater.* **2019**, *29*, 1808247, doi:10.1002/adfm.201808247.
126. Meghrazi, M.A.; Tian, Y.; Mahnam, A.; Bhattachan, P.; Eskandarian, L.; Kakhki, S.T.; Popovic, M.R. Multichannel ECG Recording from Waist Using Textile Sensors. 26.

127. Heo, J.S.; Hossain, M.F.; Kim, I. Challenges in Design and Fabrication of Flexible/Stretchable Carbon- and Textile-Based Wearable Sensors for Health Monitoring: A Critical Review. *Sensors* **2020**, *20*, 3927, doi:10.3390/s20143927.

128. Arquilla, K.; Webb, A.; Anderson, A. Textile Electrocardiogram (ECG) Electrodes for Wearable Health Monitoring. *Sensors* **2020**, *20*, 1013, doi:10.3390/s20041013.

129. Wang, J.; Soltanian, S.; Servati, P.; Ko, F.; Weng, M. A Knitted Wearable Flexible Sensor for Monitoring Breathing Condition. *Journal of Engineered Fibers and Fabrics* **2020**, *15*, 155892502093035, doi:10.1177/1558925020930354.

130. Shahariar, H.; Kim, I.; Bhakta, R.; Jur, J.S. Direct-Write Printing Process of Conductive Paste on Fiber Bulks for Wearable Textile Heaters. *Smart Mater. Struct.* **2020**, *29*, 085018, doi:10.1088/1361-665X/ab8c25.

131. Saleh, S.Md.; Jusob, S.Md.; Harun, F.K.C.; Yuliati, L.; Wicaksono, D.H.B. Optimization of Reduced GO-Based Cotton Electrodes for Wearable Electrocardiography. *IEEE Sensors J.* **2020**, *20*, 7774–7782, doi:10.1109/JSEN.2020.2981262.

132. Tang, Y.; Chang, R.; Zhang, L.; Yan, F.; Ma, H.; Bu, X. Electrode Humidification Design for Artifact Reduction in Capacitive ECG Measurements. *Sensors* **2020**, *20*, 3449, doi:10.3390/s20123449.

133. Fu, Y.; Zhao, J.; Dong, Y.; Wang, X. Dry Electrodes for Human Bioelectrical Signal Monitoring. *Sensors* **2020**, *20*, 3651, doi:10.3390/s20133651.

134. Wang, J.; Lee, S.; Yokota, T.; Jimbo, Y.; Wang, Y.; Nayeem, M.O.G.; Nishinaka, M.; Someya, T. Nanomesh Organic Electrochemical Transistor for Comfortable On-Skin Electrodes with Local Amplifying Function. *ACS Appl. Electron. Mater.* **2020**, *2*, 3601–3609, doi:10.1021/acsaelm.0c00668.

135. Nigusse, A.B.; Malengier, B.; Mengistie, D.A.; Tseghai, G.B.; Van Langenhove, L. Development of Washable Silver Printed Textile Electrodes for Long-Term ECG Monitoring. *Sensors* **2020**, *20*, 6233, doi:10.3390/s20216233.

136. Kim, S.; Lee, S.; Jeong, W. EMG Measurement with Textile-Based Electrodes in Different Electrode Sizes and Clothing Pressures for Smart Clothing Design Optimization. *Polymers* **2020**, *12*, 2406, doi:10.3390/polym12102406.

137. Cao, R.; Pu, X.; Du, X.; Yang, W.; Wang, J.; Guo, H.; Zhao, S.; Yuan, Z.; Zhang, C.; Li, C.; et al. Screen-Printed Washable Electronic Textiles as Self-Powered Touch/Gesture Tribo-Sensors for Intelligent Human–Machine Interaction. *ACS Nano* **2018**, *12*, 5190–5196, doi:10.1021/acsnano.8b02477.

138. Sliz, R.; Huttunen, O.-H.; Jansson, E.; Kemppainen, J.; Schroderus, J.; Kurkinen, M.; Fabritius, T. Reliability of R2R-Printed, Flexible Electrodes for e-Clothing Applications. *npj Flex Electron* **2020**, *4*, 12, doi:10.1038/s41528-020-0076-y.
139. Qureshi, Y.; Tarfaoui, M.; Lafdi, K.; Lafdi, K. A Flexible Strain Sensor Design Based on Ny-6 Yarn Coated with Ag Nanoparticles for Real Time Strain Monitoring Application. 5.
140. Zhao, X.; Hua, Q.; Yu, R.; Zhang, Y.; Pan, C. Flexible, Stretchable and Wearable Multifunctional Sensor Array as Artificial Electronic Skin for Static and Dynamic Strain Mapping. *Adv. Electron. Mater.* **2015**, *1*, 1500142, doi:10.1002/aelm.201500142.
141. Zhang, X.; Zhong, Y. A Silver/Silver Chloride Woven Electrode with Convex Based on Electrical Impedance Tomography. *The Journal of The Textile Institute* **2020**, 1–13, doi:10.1080/00405000.2020.1800926.
142. Islam, G.M.N.; Ali, A.; Collie, S. Textile Sensors for Wearable Applications: A Comprehensive Review. *Cellulose* **2020**, *27*, 6103–6131, doi:10.1007/s10570-020-03215-5.
143. Tseghai, G.B.; Malengier, B.; Fante, K.A.; Nigusse, A.B.; Langenhove, L.V. Integration of Conductive Materials with Textile Structures, an Overview. **2020**, 28.
144. Jin, H.; Matsuhisa, N.; Lee, S.; Abbas, M.; Yokota, T.; Someya, T. Enhancing the Performance of Stretchable Conductors for E-Textiles by Controlled Ink Permeation. *Adv. Mater.* **2017**, *29*, 1605848, doi:10.1002/adma.201605848.
145. Ryan, J.D.; Mengistie, D.A.; Gabrielsson, R.; Lund, A.; Müller, C. Machine-Washable PEDOT:PSS Dyed Silk Yarns for Electronic Textiles. *ACS Appl. Mater. Interfaces* **2017**, *9*, 9045–9050, doi:10.1021/acsami.7b00530.
146. Yu, X. Piezoelectric Materials and Devices Based Flexible Bio-integrated Electronics. In *Flexible and Wearable Electronics for Smart Clothing*; Wang, G., Hou, C., Wang, H., Eds.; Wiley, 2020; pp. 237–251 ISBN 978-3-527-34534-2.
147. Logothetis, I.; Vatansever Bayramol, D.; Gil, I.; Dabnichki, P.; Pirogova, E. Evaluating Silver-Plated Nylon (Ag/PA66) e-Textiles for Bioelectrical Impedance Analysis (BIA) Application. *Meas. Sci. Technol.* **2020**, *31*, 075101, doi:10.1088/1361-6501/ab78c3.
148. Ig Mo Koo; Kwangmok Jung; Ja Choon Koo; Jae-Do Nam; Young Kwan Lee; Hyouk Ryeol Choi Development of Soft-Actuator-Based Wearable Tactile Display. *IEEE Trans. Robot.* **2008**, *24*, 549–558, doi:10.1109/TRO.2008.921561.

149. Afroj, S.; Tan, S.; Abdelkader, A.M.; Novoselov, K.S.; Karim, N. Highly Conductive, Scalable, and Machine Washable Graphene-Based E-Textiles for Multifunctional Wearable Electronic Applications. *Adv. Funct. Mater.* **2020**, *30*, 2000293, doi:10.1002/adfm.202000293.
150. Daňová, R.; Olejnik, R.; Slobodian, P.; Matyas, J. The Piezoresistive Highly Elastic Sensor Based on Carbon Nanotubes for the Detection of Breath. *Polymers* **2020**, *12*, 713, doi:10.3390/polym12030713.
151. Wang, Z.; Volakis, J.L.; Kiourti, A. Embroidered antennas for communication systems. In *Electronic Textiles*; Elsevier, 2015; pp. 201–237 ISBN 978-0-08-100201-8.
152. Kellomäki, T.; Virkki, J.; Merilampi, S.; Ukkonen, L. Towards Washable Wearable Antennas: A Comparison of Coating Materials for Screen-Printed Textile-Based UHF RFID Tags. *International Journal of Antennas and Propagation* **2012**, *2012*, 1–11, doi:10.1155/2012/476570.
153. *Innovation in Wearable and Flexible Antennas*; Khaleel, H.R., Ed.; Wit Press: Southampton, UK ; Billerica, MA, 2015; ISBN 978-1-84564-986-9.
154. Garnier, B.; Mariage, P.; Rault, F.; Cochrane, C.; Koncar, V. Textile NFC Antenna for Power and Data Transmission across Clothes. *Smart Mater. Struct.* **2020**, *29*, 085017, doi:10.1088/1361-665X/ab8a6d.
155. Lee, J.H.; Dzagbletey, P.A.; Jang, M.; Chung, J.-Y.; So, J.-H. Flat Yarn Fabric Substrates for Screen-Printed Conductive Textiles. *Adv. Eng. Mater.* **2020**, *22*, 2000722, doi:10.1002/adem.202000722.
156. Guibert, M.; Massicart, A.; Chen, X.; He, H.; Torres, J.; Ukkonen, L.; Virkki, J. Washing Reliability of Painted, Embroidered, and Electro-Textile Wearable RFID Tags. In Proceedings of the 2017 Progress in Electromagnetics Research Symposium - Fall (PIERS - FALL); IEEE: Singapore, November 2017; pp. 828–831.
157. Kazani, I.; Scarpello, M.L.; Hertleer, C.; Rogier, H.; de Mey, G.; Guxho, G.; Van Langenhove, L. Washable Screen Printed Textile Antennas. *AST* **2012**, *80*, 118–122, doi:10.4028/www.scientific.net/AST.80.118.
158. Liu, Z.; Li, H.; Shi, B.; Fan, Y.; Wang, Z.L.; Li, Z. Wearable and Implantable Triboelectric Nanogenerators. *Adv. Funct. Mater.* **2019**, *29*, 1808820, doi:10.1002/adfm.201808820.
159. Weng, W.; Chen, P.; He, S.; Sun, X.; Peng, H. Smart Electronic Textiles. *Angew. Chem. Int. Ed.* **2016**, *55*, 6140–6169, doi:10.1002/anie.201507333.

160. Wilson, J.I.B.; Mather, R.R. Photovoltaic energy harvesting for intelligent textiles. In *Electronic Textiles*; Elsevier, 2015; pp. 155–171 ISBN 978-0-08-100201-8.
161. Wu, H.; Huang, Y.; Xu, F.; Duan, Y.; Yin, Z. Energy Harvesters for Wearable and Stretchable Electronics: From Flexibility to Stretchability. *Adv. Mater.* **2016**, *28*, 9881–9919, doi:10.1002/adma.201602251.
162. Zopf, S.F.; Manser, M. Screen-Printed Military Textiles for Wearable Energy Storage. *Journal of Engineered Fibers and Fabrics* **2016**, *11*, 155892501601100, doi:10.1177/155892501601100303.
163. Li, Y.; Yong, S.; Hillier, N.; Arumugam, S.; Beeby, S. Screen Printed Flexible Water Activated Battery on Woven Cotton Textile as a Power Supply for E-Textile Applications. *IEEE Access* **2020**, *8*, 206958–206965, doi:10.1109/ACCESS.2020.3038157.
164. Stoppa, M.; Chiolerio, A. Wearable Electronics and Smart Textiles: A Critical Review. *Sensors* **2014**, *14*, 11957–11992, doi:10.3390/s140711957.
165. IDTechEx Research Available online: https://printpackmea.com/2020/08/24/future-opportunities-for-thin-film-flexible-and-printed-batteries/.
166. Ismar, E.; Tao, X.; Rault, F.; Dassonville, F.; Cochrane, C. Towards Embroidered Circuit Board From Conductive Yarns for E-Textiles. **2020**, *8*, 9.
167. Das, S.C.; Paul, D.; Hasan, S.M.; Chowdhury, N.; Nizam, E.H.; Student, M. Smart Textiles- New Possibilities in Textile Engineering. 7.
168. Chow, P.C.Y.; Someya, T. Organic Photodetectors for Next-Generation Wearable Electronics. *Adv. Mater.* **2020**, *32*, 1902045, doi:10.1002/adma.201902045.
169. Ma, Y.; Zhang, Y.; Cai, S.; Han, Z.; Liu, X.; Wang, F.; Cao, Y.; Wang, Z.; Li, H.; Chen, Y.; et al. Flexible Hybrid Electronics for Digital Healthcare. *Adv. Mater.* **2020**, *32*, 1902062, doi:10.1002/adma.201902062.
170. Wang, B.; Facchetti, A. Materials and Processes for Stretchable and Wearable e-Textile Devices. In *Flexible and Wearable Electronics for Smart Clothing*; Wang, G., Hou, C., Wang, H., Eds.; Wiley, 2020; pp. 305–334 ISBN 978-3-527-34534-2.
171. Buechley, L.; Eisenberg, M. Fabric PCBs, Electronic Sequins, and Socket Buttons: Techniques for e-Textile Craft. *Pers Ubiquit Comput* **2009**, *13*, 133–150, doi:10.1007/s00779-007-0181-0.
172. Hardy, D.A.; Rahemtulla, Z.; Satharasinghe, A.; Shahidi, A.; Oliveira, C.; Anastasopoulos, I.; Nashed, M.N.; Kgatuke, M.; Komolafe, A.; Torah, R.; et al. Wash Testing of Electronic Yarn. *Materials* **2020**, *13*, 1228, doi:10.3390/ma13051228.

173. Cherenack, K.; Zysset, C.; Kinkeldei, T.; Münzenrieder, N.; Tröster, G. Woven Electronic Fibers with Sensing and Display Functions for Smart Textiles. *Adv. Mater.* **2010**, *22*, 5178–5182, doi:10.1002/adma.201002159.

174. Locher, I.; Troster, G. Fundamental Building Blocks for Circuits on Textiles. *IEEE Trans. Adv. Packag.* **2007**, *30*, 541–550, doi:10.1109/TADVP.2007.898636.

175. Linz, T.; Kallmayer, C.; Aschenbrenner, R.; Reichl, H. Embroidering Electrical Interconnects with Conductive Yarn for The Integration of Flexible Electronic Modules into Fabric. In Proceedings of the Ninth IEEE International Symposium on Wearable Computers (ISWC'05); IEEE: Osaka, Japan, 2005; pp. 86–91.

176. Linz, T.; von Krshiwoblozki, M.; Walter, H. Novel Packaging Technology for Body Sensor Networks Based on Adhesive Bonding A Low Cost, Mass Producible and High Reliability Solution. In Proceedings of the 2010 International Conference on Body Sensor Networks; IEEE: Singapore, Singapore, June 2010; pp. 308–314.

177. Linz, T.; von Krshiwoblozki, M.; Walter, H.; Foerster, P. Contacting Electronics to Fabric Circuits with Nonconductive Adhesive Bonding. *Journal of The Textile Institute* **2012**, *103*, 1139–1150, doi:10.1080/00405000.2012.664867.

178. Capineri, L. Resistive Sensors with Smart Textiles for Wearable Technology: From Fabrication Processes to Integration with Electronics. *Procedia Engineering* **2014**, *87*, 724–727, doi:10.1016/j.proeng.2014.11.748.

179. Scarpello, M.L.; Kazani, I.; Hertleer, C.; Rogier, H.; Vande Ginste, D. Stability and Efficiency of Screen-Printed Wearable and Washable Antennas. *Antennas Wirel. Propag. Lett.* **2012**, *11*, 838–841, doi:10.1109/LAWP.2012.2207941.

180. Miao, M. Carbon nanotube yarns for electronic textiles. In *Electronic Textiles*; Elsevier, 2015; pp. 55–72 ISBN 978-0-08-100201-8.

181. de Vries, H.; Peerlings, R. Predicting Conducting Yarn Failure in Woven Electronic Textiles. *Microelectronics Reliability* **2014**, *54*, 2956–2960, doi:10.1016/j.microrel.2014.07.008.

182. Paul, G.; Torah, R.; Yang, K.; Beeby, S.; Tudor, J. An Investigation into the Durability of Screen-Printed Conductive Tracks on Textiles. *Meas. Sci. Technol.* **2014**, *25*, 025006, doi:10.1088/0957-0233/25/2/025006.

183. Zeagler, C.; Gilliland, S.; Audy, S.; Starner, T. Can i Wash It?: The Effect of Washing Conductive Materials Usedin Making Textile Based Wearable Electronic Interfaces. In Proceedings of the Proceedings of the 17th annual international symposium on

International symposium on wearable computers - ISWC '13; ACM Press: Zurich, Switzerland, 2013; p. 143.

184. Hughes-Riley, T.; Dias, T.; Cork, C. A Historical Review of the Development of Electronic Textiles. *Fibers* **2018**, *6*, 34, doi:10.3390/fib6020034.

185. Lund, A.; van der Velden, N.M.; Persson, N.-K.; Hamedi, M.M.; Müller, C. Electrically Conducting Fibres for E-Textiles: An Open Playground for Conjugated Polymers and Carbon Nanomaterials. *Materials Science and Engineering: R: Reports* **2018**, *126*, 1–29, doi:10.1016/j.mser.2018.03.001.

186. Wilson; Laing Fabrics and Garments as Sensors: A Research Update. *Sensors* **2019**, *19*, 3570, doi:10.3390/s19163570.

187. Hwang, B.; Lund, A.; Tian, Y.; Darabi, S.; Müller, C. Machine-Washable Conductive Silk Yarns with a Composite Coating of Ag Nanowires and PEDOT:PSS. *ACS Appl. Mater. Interfaces* **2020**, *12*, 27537–27544, doi:10.1021/acsami.0c04316.

188. Ismar, E.; Zaman, S. uz; Tao, X.; Cochrane, C.; Koncar, V. Effect of Water and Chemical Stresses on the Silver Coated Polyamide Yarns. *Fibers and Polymers* **2019**, *20*, 2604–2610, doi:10.1007/s12221-019-9266-4.

189. uz Zaman, S.; Tao, X.; Cochrane, C.; Koncar, V. Launderability of Conductive Polymer Yarns Used for Connections of E-Textile Modules: Mechanical Stresses. *Fibers and Polymers* **2019**, *20*, 2355–2366, doi:10.1007/s12221-019-9325-x.

190. Rotzler, S.; Kallmayer, C.; Dils, C.; von Krshiwoblozki, M.; Bauer, U.; Schneider-Ramelow, M. Improving the Washability of Smart Textiles: Influence of Different Washing Conditions on Textile Integrated Conductor Tracks. *The Journal of The Textile Institute* **2020**, 1–12, doi:10.1080/00405000.2020.1729056.

191. Kazani, I.; De Mey, G.; Klepacko, R.; Hertleer, C.; Guxho, G.; Van Langenhove, L.; Napieralski, A. Influence of Dry Cleaning on the Electrical Resistance of Screen Printed Conductors on Textiles. *Autex Research Journal* **2016**, *16*, 146–153, doi:10.1515/aut-2015-0019.

192. Kazani, I.; Declercq, F.; Scarpello, M.L.; Hertleer, C.; Rogier, H.; Vande Ginste, D.; De Mey, G.; Guxho, G.; Van Langenhove, L. Performance Study of Screen-Printed Textile Antennas after Repeated Washing. *Autex Research Journal* **2014**, *14*, 47–54, doi:10.2478/v10304-012-0049-x.

193. Salavagione, H.J.; Shuttleworth, P.S.; Fernández-Blázquez, J.P.; Ellis, G.J.; Gómez-Fatou, M.A. Scalable Graphene-Based Nanocomposite Coatings for Flexible and

Washable Conductive Textiles. *Carbon* **2020**, *167*, 495–503, doi:10.1016/j.carbon.2020.05.108.

194. Liang, A.; Stewart, R.; Freire, R.; Bryan-Kinns, N. Effect of Bonding and Washing on Electronic Textile Stretch Sensor Properties. In Proceedings of the Proceedings of the 2019 ACM International Joint Conference on Pervasive and Ubiquitous Computing and Proceedings of the 2019 ACM International Symposium on Wearable Computers - UbiComp/ISWC ’19; ACM Press: London, United Kingdom, 2019; pp. 121–124.
195. Gaubert, V.; Gidik, H.; Bodart, N.; Koncar, V. Investigating the Impact of Washing Cycles on Silver-Plated Textile Electrodes: A Complete Study. *Sensors* **2020**, *20*, 1739, doi:10.3390/s20061739.
196. Ojstršek, A.; Gorgieva, S. Tailoring of Durable Conductive and UV-Shielding Properties on Cotton and Polyester Fabrics by PEDOT:PSS Screen-Printing. *Polymers* **2020**, *12*, 2356, doi:10.3390/polym12102356.
197. Schwarz, A.; Kazani, I.; Cuny, L.; Hertleer, C.; Ghekiere, F.; De Clercq, G.; De Mey, G.; Van Langenhove, L. Electro-Conductive and Elastic Hybrid Yarns – The Effects of Stretching, Cyclic Straining and Washing on Their Electro-Conductive Properties. *Materials & Design* **2011**, *32*, 4247–4256, doi:10.1016/j.matdes.2011.04.021.

3. Materials and Methods

Introduction

The early-stage e-textile products are yet far from being integrated into a comprehensive Internet-of-Things infrastructure, with standard protocols for secure data access from/to the cloud and as platforms for smart textiles. A lack of the possibility exists, for both the users and development communities, to build innovative solutions by integrating them with new functionalities, still guaranteeing the elevated level of security and safety that is essential to secure user acceptance. From that perspective, there is still room for improvement to build an entirely new industry of smart e-textiles. It will constitute the future IoT nodes for wearable electronics, smart and communicating composite parts, and integrate fully with existing IoT infrastructures, standardized interfaces, and open tools for application developers. Solving this dilemma and unlocking the IoT of smart wearable e-textiles and smart technical textiles is exactly the future vision. Once this is done and validated in the use-case scenarios that may be envisaged, the market opportunity seems enormous under the condition that all new exciting smart textile connected devices are reliable and washable, if necessary.

This study is designed first to understand the different types of washing processes for home laundry and then to finalize the effect of different washing cycles on smart textile components in terms of their conductivity. The second part is to co-relate available textile testing methods with the washability behavior of smart textile components. Preparing the samples repeatedly and destroying them in the washing is a difficult task and not budget-friendly. Therefore, there should be a better way to understand washing cycles, separate different washing factors, and co-relate them with available testing methods. As a result, we can predict some statements that specific smart textiles will work up to a certain number of washing cycles.

Many researchers had worked on e-textile standards. The previous chapter explained the usage of available standards by various groups according to their local requirements and how to follow these standards. They claimed the washability and reliability of their prototypes with different washing standards and the various washing cycles according to their availability. For example, some of them can state the product reliability based on some specific standard, but it may not be a good nom to follow for others. As those standards are not designed for e-textile systems, their abusive adoption for e-textile systems may raise questions regarding market adaptability issues. The need for well-developed standards or procedures is essential to produce reliable e-textile systems acceptable for customers worldwide.

3.1 Plan of experiments

Different experiments were performed on various e-textile components depending on the component requirements. Table 3.1 and Figure 3.1 explain in detail information about these experiments. Experimental work is divided into three main portions: washing programs analysis, washing actions analysis, and e-textile system components damage analysis. In the first portion of the experiments, six different washing programs available in the household washing machine were investigated using their running time, stop time, and high-speed tumbling time. Different washing stresses experienced in the process were also studied. In the second phase, various washing actions undergo in the washing machines were investigated using the accelerometer placed in the washing machine. In the last portion, various e-textile system components were examined for washing stresses triggered during the washing process. Finally, alternate available test methods were experimented on the e-textile systems to predict the washing stress damages without actually washing the products.

Table 3.1. Experiment plan

Washing program analysis					
Silk washing	*Express* washing	*Wool* washing	*Delicate* washing	*Delicate short* washing	*Cotton normal* wash

Washing actions analysis with an accelerometer		
Low-speed action	High-speed action	Resting (stop) action

E-textile system damage analysis							
Type of Component	*Silk* washing	*Express* washing	Martindale Abrasion	Pilling box	Bending test	Water test	Detergent test
Transmission lines	✓	✓	✓	✓	×	✓	✓
Skin electrode	✓	✓	✓	✓	×	✓	✓
Flexible modules	✓	✓	×	×	✓	✓	✓
Antennas	✓	✓	✓	✓	×	✓	✓

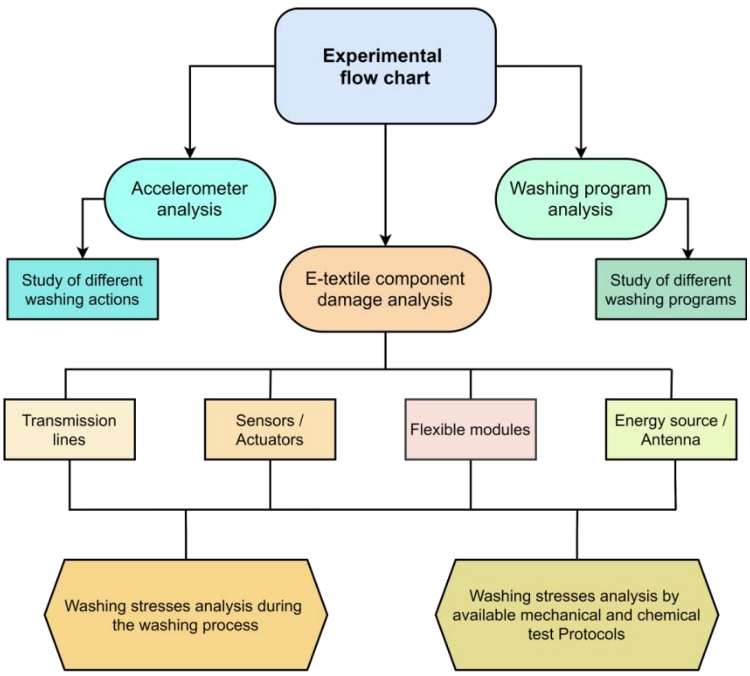

Figure 3.1. Details of experimental work

3.2 Washing Analysis

Washing analysis is critical to talk about before discussing the washing standardization. It is essential to realize the wash process and to understand what is going on. Washing factors can be divided into washing parameters, washing stresses, and post washing processes. Figure 3.2 shortlists these washing factors. They are explained in detail in the following discussion, and complete washing analysis is presented in Figure 3.3.

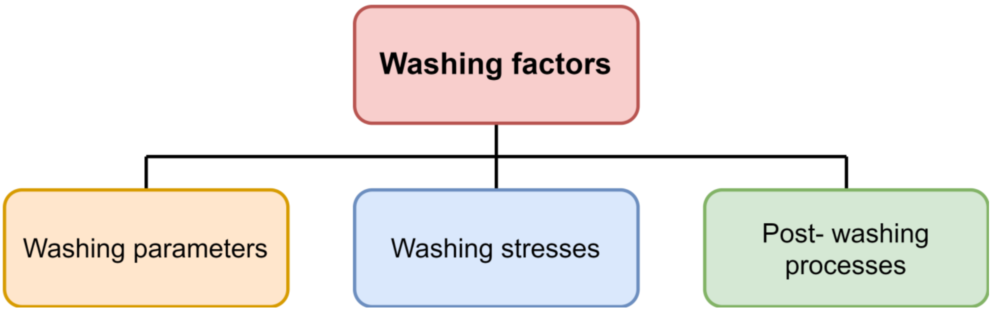

Figure 3.2. Washing factors decomposition

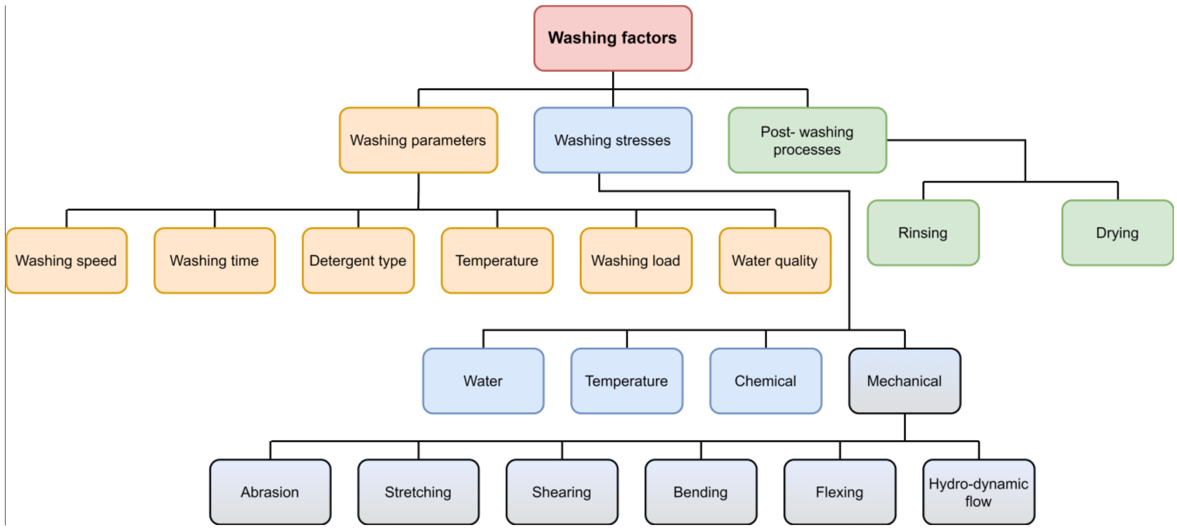

Figure 3.3. Detailed washing factors analyses

3.2.1 Washing parameters

During the washing process, some parameters should be decided for the washing process based on the product being washed. Typically, these parameters have a wide range of selections, from minimal values to extreme conditions. They include washing speed, washing time, detergent solution type and quality, the washing temperature, washing load along with the product, and water quality. These parameters are detailed in Figure 3.4.

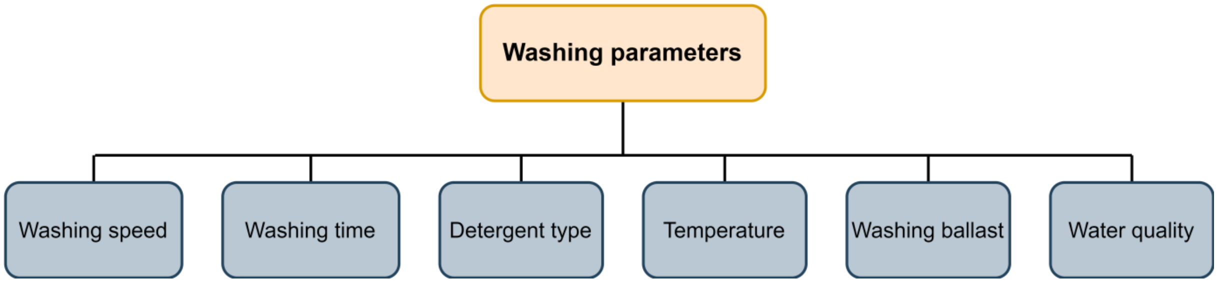

Figure 3.4. Washing parameters

Washing speed and washing time can be adjusted according to the requirements of the product. In recent washing machines, predefined washing programs have different washing speeds and time settings, and in some cases, they can be modified according to the user requirements. Usually, washing speed can be adjusted from 15 RPM (revolutions per minute) to 44 RPM for the washing process and 400 RPM to 1600 RPM for the tumbling process. Similarly, washing time has variation from 30 minutes to 90 minutes and so on.

Detergent type and quantity can be discussed and finalized based on the product type and its possible reaction with the conductive materials present in the product. Special detergents suitable for conductive components of e-textile products may be prepared to avoid any damage during the washing process. Washing temperature, commonly available in the machines, ranges from room temperature (cold) to 90°C. Some sensitive products are usually washed at a maximum of 30°C.

In routine washing, different products are washed together in the washing machines. These wash loads may be of different types and can damage the sensitive product being washed with them. The washing ballast can be divided into mainly three categories, including cotton, synthetic and blended (Figure 3.5). For sensitive e-textile product washing, it can be discussed and decided which ballast type is suitable and possibly used during the home laundering process.

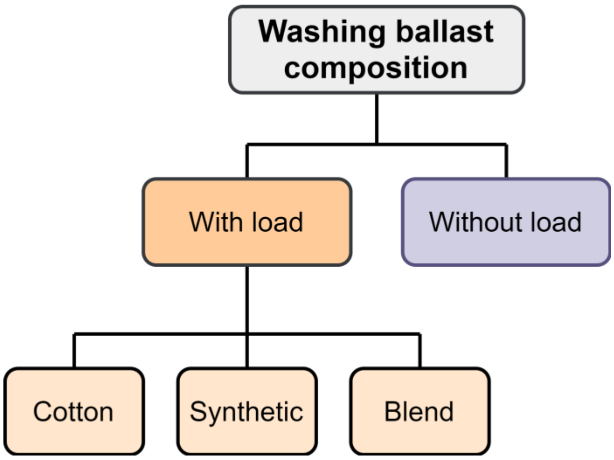

Figure 3.5. Washing ballast

3.2.2 Washing stresses

The washing process can be divided mainly into four phases (soaking, washing, rinsing, and tumbling). In most of the washing options, the soaking phase is categorized as an optional phase, and that may be added to adjust the soaking time or entirely skip this. Each phase has different stresses working in it, and their intensity varies in other parts of the washing process. The main stresses acting during the washing include water, mechanical, chemical, and temperature stresses [1–4].

Among these, mechanical and chemical stresses are the most dangerous and difficult to control according to the people's perception. During the soaking phase, only water and chemical stresses are acting as there are no rotation movements during it. Similarly, there is no chemical stress during the rinsing and tumbling phases because detergent solutions are removed before these phases and rinsing is performed with water only. Temperature stresses are impacted during the washing phase as we have various water temperatures ranges for this phase. Usually, rinsing and soaking are performed with normal tap water temperature. Table 3.2 explains different stresses and their intensities in wash actions.

Table 3.2. Washing stresses in washing process [5]

Phases / Stresses	Soaking	Washing	Rinsing	Tumbling
Water	X	X	X	0
Chemical	X	X	0	0
Mechanical	0	XX	XX	X
Temperature	0	X	0	0

X: Moderate Stress; XX: High Stress; 0: No Stress

3.2.2.1 Water and temperature Stresses

The wash process is ultimately carried out in the water. Water quality itself has an impact on prototypes being washed. Water quality, such as hardness, purity, PH value, is different in different geographic areas, and water molecules and particles present in water can attack the conductive surface or enhance the oxidation process. These probabilities are multiplied in the soaking process because clothes are soaked in water for a long duration and in standstill condition. As a result, the chances of chemical reactions are increased [1].

The temperature of the wash process can also impact the conductive behavior of the e-textiles. The wash process has temperature ranges typically varying from 30°C to 90°C, but these problems can be controlled by washing the e-textiles at room temperature.

3.2.2.2 Chemical stresses

During the wash process, detergent and surfactants are used. Commercially available detergents have different particles and oxidizing agents, added to enhance the stain removing phenomenon. On the other hand, there are also chances that these particles would attack conductive textile surfaces and affect their electrical conductivity. One idea is to develop specially designed and particle-controlled detergents suitable for specific types of e-textiles surfaces to reduce the reaction procedures.

3.2.2.3 Mechanical stresses

Mechanical actions are one of the most important and dangerous stresses working in the wash process. These actions are probably the most damaging on smart textile structures, particularly on conductive yarns and the interconnection between the conductive yarn and the electronic component. Before the washing machine invention, the wash process was carried out by hands, and some harsh mechanical actions were carried out to remove the strains [6]. With the wash machines, these mechanical actions can be controlled by different wash programs. But still, mechanical actions are an essential part of all wash programs and can't be obsoleted from the wash process [2,5,7–9]. In modern wash machines, these mechanical actions are carried out by revolving the textile products around the wash drum at a different speed. Then these products fall at various points during the drum circulations process [2].

These mechanical actions can be divided into different possible mechanical stresses based on the type and speed of washing. These actions may include abrasion actions, stretching, shearing, bending, flexing, soaking, and hydrodynamic flow (Figure 3.6). There is a possibility that all or some of them work simultaneously during the washing process. They are difficult to avoid but can be reduced by adjusting the washing parameters.

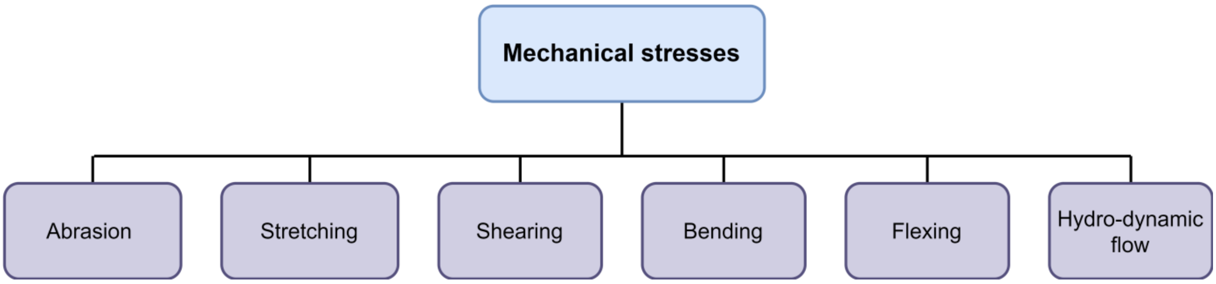

Figure 3.6. Washing stresses in term of mechanical actions performed

3.2.3 Post-washing processes

Post-washing processes include tumbling and drying (Figure 3.7). Drying and tumbling processes are normally optional and they can be excluded or reduced depending on the requirements. We can adjust the time and speed of these processes based on the sensitivity of the washing products. Similarly, numbers of tumbling cycles are also varied in different washing programs and even we can skip this process, but usually, it is considered as an essential part of the washing. On the other side, intensive washing options include two to three tumbling cycles between washing cycles. The post-washing processes can be adjusted accordingly, and they are not as dangerous as the washing processes for sensitive products.

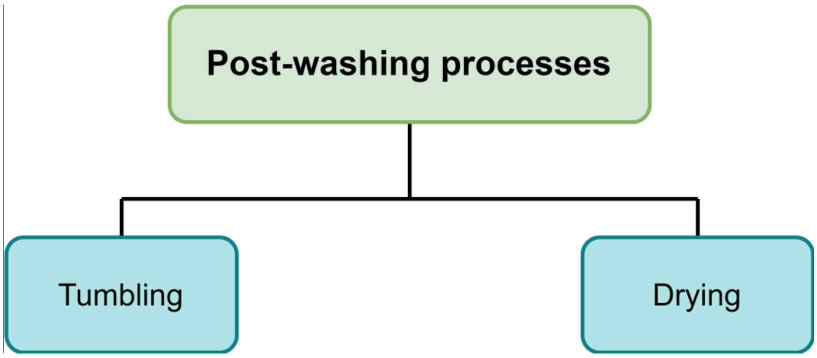

Figure 3.7. Post-washing processes

3.3 Washing programs analysis

The front-load washing machine MIELE W3240 was used in this discussion. It is one of the most commonly available brands in Europe and across the world. All experiments related to the washing are performed on the MIELE W3240 available in our laboratory (Figure 3.8).

Six most commonly used washing programs are performed in these experiments. They are *Cotton, Express, Delicate, Delicate short, Silk,* and *Wool*. Table 3.3 explains the total time duration summary of each cycle performed in this experiment. Time durations of different washing phases and washing actions are shortlisted in this table. Each washing program was performed separately for the complete process using 2 kg of washing load in the machine and following the procedure in the standard test method ISO 6330 with the exception that no detergent was used in this experiment. The temperature was kept at 40°C for all washing programs.

Table 3.3. Washing programs durations [5]

Program	Total Time	Washing speed (RPM)	Duration (MM: SS)								
			Phases								
			Washing		Rinsing			Tumbling/Spinning			Interim Tumbling
			Low-speed	Stop	Low-speed	Stop	High-speed	Low-speed	Stop	High-speed	
Cotton Normal	89:28	38.5...47.5	46:14	06:28	15:16	07:57	05:59	00:28	00:52	06:14	Yes
Delicate	56:27	38.5	14:51	19:31	07:06	11:09	00:00	00:49	00:56	02:05	No
Delicate Short	42:33	38.5	11:27	15:29	04:42	05:57	00:00	00:45	02:00	02:13	No
Express	34:43	38.5	08:39	05:22	06:41	06:10	02:45	00:10	00:10	04:46	Yes
Silk	35:41	15	05:37	17:13	03:18	08:22	00:00	00:00	00:00	01:11	No
Woolen	40:06	15	00:44	17:25	00:34	15:39	01:40	00:00	01:04	03:00	Yes

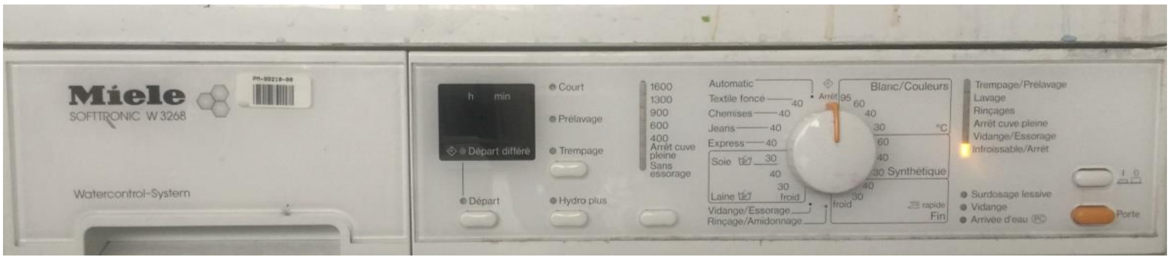

Figure 3.8. Miele W3268 machine washing programs

3.3.1 Video Record Analysis Method

To analyze the duration of each action for different washing programs and to calculate the complete time for each washing phase, video records have been done by using a camera. The duration of each action and phase was calculated by replay the videos (Figure 3.9).

Figure 3.9. Screenshots from washing videos at different washing actions

The washing process consists of three phases (washing, rinsing, and tumbling) based on different drum rotation speeds. We can observe different actions in each phase, such as low-speed rotation, high-speed rotation, and stop (resting time). Figure 3.10 explains the configuration of various washing phases and washing actions performed in the washing cycles. During the low-speed rotation action, the drum speed ranges from 15 RPM, for the *Silk* and Wool program, to 38.5 RPM for the Cotton, Delicate, and Delicate short programs. The high-speed rotation action occurs during the tumbling phase that ranges from 400 to 1600 RPM. In our experiments, we used 400 RPM for all washing programs keeping in mind that e-textile systems are sensitive products compared to the textile products and should be treated gently where possible. Secondly, it was recommended to use 400 RPM for *Silk* washing process, and for better comparison, it was kept the same for all other washing programs. During the washing phase, several low-speed rotation actions with alternate stop actions were observed. The rinsing phase could contain all three actions. The high-speed rotation occurs in the rinsing phase only for Cotton and *Express* programs. In *Silk*, Wool, and Delicate programs, the high-speed rotation action was not observed in the rinsing phase. Finally, the tumbling phase contained the low-speed rotation and high-speed rotation actions.

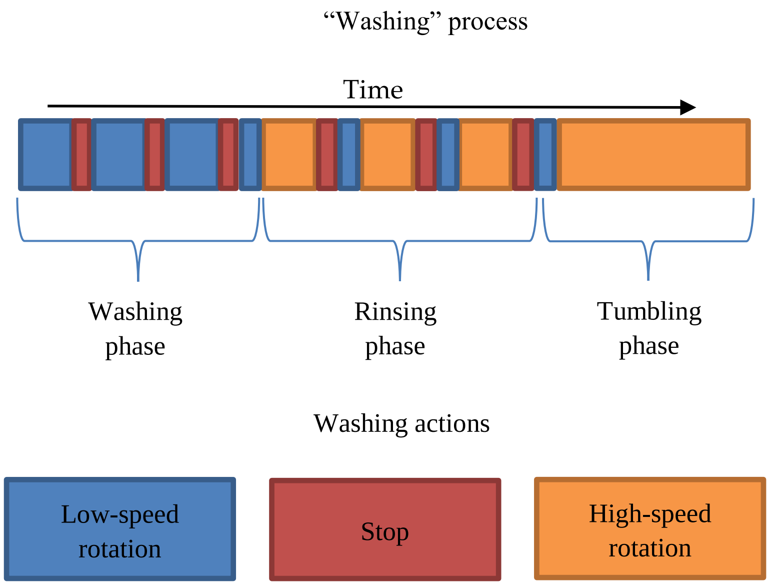

Figure 3.10. Configuration of washing phases and actions

Figure 3.11 shows the duration time analysis of the washing process according to the videos for whole washing cycles. Among these experimental analyses, total washing durations are 89 minutes for the Cotton program, 56 minutes for the Delicate program, 42 minutes for the Delicate short program, 35 minutes for *Express* program, 36 min for the *Silk* program, and 42 minutes for the Wool program. The *Silk* and *Express* programs have the least total washing time, but the Wool program has the least percentage of low-speed rotation action. From the perspective of people's traditional concept, it is considered that a long duration in washing is more dangerous than a short washing duration. However, from these experiments, it is observed that the actual rotation and stop durations should be considered instead of the total washing process time. For example, in comparison with *Silk* and *Express* washing programs, they have almost the same total washing duration, but the percentage of stop (resting) action increases from 34 % to 72 %. Similarly, the Wool program has a whole washing process time of 40 minutes, and the percentage of its stop action is the maximum (85 %) among all programs. The Delicate short program also has a total time of 42 minutes, close to the Wool programs; the percentage of its stop (resting) action is 55%, almost 30 % less compared with the Wool program. When the fabric is in low-/high-speed rotation actions, it remains under the stress of water, chemical, or temperature stresses. But when it is in the stop action, mechanical stresses can be neglected, and overall damages should be reduced.

From the video analysis, it has been concluded that the duration of the low-speed and high-speed rotation actions should be privileged comparing to the duration of the whole washing process. The high-speed rotation action duration percentage is 22 % for the *Express* program and only 3% for the *Silk* program, although their total washing times are almost the same. The Cotton program has the longest total washing process time, but its percentage of high-speed rotation action is about 13 %, less than *Express* wash having the least total washing time.

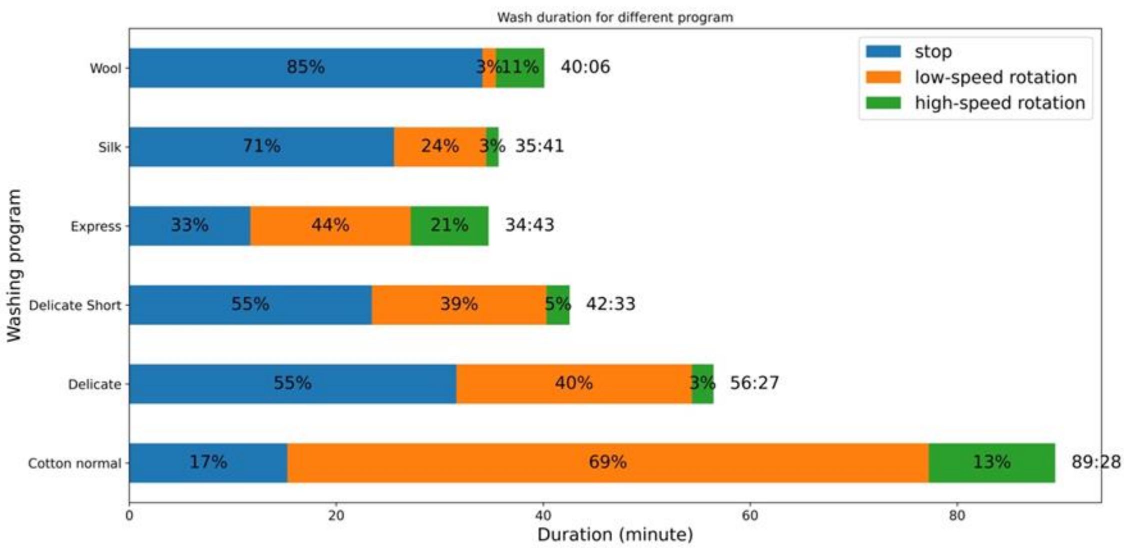

Figure 3.11. Washing time configurations for different washing programs (percentage of total time)

3.4 Accelerometer Analysis method

To investigate mechanical stresses underwent in the e-textile devices, during a washing process, a flexible PCB integrated with an accelerometer (MPU-6050) and Bluetooth communicator (RDF 77101) has been designed and manufactured. It has been sewn onto a piece of cotton fabric. The fabric was then sealed in an airtight plastic envelope to avoid water and chemical damages. The accelerometer records “Proper acceleration” in all three directions (X, Y, Z relative to its coordinate system) in its instantaneous rest frame without any continuous movement problem. The measurement range is ±16 g with a 40 Hz sampling frequency. Acceleration signals were collected and transmitted by Bluetooth protocol. Figure 3.12 explains the circuit diagram. The low-speed rotation speed used for accelerometer analysis was 38 RPM, and high-speed rotation experimented at 400 and 600 RPM separately. The working diagram of this experiment is explained in Figure 3.13.

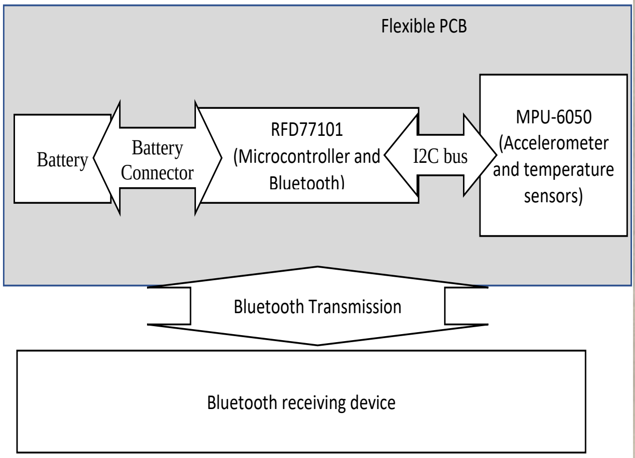

(a)

(b)

Figure 3.12. (a) Accelerometer diagram (b) An accelerometer is sealed in an airtight envelope

Figure 3.13. Working diagram of the accelerometer used for washing analysis

3.5 Samples preparations

Different e-textile components were developed for this study. E-textile systems will vary from complex models to simple ones depending on the requirements. The simplest model containing transmission lines, electrodes, flexible PCBs, and antennas was selected for this study. The material selection was carried out based on the suggestions from different groups in research lab working specifically in these areas. The components details are explained in the following sections.

3.5.1 Connection yarns/ Transmission lines

Three different types of conductive yarns were used in these experiments. These yarns were coded as Type A, Type B, and Type C. In all future discussions, these yarns are labeled accordingly (Table 3.4). Type A yarn was “Statex-Shieldex 117f17 2-ply HC+B” purchased from Statex Produktions+Vertriebs GmbH, Bremen, Germany. It was a two-ply sliver plated polyamide yarn having 17 filaments of 117 dtex in each ply, and the overall yarn diameter was 0.62mm. “Type B” yarn was similar to “Type A” yarn with some modifications in silver coating techniques. It was purchased from Madeira Garnfabrik GmbH, Freiburg, Germany, with the brand name HC-40. The final count for silver-plated yarn was 290 dtex. “Type C” yarn was three-ply yarn but having only one silver-plated ply, and the other two plies were non-conductive polyester filament. The technical name was Amann silver-tech 120, and the final yarn count was 280 dtex.

Table 3.4. Type of conductive yarns used.

Yarn type	Brand name	Company	Resistivity (Ω/m)
Type A yarn	Statex-Shieldex 117f17	Statex Produktions	< 300
Type B yarn	HC-40	Madeira Garnfabrik	< 300
Type C yarn	silver-tech 120	Amann	< 530

In all the experiments, cotton fabric was used as a substrate for these conductive transmission lines. All the yarns were stitched on cotton fabric with a ZSK embroidery machine (ZSK Stickmaschinen GmbH, Krefeld, Germany) (Figure 3.14). These conductive yarns were used as needle yarn, and the normal polyester yarn was used as bobbin/spool yarn during the stitching process. Figure 3.15 explains the stitch composition in terms of bobbin yarn and needle yarn.

Figure 3.14. ZSK embroidery machine

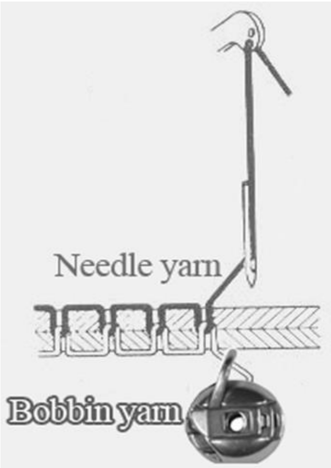

Figure 3.15. Needle yarn and bobbin yarn composition

These yarns were stitched in three different arrangements, including single line stitch, two-line zig-zag stitch, and three-line zig-zag network stitch. The stitch patterns were designed using the software BASE PAC8 provided by ZSK Company (ZSK Stickmaschinen GmbH, Krefeld, Germany). Two and three-line network stitch patterns (Figure 3.16) increase the conductive paths by surface-to-surface cross-contact in between stitched lines. Thus, if one yarn is damaged at any point, still current can pass through other conductive yarns in a zig-zag pattern, thanks to multiple connecting points. The total length (consumption of yarn) of two and the three-line pattern will be more than the single-line pattern. In comparison, a change in linear resistance from original values was used in these experiments. In fact, for 20 cm stitched length, the consumption of conductive yarn was 30, 97, and 153 cm for single, double, and three-line stitch, respectively.

Figure 3.16 explains different stitching techniques used in these experiments.

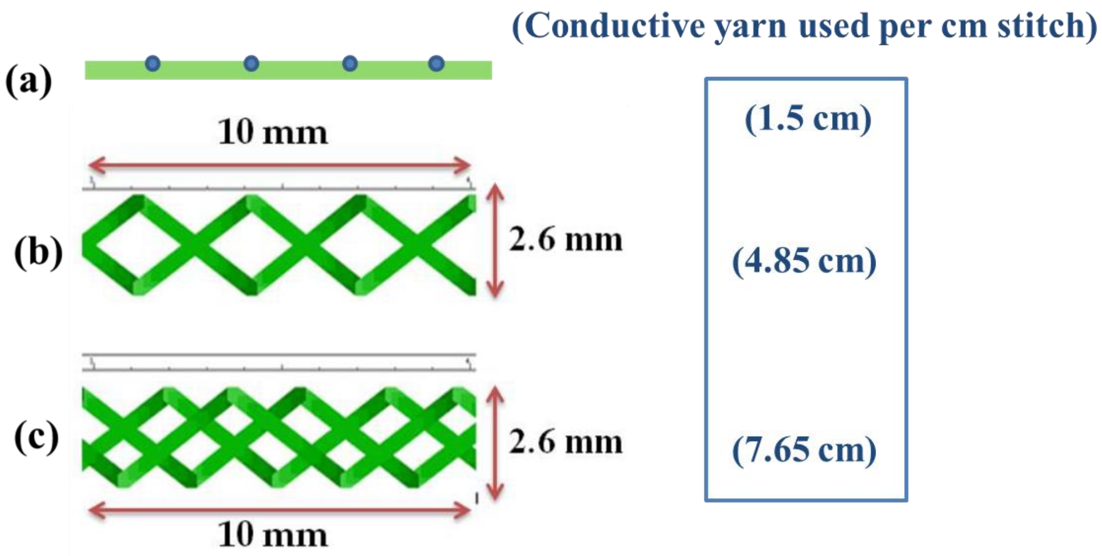

Figure 3.16. Composition of single, two, and three-line stitched transmission lines

In the next step, the transmission lines were protected with two different techniques. TPU (Thermoplastic polyurethane) films were attached to these conductive transmission lines. In another set of samples, an extra layer of embroidered yarn was used to protect the inner conductive tracks. Thermoplastic polyurethane films were purchased from BEMIS, Brigg, United Kingdom. These TPU films were fixed on the samples using a heated press for 20 seconds at 140°C. In a separate set of samples, an extra layer of yarn was stitched over the conductive transmission lines. This layer worked as the bridge and protected the conductive lines from wear and tear during washing and mechanical testing. Figure 3.17 shows the example of transmission lines without protection, with TPU protection, and with embroidered layer protection.

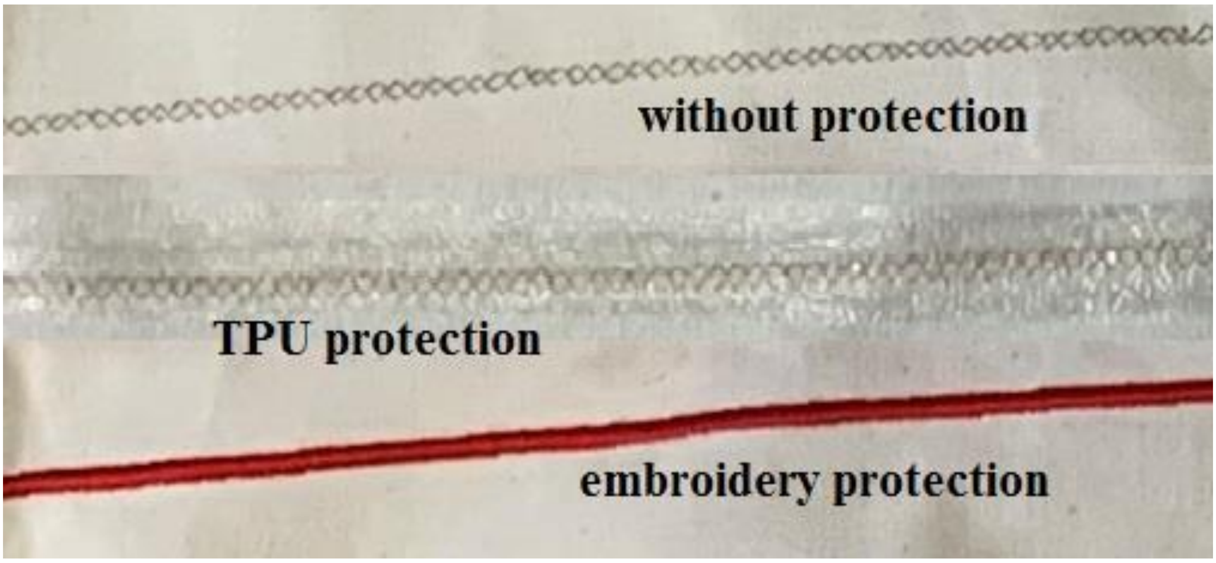

Figure 3.17. Conductive transmission lines without protection, with TPU protection, and with embroidered protection

Both edges of transmission lines were coated with silver paste, and then a snap button was mounted to them, as shown in Figure 3.18. The metallic snap button has negligible electrical resistance. It helped avoid wear and tear from edges during experiments and easy connection with multi-meter for resistance measurements. Silver paste helped to minimize the contact resistance between conductive lines and snap buttons.

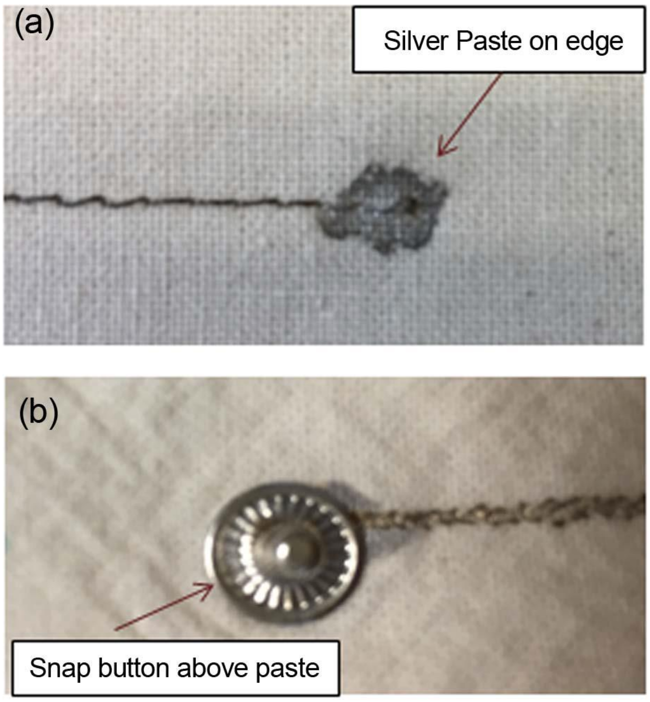

Figure 3.18. Transmission lines (a) silver paste on edge, (b) snap button mounted on the silver paste

Figure 3.19 explains the schematic diagram of transmission lines experiments performed in this study. A separate set of samples were prepared for each type of test, and all transmission lines were stitched on plain cotton fabric.

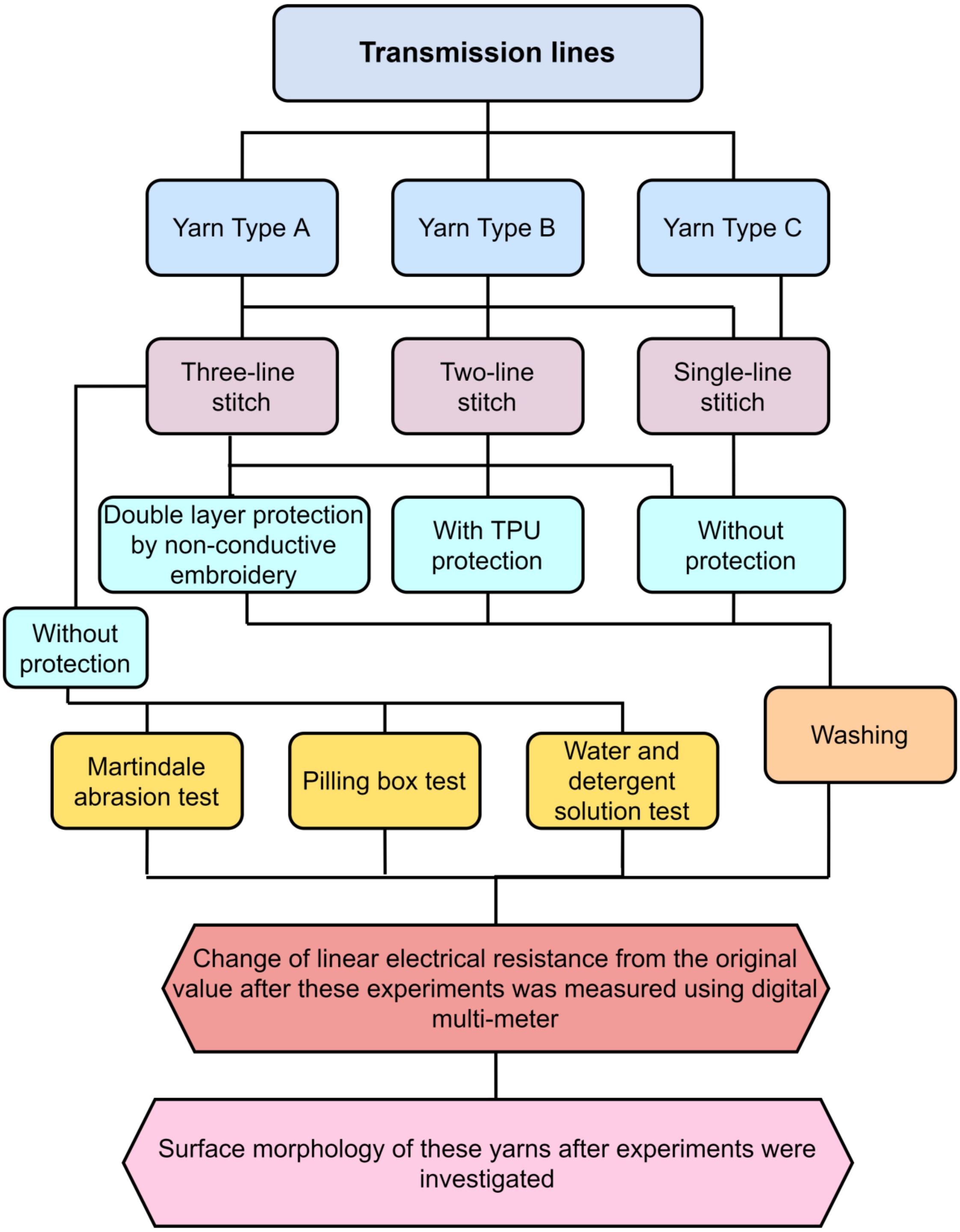

Figure 3.19. Flow chart of experiments for transmission lines

3.5.2 ECG electrodes

Skin dry electrodes were prepared for ECG measurement purposes. Different types of electrodes with various structural properties are used for experiment purposes, and there is no degradation link between them. Their degradation coefficient will differ from each other and should be treated separately for analysis.

The circular shape electrodes were prepared by a double-layer conductive stitch pattern. The circular electrodes were then connected with snap buttons through conductive transmission lines. The transmission lines were designed by a three-line stitch with a protective layer over them. The non-conductive polyester yarn was used for this purpose. The pattern for transmission lines was selected based on the results for different types of transmission lines from previous experiments. Transmission lines were embroidered 3 mm inside the electrode for better electrical connections.

Similarly, a circular connector of 8 mm diameter was embroidered on edge for better electrical transmission through snap buttons. The distance between the ECG electrode and connector was kept 65 mm, and the diameter of the ECG electrode was 30 mm. Figure 3.20 explains the pattern of one ECG electrode. The electrodes were prepared in three electrodes set on the fabric belt for real-time ECG measurement on the human body, as shown in Figure 3.21.

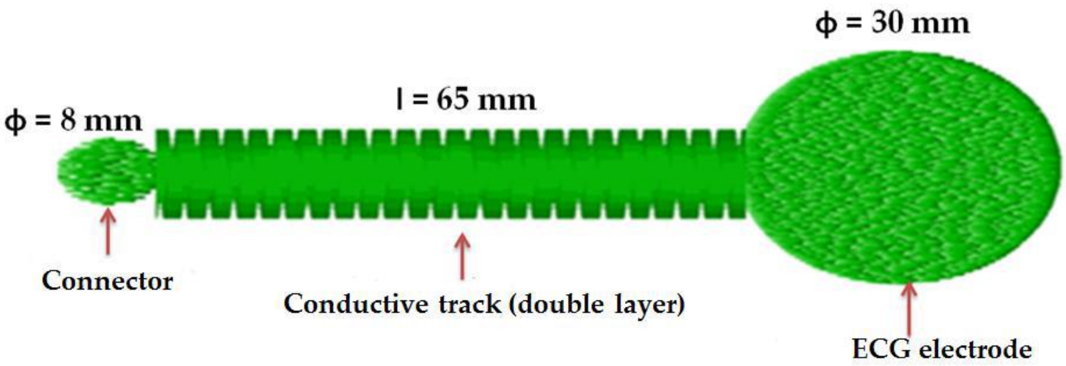

Figure 3.20. Skin-dry electrode pattern [10]

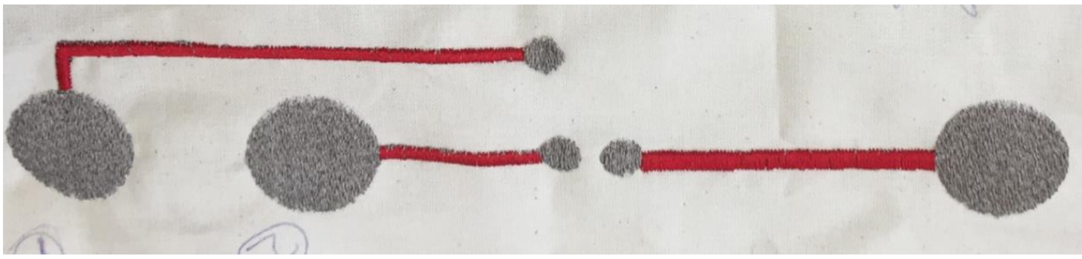

Figure 3.21. Set of three skin electrodes embroidered on cotton fabric belt for ECG measurement

A separate set of electrodes were prepared by conductive fabrics. Four different types of conductive fabrics were used for this purpose. These fabrics include RF shielding Silver fabric (F1), RF shielding Nickel Copper fabric (F2), RF shielding Copper fabric (F3), and silver-plated fabric (F4). Fabrics F1, F2, and F3 were obtained from Faradaydefence LLC, Unites States, and F4 were received from Innovative textile, Italy. Table 3.5 explains the sample coding and type of materials used for these experiments. Fabric samples were cut in rectangular shapes of size 20mm x 60mm and stitched on a plain cotton fabric belt. Each cotton fabric belt consists of three electrodes, and snap buttons were attached on the edge of each electrode.

Table 3.5. List of different materials used for skin-electrode preparation along with sample coding

Sample	Material	Brand	Initial surface resistance (Ω/sq.)	Surface thickness (mm)
E1	Silver-plated Yarn, Embroidered	Shieldex-117f17 HC+B	0.12	1.39
E2	Silver-plated Yarn, Embroidered	Madeira HC-40	0.23	1.40
F1	RF Shielding Silver Fabric	Faradaydefense LLC	0.33	0.28
F2	RF Shielding Nickel Copper Fabric	Faradaydefense LLC	0.04	0.09
F3	RF Shielding Copper Fabric	Faradaydefense LLC	0.04	0.08
F4	Silver-plated Fabric	Innovative textile	1.45	0.5

The samples (E1-E2, and F1-F4) were tested on three different subjects including two males and one female, ages ranging from 25 to 55 years old. Three electrodes were placed on the chest position and all subjects were in the sitting position for at least three minutes before testing. The ECG signals were recorded for 40 seconds and repeated three times. The fabric belt containing the ECG sensors was tightened with the help of an external belt to guarantee proper contact with the human body. However, this ECG testing protocol was not the main focus of the Ph.D. thesis, it has been applied to assess the textile electrodes' robustness upon washing cycles up to 50 and the relationship between the recorded ECG signal quality and the electrode surface resistance.

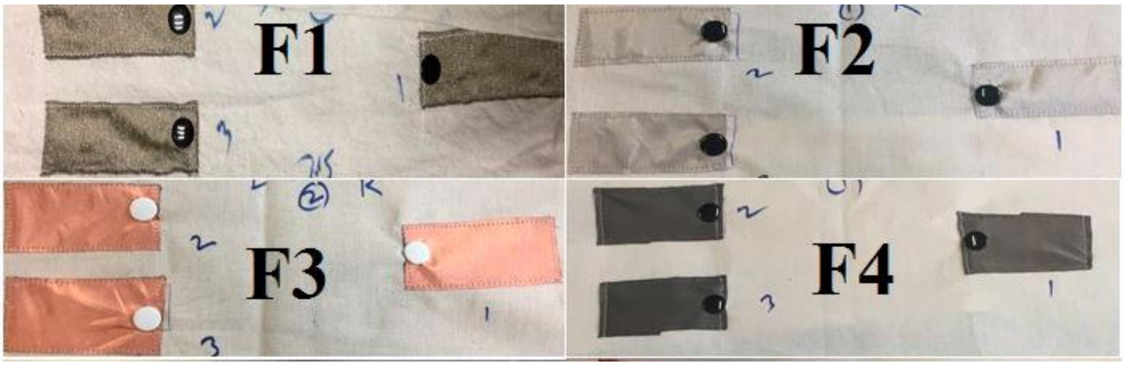

Figure 3.22. Set of three skin electrodes prepared with the pieces of conductive fabrics for ECG measurement

ECG electrodes prepared with four different types of conductive fabric pieces are shown in Figure 3.22. Same as embroidered electrodes, snap buttons are used for proper connection between electrodes and the ECG measuring devices. Flow charts of experiments performed on electrodes are described in Figure 3.23.

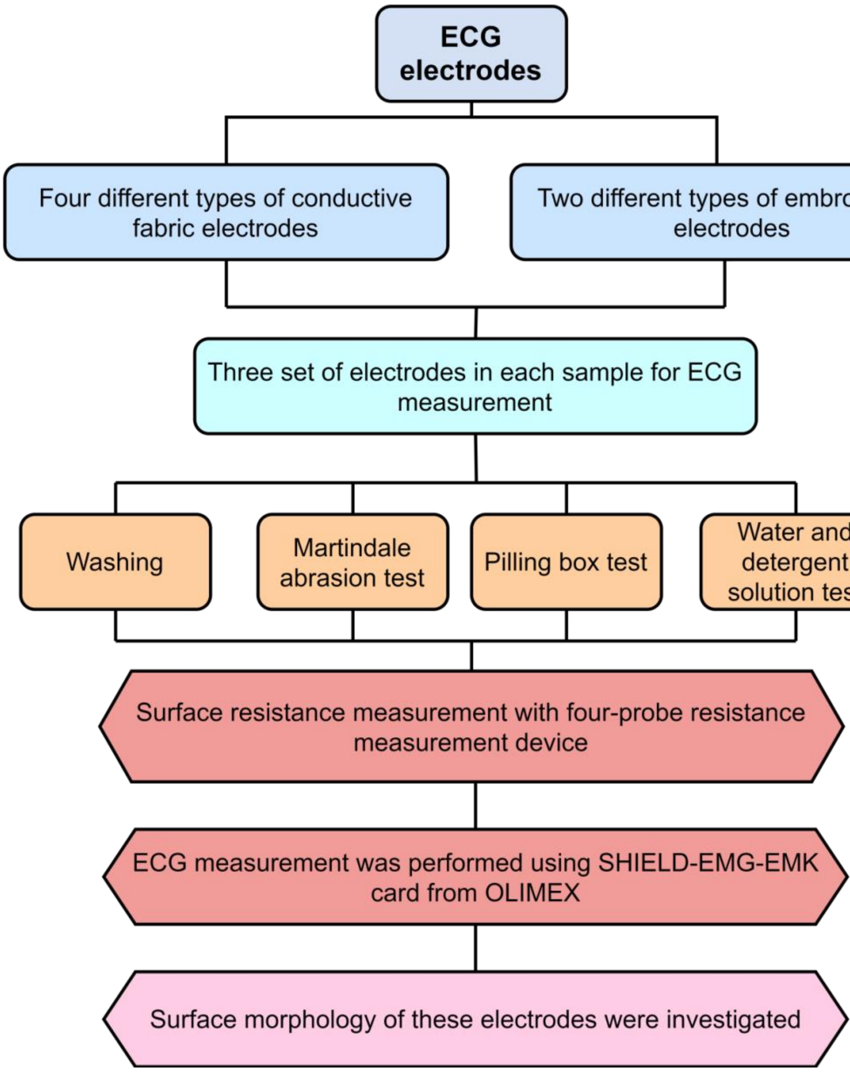

Figure 3.23. Flow chart of experiments for ECG electrodes

3.5.3 The flexible printed circuit board (PCBs)

PCBs were prepared by designing a circuit with tracks of diverse width, and two different types of SMD (surface-mount device) resistances were mounted on these tracks. First of all, circuit designs were prepared using "Kicad software." These designs include tracks of eight different widths including 0.15mm, 0.2mm, 0.25mm, 0.30mm, 0.45mm, 0.60mm, 0.75mm, and 1.00mm (Figure 3.24). SMD resistor 1206 and 0805 sizes were used in these PCBs separately for each track. Two distinct sets of resistances mounted tracks were prepared based on the horizontal and vertical assembling of these SMDs. Eight 1206 SMD resistors mounted horizontally to each track and eight mounted vertically to tracks were prepared.

Similarly, overall, sixteen tracks with SMD resistors 0805 were designed in one set of samples. The defined resistance of these SMD resistors was 5.1Ω. Each SMD resistor has a separate measuring connection pad for resistance measurement.

The PCB designs were printed on PNP (press and peel) blue sheet, purchased from SEEIT SARL, France. Then the positives were transferred from the PNP sheet to a thin copper sheet. A flexible single-face copper sheet of 35µm was obtained from Circuit Imprimé Français (CIF). These sheets were cleaned throughout, and PNP printed sheets were placed on them in the face-to-face direction (Figure 3.25). Transfer of design was carried out by putting them in the heated press for 180 seconds at 170°C.

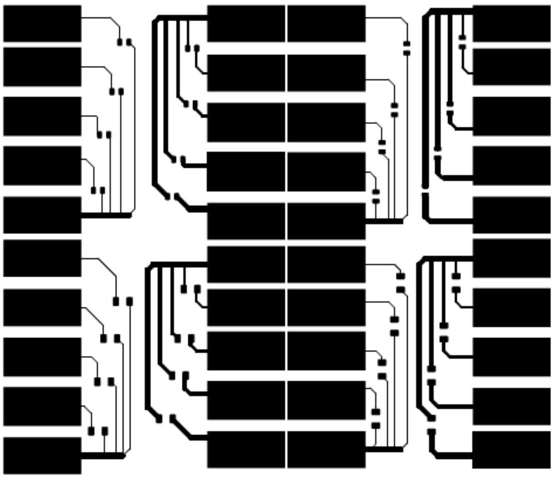

Figure 3.24. Screenshot of PCB design prepared on Kicad software

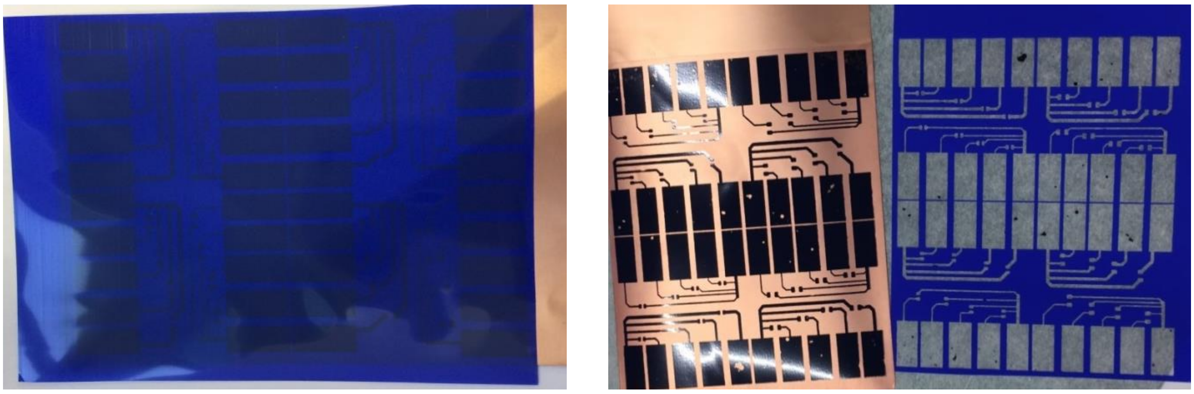

(a) (b)

Figure 3.25. PCB preparation, (a) face to face placement of PNP sheet and copper sheet before the heated press, (b) transfer of design on the copper sheet after heated press

These printed copper sheets were then dipped in a vertical etching tank (Velleman), having a temperature-controlled rod and vacuum pump (Figure 3.26). This tank was filled with Iron Chloride ($FeCl_3$) solution. Copper sheets were dipped in the solution until all copper from the surface was dissolved except protected by the printed design. These sheets were then completely washed and dried.

Figure 3.26. Vertical etching tank

In the next step, SMD resistors were mounted using conductive paste and a heated air pump (Toolcraft). The temperature of heated air was kept at 300°C (Figure 3.27).

(a) (b)

Figure 3.27. (a) Heated air pump, (b) attachment of SMDs in printed circuits

The PCBs were machine washed without any protective measurements and with flexible silicon coating (Bluesil™ TCS 7550, ELKEM) on them. The curing time for silicon was more than 16 hours at room temperature. The two-part silicon was mixed in the 1:1 by weight ratio as recommended by manufacturer. After mixing it with the stirrer, it was placed in the vacuum tank to remove air bubbles from the silicon solution. This practice was performed to avoid holes in the dried silicon after settlement. The silicon solution was poured on the PCBs and then kept in the oven for 4-5 minutes at 80°C. Figure 3.28 shows the silicon solution used in these experiments and the airtight vacuum jar used to remove the air bubbles from the silicon solution.

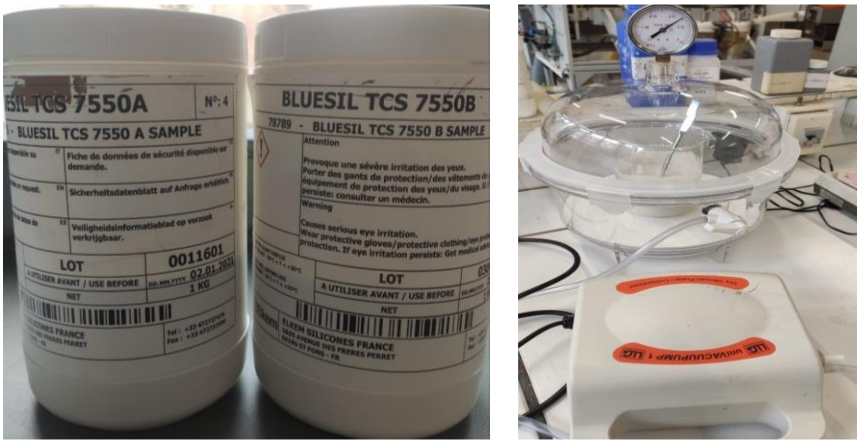

(a) (b)

Figure 3.28. (a) Elkem silicon used for the protective layer, (b) vacuum pump with the airtight jar to remove air bubble from solution

Figure 3.29 shows the set of all samples used in experiments. In one set of samples, silicon protection is applied only on SMDs soldering points. Whereas, in other sets of samples, complete PCBs were covered with 2-3 mm thin silicon layer just keeping connection point for measurement (Figure 3.30). This silicon was used for two purposes, a protective layer, and the adhesive layer. An adhesive layer was used to stick these PCBs on cotton fabric for further experiments.

An overview of PCB samples and experiments performed is explained in Figure 3.31.

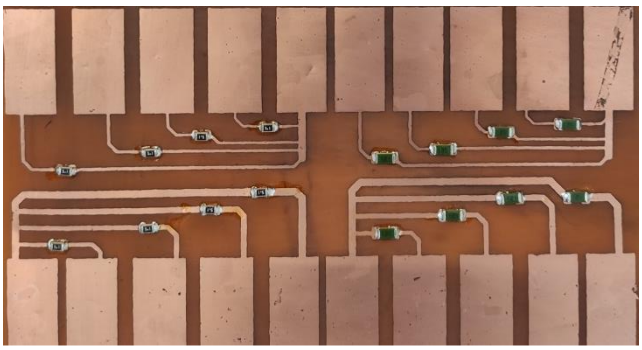

Figure 3.29. Four sets of ready to use PCBs

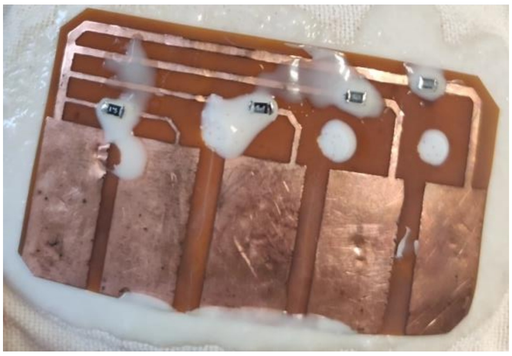

(a)

(b)

Figure 3.30. (a) PCB with SMD resistor protected with silicon, (b) PCB completely protected with a silicon-coated layer

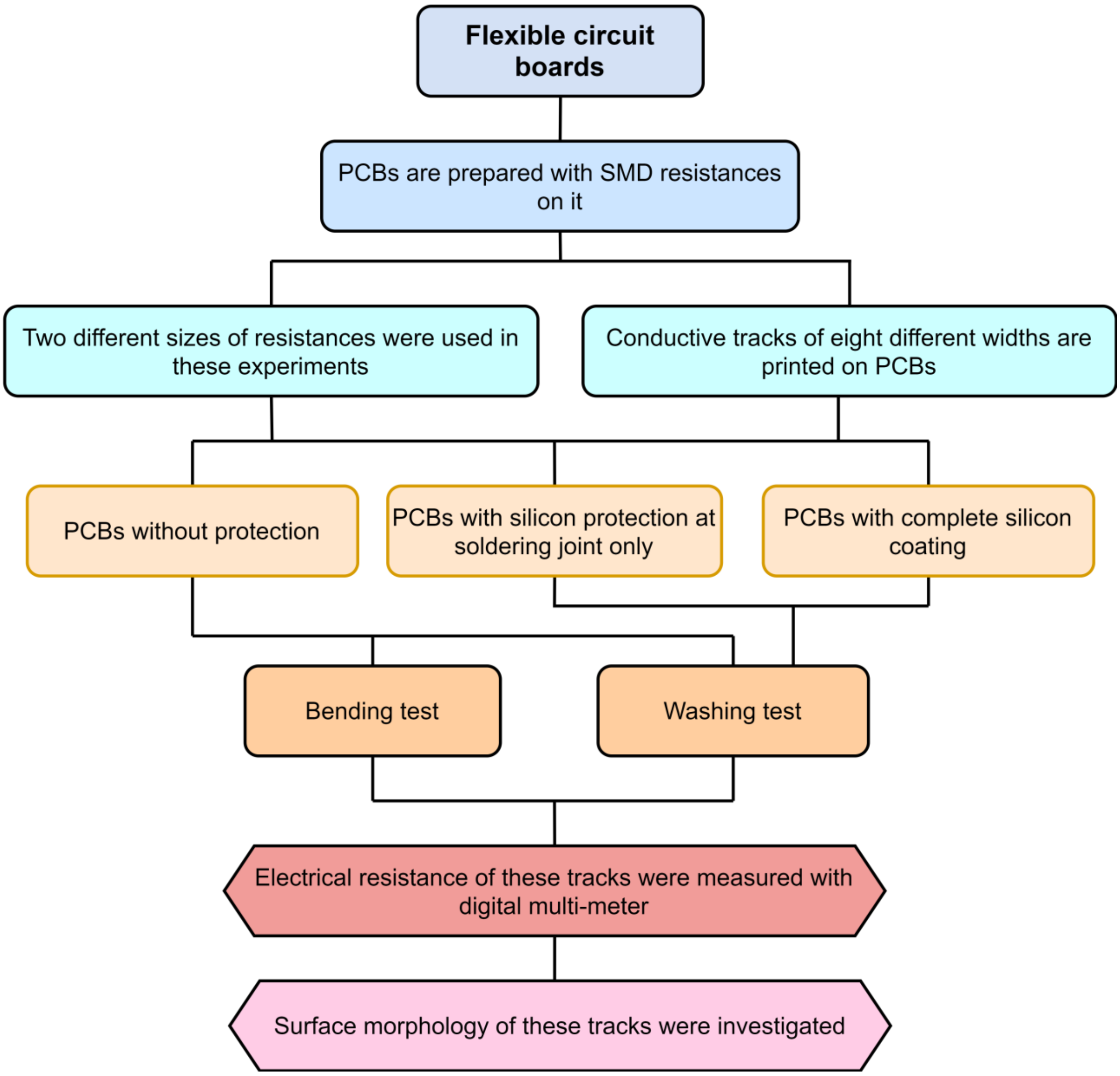

Figure 3.31. Flow chart of experiments for PCBs

3.5.4 Textile antennas

Textile antennas are prepared to provide induction, resistance, and capacity to create the RLC circuit resonant at the target frequency kept at 13.56 MHz (NFC standard). These antennas were composed of 6 circular spirals with a 40 mm outer radius (Figure 3.32). The number of spiral turns and radius directly impact the inductance of the antennas. Different combinations were performed to get resonant frequency at 13.56 MHz, and then finally, 6 circles of yarn with a 40 mm radius were finalized. The antennas were attached with 200 mm long transmission lines. Transmission lines were used to transfer modulated power signals to the terminal component with the help of the SMA connector. The length and width of the transmission lines also impact the overall resonance frequency of the system. The conductive yarn used was Datatrans, from “TIBTECH innovations,” having enameled wires with 30% stretch capacity and linear resistance was 4.2 Ω/m. It was composed of four copper strands that were twisted on PET filaments. The total covering ratio of the conductive part on the core yarn was approximately 42.5%.

The yarns were embroidered on the plain cotton fabric with an embroidery machine, and the resonant frequency of these antennas was measured with the help of an impedance analyzer Agilent 4964A. The following equation was used to adapt the resonance frequency at 13.56 MHz.

$$f_0 = \frac{1}{2\pi\sqrt{L(C_1 + C_2)}}$$

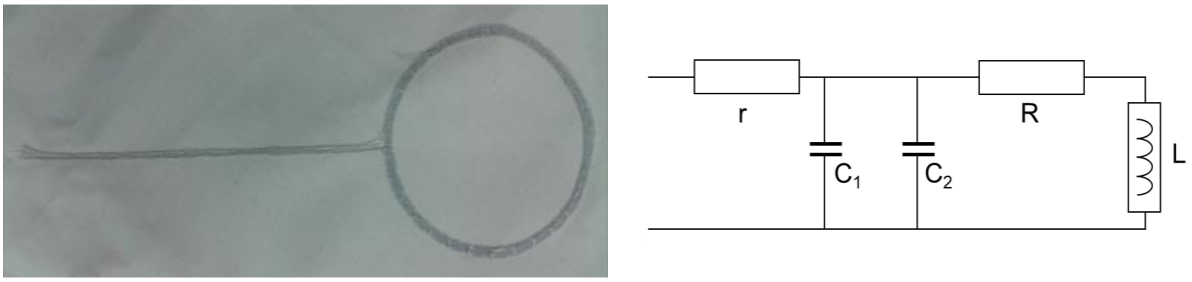

(a) (b)

Figure 3.32. Photography of the textile NFC antenna and (b) its electric diagram

As in the PCBs experiments, the textile antennas were protected with silicone coating on them. Silicon solution was poured on textile antennas, and then they were oven-dried at 80°C for 4-5 minutes. Textile antennas protected with silicon coatings are shown in Figure 3.33. The detailed experimental design of textile antennas is described in Figure 3.34.

Figure 3.33. Silicon protected textile antenna

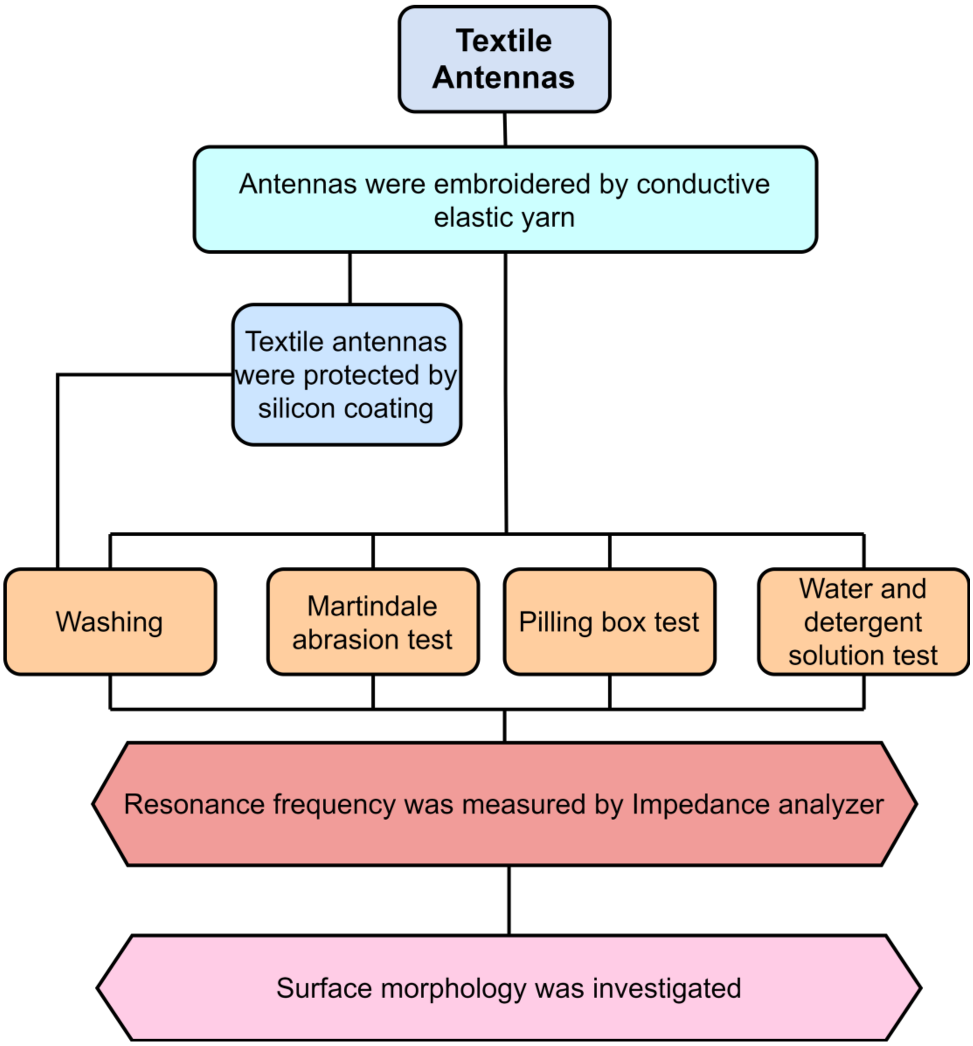

Figure 3.34. Flowchart of textile antenna experiments

3.6 Washing tests

All e-textile components prepared were washed up to 50 washing cycles. Two different washing programs were used on a separate set of samples. The *Silk* washing program and *Express* washing program were used for these experiments based on washing cycle analysis. These experiments were performed in the Miele W3268 washing machine according to the ISO 6330 washing standards. The washing load was 2 kg of cotton fabrics, and the washing temperature was kept at 40°C. “Total Extra” detergent was used in these experiments. A total of 20g of detergent was used in each washing cycle. The quantity of detergent was calculated from ISO 6330 standard, which states that detergent should be used as 4g/L. The detergent composition is shown in Figure 3.35. Table 3.6 shortlists the samples prepared for washing tests in this study.

Table 3.6. List of samples used for washing tests

Type of samples	Total samples	Total readings
Single-line stitched connection yarn Type A	06 Samples	18 Readings
Single-line stitched connection yarn Type B	06 Samples	18 Readings
Single-line stitched connection yarn Type C	06 Samples	18 Readings
Two-line stitched connection yarn Type A	06Samples	18 Readings
Two-line stitched connection yarn Type B	06 Samples	18 Readings
Three-line stitched connection yarn Type A	06 Samples	18 Readings
Three-line stitched connection yarn Type B	06 Samples	18 Readings
Two-line stitched yarn Type A (TPU protected)	06 Samples	18 Readings
Three-line stitched yarn Type A (TPU protected)	06 Samples	18 Readings
Two-line stitched yarn Type B (TPU protected)	06 Samples	18 Readings
Three-line stitched yarn Type B (TPU protected)	06 Samples	18 Readings
Two-line stitched connection yarn Type A (Non-conductive embroidery protection)	06 Samples	18 Readings
Three-line stitched connection yarn Type A (Non-conductive embroidery protection)	06 Samples	18 Readings
Two-line stitched connection yarn Type B (Non-conductive embroidery protection)	06 Samples	18 Readings

Three-line stitched connection yarn Type B (Non-conductive embroidery protection)	06 Samples	18 Readings
ECG electrode F1	06 Samples	24 Readings
ECG electrode F2	06 Samples	24 Readings
ECG electrode F3	06 Samples	24 Readings
ECG electrode F4	06 Samples	24 Readings
ECG electrode E1	06 Samples	24 Readings
ECG electrode E2	06 Samples	24 Readings
PCBs without protection	03 Samples	24 Readings
PCBs with silicon protection on SMD joint	03 Samples	24 Readings
PCBs with silicon protection complete	03 Samples	24 Readings
Textile antenna	04 Samples	04 Readings
Textile antenna (silicon Protected)	04 Samples	04 Readings

Figure 3.35. Detergent composition

3.7 Washing simulation tests

3.7.1 Chemical and water tests

Chemical and water stresses acting on the e-textile products were investigated by putting the samples in water and water detergent solutions for a specific time. Universal hot plate magnetic stirrer IKA by IKAMAG™ was used for these experiments (Figure 3.36). A magnetic stirrer was used to guarantee the same temperature throughout the beaker containing the samples and solutions. The time for these experiments was ranged from 30 min to 72 hours, and the temperature was kept at 40°C. Results were calculated after 30 min, 2 hours, 24 hours, 48 hours, and 72 hours. A separate set of samples were used for water and water detergent solutions. Usually, delicate fabrics are washed at room temperature (25°C) to 40°C. That's why; all these experiments were performed at 40°C. For water detergent solutions, 4g/L detergent was mixed in the water. "Total Extra" detergent, same as in the washing tests, was used in these experiments. List of samples are shown in Table 3.7.

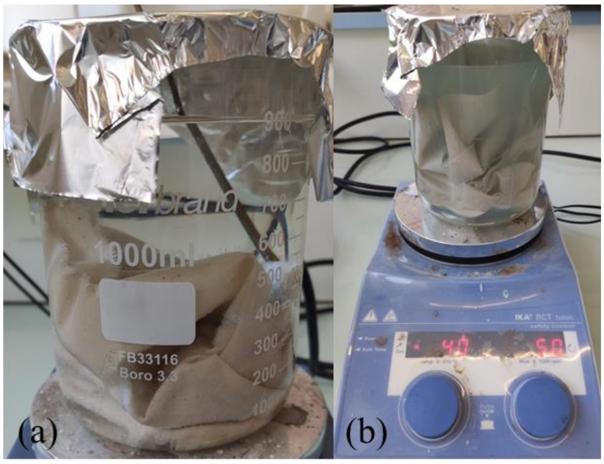

Figure 3.36. (a) Experimental set-up of chemical and water test, (b) Hot plate magnetic stirrer

Table 3.7. List of samples used for water and chemical analysis

Type of samples	Total samples	Total readings
Three-line stitched connection yarn Type A	06 Samples	06 Readings
ECG electrode F1	06 Samples	12 Readings
ECG electrode F2	06 Samples	12 Readings
ECG electrode F3	06 Samples	12 Readings
ECG electrode F4	06 Samples	12 Readings
ECG electrode E1	06 Samples	12 Readings
ECG electrode E2	06 Samples	12 Readings
Textile antenna	04 Samples	04 Readings

3.7.2 Martindale Abrasion test

Martindale abrasion resistance was performed on Martindale Abrasion Tester by "James H. Heals & Co Ltd.". The top weight on the sample (sample Load) during testing was kept at 9

K.Pa as defined in the testing manual. Standard woven felt (140 mm diameter) was placed as the lower surface for abrasion resistance testing. These woven felt were prepared by James H. Heals under ISO-129471 testing standards (Figure 3.37).

Figure 3.37. Woven felt specifications used in experiments

Unidirectional movement of Martindale top motion plate was selected for tests. The speed of the top motion plate was 0.8 sec/cycle, and the total distance covered in each cycle was 5.5 cm.

Martindale abrasion test was used to investigate the mechanical damages on different components of e-textile systems. Table 3.8 presents the various sampling components used for Martindale testing. Depending on the type of samples, different numbers of readings were obtained, and then mean values were calculated. Six samples can be tested on this specific machine at the same time. Samples related to transmission lines were stitched with three lines on each sample. These lines were 7 cm long and 1cm away from each other. Figure 3.39 shows the schematic diagram of these samples used for abrasion testing. ECG electrodes and textile antennas were tested as one specimen on each sample, and four output readings from four different points were calculated for each sample. All these experiments were performed under standard testing conditions 20 ± 2°C and 65 ± 5 % R.H. After Martindale abrasion testing, these samples were conditioned for 24 hours under room temperature before final output readings.

Table 3.8. List of samples used for Martindale abrasion tests

Type of samples	Total samples	Total readings
Three-line stitched connection yarn Type A (Dry)	06 Samples	18 Readings
Three-line stitched connection yarn Type B (Dry)	06 Samples	18 Readings
Three-line stitched connection yarn Type A (Wet)	06 Samples	18 Readings
Three-line stitched connection yarn Type B (Wet)	06 Samples	18 Readings
ECG electrode F1	06 Samples	24 Readings
ECG electrode F2	06 Samples	24 Readings
ECG electrode F3	06 Samples	24 Readings
ECG electrode F4	06 Samples	24 Readings
ECG electrode E1	06 Samples	24 Readings
ECG electrode E2	06 Samples	24 Readings
Textile antenna	04 Samples	04 Readings

Figure 3.38. Martindale abrasion test machine, (a) Configuration of upper arm movement, (b) Sample placement unit, (c) Testing machine front panel

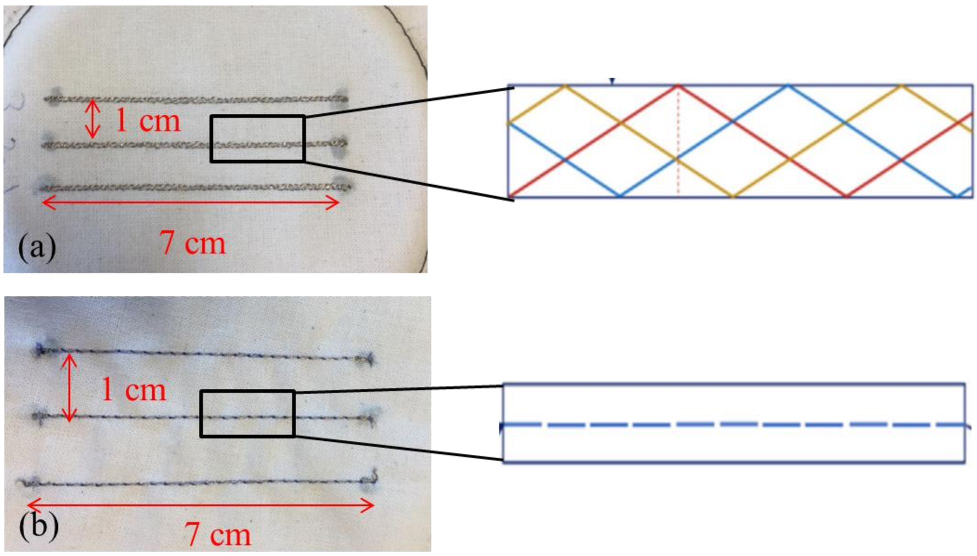

Figure 3.39. Schematic overview of transmission lines samples prepared for Martindale test (Three transmission lines per samples with 1 cm distance between them, (a) single-line stitch, (b) three-line stitch

3.7.3 Pilling box test

An orbiter pilling and snagging tester by "James H. Heals & Co Ltd., United Kingdom" was used in these experiments (Figure 3.40). All the samples were first stitched on plain cotton fabric, and then both edges of the fabric were stitched together to make them in a tube shape. These samples were mounted on the rubber tube specimens and finally placed into a revolving drum. Pilling box speed was adjusted to 60 RPM for all experiments. All experiments were performed under standard testing conditions 20 ± 2°C and 65 ± 5 % R.H and conditioned for 24 hours under room temperature before final output observations.

Three transmission lines of 10 cm each were stitched on each sample prepared for pilling box tests. ECG electrodes were stitched as two electrodes per sample, and textile antennas were prepared as one specimen for each sample (Figure 3.41). Total four samples each were prepared for these testing of e-textile components. Table 3.9 explains the sampling quantity in detail for e-textile components for pilling box testing.

Figure 3.40. An Orbitor pilling box machine

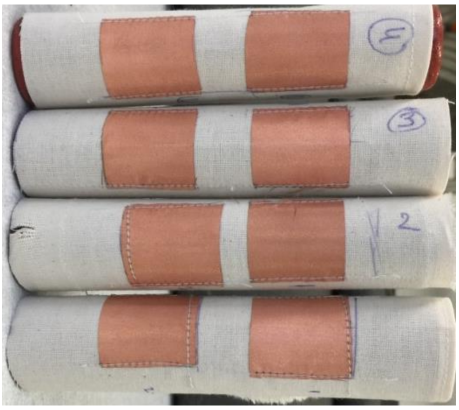

Figure 3.41. Set of four electrodes samples prepared for Pilling box test

Table 3.9. List of samples used for Pilling box test

Type of samples	Total samples	Total readings
Three-line stitched connection yarn Type A	04 Samples	12 Readings
Three-line stitched connection yarn Type B	04 Samples	12 Readings
ECG electrode F1	04Samples	16 Readings
ECG electrode F2	04 Samples	16 Readings
ECG electrode F3	04 Samples	16 Readings
ECG electrode F4	04 Samples	16 Readings
ECG electrode E1	04 Samples	16 Readings
ECG electrode E2	04 Samples	16 Readings
Textile antenna	04 Samples	04 Readings

3.7.4 Bending test

A bending test was performed for flexible PCBs. The bending machine was prepared using a double-acting pneumatic round line cylinder. The double-acting cylinder was used to create a backward and forward movement to the attached long rod. Fabric containing PCBs was fixed from one side, and a hanging weight of 1 kg was attached on the other side. PCB was bending around the circular road of 12 mm diameter with forwarding and backward movements under the load of 1 kg. Figure 3.42 and Figure 3.43 presents the bending machine and its schematic diagram, respectively. Speed was adjusted 80 cycles per minute, and a total of 32 samples were investigated for the flexible PCBs bending test.

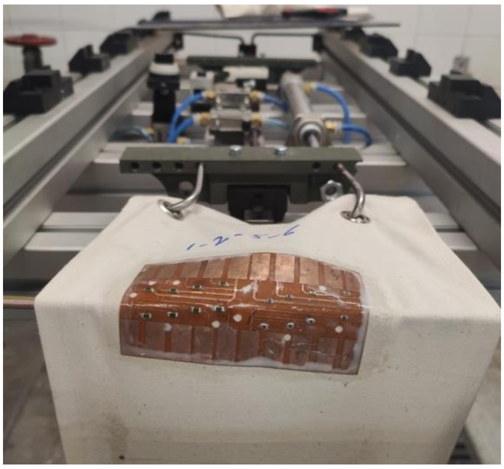

Figure 3.42. Bending test machine

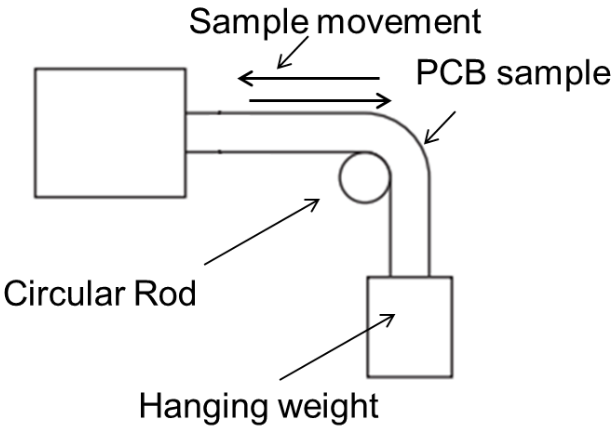

Figure 3.43. Schematic diagram of bending test

3.8 Measuring techniques

3.8.1 Linear electrical resistance measurement

Linear electrical resistance was measured by using Agilent 34401A digital multi-meter (Figure 3.44). Same leads and probes are used for all experimental testing. For validation purposes, each reading was repeated three times before noting down the measurement. Linear electrical resistance was measured for samples related to transmission lines. The ratio of change in resistance from actual resistance was calculated for better comparison and understanding.

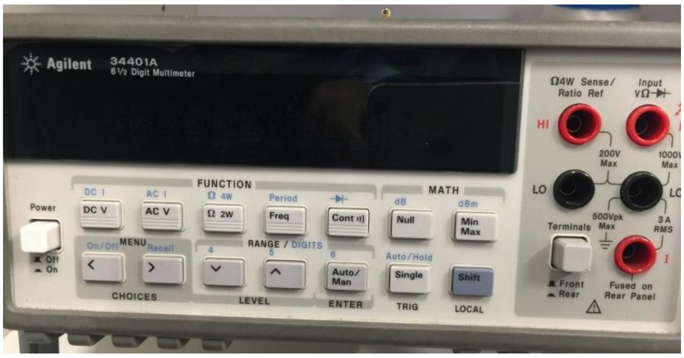

Figure 3.44. Agilent digital multi-meter

3.8.2 Four probe surface resistance measurement

Surface sheet resistance was measured using a Four-Probe system from Ossila, United Kingdom. This device works on the four-probe method having four equally spaced probes. The distance between these probes was 1.27 mm. AC supply is passed between two outer probes, and the voltage drop is measured between two inner probes (Figure 3.45). Then SMU (source measurement unit) is used to calculate the sheet resistance in Ohm per square unit (Figure 3.46). V/I curve data was used in the following equation to measure the surface resistance of ECG electrodes.

$$Rs = 4.53236\frac{\Delta V}{I}$$

I is the current applied between outer probes, and ΔV is the change in voltage measured between inner probes.

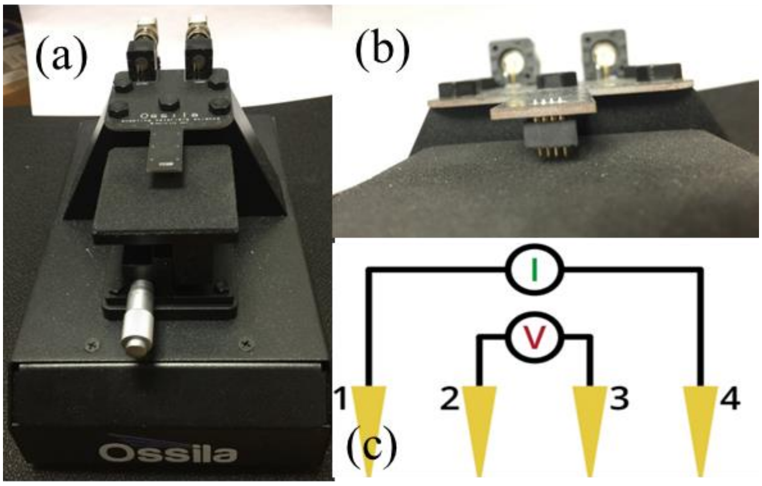

Figure 3.45. (a) Ossila four-probe device, (b) Close-up of measuring probes, (c) Schematic diagram of the four-probe calculation

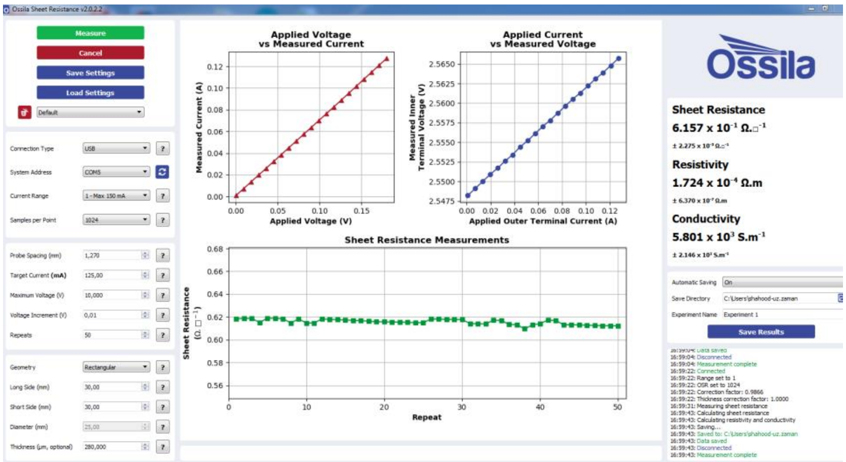

Figure 3.46. An overview of surface resistance measurement software tool

3.8.3 Impedance meter

The Agilent impedance analyzer 4294A was used to investigate the textile antennas (Figure 3.47). The real and imaginary part of impedance was measured against the frequency range 1 KHz to 30 MHz. The resonance frequency was calculated, from the received data, at the frequency when the impedance of the imaginary part comes to zero. Then quality factor was calculated using the following equation.

$$Q = \frac{fo}{\Delta f}$$

Where Δf is the bandwidth of resonance structure.

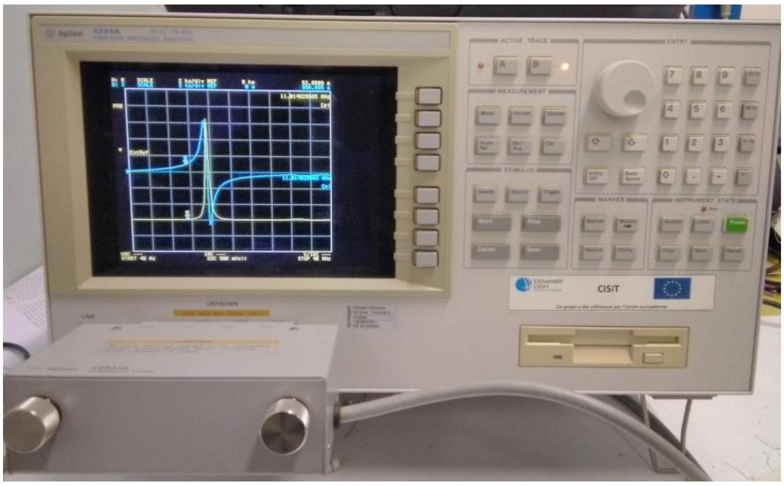

Figure 3.47. Agilent 4294A Impedance analyzer

3.8.4 ECG signal analysis

ECG measurements for these fabricated and embroidered skin electrodes were performed by SHIELD-EKG-EMG card from OLIMEX. This device uses a dedicated embedded 10-bit ADC integrated with the MCU of the baseboard to receive a digital output value ranging from 0-1024. This OLIMEX card was connected to an Arduino UNO board. The sampling rate was kept at 250 Hz, and the data obtained were analyzed by processing it by MATLAB (R2013a). These signals were filtered by a Butterworth pass-band filter (0.5–100 Hz) to remove motion artifacts and a Notch filter at 50 Hz to remove power line noises [10].

3.8.5 SEM and microscopic analysis

These samples are analyzed by Scanning electron microscopy (SEM) to investigate the damages and their intensity. Phenom ProX SEM (FEI Company, Hillsboro, USA) (Figure 3.48) was used for this purpose. Conductive transmission lines and skin-dry electrodes were investigated by random sampling from the samples. Removal of silver or other conductive material from these surfaces was highlighted by changing the image color from white to black on that specific point, reflecting the inner non-conductive polyamide material.

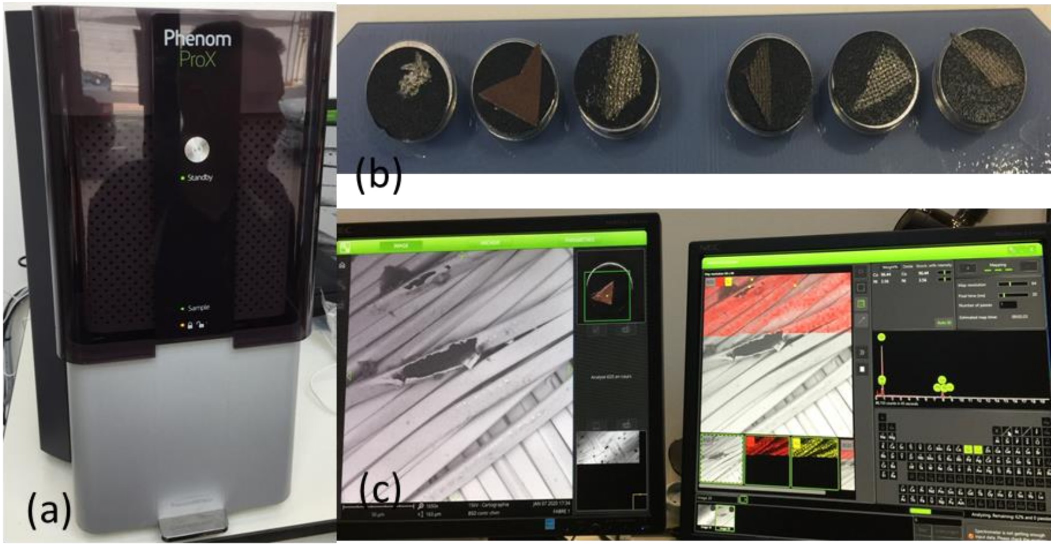

Figure 3.48. (a) SEM analyzing device, (b) sample preparation for SEM, (c) SEM results display

The following chapter 4 explains the results obtained from these experiments and their interpretation along with detailed explanations and discussions.

References

1. Ismar, E.; Zaman, S. uz; Tao, X.; Cochrane, C.; Koncar, V. Effect of Water and Chemical Stresses on the Silver Coated Polyamide Yarns. *Fibers and Polymers* **2019**, *20*, 2604–2610, doi:10.1007/s12221-019-9266-4.
2. Kim, H.; Yun, C.; Park, C.H. Fabric Movement and Washing Performance in a Front-Loading Washer with a Built-in Pulsator. *Textile Research Journal* **2019**, *89*, 4732–4745, doi:10.1177/0040517519835757.
3. Yun, C.; Choi, H.R.; Park, S.; Park, C.H. The Effect of Fabric Movement on Washing Performance in a Front-Loading Washer V: Focusing on the Role and Shape of the Lifter. *Textile Research Journal* **2019**, *89*, 364–374, doi:10.1177/0040517517743741.
4. Yu, X.; Li, Y.; Ding, X. Dynamics of Cotton Textile Motion in a Domestic Tumble Dryer and Its Effect on Drying Performance. *Textile Research Journal* **2020**, 004051752096075, doi:10.1177/0040517520960751.
5. uz Zaman, S.; Tao, X.; Cochrane, C.; Koncar, V. Launderability of Conductive Polymer Yarns Used for Connections of E-Textile Modules: Mechanical Stresses. *Fibers and Polymers* **2019**, *20*, 2355–2366, doi:10.1007/s12221-019-9325-x.
6. Merilampi, S.; Björninen, T.; Haukka, V.; Ruuskanen, P.; Ukkonen, L.; Sydänheimo, L. Analysis of Electrically Conductive Silver Ink on Stretchable Substrates under Tensile Load. *Microelectronics Reliability* **2010**, *50*, 2001–2011, doi:10.1016/j.microrel.2010.06.011.
7. Ryan, J.D.; Mengistie, D.A.; Gabrielsson, R.; Lund, A.; Müller, C. Machine-Washable PEDOT:PSS Dyed Silk Yarns for Electronic Textiles. *ACS Appl. Mater. Interfaces* **2017**, *9*, 9045–9050, doi:10.1021/acsami.7b00530.
8. Gaubert, V.; Gidik, H.; Bodart, N.; Koncar, V. Investigating the Impact of Washing Cycles on Silver-Plated Textile Electrodes: A Complete Study. *Sensors* **2020**, *20*, 1739, doi:10.3390/s20061739.
9. Rotzler, S.; Kallmayer, C.; Dils, C.; von Krshiwoblozki, M.; Bauer, U.; Schneider-Ramelow, M. Improving the Washability of Smart Textiles: Influence of Different Washing Conditions on Textile Integrated Conductor Tracks. *The Journal of The Textile Institute* **2020**, 1–12, doi:10.1080/00405000.2020.1729056.
10. Ankhili, A.; Zaman, S.U.; Tao, X.; Cochrane, C.; Koncar, V.; Coulon, D. How to Connect Conductive Flexible Textile Tracks to Skin Electrocardiography Electrodes

and Protect Them Against Washing. *IEEE Sensors Journal* **2019**, *19*, 11995–12002, doi:10.1109/JSEN.2019.2938333.

4. Results and Discussion

Detailed analyses of damages provoked during the washing process on e-textile systems' components have been explained with results. Different textile testing techniques have been performed on these components. Relations between different damages from washing process and from textile testing techniques have been investigated, and projected outputs have been discussed. These experiments were performed in standard working conditions following all available standard protocols.

4.1 Accelerometer Analysis

Accelerometer analysis was performed to understand the washing behavior during the process and calculate the stresses on the e-textile components. As described previously, the washing process may be divided into three main phases, including washing, rinsing, and tumbling. During these phases, three washing actions are carried out that are low-speed rotation, stop (resting), and high-speed rotation action. An accelerometer was used to investigate the impact of different washing actions during various washing phases. It was attached to a flexible PCB sewn on cotton fabric, sealed in a plastic bag, and then placed in the washing machine.

The accelerometer measures its proper acceleration, which is not the same as coordinate acceleration. The X, Y, and Z directions of the accelerometer were fixed with itself. The X (left/right) and Y (forward/backward) directions are on the PCB surface, and the Z (up/down) direction is perpendicular to itself. The fabric containing the accelerometer fixed on it is revolving in all directions and orientations. Figure 4.1 describes the coordinate system during different accelerometer positions in the washing machine.

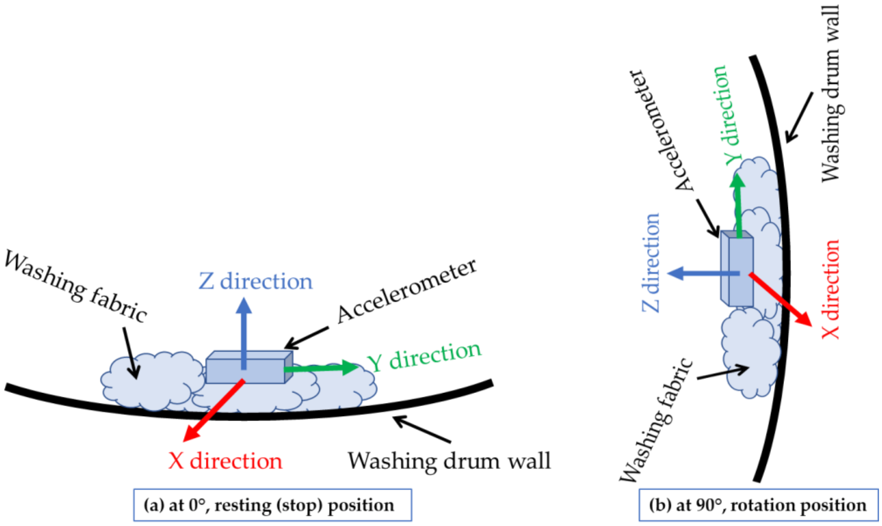

Figure 4.1. Coordinate system (X, Y, Z) of the accelerometer, fixed to the plain fabric that is moving during the washing cycle, (a) at 0° position, (b) at 90° position [1]

Figure 4.2 explains the accelerometer sensor movements during the washing phase of the process. During this process, the fabric revolves several times with some resting (stop) intervals between two low-speed rotation movements. Throughout fabric rotation, it revolves along with the washing drum and then falls. This phenomenon is repeated again and again, and it is visible in Figure 4.2.

The accelerometer output values helped us to identify the low-speed rotation and stop positions during the whole process. Different peaks correspond to all three actions are noticeable, and we recognized them as falling peaks because their readings were more significant than 1g. These falling peaks are created due to the free fall of fabric after half revolving cycle in the wash drum and then falls. This phenomenon was verified outside the washing machine by dropping the accelerometer on the floor from the height of 0.47 m (equal to the washing drum diameter).

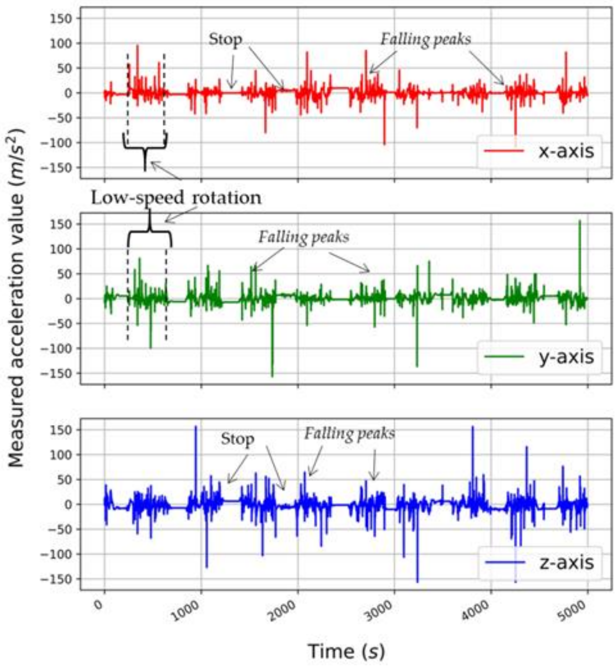

Figure 4.2. Accelerometer analysis in the washing phase (low-speed rotation), three separate graphs for X, Y, and Z-axis [1]

Figure 4.3 explain the accelerometer analysis for high-speed rotation at 400 RPM and Figure 4.4 highlight the behavior at 600 RPM in the tumbling phase of the washing process. The rotation speed starts from 0 RPM, and it achieves the required rate in several seconds. For the initial seconds, its behavior is similar to the low-speed rotation. The fabric repeatedly falls after half rotation cycles due to gravity until the rotational speed reaches certain momentum and fabric stuck with drum the wall under centrifugal force. The pressure force, generated due to the centrifugal force, acts perpendicular (Z-axis) to the fabric that causes the fabric to stick with the wall. Once the fabric is stuck with the drum, X and Y-axis are zero, and a straight line only in the Z-axis is observed because the centrifugal force is acting in the Z-axis only.

Newton's second law ($F=a*m$) may be used to calculate the pressure generated by the centrifugal force. Here a is acceleration (m^2/s), m mass (kg) and $a = \omega^2 * r$ (ω angular speed (rad/s) and r radius (m)). The washing drum diameter was d = 0.47 m, and its rotational speed was 400 RPM. The calculated acceleration value is 42 g, which is much higher than the tested accelerometer capacity (16 g). Hence a straight line at maximum detectable level (16 g) is observed on the Z-axis. This equation authenticates the accelerometer analysis performed and its creditability to sense the washing process's washing forces.

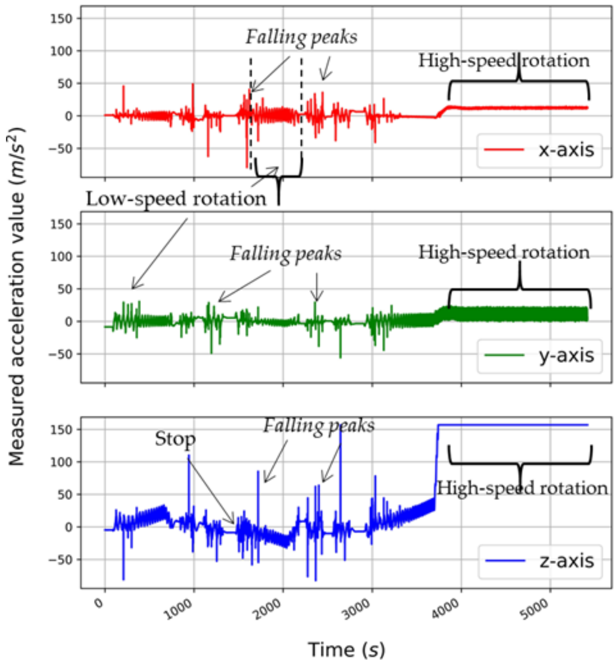

Figure 4.3. Accelerometer analysis in the tumbling phase (400 RPM), three separate graphs for X, Y, and Z-axis [1]

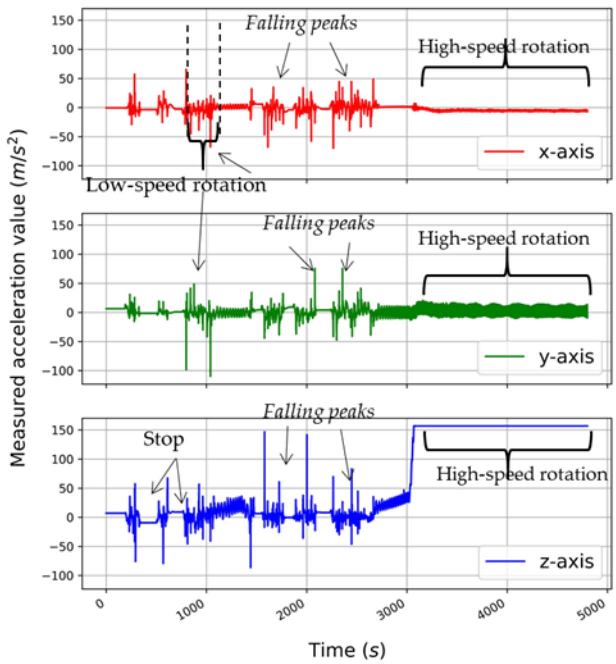

Figure 4.4. Accelerometer analysis in the tumbling phase (600 RPM), three separate graphs for X, Y, and Z-axis [1]

In common sense, it is usually considered that high-speed rotation will create a more damaging impact in terms of the mechanical stresses acting on the washed substrates. However, this study of the accelerometer analysis concluded that continuous falling during the low-speed rotation is more damaging than the high-speed when the fabric is stuck on the wall due to centrifugal forces in the washing drum. Because for low-speed rotations, the fabric repeatedly falls due to gravity, and e-textile systems are damaged. Consequently, the low-speed process, which varies between 15 RPM to 38 RPM, provoked more damages than the high-speed circulation ranging from 400 RPM to 1600 RPM.

4.1.1 Power Spectral Density (PSD)

The power spectral density of the data collected from the accelerometer movements placed in the washing drum was plotted for low and high-speed rotation actions. This practice aimed to highlight the intensity of the falling impact in the drum during the washing process. For Power Spectral Density (PSD), separate plots for each axis and then combined graphs for all three directions were prepared using root mean square (RMS).

4.1.1.1 PSD analysis of washing phase (low-speed rotation action)

Figure 4.5 describes the PSD for low-speed rotation. It is easily noticed that the gravity is visible on all three axes plotted as they move in all directions during the washing process, as shown in PSD accelerations for 0 Hz frequency. Like the X, Y, and Z accelerations, PSD signals are quite noisy, but without specific plots, it is possible to conclude that there are some peaks created due to the low-speed rotation. It is, however, possible to identify a small peak at low frequencies around 1 Hz specifying that the accelerometer was falling from the upper position as the RPM was less and the centrifugal force not strong enough to keep it stuck to the drum wall. Therefore, if the e-textile system containing sensitive parts is exposed to this repetitive falling stresses, it may be damaged. It is difficult to establish a quantitative equation between the PSD information and the possible damages, but some kinds of the threshold value (maximal stress at a given frequency) of PSD peaks not to exceed could be defined. In that case, the probability for the e-textile system to be damaged would be lower.

The PSD information could also be used to simulate the wash process by some other means such as a pilling box instance. This PSD information may also be interpreted as a signature of the washing machine and may be used to compare different types of washing machines to determine which one is mild towards the e-textile systems, or not, at the same washing programs.

The accelerometer motion average values in three directions are probably quasi-isotropic during the long period, explaining similar X, Y, and Z accelerometer outputs and their PSD plots in low-speed rotation actions. As the accelerometer, along with other fabrics, is constantly moving, it is impossible to predict the movements and random behavior in the washing cycle. That's why the non-isotropic accelerometer motions were observed.

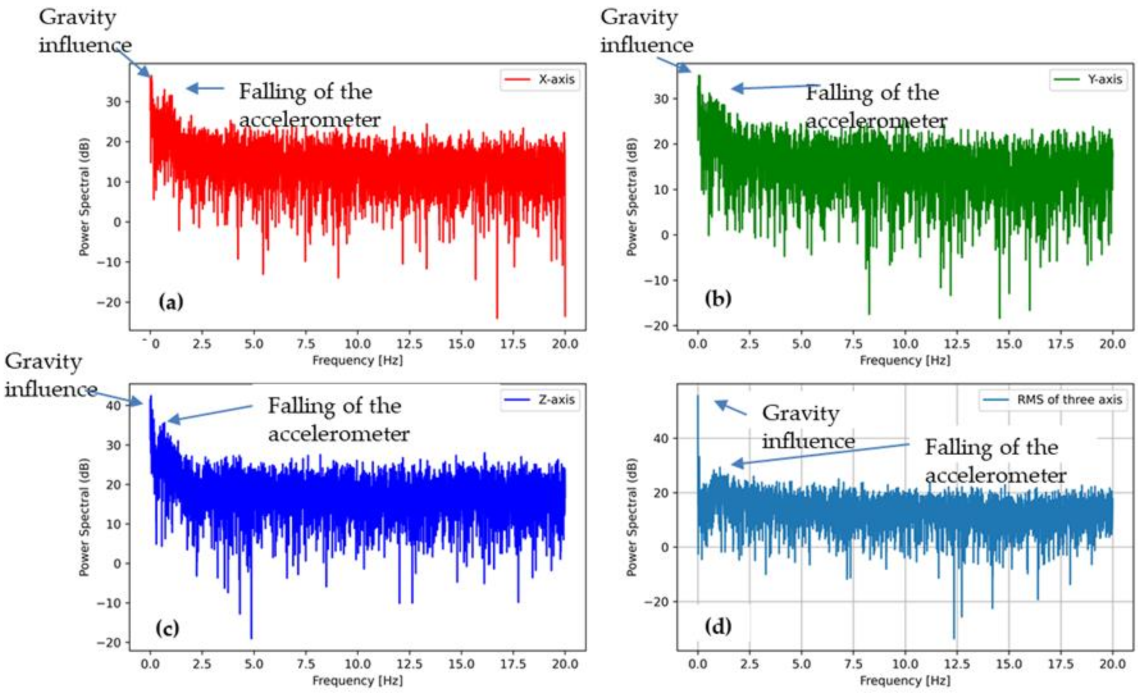

Figure 4.5. PSD of the accelerometer outputs of washing phase (low-speed rotation action), (a) in the X direction, (b) in the Y direction, (c) in the Z direction, and (d) the sum of all the accelerations [1]

4.1.1.2 PSD analysis of tumbling phase (high-speed rotation action)

The PSD for high-speed rotation in the tumbling phase is plotted in Figure 4.6 and Figure 4.7. It is noticeable that all plots show the same trend regardless of the rotational speed. In the Z direction, the centrifugal force of acceleration at 0 Hz is quite visible in these plots. Vibration peaks primarily visible in the Y directions are probably created due to the washing machine vibrations when rotating at a high-rotation speed. These vibrations themselves can cause damages to sensitive e-textile components. These peaks are visible at 7 Hz for 400 RPM and 10 Hz for 600 RPM.

Another power spectral peak at 1 Hz is also visible in these plots. It is due to the angular acceleration stage (low-speed rotation) for the tumbling phase. When the fabric starts moving at 0 RPM, it falls, again and again, the washing drum until speed reached the threshold level, and the washing material got stuck with the drum. However, this intensity is far less than the washing phase due to the short duration of this rotation in the tumbling phase.

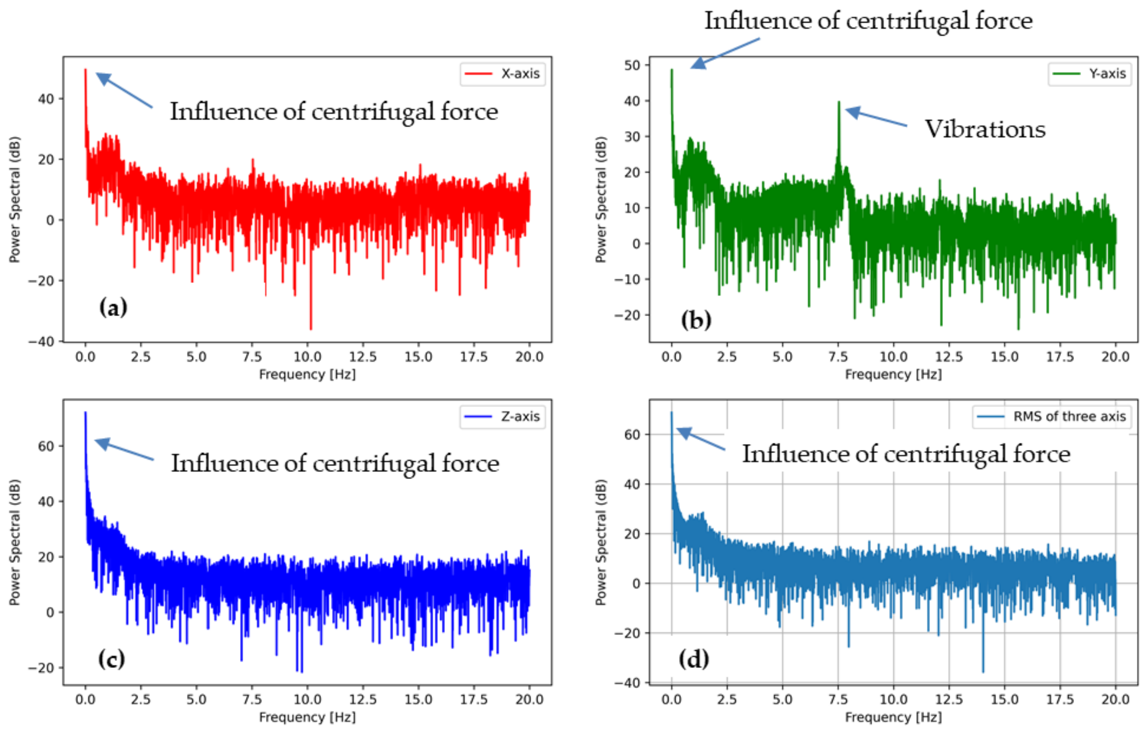

Figure 4.6. PSD of the accelerometer outputs from tumble phase (high-speed rotation 400 RPM), (a) in the X direction, (b) in the Y direction, (c) in the Z direction, and (d) the sum of all the accelerations [1]

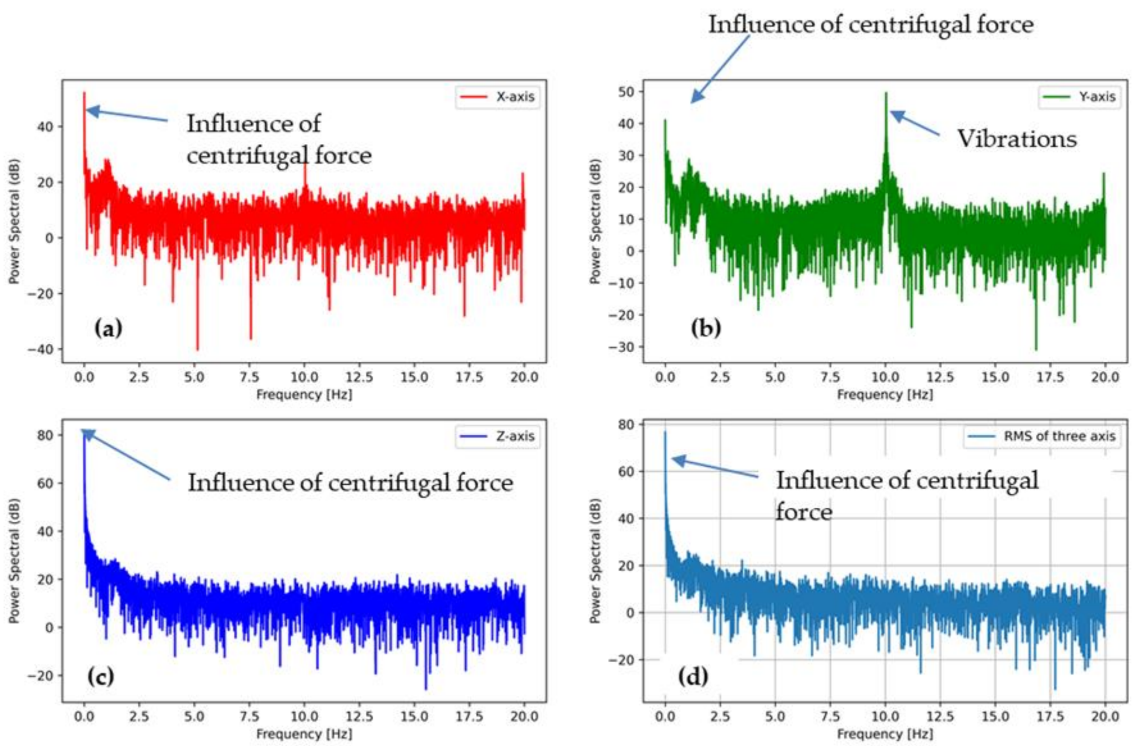

Figure 4.7. PSD of the accelerometer outputs from tumble phase (high-speed rotation 600 RPM), (a) in the X direction, (b) in the Y direction, (c) in the Z direction, and (d) the sum of all the accelerations [1]

In the next step, these PSDs for high-speed rotations (Figure 4.8 and

Figure 4.9) were plotted again after removing the initial low-speed process. These graphs show only rotational movement after the fabric was stuck on the wall due to the rotational centrifugal force created when the tumbling speed crosses the threshold level. The Z-direction's centrifugal force is visible due to the removal of noises produced by initial low-speed rotation actions. That's why the peak at 1 Hz, created by low-speed rotation, is also removed in these plots. Vibrations at 7 Hz and 15 Hz for 400 RPM rotational speed and 10 Hz and 20 Hz for 600 RPM rotational speed are visible in these graphs, mainly upon the X and Y axes, representing the possible rubbing actions of the fabric against the drum wall during this process.

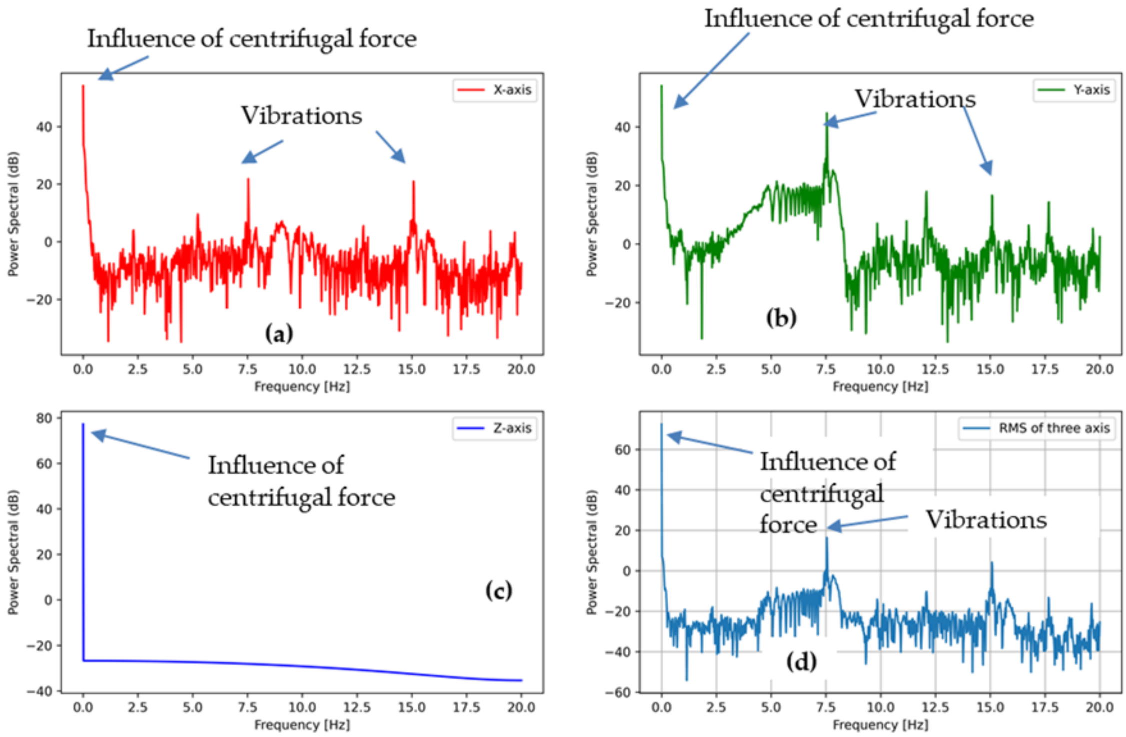

Figure 4.8. Tumble phase (400 RPM), removing initial acceleration phase, PSD of the accelerometer outputs, (a) in the X direction, (b) in the Y direction, (c) in the Z direction, and (d) the sum of all the accelerations [1]

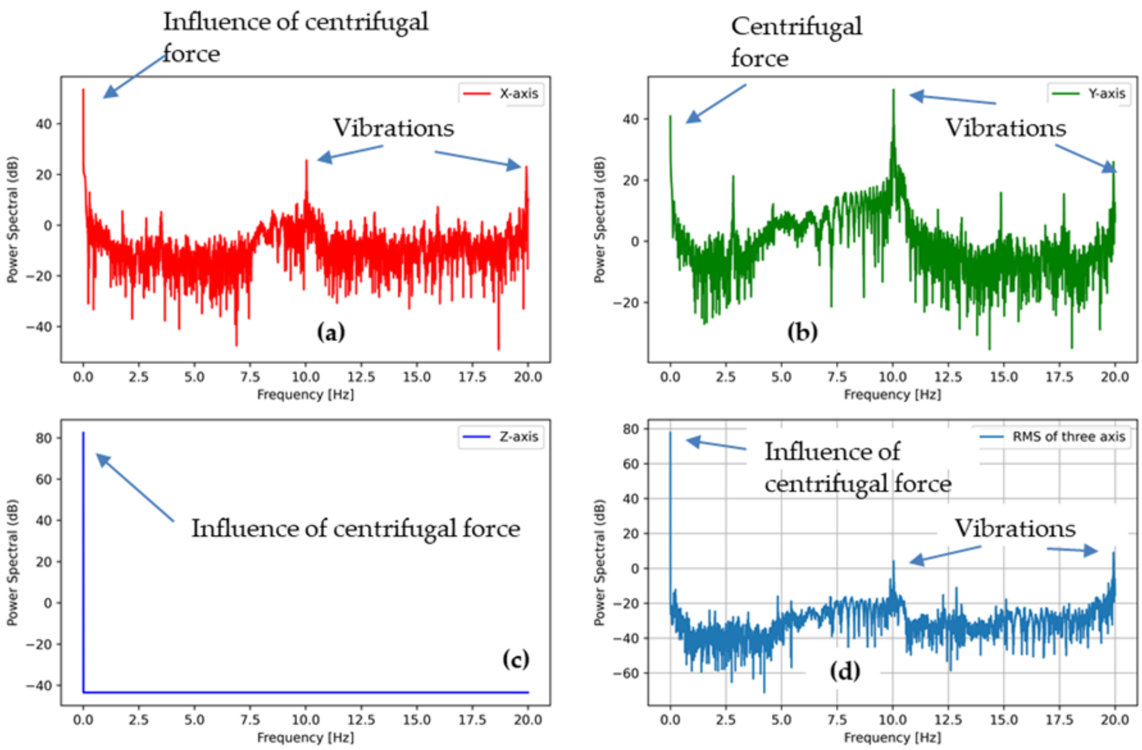

Figure 4.9. Tumble phase (high-speed rotation 600 RPM), removing initial acceleration phase, PSD of the accelerometer outputs, (a) in the X direction, (b) in the Y direction, (c) in the Z direction, and (d) the sum of all the accelerations [1]

All these experimental analyses explained two different types of behavior, in terms of mechanical stresses, for the fabric undergoing the washing process. The first type is the falling movement of the samples in the low-speed rotation due to gravity, and it is shown in the falling peaks in the previous discussion. These low-speed movements may be simulated by using the Pilling box test. This test uses the closed box containing the samples and rotating at specific revolutions per minute. Although the Pilling box is rectangular, not circular as the washing drum, the best possible simulation may be obtained from these experiments. Usually, the Pilling box test has a rotational speed ranging from 30 RPM to 60 RPM. In our previous discussion about washing time analysis, we observed that the low-speed rotational speed is kept at 38 RPM in most of the cases, close to this speed. This available test protocol can simulate the washing drum movement outside the washing machine.

In the second type of behavior, the fabric was stuck on the wall due to pressure force in Z-direction and continuous movement in the X and Y-directions during the high-speed rotation. These movements create the fabric sliding with the drum wall under a certain amount of pressure in the Z-direction perpendicular to the fabric face. The Martindale abrasion test may simulate these mechanical stresses. This test is performed by applying certain known pressure on the fabric in one direction and under-pressure sliding movements in other directions. Identified pressure of 9 KPa, in the form of pressure arm on the sample, was applied in the Martindale Abrasion machine used in these experiments. The fabric was then slid in the backward and forward motion under this pressure. This phenomenon can give a close simulation of high-speed rotation under rotational force created in Z-direction.

These two available test procedures (Pilling box and Martindale) can simulate and predict similar damage in the washing process without going into the washing machine. Figure 4.10 demonstrates the proposed idea to expect the washing damages caused by specific stresses working on it. As a result, the actual washing process can be replaced by mechanical tests, and the reliability of e-textile components can be tested at each step during the manufacturing process of the e-textile systems.

The following sections of this chapter explain the proposed test results on various e-textile components.

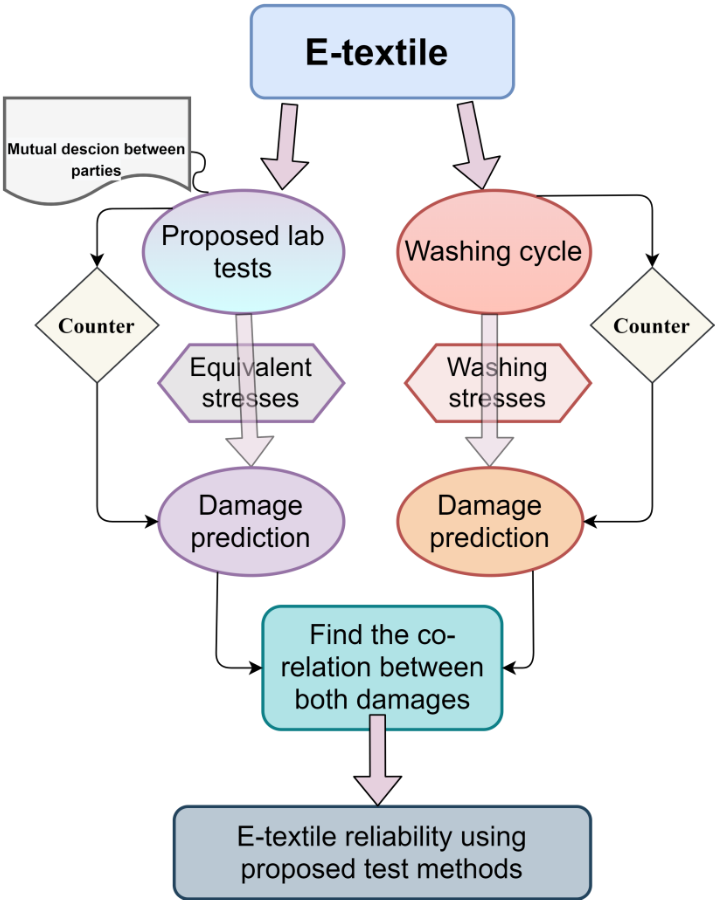

Figure 4.10. The layout of the proposed model for washing predictions

4.2 Connection yarns/ Transmission lines

4.2.1 Washing tests

Different transmission line samples were prepared and tested for washing. Two different types of washing programs were investigated in these experiments. These washing programs were selected based on video analysis for various programs. *Silk* and *Express* washing program were chosen for these studies based on their different washing speed but almost equal total washing time (35 minutes). The *Silk* washing cycle uses the 15 RPM washing speed, while in the case of the *Express* washing cycle, it is 38 RPM. In both cases, the tumbling speed was adjusted at 400 RPM. Washed samples were dried for 24 hours in controlled temperature and relative humidity (20 ± 2°C and 65 ± 5 %) before final testing. Linear resistance of samples was measured with Agilent 34401A digital multimeter, and the same leads were used for all experiments to avoid any effect on results.

Figure 4.11 highlights the washing analyses for single line stitched transmission lines, prepared with yarn Type A, B, and C, against *Express* washing cycles. For Type C yarns, all samples were damaged just after one wash cycle. This yarn is a three-ply yarn with only one conductive ply among them. The other two yarns (Type A and B) were also three-ply yarn, but in this case, all plies were conductive. Hence, it was evident that Type C yarn was weak in conductivity and more volatile to damage. Its initial linear resistance was also more than twice of other two yarns. That’s why this yarn was removed from further investigation, and future experiments were focused on the remaining two yarns (Type A and B). Both Type A and B yarns were also damaged after 3 washing cycles. All samples increased their linear resistance values above 30 Ohm/cm (from initial 5 Ohm/cm) after 5 washing cycles.

Average resistance for these samples was not possible, and it is not discussed here. Further experiments were conducted with a two-line and three-line stitch and TPU and embroidered protection layer on it. In two/three-line stitch, a network was between yarn stitches, and they interconnect each other at various multiple places. If one part of one yarn is broken, electrical current can transmit through different yarn stitches thanks to these numerous connection points. Secondly, in multiple stitched transmission lines, yarn layers are placed on each other and act as a protector for the inner side layer of yarn from possible damages.

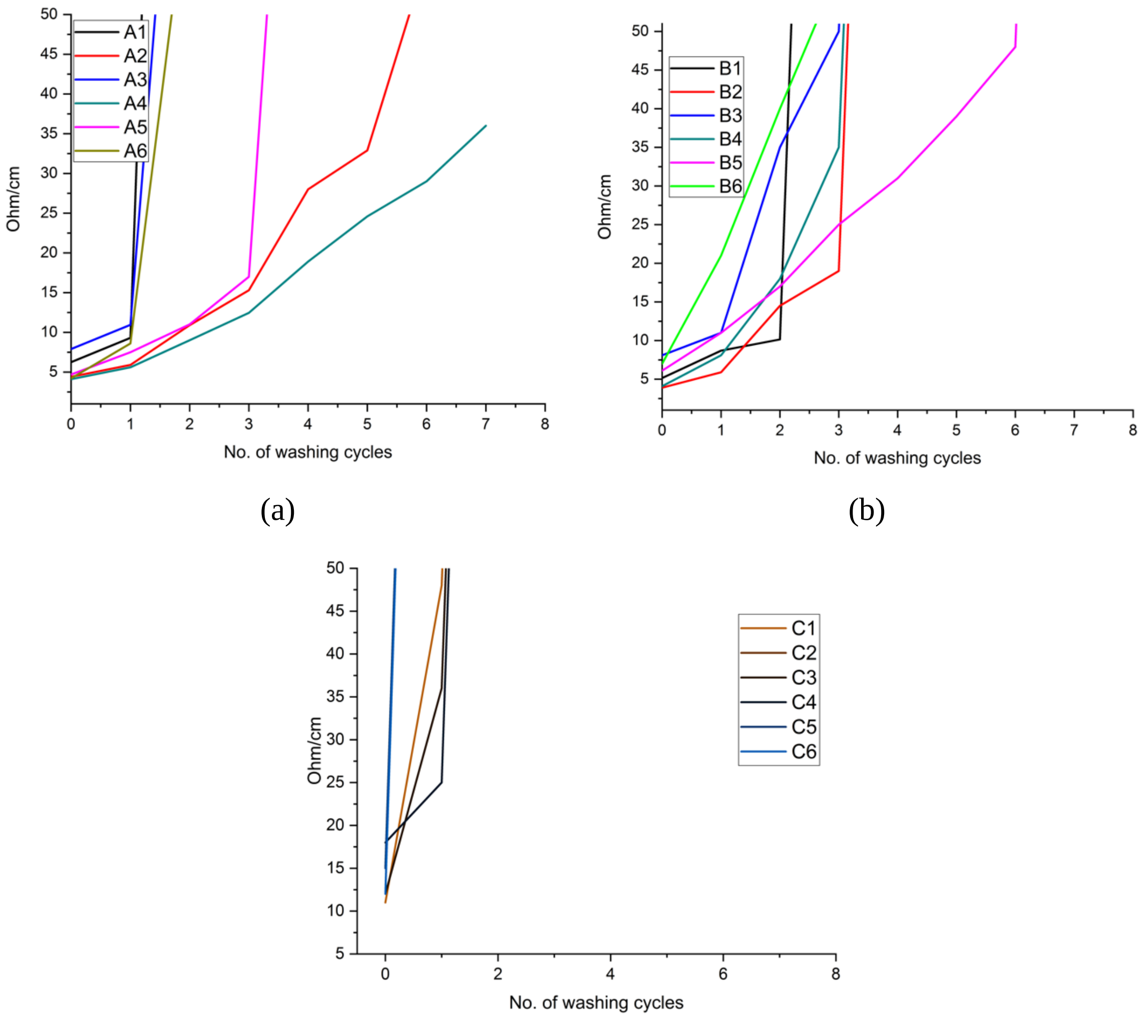

(a) (b) (c)

Figure 4.11. Washing analyses for single-stitched transmission lines stitched on the plain cotton fabric, Six samples for each type of yarns, (a) “Type A” yarn, (b) “Type B” yarn, (c) “Type C” yarn

The surface morphology for these conductive yarns was investigated, before and after the washing process, with Scanning Electron Microscopy (SEM). All the yarns showed damage to the conductive layer, and in most cases, it was removed from the surface. Black color threads in the pictures represent the non-conductive threads, and the white part corresponds to the conductive portion in these yarns (Figure 4.12).

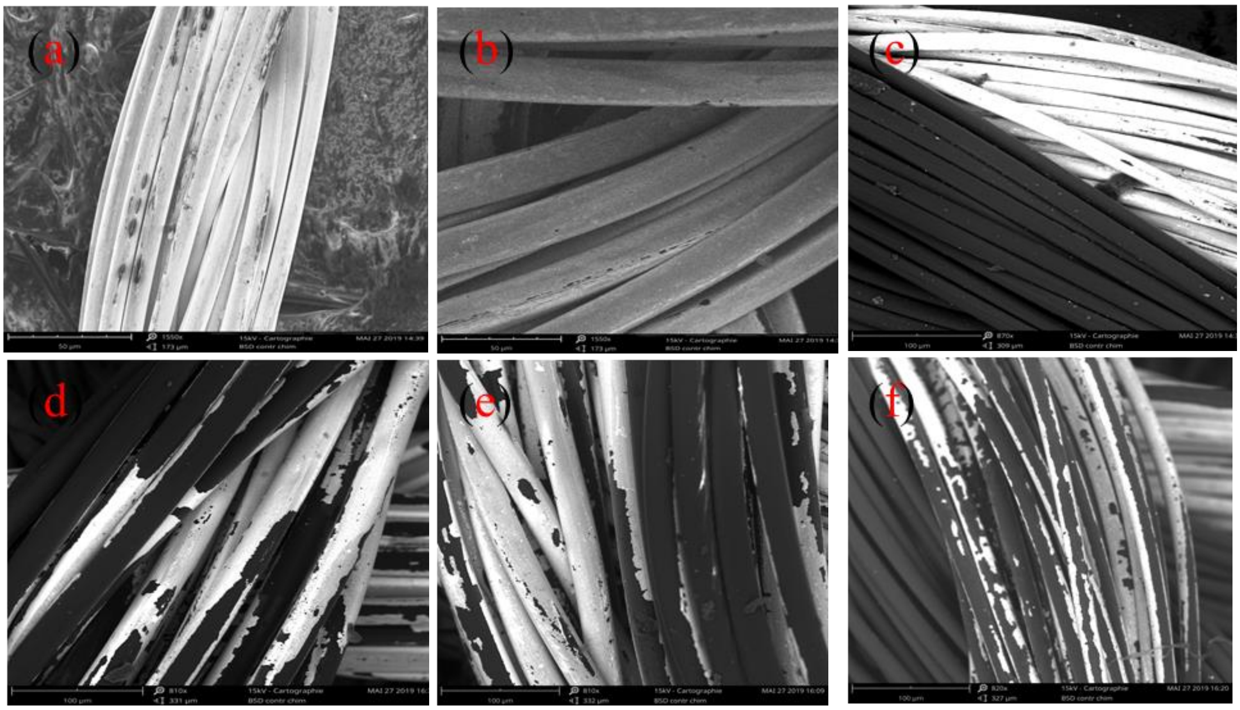

Figure 4.12. Surface morphology for three yarns before and after washing was captured using the SEM. (a) "Type A" yarn before washing, (b) "Type B" yarn before washing, (c) "Type C" yarn before washing, (d) "Type A" yarn after washing, (e) "Type B" yarn after washing, (f) "Type C" yarn after washing.

Figure 4.13a explains the relative resistance ratio R'/R (a ratio of change in resistance from initial value) for "Type A" yarn with two-line stitched and three-lined stitched conductive tracks. Two-line stitched samples increased their resistance after five washing cycles, and the calculated R_i/R_o value was 5.5, and it increased more than value 10 after 10 washing cycles. These graphs show the R_i/R_o values up to 10 only because we considered that output values increased 10 times from original values could not be stated good conductive for e-textile systems. On the other side, three-lined stitched tracks showed more resistance to damages in washing cycles, and R_i/R_o was 3.04 after 10 washing cycles. But after 10 washing cycles, they also lost their conductivity and the increase in linear resistance was more than 10 times from their original values. In the next step, these conductive tracks were protected by TPU and simple yarn embroidered in a zig-zag pattern over the transmission lines. As in these cases, conductive paths were covered for possible damages during the washing process and we continued the *Express* washing up to 50 washing cycles. The samples were tested after each 10 washing cycles. Two-line stitched with TPU protection samples increased their linear resistance by the ratio of 6.04 times. It is further reduced to 3.60 in the case of embroidered yarn protection over conductive tracks. It is acceptable that protections reduced the damage proportion rapidly. These conductive paths are still useable after 50 washing cycles as these protections, which are already known to resist the damages, increased the extra layer over sensitive portions.

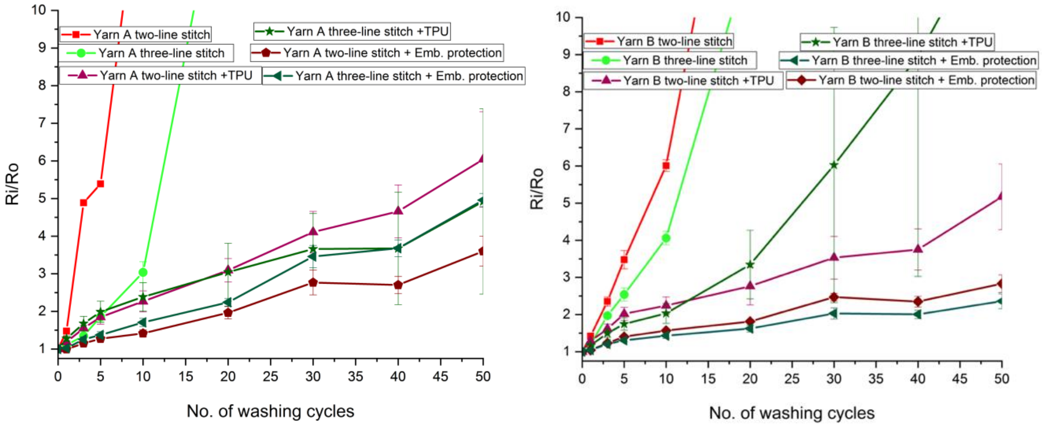

(a) (b)

Figure 4.13. R_i/R_o values for “Type A” yarn with two and three-line stitch after 50 washing cycles (a) type A (b) type B

Figure 4.13b explains the R_i/R_o for Type B yarn samples up to 50 washing cycles. Two and three-line stitched samples without any protection increased their resistivity rapidly. R_i/R_o value for two-line stitched after 10 washing cycles was 6.03, and it was calculated 4.01 for three-lined stitched samples. Type B yarn showed better resistance to damages than “Type A” yarn which explains better silver coating and its adhesion with base nylon fibers.

A similar trend is also visible in protected conductive tracks for Type B yarn. Two-line stitched with TPU protection reduced the ratio to 5.17 after 50 washing cycles. This value is further reduced to 2.83 for two-lined stitched tracks with an embroidered protective layer over them. Three-lined stitched samples with embroidered protection layer over them have The R_i/R_o value of 2.36, which is the best minimum value for all these samples after 50 washing cycles. But these samples with TPU protection showed unexpected results, and linear resistance values were increased to 17.69 after 50 washing cycles. A higher standard deviation for these specific samples explains that some prototypes were damaged out of the routine from others. As TPU coating was performed under the heated press at 140°C and there is a possibility that this temperature damaged the outer conductive silver coating for some samples, which ultimately increased their conductivity after the impact of washing stresses. This hypothesis is acceptable as in all samples for both types of yarns, TPU coated samples increased their conductivity more rapidly compared to the prototypes with embroidered protection layers over transmission lines. Although the acceptable temperature to withstand is mentioned in neither of the yarns' datasheets, a heated plate with high pressure ultimately created damage to the silver-plated yarn, visible from the results.

In the comparison of two-line and three-line stitched tracks, the last one performed better in all samples. In three-lined stitched channels, there is one more line available for the current to pass, and also, more connection points among them are offered to transfer the current in case of damage at any single area or line throughout the track length. In a three-line stitch, there is also more space for the outer line to protect the inner two lines at any point during the washing stresses acting on them. In comparing Types A and B yarns, Type B yarn showed somehow a little better performance in washing tests. "Type B" yarn is prepared with 100% polyamide silver-plated yarn (Shieldex, "Type A") with some modifications in the silver coating, which ultimately increased its performance in terms of resistance to damages. Finally, it was concluded that three-lined stitched yarn with an embroidered protected layer above the conductive tracks showed the best performance in all samples.

Surface morphology of "Type A" and "Type B" yarns after 50 *Express* washing cycles are presented in Figure 4.14. Some damages on the surface are visible, but as these are three-line stitched transmission lines, current can still pass through inner lines that are not damaged and are in contact at multiple points.

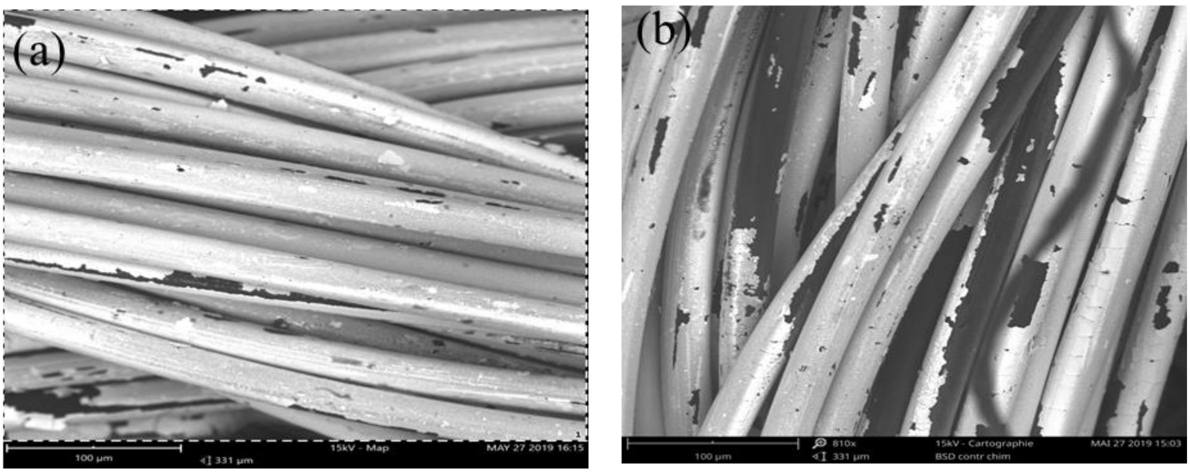

Figure 4.14. SEM images for Type A and B yarns in a three-line stitched pattern after 50 washing cycles

4.2.2 Martindale abrasion resistance test

Martindale abrasion test was performed on these transmission line samples in wet and dry states. Figure 4.15 describes the evolution of the relative resistance ratio against the abrasion cycles. The rate of change in resistance from initial values (R'/R) after 3000 abrasion cycles was 2.89 and 1.7 for "Type A" and "Type B" yarn, respectively. Like at beginning of washing cycles for three-line stitched yarns, Martindale abrasion cycles also showed the linear trend, and it is possible to plot the regression models. This linear regression model fits well and proves the linear trend for electric resistance change against abrasion cycles. Both yarns showed a sharp increase of change in electric resistance at the beginning of the abrasion test. This initial change may be due to the initial damage of superficial silver coating that is not adequately adhered to with the yarn's base polyamide surface. Both "Type A" and "Type B" yarns showed a similar trend in Martindale abrasion tests, and it is possible to find a co-relation between washing tests and Martindale abrasion tests.

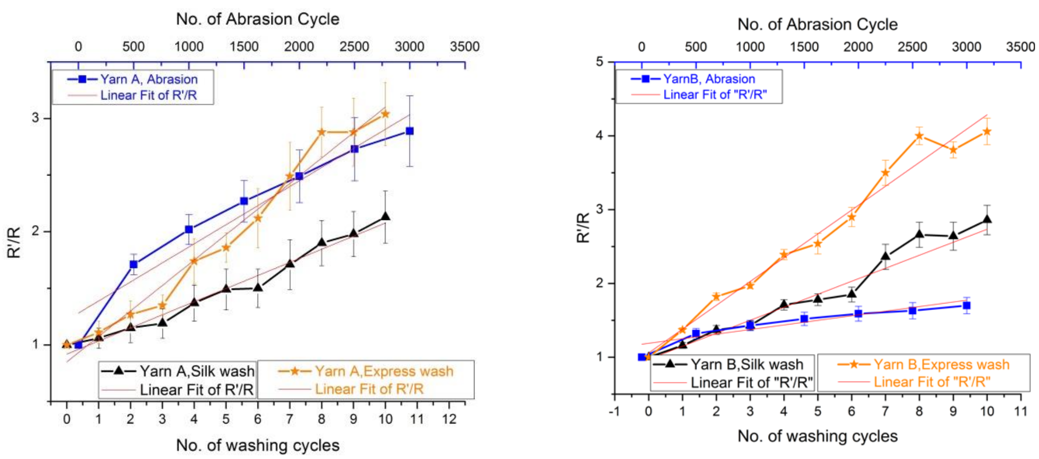

(a) (b)

Figure 4.15. (b) R'/R values after 50 washing cycles, and 3000 abrasion cycles, (a) Type A (b) Type B [2]

In Figure 4.15 all the plots show the linear trend, and adjacent R square values are presented in Table 4.1 Linear regression equations for all these plots are also added to this table. Adjacent R square values for the *Express* and *Silk* washing cycles experimented on "Type A" yarn are 0.97 and 0.98, respectively. In the case of abrasion resistance for "Type A" yarn, the adjacent R square value was 0.93, just below the threshold level of 0.95. "Type B" samples for washing tests showed adjacent R square values 0.96 and 0.97 for *Silk* and *Express* washing cycles, respectively. Martindale abrasion tests for this yarn gave the adjacent R square value of 0.85. In both yarns, a sharp increase of electric resistance change at the beginning of the abrasion test was noted, and this behavior impacted the adjacent R square values for these transmission lines. The initial abrupt increase of electrical resistance has been ignored for better fitting of the linear model by starting modeling from 500 cycles (Figure 4.16). Hence, adjacent R square values for both types of transmission lines increased well above the threshold level of 0.95. These regression equations may be used to predict the damages caused after a certain number of washing cycles or Martindale abrasion cycles.

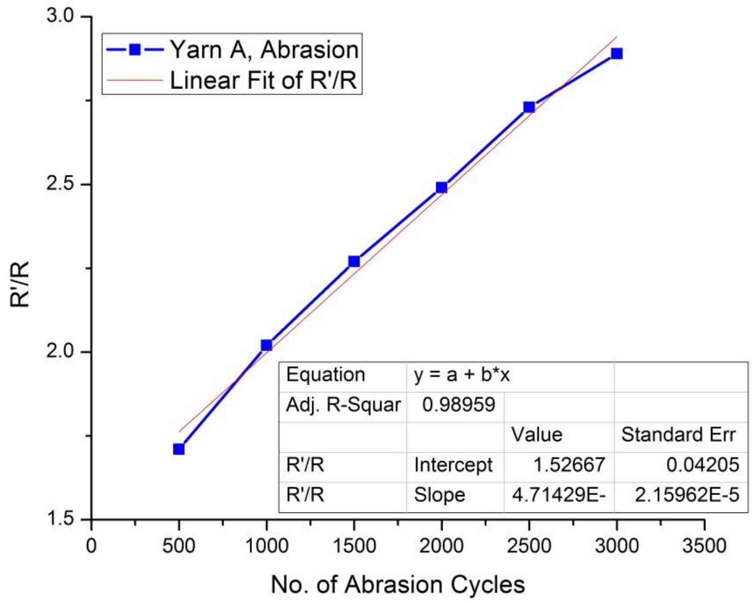

Figure 4.16. R'/R values for Type A yarn after removing initial 500 abrasion cycles [2]

With the help of comparison graphs plotted for both yarns, it is also possible to predict the equivalent numbers of abrasion cycles corresponding to washing cycles in terms of damages provoked, and thus, to skip the washing procedure. For example, in the case of "Type A" yarn, 1000 abrasion cycles gave almost equivalent damage provoked for 8 *Silk* washing cycles or 5 *Express* washing cycles. These predictions may be used to predict the number of washes e-textile prototype can withstand tolerable conductivity with the help of available abrasion resistance equipment in the laboratories. Consequently, the need to test the e-textile prototypes with multiple washing cycles may be reduced.

Table 4.1. Regression equations and Adjacent R square values for Type A and B yarns after washing, Abrasion testing, and Pilling box testing [2]

Specifications	Regression Equation (y= a+bx)	Adj. R-Sq. Value
Silk washing Yarn A	y = 0.91864 + (0.11591)*xw	0.98
Silk washing Yarn B	y = 0.93409 + (0.19173)*xw	0.97
Express washing Yarn A	y = 0.85045 + (0.22518)*xw	0.97
Express washing Yarn B	y = 1.07045 + (0.31973)*xw	0.97
Martindale test Yarn A	y = 1.28214 + (0.000584286)*xa	0.93
Martindale test Yarn B	y = 1.14714 + (0.000205714)*xa	0.85
Pilling test Yarn A	y = 1.072 + (0.000244)*xa	0.97
Pilling test Yarn B	y = 1.104 + (0.000236)*xa	0.93

"xw" is the number of washing cycles, "xa" number of abrasion cycles (Martindale or Pilling), and y is the R'/R value.

To further enhance the Martindale abrasion testing experience, these conductive transmission lines have also experimented within a wet state. The samples were immersed in water and water detergent solutions separately for 30 minutes. They were then placed on the absorbing fabric for 10 minutes to remove the excess surfaces liquids. The wetted samples were firstly tested for abrasion tests and then dried for 24 hours before the final electrical resistance measurements. Martindale abrasion tests, with wet samples, helped to get close washing stresses simulations because in this case, chemical stresses and mechanical stresses are working together simultaneously.

Although still, it is not the exact situation because, in the washing process, the samples are always immersed in the solution together with the mechanical stresses working on it. However, these experiments were executed on the three-line stitched yarns, prepared with "Type A" and "Type B" yarns.

Figure 4.17 shows the graphs plotted for these experiments. Here two trends are observed. Firstly, "Type A" yarn increased the R'/R values more than "Type B" yarn. R'/R values for "Type A" yarn were 4.32 and 5.93 for water and water detergent solutions, respectively. For "Type B" yarns, these values recorded 3.56 and 2.82 for water and water detergent solutions, respectively. This trend is already observed in dry Martindale tests, where the R'/R value for "Type A" yarn was more than "Type B" yarn. Secondly, samples wetted with only water solution showed more damages than that with water detergent solutions. It means that the detergent solution reduces the damage. The phenomenon will be explained in the chemical stresses testing discussion section. Overall, it is also observed that wet abrasion test results showed more R'/R values than the dry abrasion results. It is obvious to get more damages and higher R'/R values in this case because of the presence of chemical stresses along with mechanical stresses during the Martindale abrasion tests. Separate experiments for chemical tests are completed, and the impact of water and water detergent solutions are explained in detail in the coming discussions.

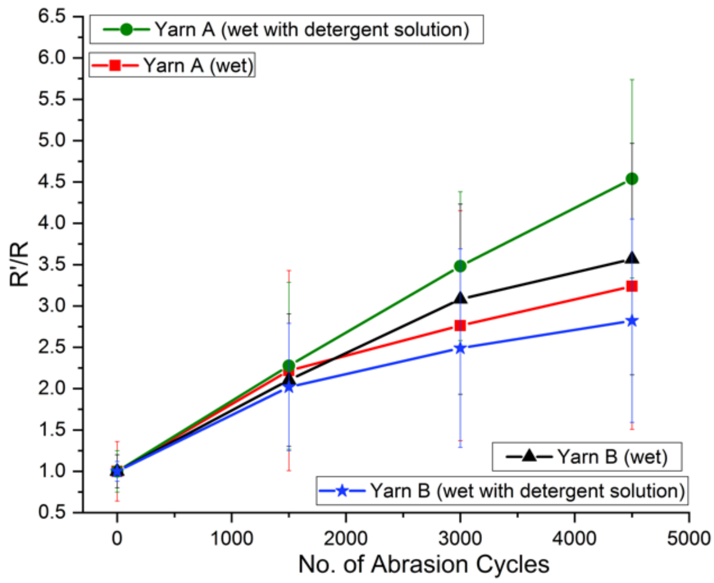

Figure 4.17. R_i/R_o values for Type A and B yarn with a three-line stitch after 4500 abrasion cycles

Finally, the surface morphology of the yarns after Martindale abrasion tests is presented in Figure 4.18. It is explained earlier that three-line stitched yarn has the advantage of passing the current through any of these lines if one is damaged due to external stresses. The samples also showed some damages on the upper surface of the transmission lines. However, these yarns were conductive enough because current can pass through other lines having contact at multiple points.

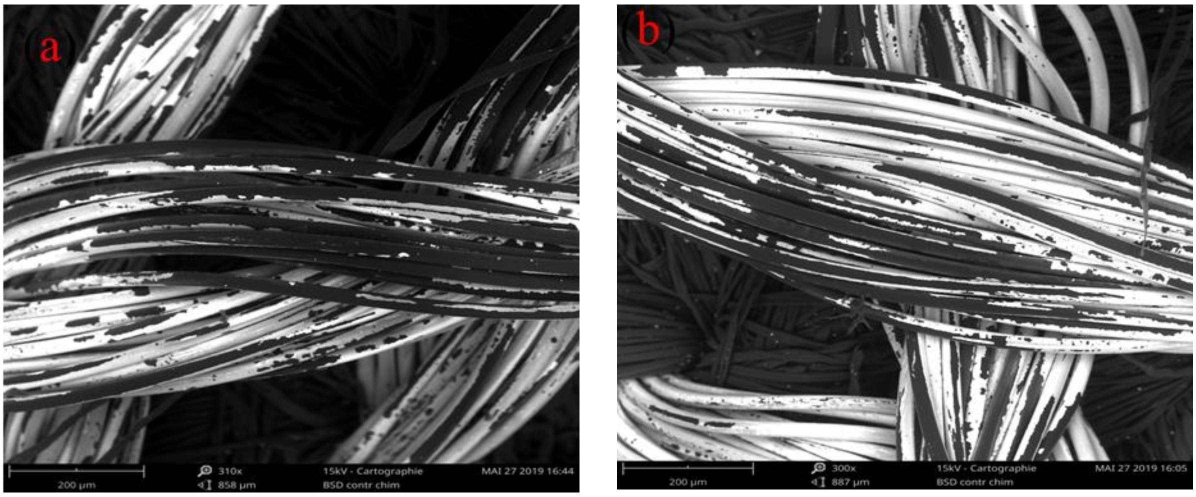

Figure 4.18. SEM analysis for Type A and B yarns after Martindale abrasion testing, black part shows the removal of conductive coating

4.2.3 Pilling Box tests

Pilling Box test was performed for three-line stitched transmission lines prepared with "Type A" and "Type B" yarns. 4000 Pilling cycles were tested for these samples, and the ratio of change in resistance from original values (R'/R) was calculated after every 1000 cycles. R'/R values after 4000 pilling cycles were 1.99 and 1.97 for "Type A' and "Type B" yarns, respectively. Like previous experiments, all these results obtained from Pilling box tests also showed the linear trend, and linear regression models can be plotted for these graphs. Table 4.1 shortlists the adjacent R square values and regression equations for these samples. The adjacent R square values were 0.97 and 0.93 for "Type A' and "Type B" yarns, respectively. Comparison plots for these results along with washing results are shown in Figure 4.19. Both pilling cycle and washing cycles exhibit the quasi-linear trend in electric resistance change against the number of pilling or washing cycles, and their R square values are above the 0.95 threshold level. The regression equations may be used to predict the change in electric resistance against a certain number of washing and pilling cycles.

The comparisons can also be used to co-relate the washing damages without actually washing the samples. For example, from the comparison graphs, it can be concluded that, in the case of "Type A' yarn, 1000 pilling cycles give equivalence damage to the transmission lines as 4 number of *Silk* washing cycles or 3 number of *Express* washing cycles. In the case of "Type B" yarns, 1000 abrasion cycles showed the equivalent change in resistance (R'/R) as 3 *Silk* washing cycles or 1 *Express* washing cycle. This equivalence may be used to predict the damage after a given number of washing cycles by performing specific pilling box test cycles in the laboratory and skipping the actual washing procedure.

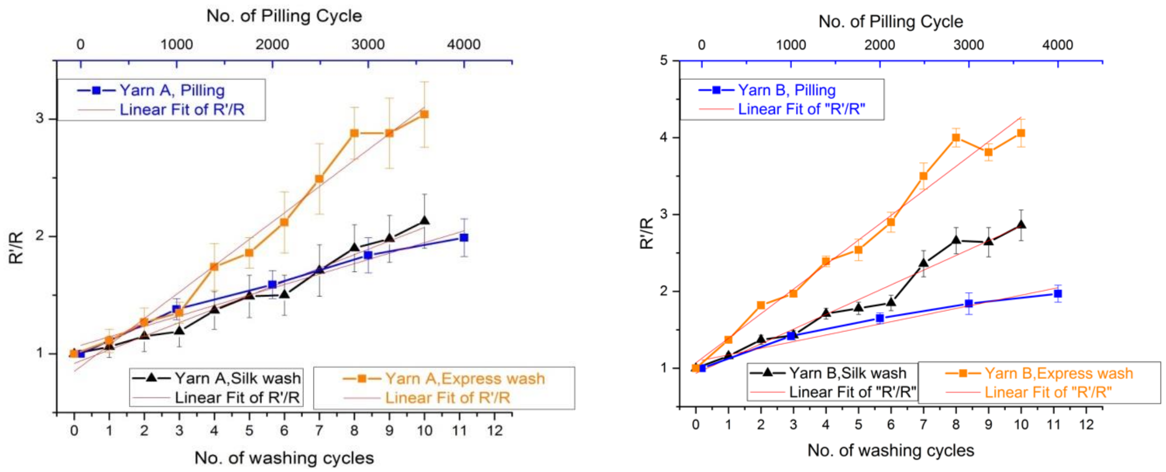

(a) (b)

Figure 4.19. R_i/R_o values for yarns with a three-line stitch after 4000 pilling cycles, (a) Type A (b) Type B [2]

4.2.4 Chemical tests

The transmission lines have been exposed to chemical tests. As both yarns are silver-plated polyamide yarns, only “Type A” yarn is used in these experiments. For these tests, 8 cm lengths of yarns were dipped in the 25 ml liquid in the beaker. Two separate sets of samples for water and water detergent solutions were used for these experiments. 1.25 g/L detergent was used in water water-detergent solution. Single yarns without any protective treatments were used to get the best possible idea of chemical stresses on these samples. The immersion duration of yarns varied between 30 minutes and 72 hours to better understand the water and detergent effects. Washing machines have different types of washing cycles, but all of them last a minimum of 30 minutes each. The washing cycle time justifies why the first reading was noted after 30 minutes dipping in liquid and repeated up to 72 hours to simulate the lifetime expected for the e-textile product. The solution temperature was maintained at 30^{o}C because, in most cases, sensitive fabrics are washed at 30^{o}C in ordinary household washing machines. Figure 4.20 describes the schematic diagram of the experimental setup for these tests.

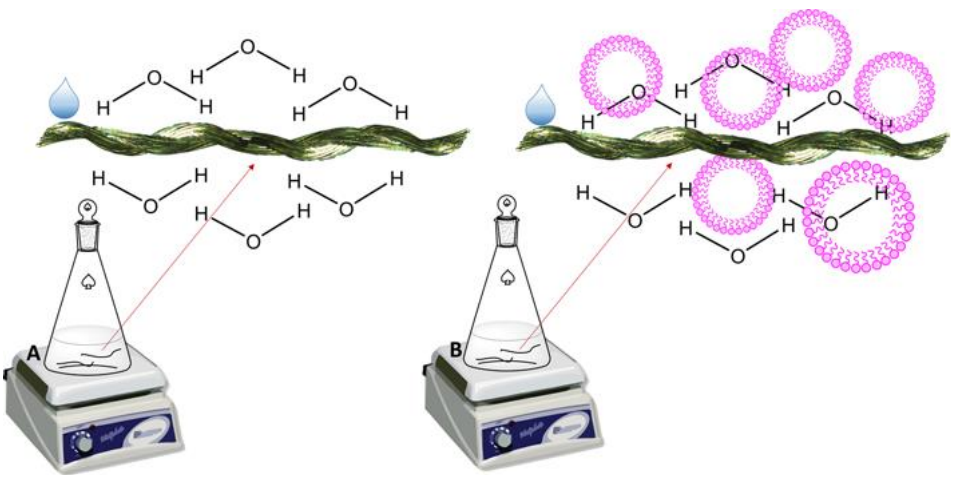

Figure 4.20. Schematic description of the experimental setup [3], (A) only water, (B) water, and detergent [3]

Initial linear resistance for all the samples was approximately 5 ohm for 8 cm length of the yarn. The samples were dipped for a maximum of 72 hours, and electrical resistance was measured after 30 minutes, 2 hours, 24 hours, 48 hours, and 72 hours. For both solutions (water and water detergent), linear electrical resistance was increased to approximately 8 ohms for all samples, as shown in Figure 4.21.

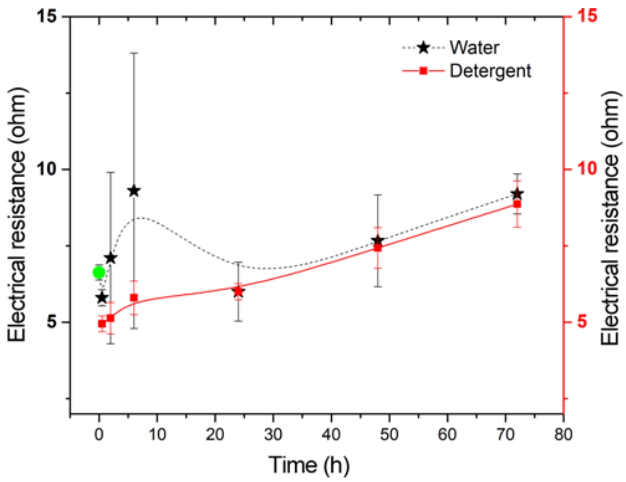

Figure 4.21. The electrical resistance of the “Type A” yarn, measured after 72 hours of immersion in the water [3]

The solution dipped samples were further investigated with the help of FTIR-ATR. The chemical structure of Polyamide fiber is explained in Figure 4.22(a). Polyamide is composed of C=O bonding, N-H bonding, C-C bonding, and C-H bonding. It is a crystalline polymer that is derived from basic amine structures, and it is quite possible to modify its properties [4]. FTIR-ATR results are presented in Figure 4.22(b) and (c) highlight various peaks assigned to different bonding. A peak around 1540 cm^{-1} is allocated to N-H bonding, resulting from in-plane bending deformation [4], [5]. Peaks at 1637 cm^{-1} and 3297 cm^{-1} are reserved for O=C stretching and N-H stretching vibration, respectively, and the width of these peaks gives an idea about the crystalline characteristics of the nylon [4], [6]. Similarly, peaks at 1200 cm^{-1} and 930 cm^{-1} were recognized as the α-crystalline phase of the polyamide [7]. Peaks at 2930 and 2860 cm^{-1} were allocated for CH_2 symmetric stretching [8].

When the yarns were immersed in water and water detergent solutions for a given time, different polyamide characteristics peaks became prominent. The polyamide peaks' presence highlights that silver coating on the polyamide surface is removed due to chemical stresses. When peak intensities were compared, the water solution has a slightly aggressive impact on the specimen surface compared to the detergent solution. Detergents are composed of different types of surfactants having hydrophilic and hydrophobic molecular structures.

Due to this extraordinary combination of detergents, they serve an exceptional property as an interfacial activity. For example, water solvents with surfactants interfacial activity displaying as an amendment in the system properties and finally decreasing the interfacial tension between the water and the adjacent phase. It also alters the wetting properties and the formation of the electrical double layer at the interface [9]. It is likewise visible that peak intensities were increased with the increasing dipping time. For the first 6 hours or so, the curve is almost straight, showing no damage at all for the silver coating. Hence, the highest peak intensities were observed for 72 hours in both water and water detergent solutions. The absorbance ratio for the yarn immersed in water is also higher than the water detergent solution (Figure 4.23).

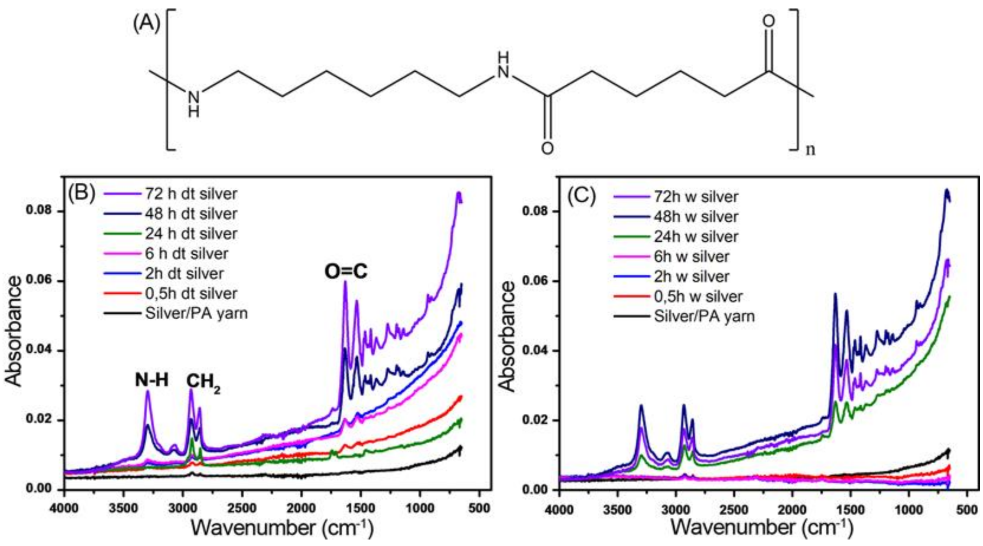

Figure 4.22. Chemical structure of polyamide yarn [3], (a), FTIR-ATR results of silver-coated PA yarns which are immersed in water detergent solution, (b) and immersed in water (c)

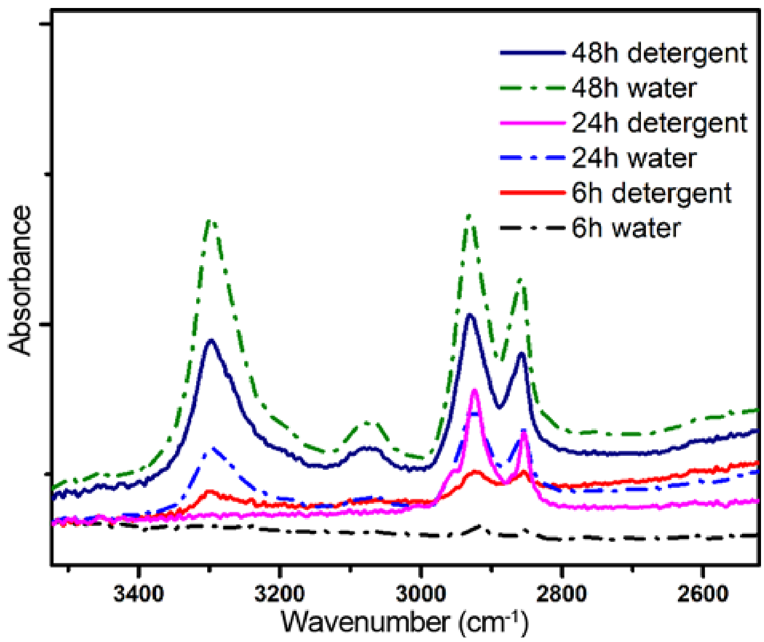

Figure 4.23. Absorbance differences of the immersed yarns water with straight lines and the detergent with the dashes [3]

The surface morphology of the yarns after 72 hours immersion in the water and water detergent solution was investigated with SEM analysis, as shown in Figure 4.24. Immersion of yarns in the liquid causes to weaken the upper conductive layer, and hence silver nanoparticles are somehow dissolved in the solutions. The conductive layer's removal highlights the inner polyamide yarns, and it is visible in black shade in the SEM analysis. It is explained earlier that water solution has a more aggressive impact on the conductive yarn, which causes the cracks at the silver plating and provokes the rupture of electrical conduction. It is also visible from the SEM pictures, where a rough surface is visible after 72 hours of immersion in the water. On the other side, the detergent solution removes the silver coating in the form of nanoparticles, and a relatively fair surface is visible in the SEM analysis.

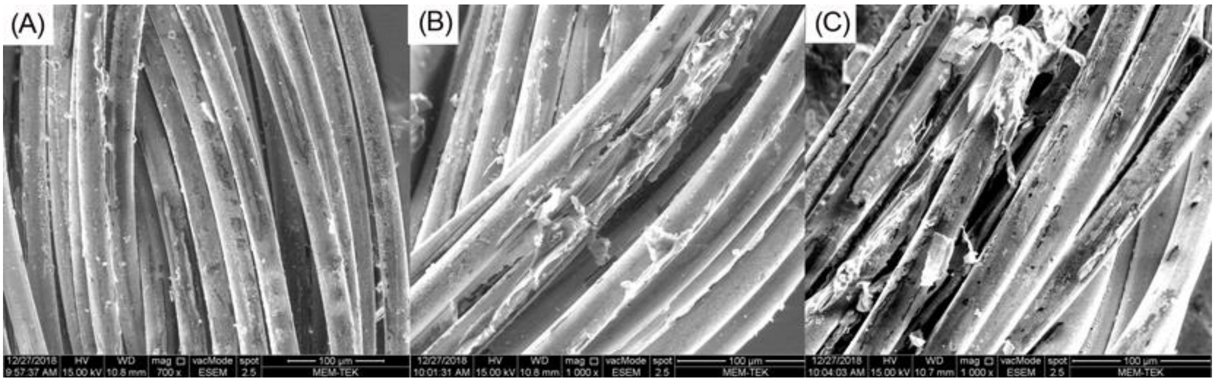

Figure 4.24. SEM images of; (A) silver-coated PA yarn before treatments, (B) silver-coated PA yarn after waiting for 72 h in water/detergent mixture, and (C) silver-coated PA yarn after waiting for 72 h in water [3]

Finally, UV-Visible Spectroscopy tests were performed to examine the remaining liquids after the 72 hours of immersion of the yarns in these liquids. Water and water detergent solutions before the experiment were used as the reference cell. This test was performed to detect any silver nanoparticles present in the solution. Obtained peak (Figure 4.25) verifies SEM analysis and previous results by detecting the nanoparticles in the water and water detergent solutions.

A broader peak visible around 424 nm is related to silver nanoparticles [10], [11]. The doublet peaks in the range of 500-600 nm may be recorded caused by the different silver nanoparticle sizes [12]. Peaks at the 575 nm region are also due to the silver nanoparticles' presence in the solutions [13]. The absence of the peaks in the water solution indicates that water has an aggressive impact, and it causes the peel off from the surface of the conductive yarn. Hence, the silver layers are not mixed within the solution as the detergent solution with nanoparticles.

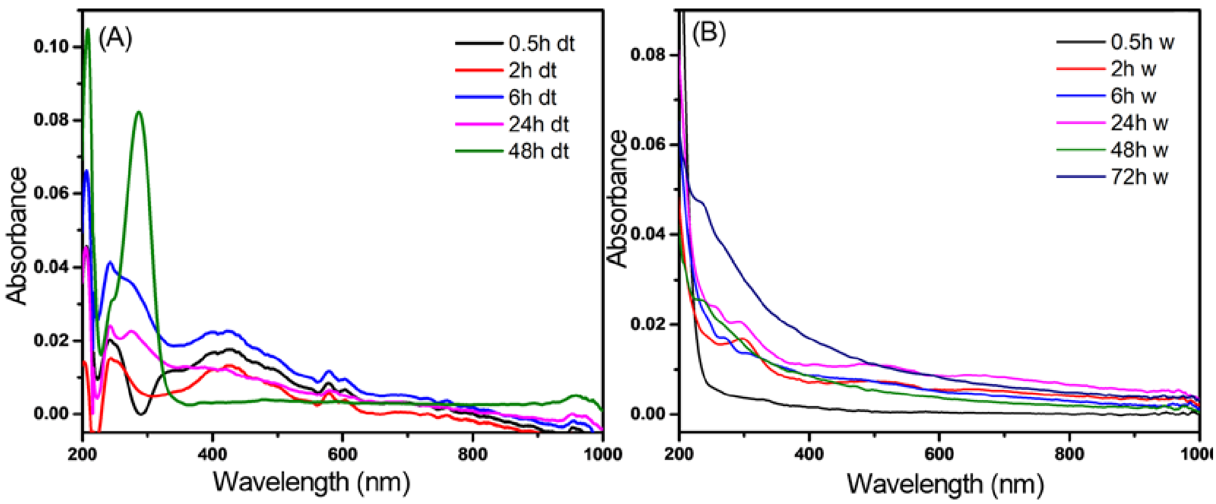

Figure 4.25. UV-Visible results of remained liquids (A) water with detergent and (B) water after immersion of yarns [3]

4.3 Skin electrodes

4.3.1 Washing tests

Prepared ECG skin electrodes were washed up to 50 washing cycles. Surface resistance was measured using the four-probe device, and R_i/R_o (ratio of change in surface resistance from the original value) was calculated. ECG measurement was recorded before and after 50 washes. Six samples for each kind of fabric were developed for both *Silk* and *Express* wash cycles. F1-F4 sample coding was used for fabricated sheet electrodes and E1-E2 for embroidered electrodes. In all further experiments, this coding was discussed.

Figure 4.26 and Figure 4.27 show the surface resistance behavior in the response of *Silk* washing cycles for fabricated skin electrodes (F1-F4). In all graphs, the left y-axis measures the ratio of surface resistance from the original value. The right y-axis (where available) explains actual surface resistance (Ohm/Sq.) measured by the four-probe device. F1 and F4 types of the skin electrodes did not show much deviation from the primary surface resistance properties even after 50 wash cycles. These electrodes were silver-based conductive fabric electrodes, and their initial surface resistance was relatively higher than F2 and F3. The initial values for F1 and F4 were 0.33 and 1.45 ohm/sq., respectively, whereas it was 0.038 and 0.042 ohm/sq., for F2 and F3, respectively. Both F2 and F3 electrodes were copper-based electrodes, and resistance started increasing after the first wash cycle. After 50 *Silk* washing cycles, resistance was increased 10 and 15 times respectively for F2 and F3 type electrodes.

Their final surface resistance was 0.35 and 0.65 ohm/sq., respectively. Those values were less than initial surface resistance values for F1 and F4, even after 50 washing cycles. The skin-electrode conductivity was fair enough to get ECG signals of good quality, thanks to low initial surface resistance values. In *Silk* wash, all four types of electrodes gave acceptable quality ECG signals, even after 50 wash cycles.

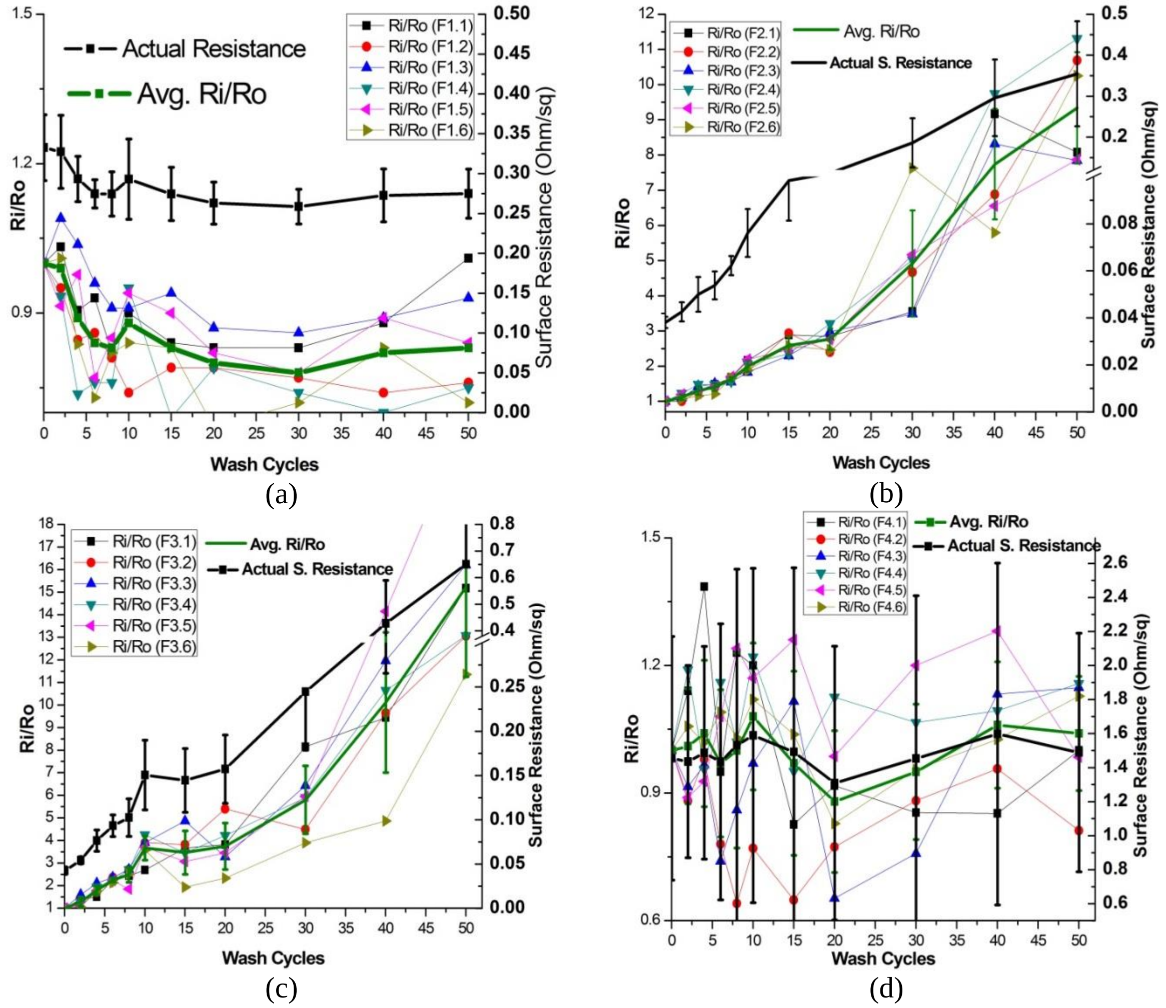

Figure 4.26. Surface resistance analysis (*Silk* wash), six samples of each electrode were tested, Fi.1 – Fi.6. The left Y-axis explains R_i/R_o, and the right Y-axis describes the actual surface resistance for each sample [14]. (a)F1 electrodes (b) F2 electrodes (c) F3 electrodes (d) F4 electrodes

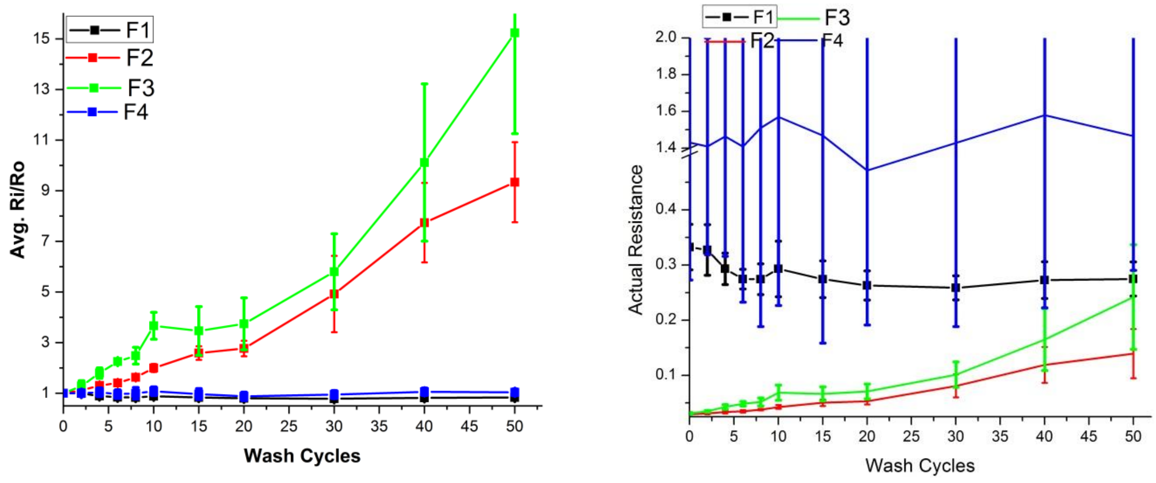

(a) (b)

Figure 4.27. Surface resistance analysis (*Silk* wash). Evaluation of all samples (F1-F4) together in one graph [14], (a) Comparison of Ri/Ro, (b) Comparison of actual surface resistance

The case of *Express* washing cycles, as explained earlier, have higher washing speed and more intense mechanical actions are undergoing during the wash. In this case (Figure 4.28 and Figure 4.29), F2 and F3 electrodes lost their conductivity entirely after the 10 wash cycles. F1 and F4 skin electrodes maintained conductive behavior, and an increase in surface resistance was less than 1.15 times from initial values.

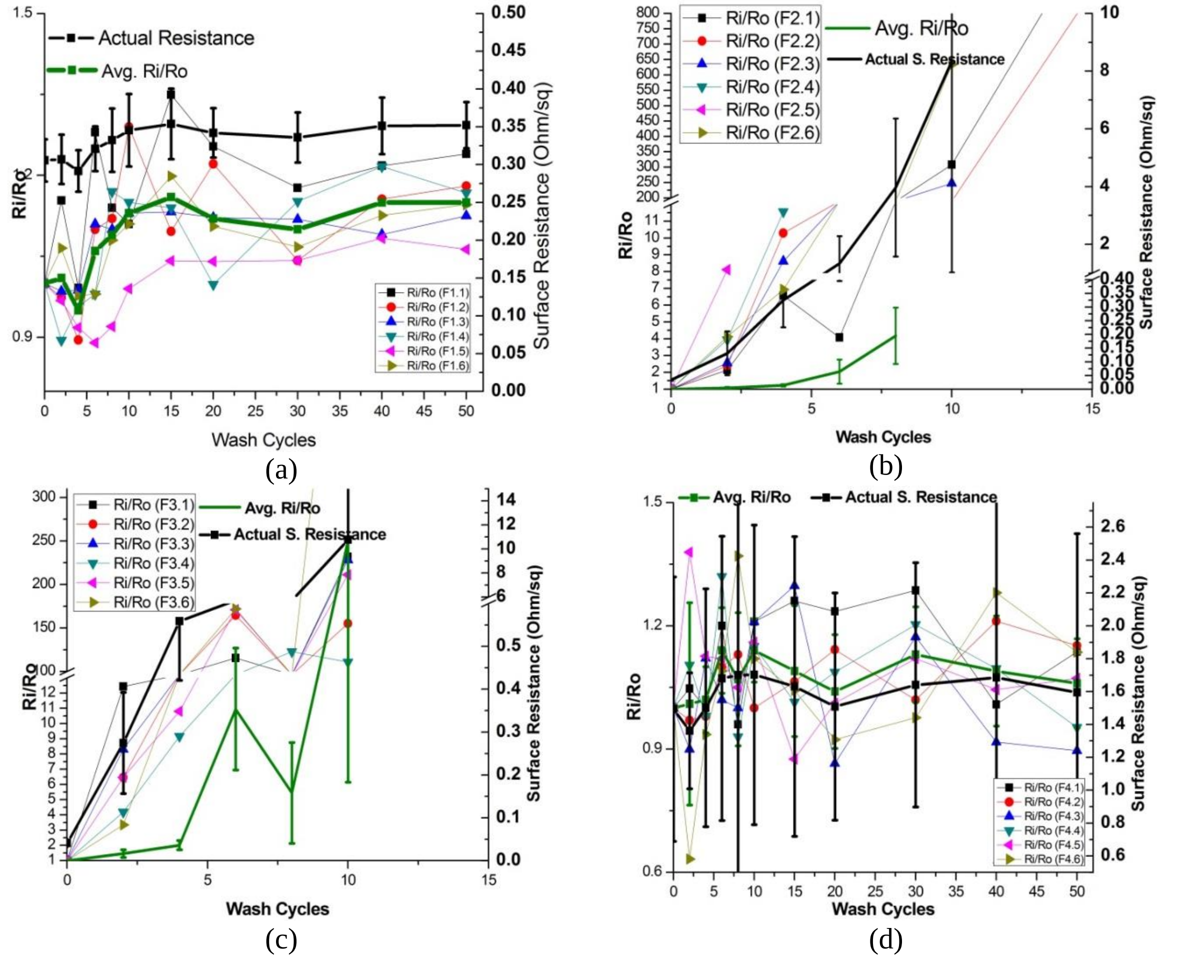

Figure 4.28. Surface resistance analysis (*Express* wash), six samples of each electrode were tested, Fi.1 – Fi.6. Fi.1 – Fi.6. Left Y-axis explain R_i/R_o, right Y-axis describe the actual surface resistance for each sample [14], (a)F1 electrodes (b) F2 electrodes (c) F3 electrodes (d) F4 electrodes

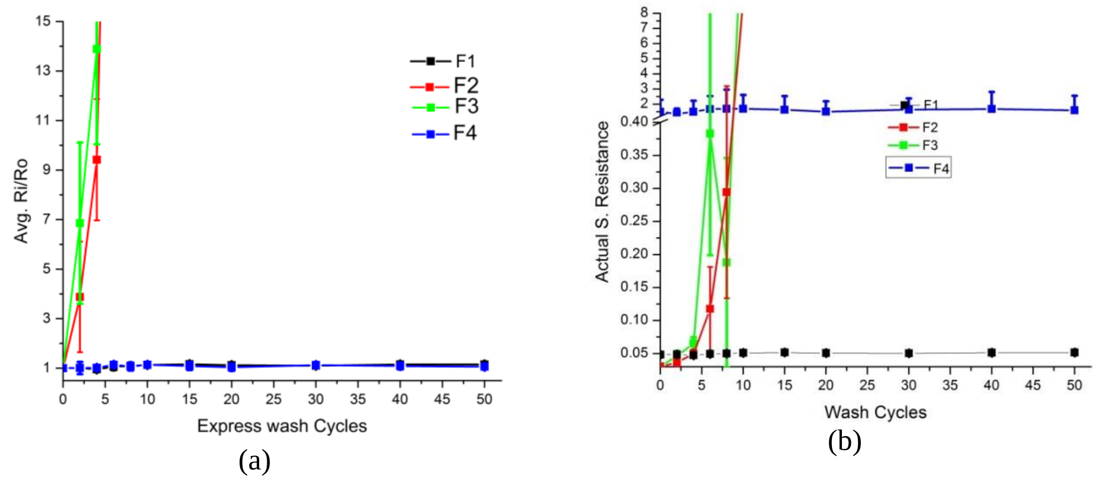

Figure 4.29. Surface resistance analysis (*Express* wash). Evaluation of all samples (F1-F4) together in one graph [14], (a) Comparison of Ri/Ro (b) Comparison of actual resistance

ECG monitoring was performed before and after 50 wash cycles for all electrodes used in these experiments. Figure 4.30 shows the ideal ECG graph. The P wave describes the atrial depolarization and the T wave gives ventricular repolarization. The QRS complex corresponds to a specific part of the ECG considering Q, R, and S waves that corresponds to the depolarization of the right and left ventricles of the human heart. ECGs are plotted with time on the horizontal and voltage on the vertical axis. Figure 4.31 highlights the testing subject sitting in an idle position with the ECG belt tightened on the body.

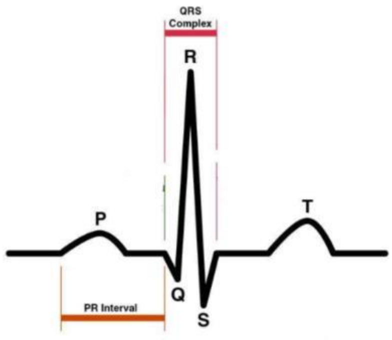

Figure 4.30. Normal ECG morphology

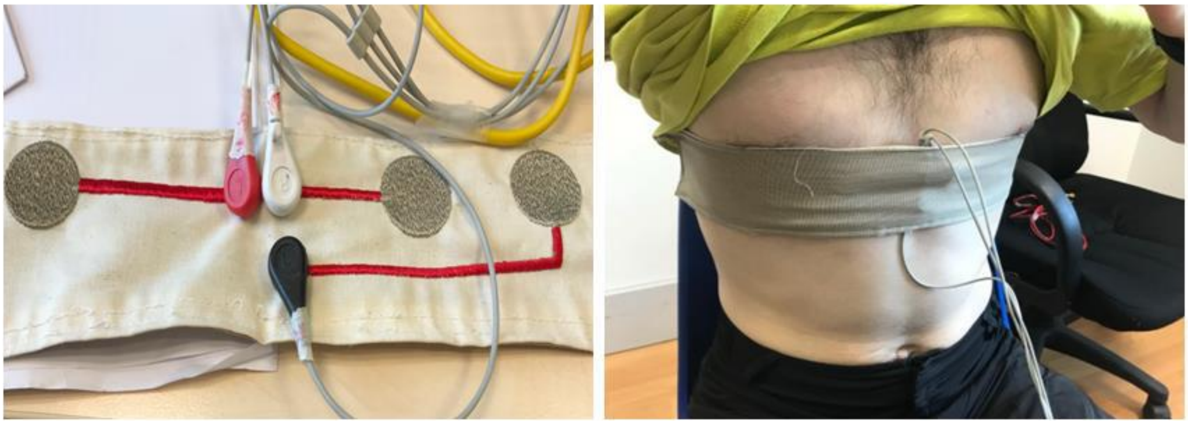

Figure 4.31. ECG recording belt

The electrodes detected the electrocardiographic waves noticeably after 50 *Silk* washing cycles (Figure 4.33). P, Q, R, S, T waves, and QRS complex can be distinguished easily in all these curves. The ECG detectable waves are quite clear and it has been stated by the cardiologists that the ECG sensor electrodes were medical grade. Power Spectral Density (PSD), before and after the washing, was plotted in Figure 4.32. Power spectral density is not detonated for all samples at frequency domain < 5Hz, which indicates the ECG signal domain. On the other side, for *Express* washing cycles, F2 and F3 skin electrodes did not sense any signals at all, and P, Q, R, S waves are not detectable, as shown in Figure 4.35.

Power spectral density for these two types of electrodes (after *Express* washing cycle) also displayed degradation all over the spectral, including < 5Hz frequency domain (Figure 4.34).

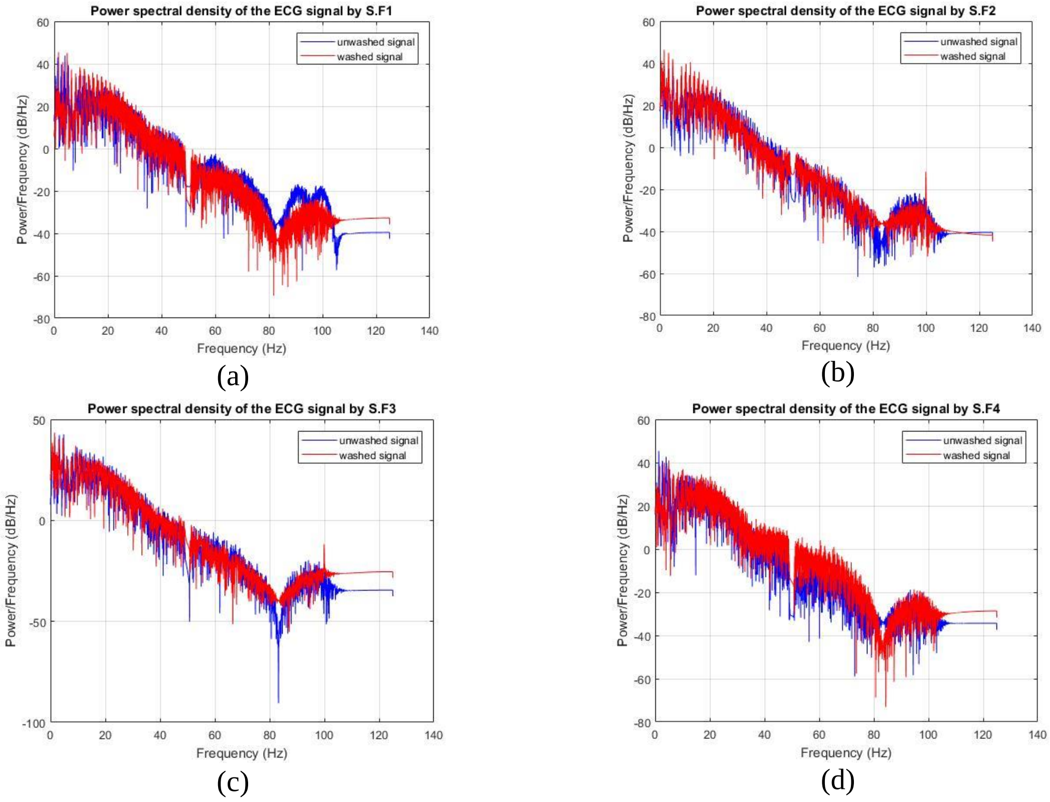

Figure 4.32. Power spectral density (*Silk* wash) before and after the 50 washing process [14], (a) F1 (b) F2 (c) F3 (d) F4

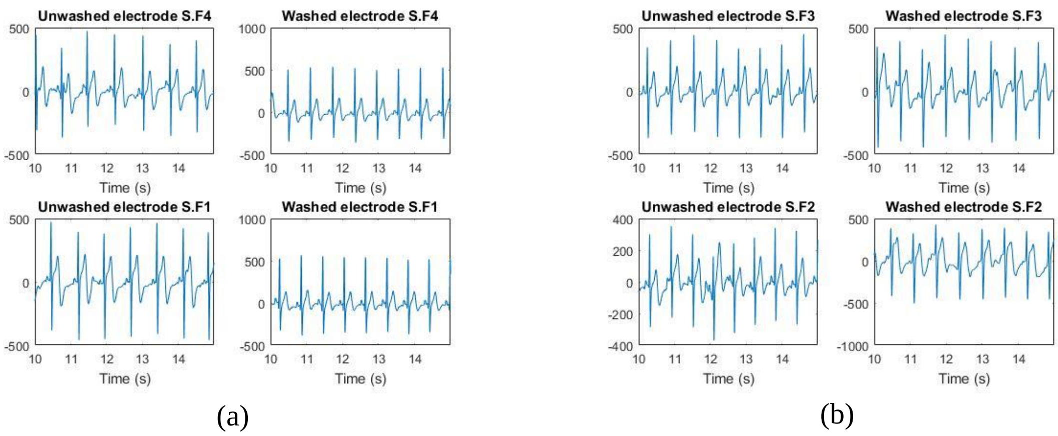

Figure 4.33. ECGs measured (*Silk* wash) before and after the 50 washing process [14]. (a) F1 and F4 (b) F2 and F3

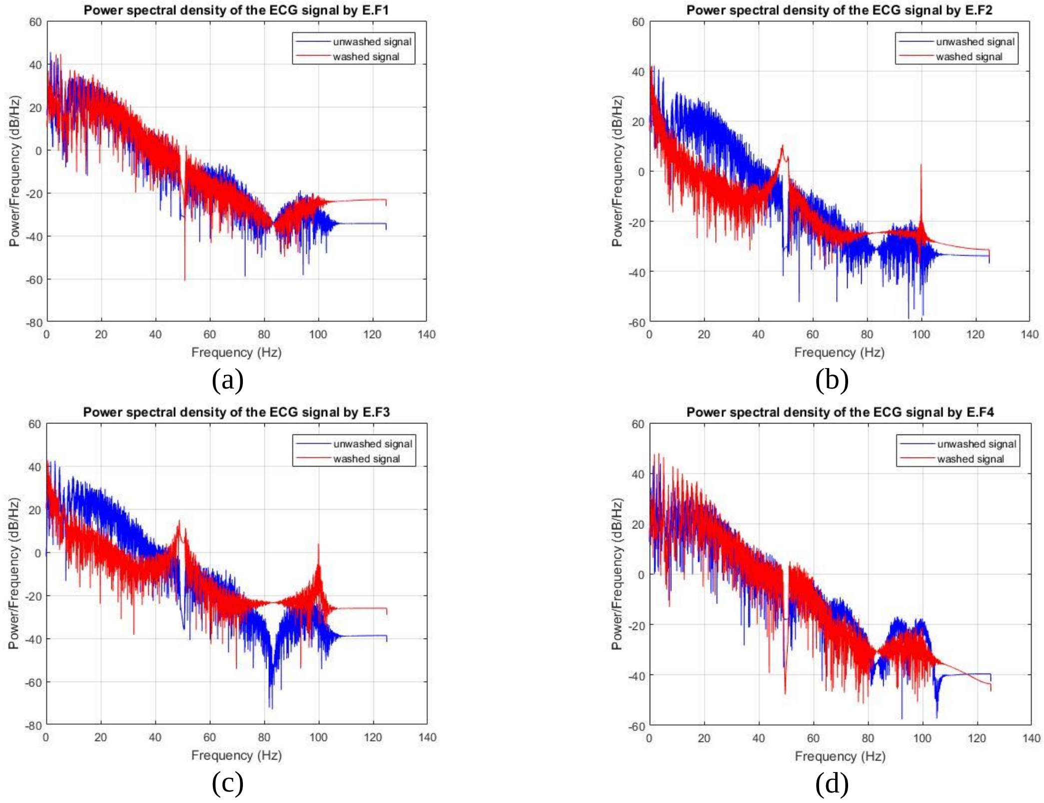

Figure 4.34. Power spectral density (*Express* wash) before and after the 50 washing process [14], (a) F1 (b) F2 (c) F3 (d) F4

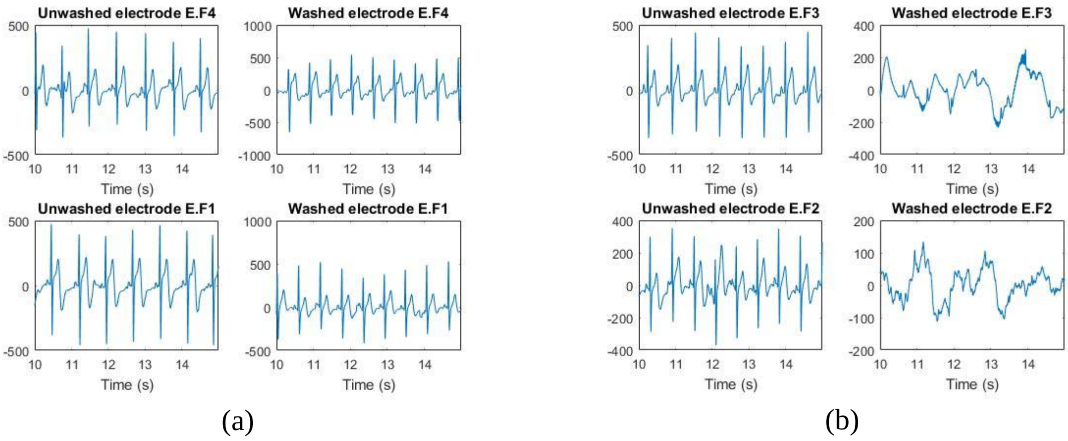

Figure 4.35. ECGs measured (*Express* wash) before and after the 50 washing process [14], (a) F1 and F4 (b) F2 and F3

These electrodes are further investigated by SEM analysis. Figure 4.36 presents the SEM images for them. It was noted that for F2 and F3 type of electrodes, the copper layer was peeled off from the nylon base fibers after washing experiments. It concludes that adhesion between Copper and Copper/Nickel coating and base Nylon fiber was not good enough to withstand the washing stresses. It lost strength either by mechanical or chemical stresses during the washing process. Indeed, copper is excellent in terms of electrically conductive properties, and it is visible from initial low resistance values. However, these values increased rapidly in the washing process, especially in the *Express* washing process, which has a higher washing speed and, ultimately, more washing stresses. Hence, we can conclude that adhesion between Copper and Nylon in these specific types of conductive fibers can withstand only mild stresses as in *Silk* washing cycles. It starts degrading as the level of stress increases.

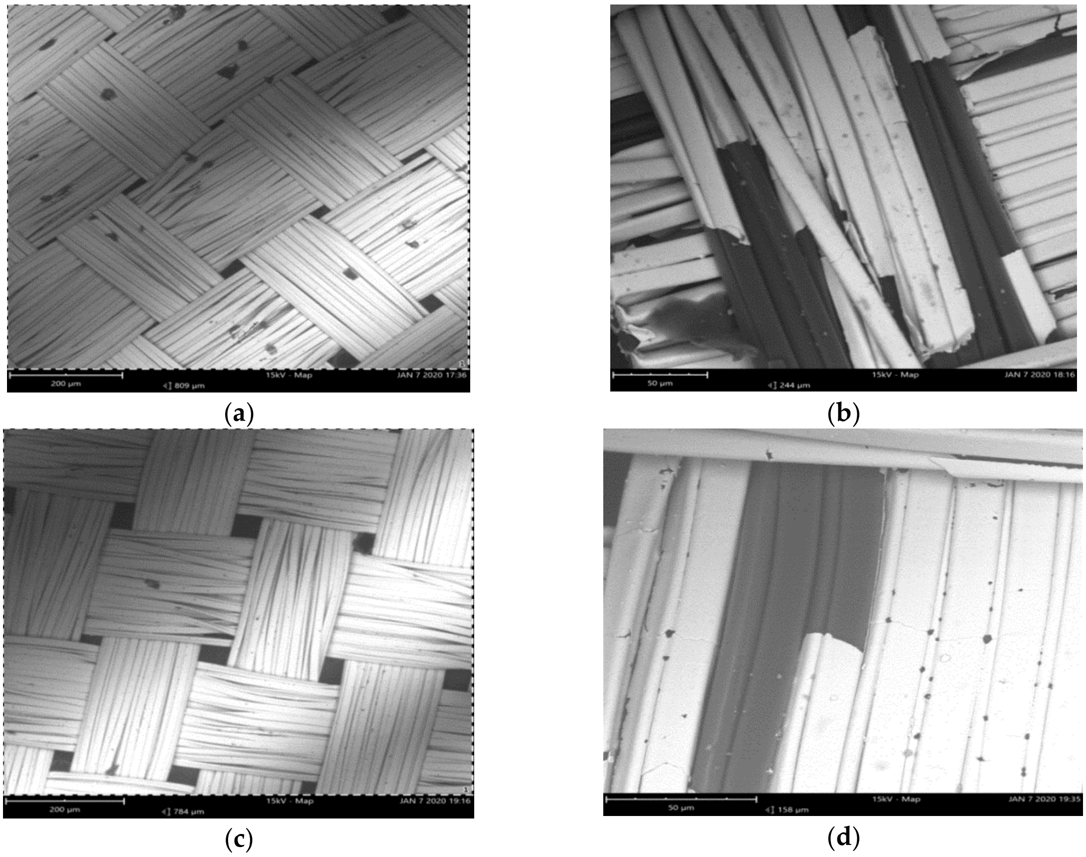

Figure 4.36. SEM analysis performed before and after the 50 *Express* washing processes, (a) F3 before wash (b) F3 after wash (c) F2 before wash (d) F2 after wash

On the other side, silver-based conductive yarns have good adhesion between silver and nylon base fibers and can withstand intensive washing stresses. Their initial values are higher because silver is not a good conductor when compared with copper. SEM analysis of these electrodes also showed almost no significant damages on the surface excepting some minor holes created in random places, as shown in Figure 4.37.

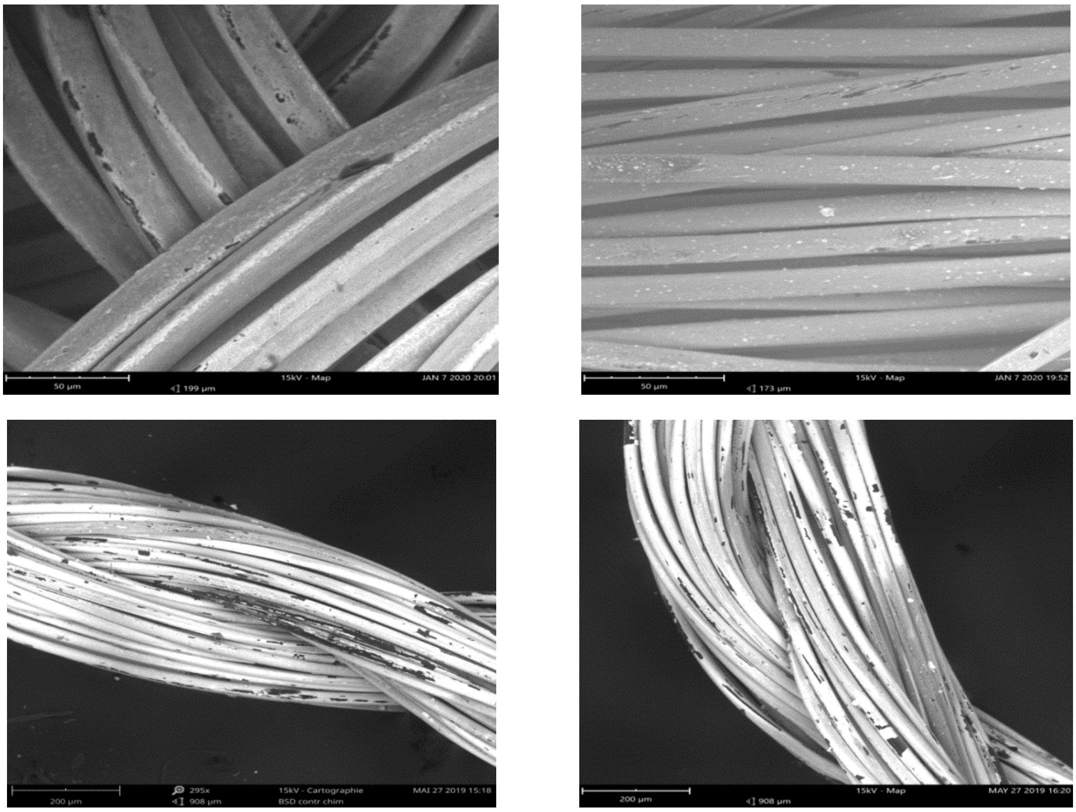

Figure 4.37. SEM analysis performed after the 50 *Express* washing processes, (a) F1 electrode (b) F4 electrode (c) E1 electrode (d) E2 electrode

All these experiments were repeated separately for embroidered bases electrodes E1 and E2. These electrodes had an initial average surface resistance of 0.14 and 0.23 ohm/sq., respectively. As in previous experiments, these electrodes were washed up to 50 washing cycles for *Silk* and the *Express* washing cycles. In all samples increase in surface resistance was less than 1.3 times the initial values (Figure 4.38 and Figure 4.39). This change was nominal and can be neglected.

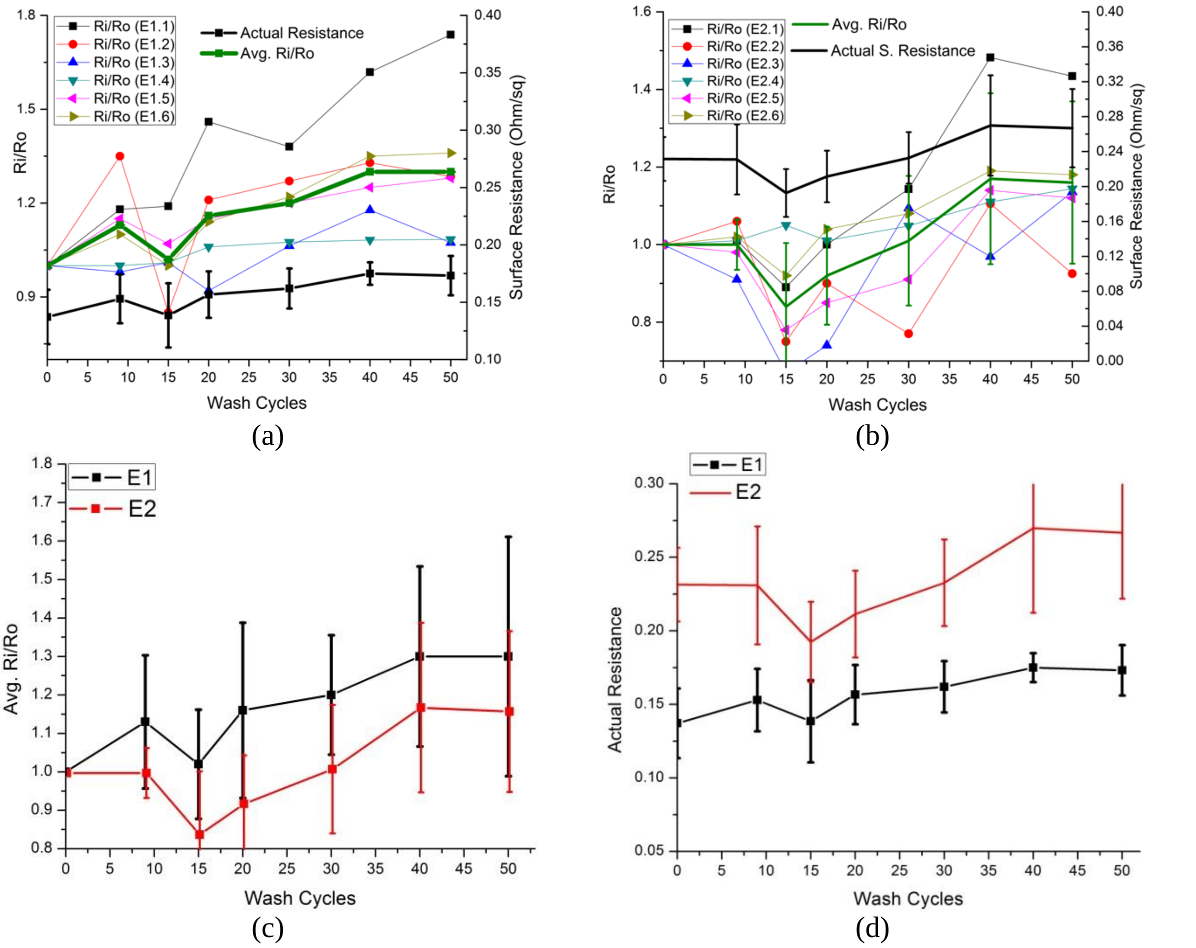

Figure 4.38. Surface resistance analysis (*Express* wash), six samples of each electrode were tested, Left Y-axis explains R_i/R_o, right Y-axis (where applicable) describe the actual surface resistance for each sample [14], (a) E1 electrode (b) E2 electrode (c) Comparison of Ri/Ro for all samples (d) Comparison of actual surface resistance for all samples

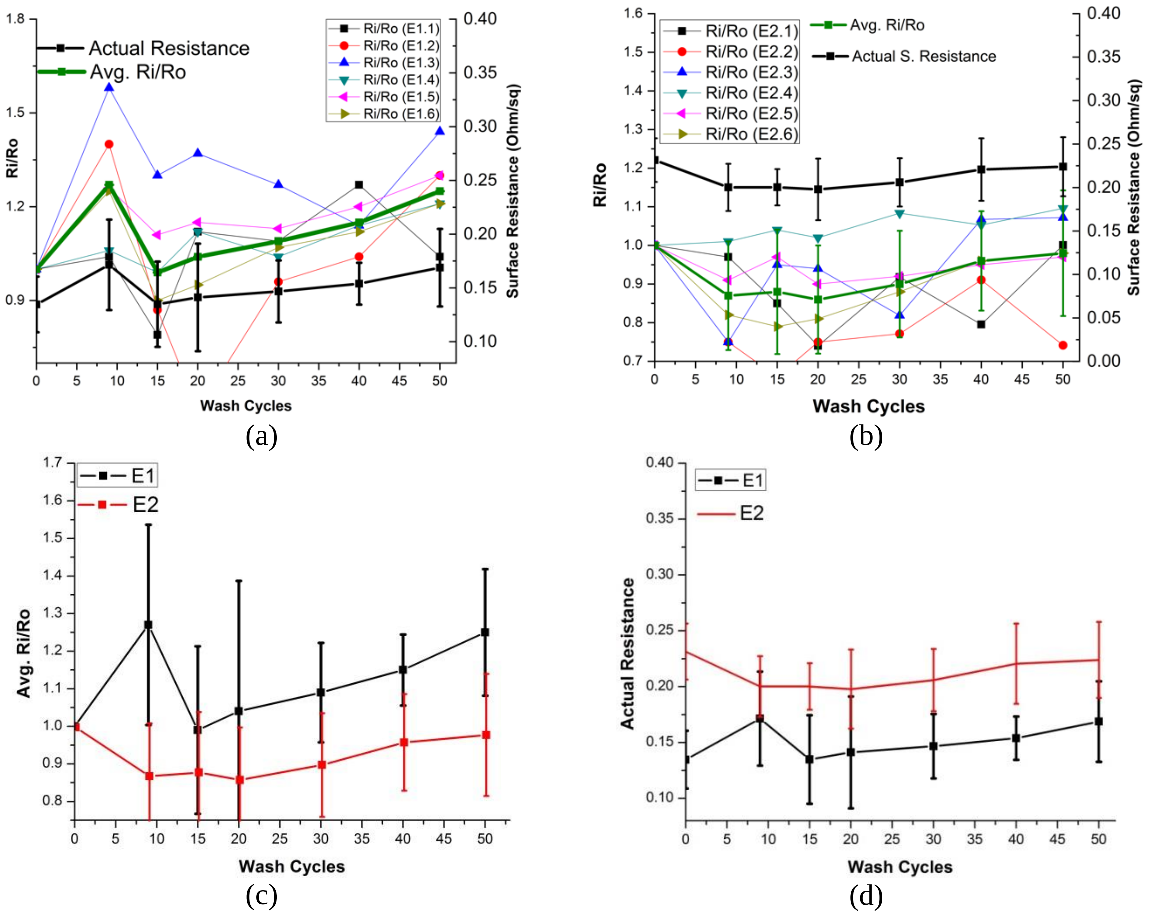

Figure 4.39. Surface resistance analysis (*Silk* wash), six samples of each electrode were tested, Left Y-axis explains R_i/R_o, right Y-axis (where applicable) describe the actual surface resistance for each tested sample [14], (a) E1 electrode (b) E2 electrode (c) Comparison of Ri/Ro for all samples (d) Comparison of actual surface resistance for all samples

These electrodes were then used for an ECG analysis. The electrocardiographic (ECG) waves are good enough to detect all peaks required to conclude good ECG signals. Similarly, power spectral density (PSD) also showed no degradation at a low frequency suitable for ECG measurement (Figure 4.40 and Figure 4.41).

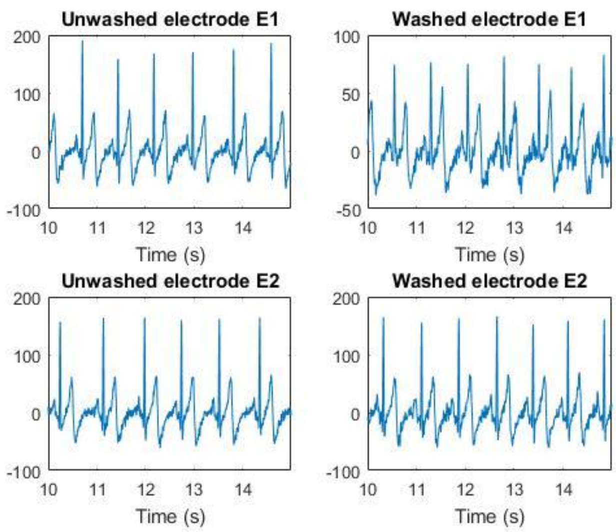

Figure 4.40. ECGs measured (*Express* wash) before and after the 50 washing process for E1 and E2 electrodes [14].

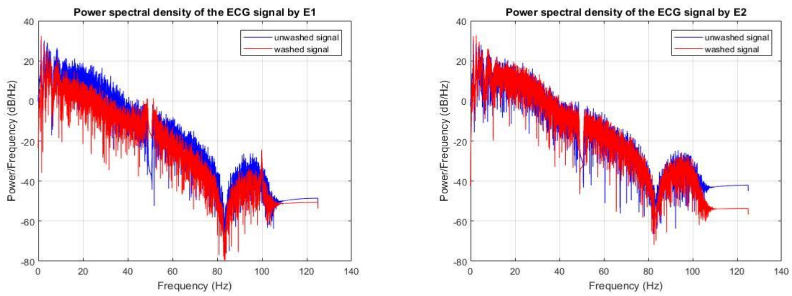

(a) (b)

Figure 4.41. Power spectral density (*Express* wash) before and after the 50 washing process [14], (a) E1 electrode (b) E2 electrode.

4.3.2 Martindale abrasion resistance test

As discussed, the washing cycle experiences different sorts of washing stresses working in it, and among these stresses, mechanical and chemical are the most damaged ones [2]. For the simulation of these mechanical forces, Martindale abrasion resistance experiments were executed. Although the effect of mechanical forces performed separately may be changed from the impact when performed in combination with other stresses during the wash process. However, the mechanical tests are executed separately to assume damages.

Overall, 10,000 abrasion cycles were performed on the skin electrodes. Figure 4.42 and Figure 4.43 highlight surface resistance change concerning the abrasion cycles for electrode samples F1 to F4. In all these samples, surface resistance increase was negligible after 10,000 abrasion cycles.

When we compare these results with washing results, F1 and F2 electrodes' behaviour in Martindale tests can be justified because they did not change the resistance values after 50 washing cycles. In the case of F2 and F3 skin electrodes, abrasion resistance showed a small change in resistance which was contrary to washing results where these electrodes were utterly damaged in *Express* washing cycles and showed surface resistance change in the acceptable range for *Silk* washing cycles. The *Silk* wash cycle involves reduced mechanical stresses compared to *Express* wash, and these samples were good enough to withstand these stresses. It was concluded that only abrasion resistance stress was not enough to peel out the upper copper layer attached with the base nylon material. However, it is already explained that different types of stresses work together in the washing process, and their impact can be different when performed separately. To further clarify those problems, chemical stresses were investigated separately on the skin electrodes.

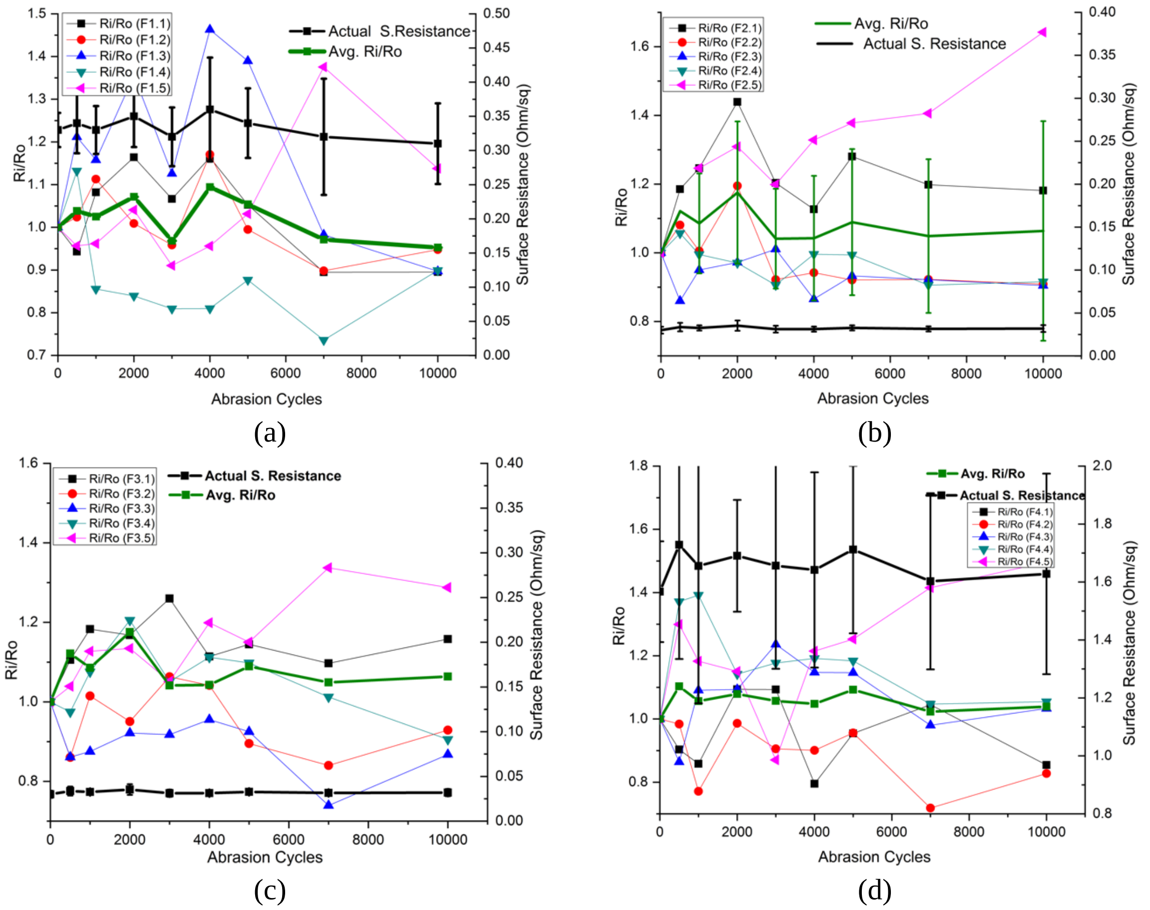

Figure 4.42. Surface resistance analysis after 10,000 abrasion cycles, five samples of each electrode were tested (Fi1-Fi5), Left Y-axis explains R_i/R_o, right Y-axis describe the actual surface resistance for each sample (a) F1 (b) F2 (c) F3 (d) F4

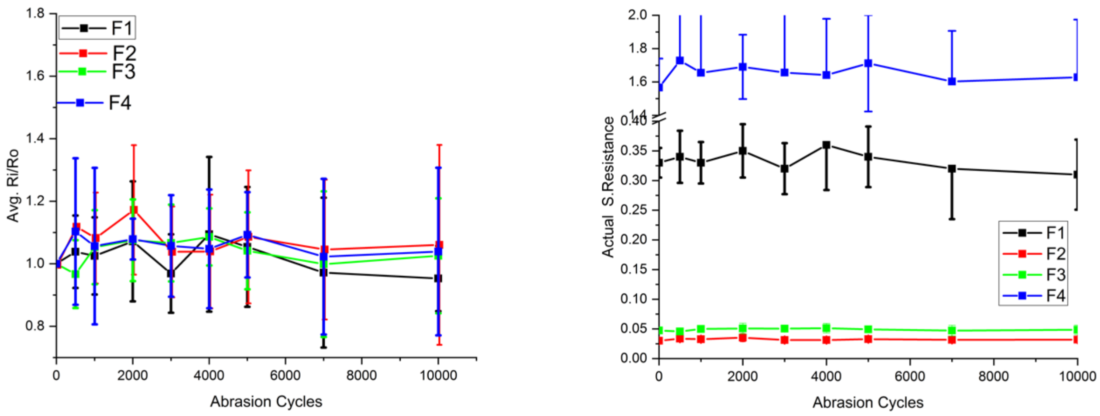

(a) (b)

Figure 4.43. Surface resistance analysis after 10,000 Abrasion cycles, evaluation of all samples together (F1-F4) (a) Comparison of Ri/Ro (b) comparison of actual surface resistance

Although there is minor change in surface resistance for F2 and F3 skin electrodes, SEM surface analysis showed slight marks of the peel-off layer at random positions. These damages did not impact the electrodes' overall properties as they are negligible compared with the broad surface. These marks are shown in Figure 4.44.

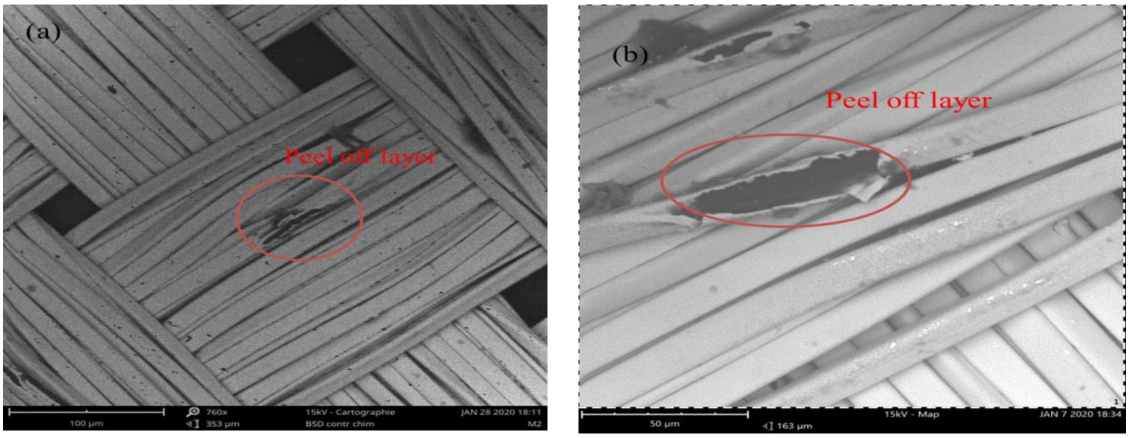

Figure 4.44. The surface investigation by SEM images, Peel-off at random positioned is circled

Those experiments were also repeated for embroidered skin electrodes type E1 and E2. Figure 4.45 highlights the change in resistance from original values for embroidered skin electrodes E1 and E2. In comparison between E1 and E2, E1 electrodes increased their surface resistance almost 2 times after 10,000 abrasion cycles, whereas it is just 1.2 times in E2 skin electrodes. It means that E2 electrodes were good enough to withstand the abrasion resistance test in contrast with E1 electrodes. The same trend was also observed in washing experiments, where E1 skin electrodes were more damaged than E2 electrodes, both in *Express* and *Silk* washing cycles. Hence, the hypothesis can be generated that the change in resistance due to the Martindale abrasion test is directly related to the washing damages.

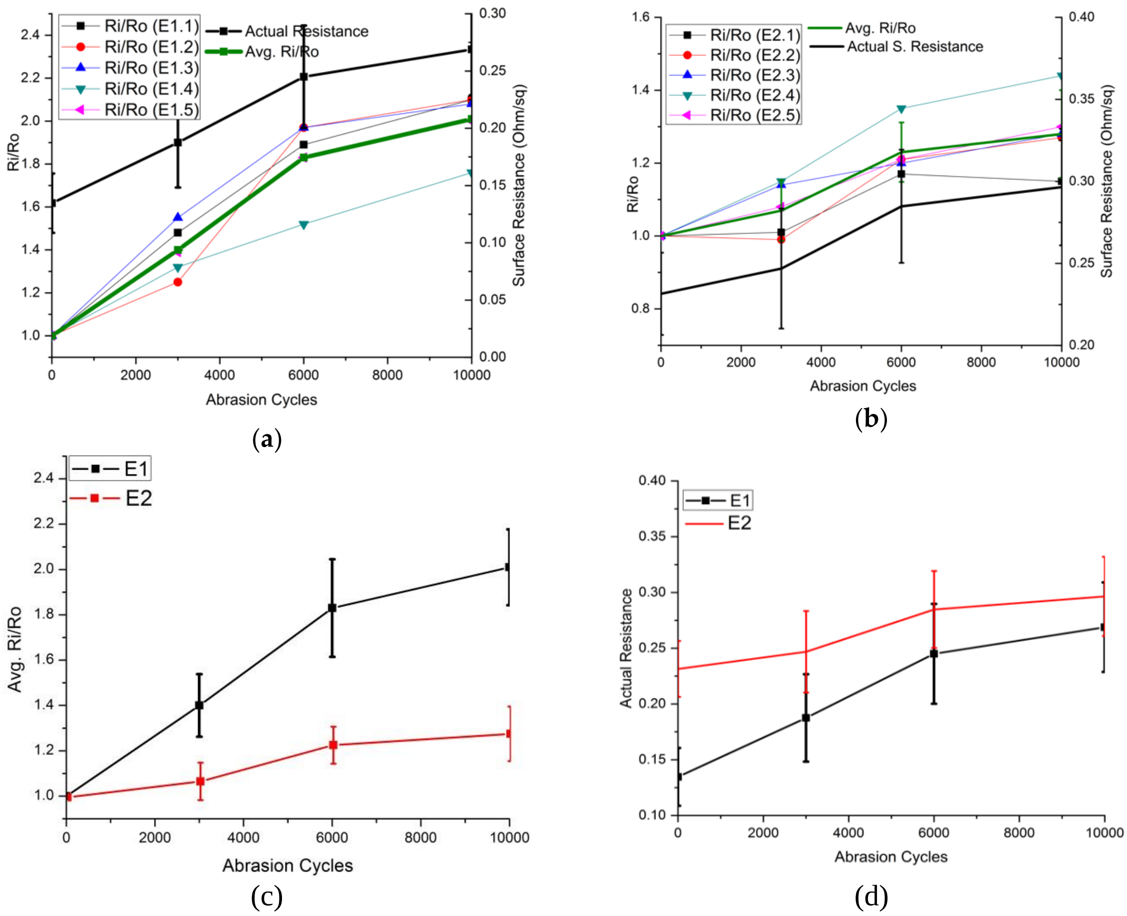

Figure 4.45. Surface resistance analysis after abrasion cycles, five samples of each electrode were tested (Ei1-Ei5), Left Y-axis explains R_i/R_o, right Y-axis (where applicable) describe the actual surface resistance for each sample [14], (a) E1 electrodes (b) E2 electrodes, (c) Comparison of Ri/Ro for E1 and E2, (d) comparison of actual surface resistance for E1 and E2

4.3.3 Pilling Box tests

The skin electrodes were also tested for Pilling box tests to provoke the possible damages co-related with the washing damages. All the samples were experienced up to 10,000 Pilling cycles, and change in surface resistance from their initial resistance was measured with the help of a Four-probe testing device.

Figure 4.46 and Figure 4.47 explain the R_i/R_o and actual surface resistance for skin electrodes. F1 and F4 electrodes showed almost no change in surface resistance from their original values even after 10,000 Pilling cycles. This trend is the same as in washing tests and Martindale abrasion tests, where these electrodes showed promising results after various experiments. F2 and F3 electrodes increased their surface resistance after 10,000 Pilling cycles, and these damages again confirmed the weak adhesion between the upper conductive coating and base nylon fibers. Although this increase was significantly less compared with washing tests, it is visible among all the samples and can be differentiated. These electrodes do not need to have the same ratio of damages in all experiments. Various test methods will have a different percentage of damaging impacts on the samples and may be used to differentiate from other samples. Any highlighted damages from these samples can be helpful to predict and to co-relate them from washing wears.

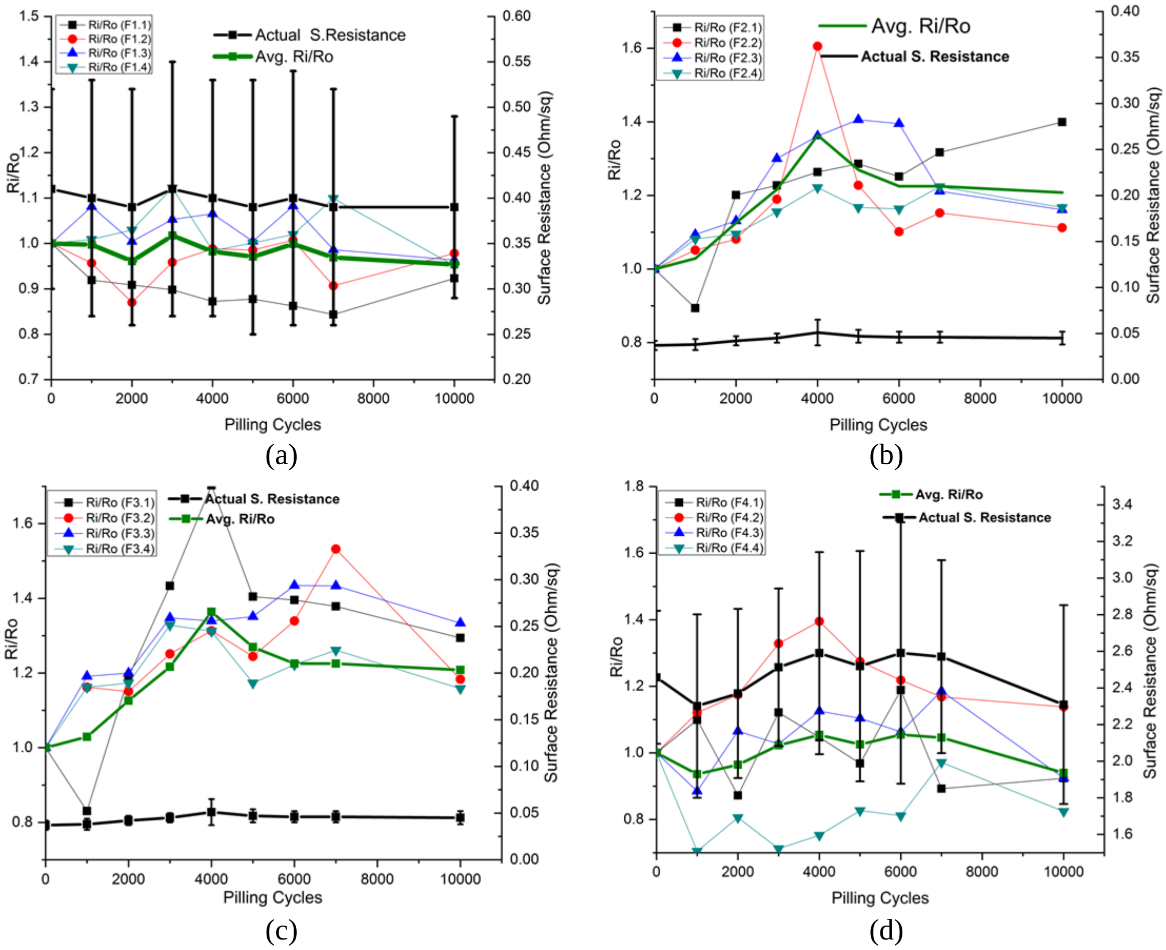

Figure 4.46. Surface resistance analysis after 10,000 pilling cycles, four samples of each electrode were tested (Fi1-Fi4), Left Y-axis explains R_i/R_o, right Y-axis describe the actual surface resistance for each sample [14], (a) F1, (b) F2, (c) F3, (d) F4

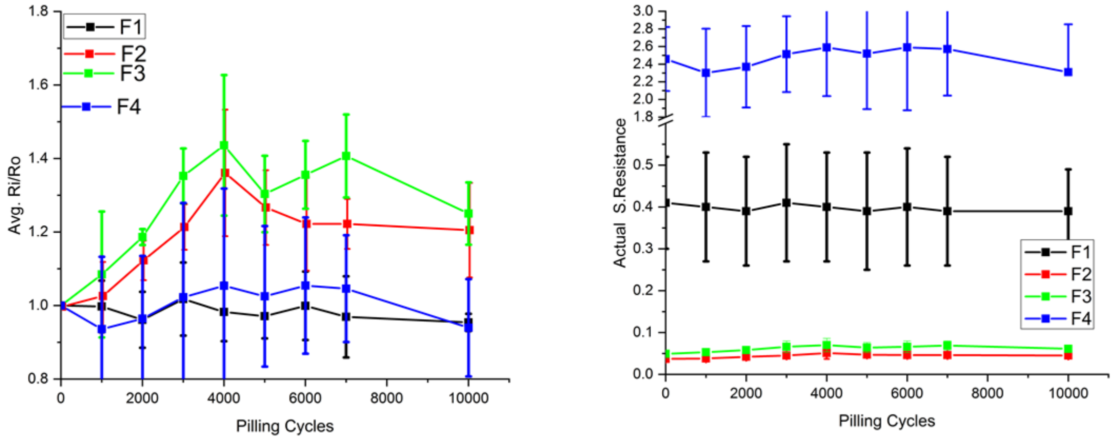

(a) (b)

Figure 4.47. Surface resistance analysis after 10,000 Pilling cycles, evaluation of all samples together (F1-F4) [14], (a) Comparison of Ri/Ro (b) comparison of actual surface resistance

Finally, these results were compared with each other for all samples separately (Figure 4.48 and Figure 4.49). All these graphs show the same trend for samples F1, F4, E1, and E2. These graphs explain that these samples have equivalent damages for proposed mechanical tests and can be used to co-relate with washing cycle damages. F2 and F3 samples showed different behavior. Here we concluded that stresses other than mechanical stresses are also working during the washing process, and some samples are not strong enough to withstand these stresses. It is further confirmed by experimenting chemical stresses experiment where only F2 and F3 samples showed an increase in surface resistance after dipping them in water and water detergent solutions. It is further explained in the coming discussion.

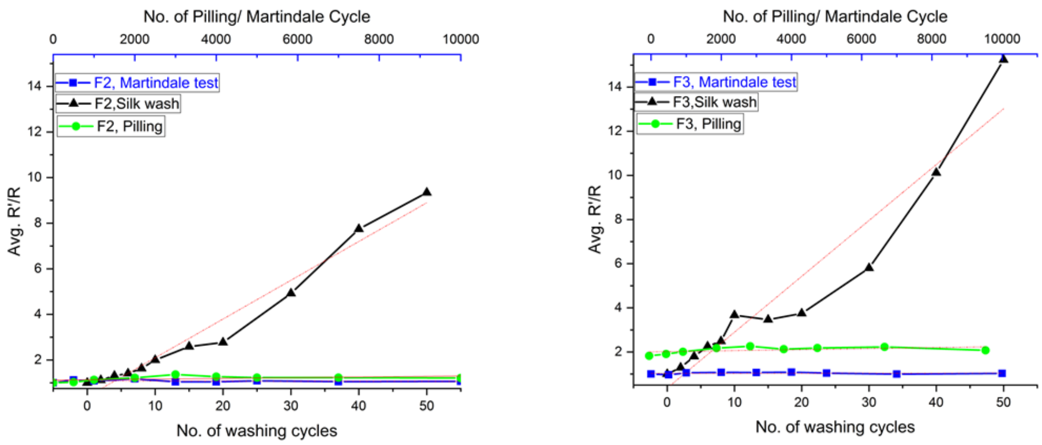

(a) (b)

Figure 4.48. Comparison of washing tests and mechanical tests performed in these experiments, (a) F2 electrodes, (b) F3 electrodes

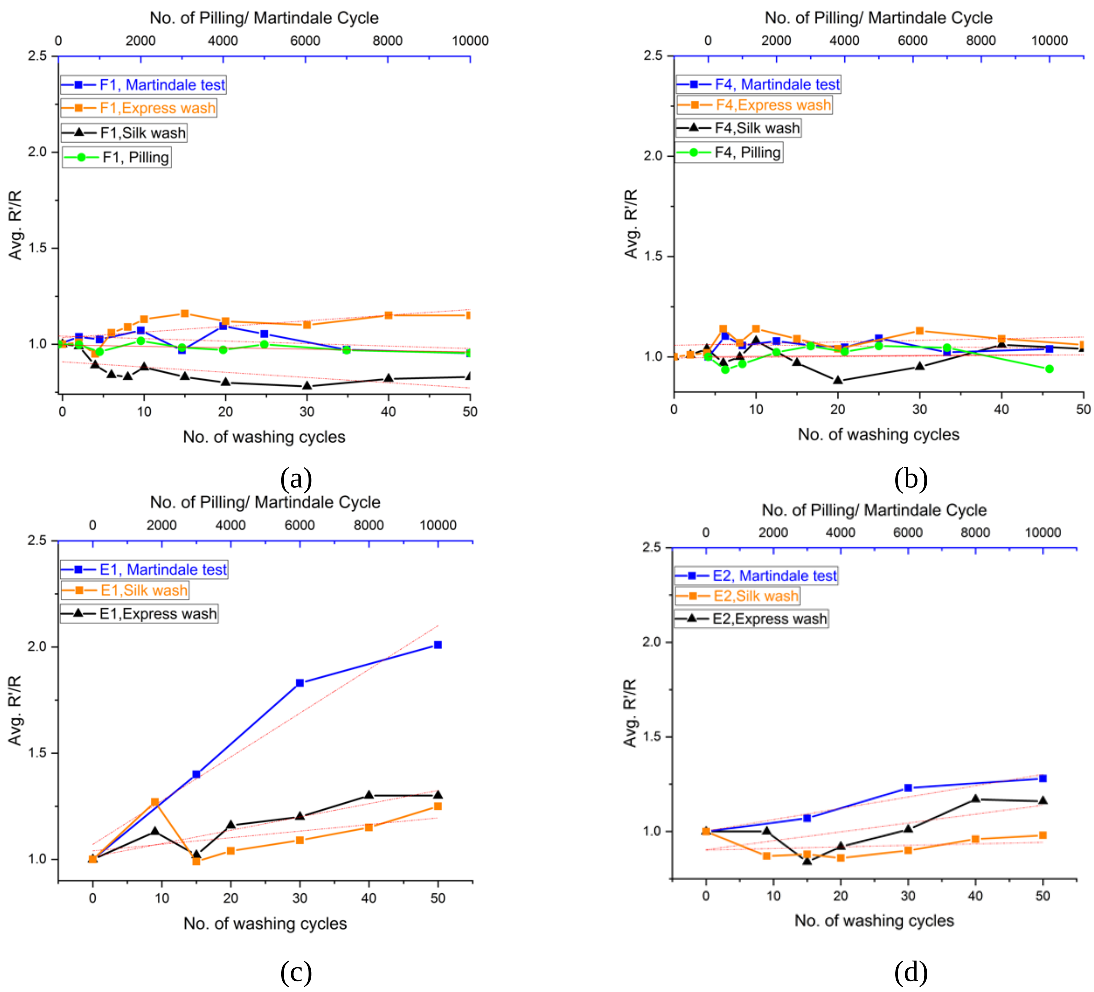

Figure 4.49. Comparison of washing tests and mechanical tests performed in these experiments, (a) F1electrodes, (b) F4 electrodes, (c) E1 electrodes, (d) E2 electrodes

4.3.4 Chemical tests

The skin electrodes were also investigated for chemical tests. These tests include water and water detergent solution tests. These samples were immersed in solutions for a maximum of 72 hours before calculating the R_i/R_o values. Samples F1, F4, E1, and E2 showed almost no difference in resistance after 72 hours of dipping in water and water detergent solution at 40°C temperature (Figure 4.50). Both solutions' temperature was kept at 40°C to avoid the damages provoked by the difference in swelling at high temperatures (above 75°C) between the core polymer and the plated metallic layer. However, samples F2 and F3 showed a change in surface resistance after these experiments, both for water and water detergent solutions. In water detergent solution, resistance was increased 1.3 and 1.7 times for F2 and F3, respectively (Figure 4.50). Copper-coated fabric electrodes were chemically attacked, and surface resistance was increased even without any mechanical force acting on it.

During the wash process, chemical forces are the second most impacting forces after mechanical forces. These forces include both water and detergent acting on electrodes during the wash process. Water molecules alone or with the detergent particles can attack chemically on the electrodes' surface or oxidize them. Oxygen in water can corrode with copper molecules, and this corrosion phenomenon can be increased in high temperatures [15], [16]. Broo *et al.* [17] discussed the copper corrosion after dipping the specimens in water for a calculated period. They claimed that with increasing time, cuprous oxide (Cu_2O) density was increased. These corrosions can reduce the adhesion bonding between metal and inner nylon materials. The phenomenon can be further damaging together with mechanical forces.

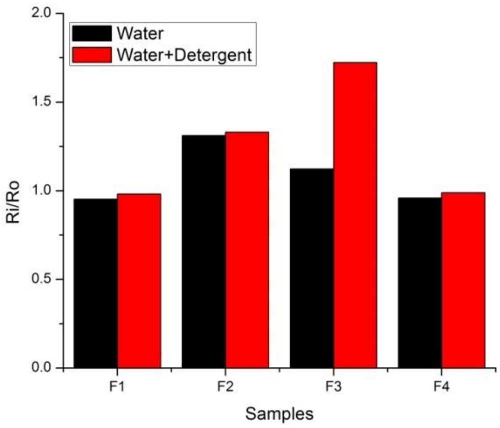

(a)

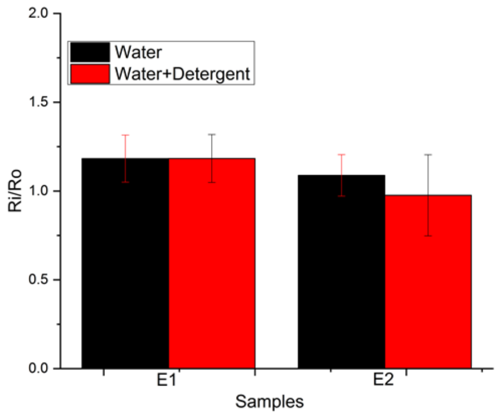

(b)

Figure 4.50. Chemical test analyses for skin electrodes with water and water detergent solution immersion for 72 hours at 40°C [14], (a) Fabric samples F1, F2, F3, and F4, (b) Embroidered samples E1 and E2

The experiments were performed on different types of electrodes having other metallurgy. Both mechanical and chemical stresses impact the e-textile system properties in terms of their performance. These stresses will have different behavior when performed separately in contrast with more than one stress combined in one experiment. Secondly, the impact of various stresses does not need to be the same on these electrodes. Different available test methods are used to predict the damage provoked on these samples and then correlate these results with other samples.

Skin electrodes F2 and F3 were more volatile to the damages when compared with other types of electrodes, and these damages were visible in all experiments, including washing, mechanical, and chemical tests. The damage intensity was different in various experiments depending on the nature of experiments and their direct impact on the electrodes. The proposed tests may have a higher effect when performed together instead of separately. Both of the samples were copper base samples, and their adhesion with base nylon fibers was not high enough to withstand these washing and alternate proposed stresses. SEM analysis highlighted the peeled-out surfaces at random positions after these experiments.

4.4 The Flexible Circuit Boards (PCBs)

4.4.1 Washing tests

The flexible PCBs were tested for the washing process. Both *Silk* and *Express* washing programs were investigated on the samples without any protection, with semi-protected and wholly protected with silicon coating over them. Eight tracks of different widths ranging from 0.15 mm to 1.00 mm were used for these experiments. SMD resistances were mounted in the PCBs in two different ways, parallel and perpendicular to the tracks (Figure 4.51). The SMD resistances in-line with conductive tracks (0° angle) are named as parallel to tracks. The resistances placed at 45° - 90° angle to conductive tracks are called perpendicular to tracks.

(a) (b)

Figure 4.51. SMD resistances mounted on the PCB, (a) parallel to tracks, (b) perpendicular to tracks

Figure 4.52 describes the impact of *Express* washing on the flexible PCBs without any protection over them. After 40 washing cycles, 75% of samples (24 out of a total of 32) were wholly damaged in terms of no resistance output. However, the remaining ones were in good condition, and their R'/R (ratio of change in resistance from initial resistance) was almost same after 40 washing cycles. In terms of damages on the different track widths, nearly all tracks were damaged after 40 *Express* washing cycles except for 1.00mm and 0.45mm track widths, which showed little resistance, 25% and 50% tracks, were working, respectively.

Figure 4.53 defines the percentage of damages in terms of parallel and perpendicular SMD resistance in these PCBs. In comparison, PCBs with SMD resistances mounted parallel to tracks were more damaged (93%) than vertical tracks (60%).

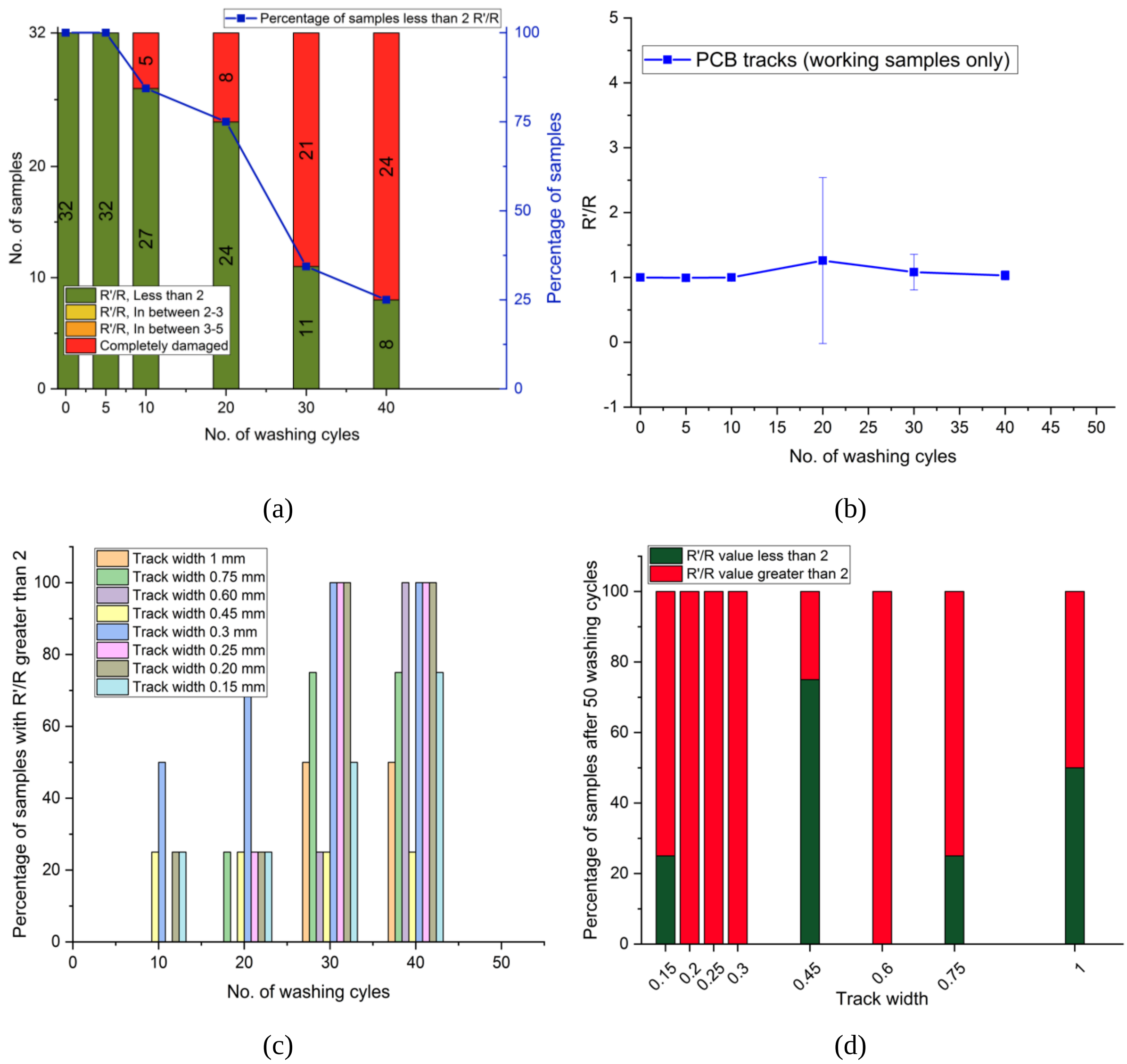

Figure 4.52. Flexible PCBs sample (without any protection) analyses after 40 *Express* washing cycles, a total of 32 samples were tested, (a) No. of samples with R'/R values increased above 2, 3, and ultimately damaged pieces on the left y-axis and percentage of samples having R'/R value below 2 on the right y-axis, (b) average R'/R value of working samples only, (c) percentage of samples with R'/R value above 2 described based on track widths, (d) ratio of samples having R'/R values below and above 2 after complete washing cycles based on track widths

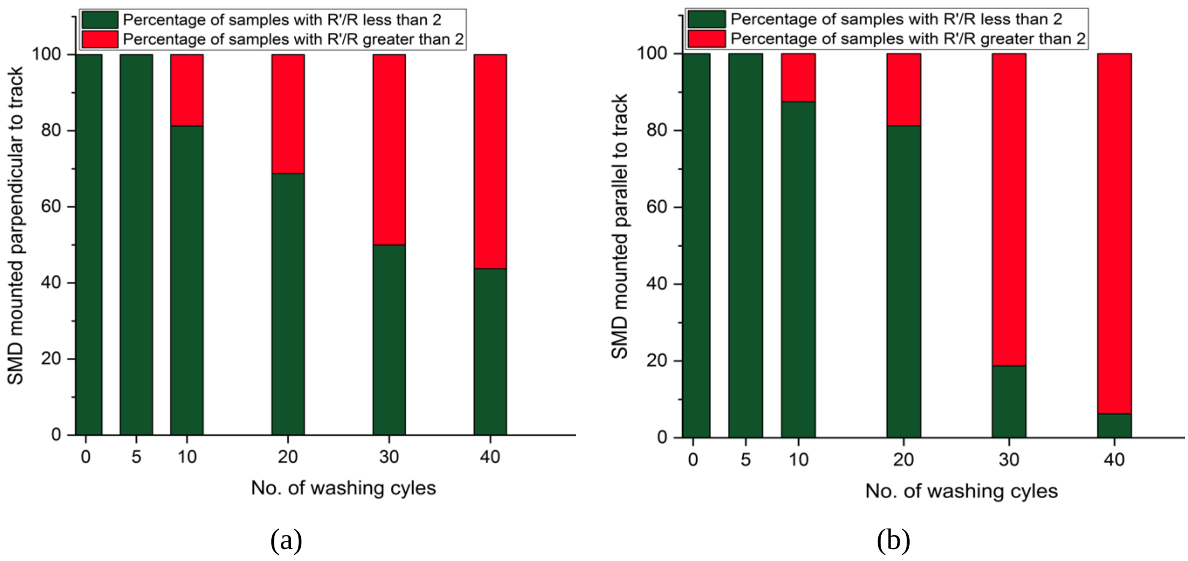

Figure 4.53. Flexible PCBs sample (without any protection) analyses after 40 *Express* washing cycles, a total of 32 samples were tested, (a) samples with SMDs mounted perpendicular to tracks, (b) samples with SMDs mounted parallel to tracks

The experiments were repeated for PCBs covered with silicone coating at SMD resistance joining points. Almost the same trend as shown in previous results is visible here, and more than 75% of samples were damaged after 40 washing cycles. The remaining ones showed nearly no change in R'/R value after 40 washing cycles (Figure 4.54). When the samples were separated based on track width, all samples were damaged except for 1.00 mm 0.75 mm, and 0.45 mm, which showed little resistance to these washing stresses. Here again, PCBs with SMD resistances mounted parallel to tracks are more damaged. All samples were entirely damaged compared to the perpendicular ones, where 60% of samples were destroyed (Figure 4.55).

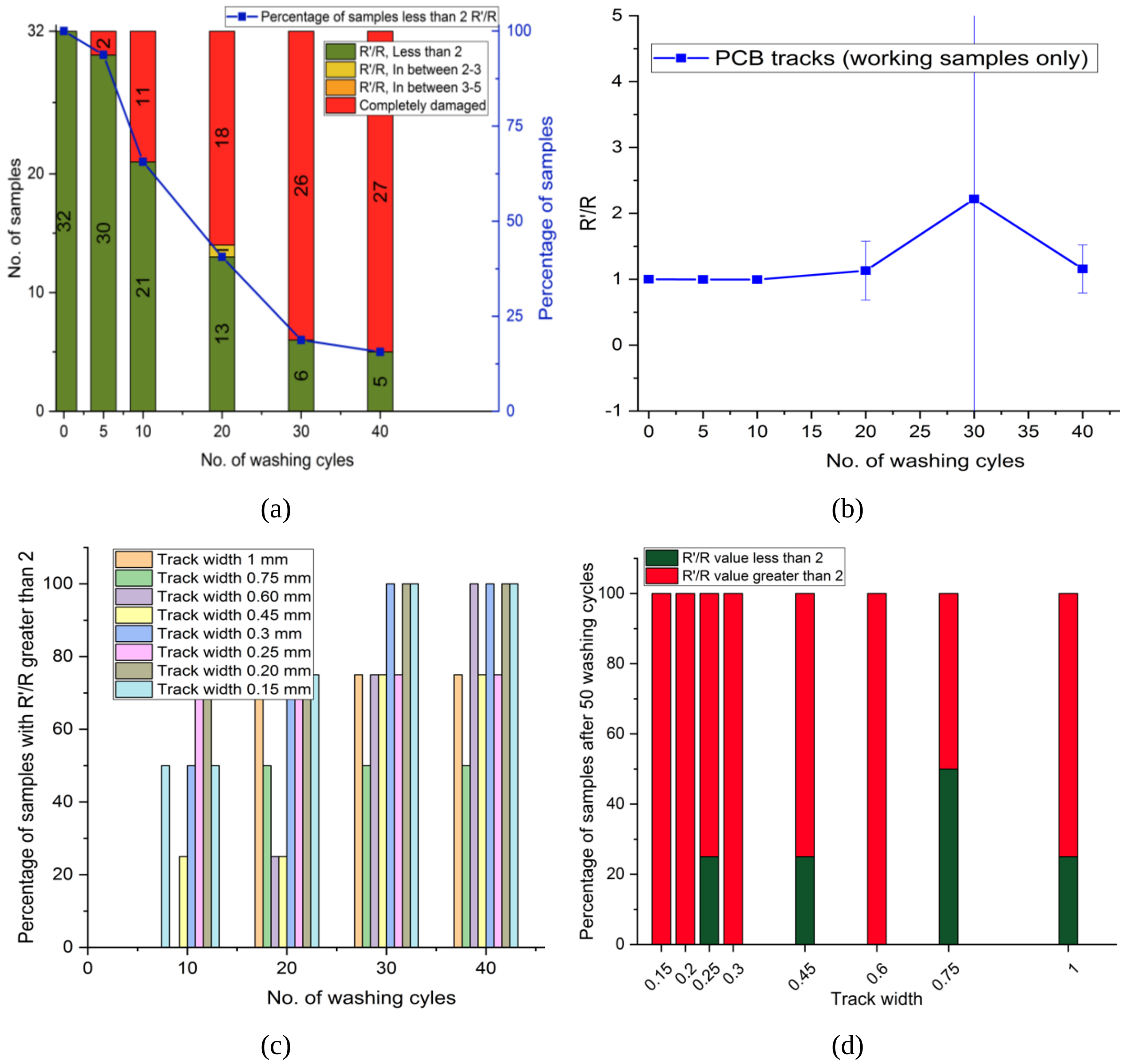

Figure 4.54. Flexible PCBs sample (with silicone protection at SMD joints only) analyses after 40 *Express* washing cycles, a total of 32 samples were tested, (a) No. of samples with R'/R values increased above 2, 3, and ultimately damaged pieces on the left y-axis and percentage of samples having R'/R value below 2 on the right y-axis, (b) average R'/R value of working samples only, (c) percentage of samples with R'/R value above 2 described based on track widths, (d) ratio of samples having R'/R values below and above 2 after complete washing cycles based on track widths

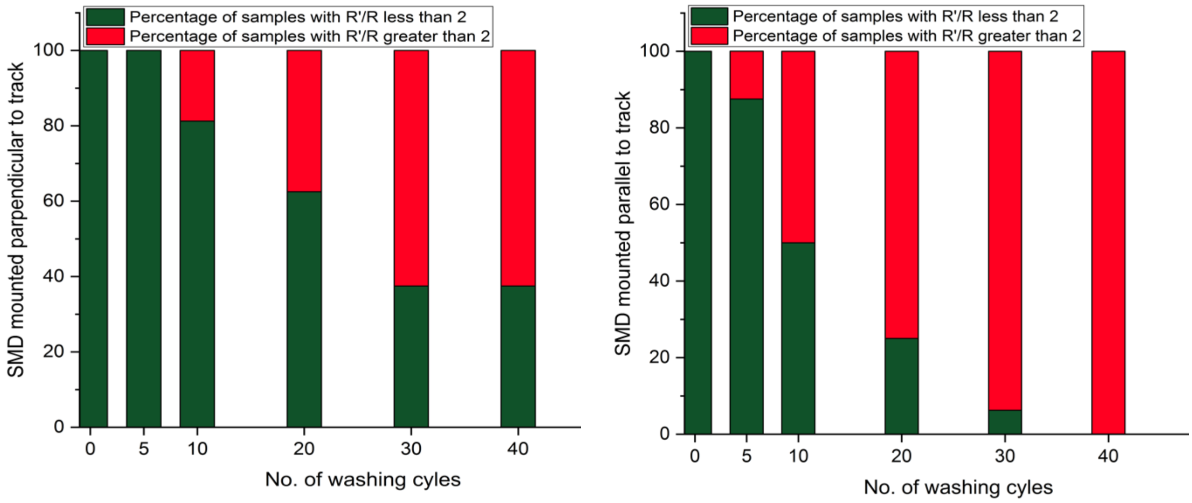

(a) (b)

Figure 4.55. Flexible PCBs sample (with silicone protection at SMD joints only) analyses after 40 *Express* washing cycles, a total of 32 samples were tested, (a) samples with SMDs mounted perpendicular to tracks, (b) samples with SMDs mounted parallel to tracks

In the third repetition, *Express* washing was performed on the entirely silicone protected PCB samples. The coating increased the resistance against provoked damages in the washing process. Only 4 samples were destroyed after 50 washing cycles compared to the 24 damaged for the samples without any protection. Among the remaining, 8 samples increased their R'/R values above 2 and 1 above 3, but still, they were working in good condition (Figure 4.56 and Figure 4.57). Overall, more than 80% of samples have R'/R values less than 2 after 50 washing cycles. Average R'/R values for working samples increased to 2, because samples were not damaged but they increased R'/R values. Here samples with higher width tracks showed better results, and only a few were damaged. Samples with 0.3 mm and 0.25 mm width showed highest damage, 100% and 75% samples increased their R'/R values above 2, respectively.

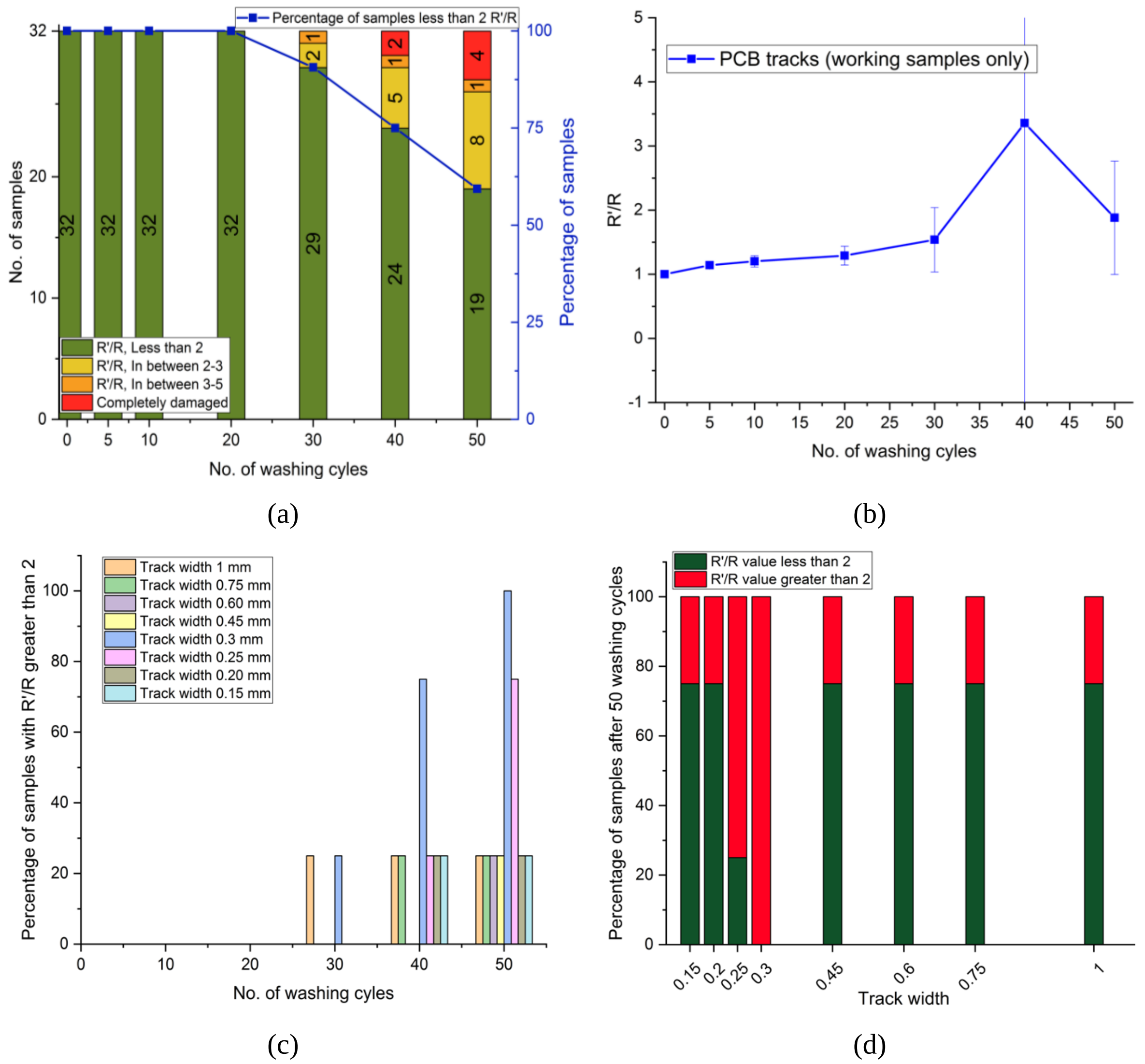

Figure 4.56. Flexible PCBs sample (with silicone protection completely) analyses after 50 *Express* washing cycles, a total of 32 samples were tested, (a) No. of samples with R'/R values increased above 2, 3, and ultimately damaged pieces on the left y-axis and percentage of samples having R'/R value below 2 on the right y-axis, (b) average R'/R value of working samples only, (c) percentage of samples with R'/R value above 2 described based on track widths, (d) ratio of samples having R'/R values below and above 2 after complete washing cycles based on track widths

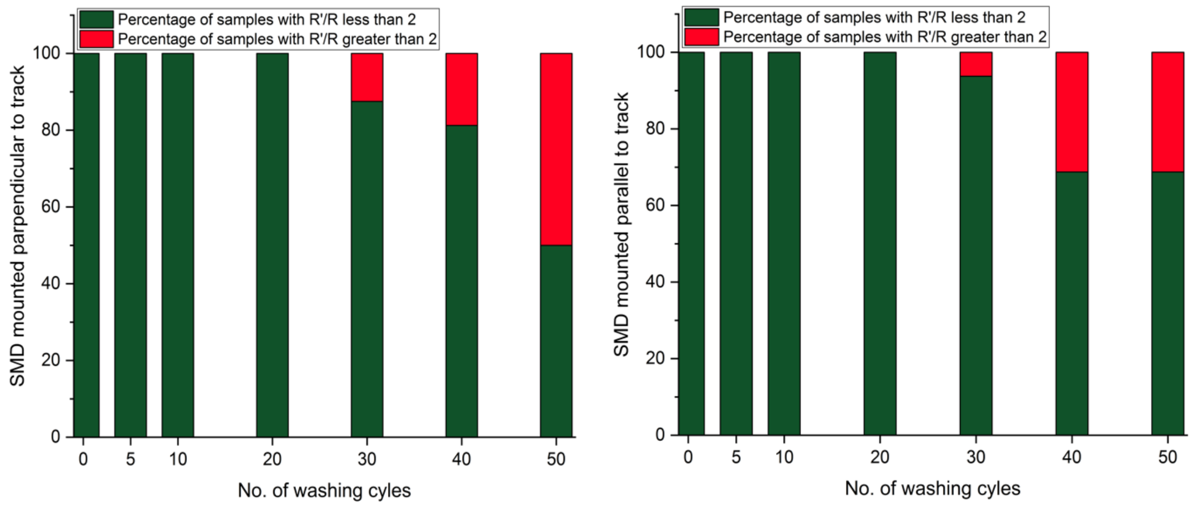

(a) (b)

Figure 4.57. Flexible PCBs sample (with silicone protection completely) analyses after 40 *Express* washing cycles, a total of 32 samples were tested, (a) samples with SMDs mounted perpendicular to tracks, (b) samples with SMDs mounted parallel to tracks

The PCB samples were also washed with the *Silk* washing cycles. The practice is performed to obtain the comparison with *Express* washing cycles in terms of intensive and mild washing stresses working on them. Figure 4.58 highlights the non-protected PCBs samples washed in *Silk* washing process. Almost 50% of samples were damaged after 50 washing cycles. The remaining samples were in good condition and showing no change in the average R'/R value. Samples with smaller track widths were more intensively damaged (80% were damaged). PCBs with 1 mm track width showed the best results, and no piece was destroyed. Comparing the parallel and perpendicular mounted SMDs samples, both types of prototypes showed almost equal damages, about 50-60% of samples were damaged (Figure 4.59).

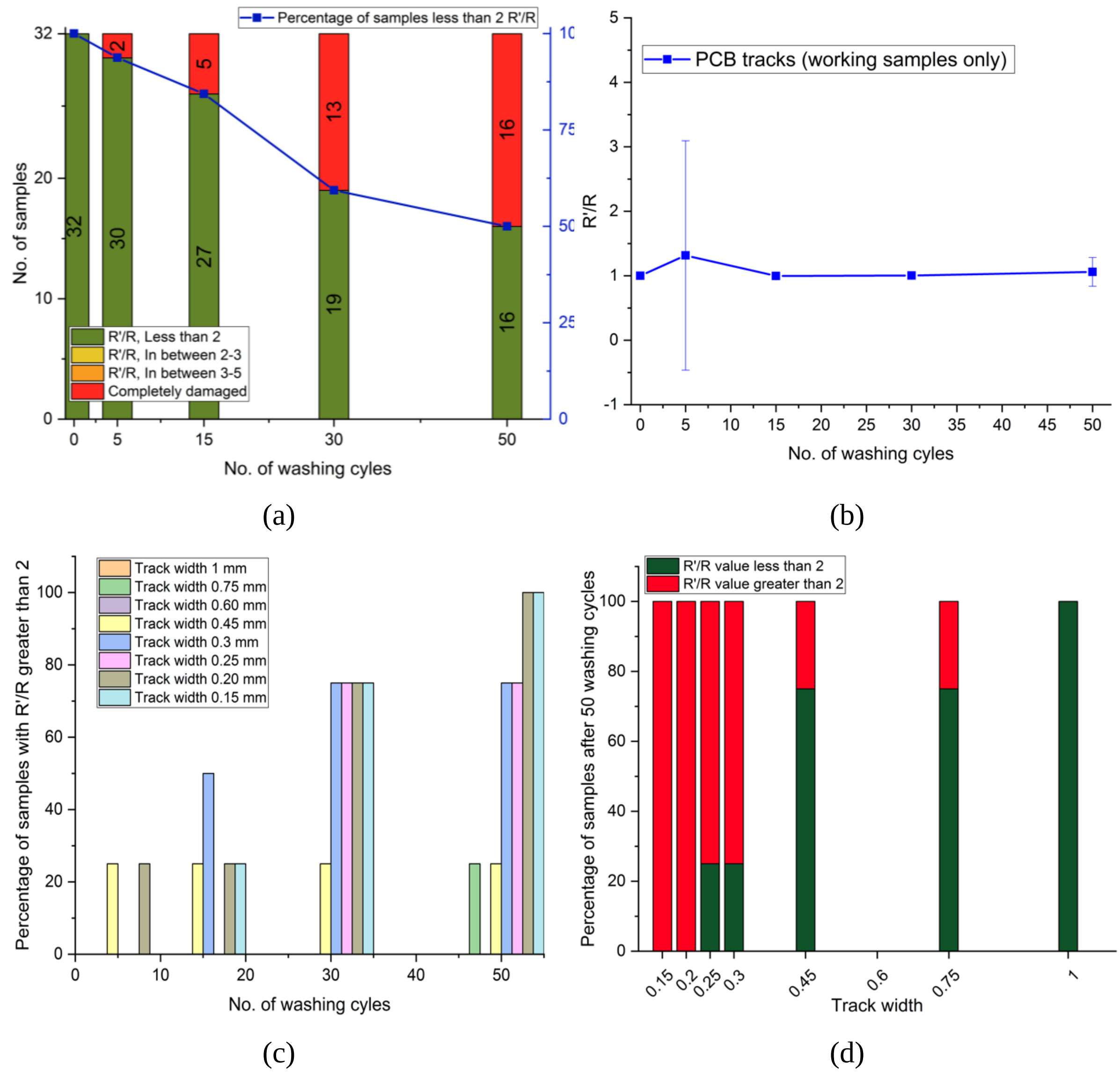

Figure 4.58. Flexible PCBs sample (without any protection) analyses after 50 *Silk* washing cycles, a total of 32 samples were tested, (a) No. of samples with R'/R values increased above 2, 3, and ultimately damaged pieces on the left y-axis and percentage of samples having R'/R value below 2 on the right y-axis, (b) average R'/R value of working samples only, (c) percentage of samples with R'/R value above 2 described based on track widths, (d) ratio of samples having R'/R values below and above 2 after complete washing cycles based on track widths.

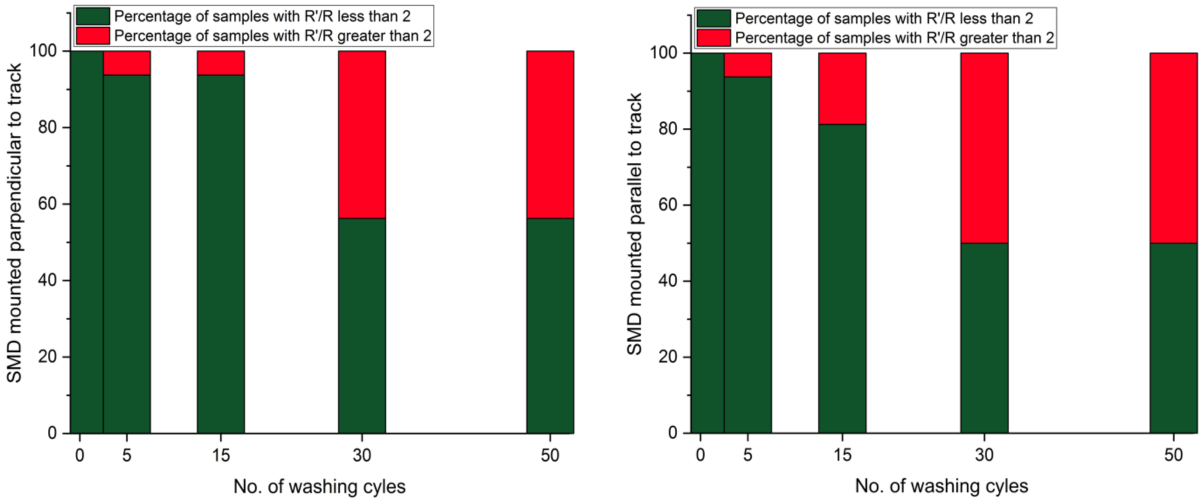

(a) (b)

Figure 4.59. Flexible PCBs sample (without any protection) analyses after 50 *Silk* washing cycles, a total of 32 samples were tested, (a) samples with SMDs mounted perpendicular to tracks, (b) samples with SMDs mounted parallel to tracks

In PCBs with silicon coating on SMD mounting point only, 75% of samples were damaged after 50 *Silk* washing cycles (Figure 4.60). This ratio is much higher than models without any protection. When we discussed the results based on the track width, samples with smaller track widths were almost wholly damaged, and samples with 0.45 to 1.00 mm width were nearly 50% damaged. In contrast to parallel and perpendicular mounted samples, 100% of samples with parallel mounted SMDs were destroyed, whereas this ratio is 50% in other case (Figure 4.61).

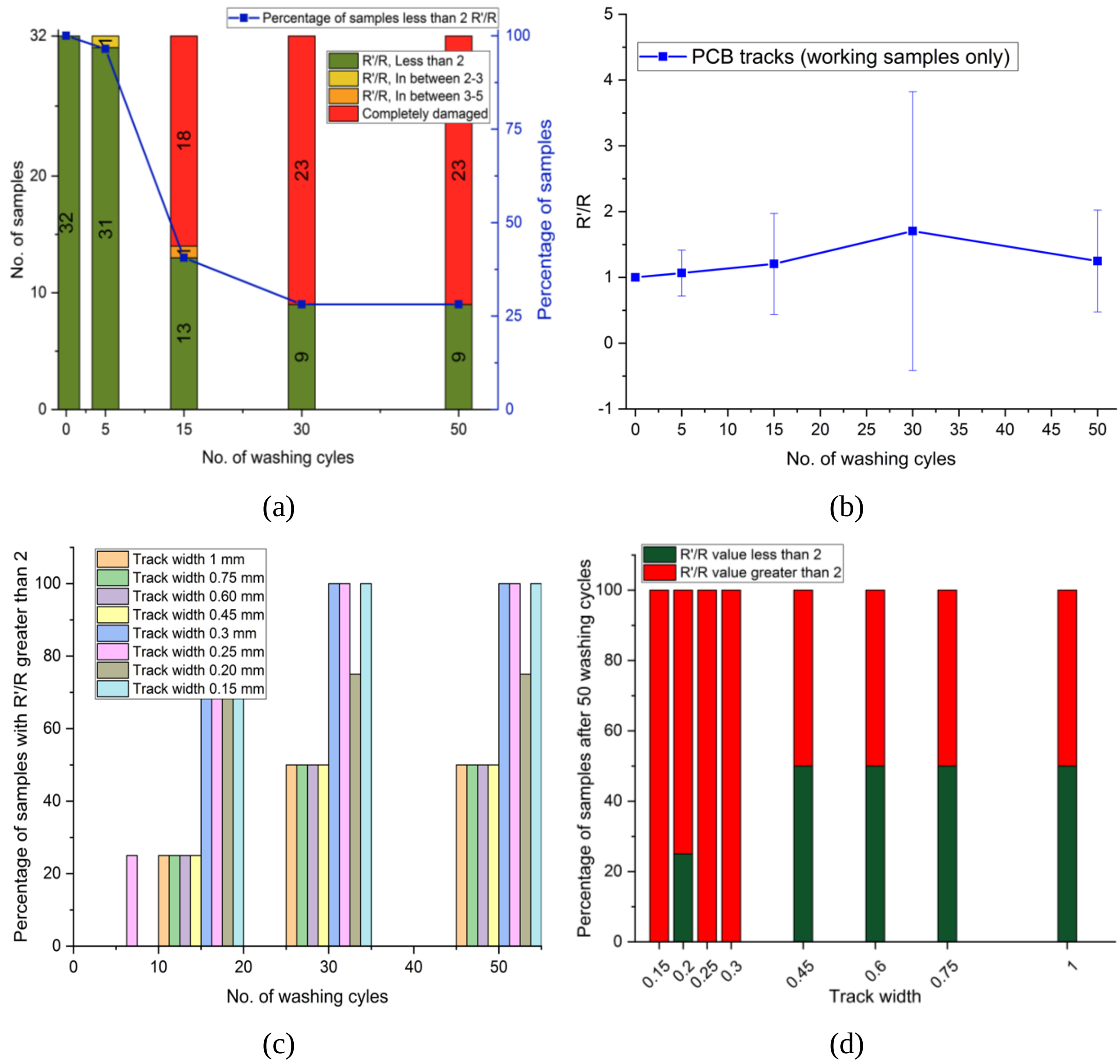

Figure 4.60. Flexible PCBs sample (with silicone protection at SMD joints only) analyses after 50 *Silk* washing cycles, a total of 32 samples were tested, (a) No. of samples with R'/R values increased above 2, 3, and ultimately damaged pieces on the left y-axis and percentage of samples having R'/R value below 2 on the right y-axis, (b) average R'/R value of working samples only, (c) percentage of samples with R'/R value above 2 described based on track widths, (d) ratio of samples having R'/R values below and above 2 after complete washing cycles based on track widths

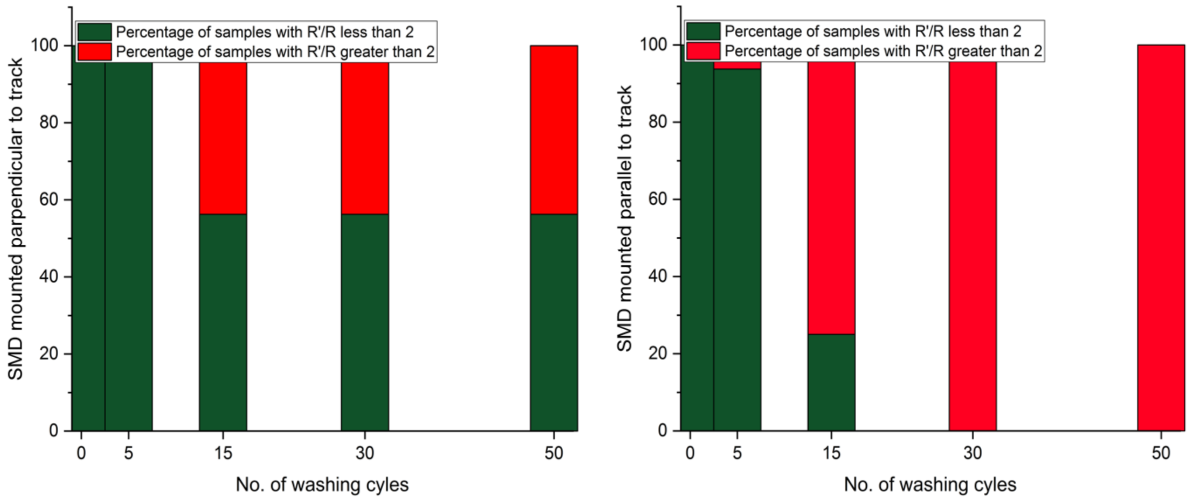

(a) (b)

Figure 4.61. Flexible PCBs sample (with silicone protection at SMD joints only) analyses after 50 *Silk* washing cycles, a total of 32 samples were tested, (a) samples with SMDs mounted perpendicular to tracks, (b) samples with SMDs mounted parallel to tracks.

Samples completely protected with silicon coating and washed in *Silk* washing cycles showed the best values among all experiments, and only 2 pieces were damaged after 50 washing cycles. About 94% of samples maintained their R’/R values below 2 (Figure 4.62). Both damaged samples were from parallel and perpendicular mounted samples each (Figure 4.63).

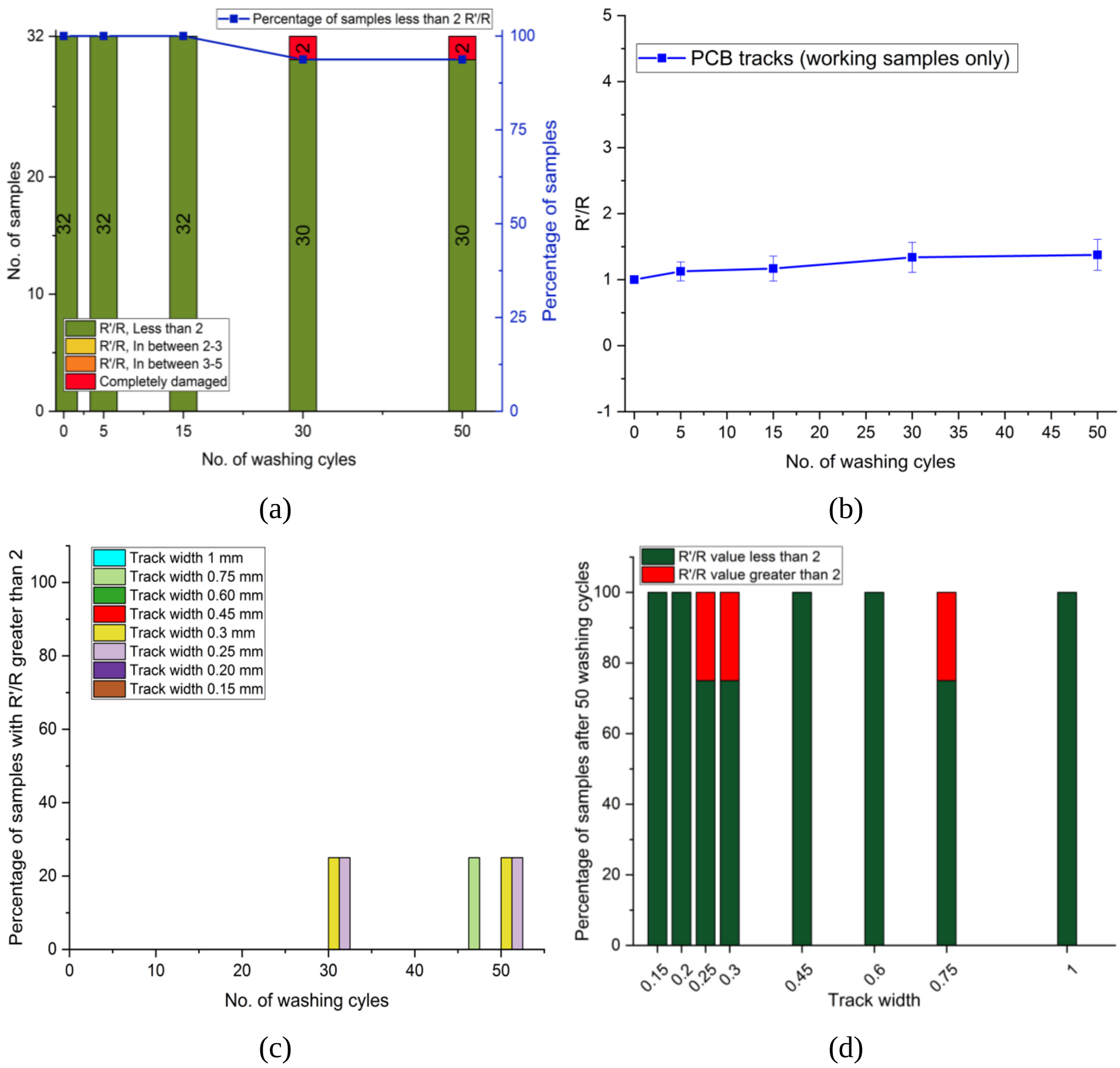

Figure 4.62. Flexible PCBs sample (with silicone protection completely) analyses after 50 *Silk* washing cycles, a total of 32 samples were tested, (a) No. of samples with R'/R values increased above 2, 3, and ultimately damaged pieces on the left y-axis and percentage of samples having R'/R value below 2 on the right y-axis, (b) average R'/R value of working samples only, (c) percentage of samples with R'/R value above 2 described based on track widths, (d) ratio of samples having R'/R values below and above 2 after complete washing cycles based on track widths

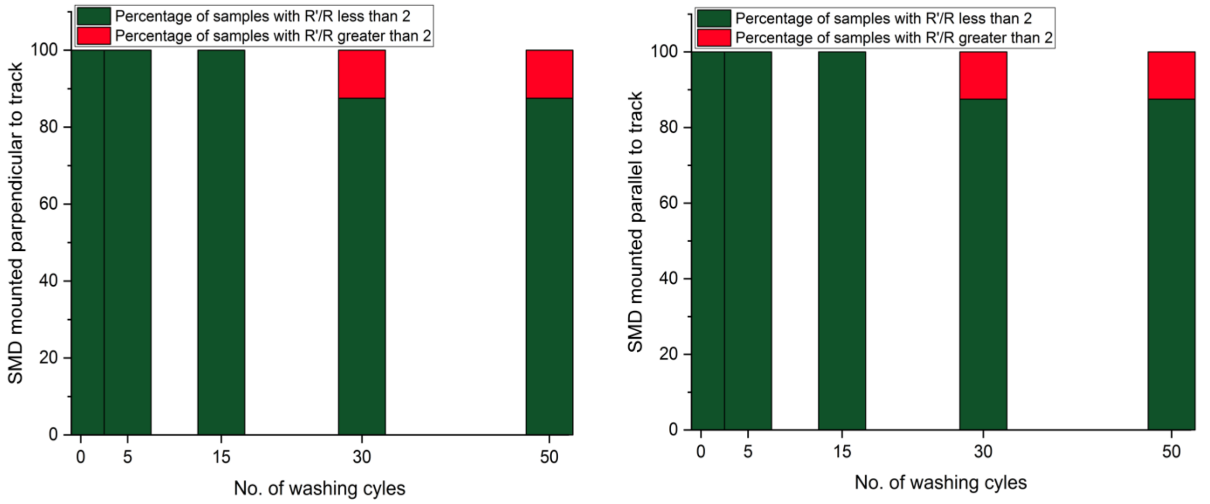

(a) (b)

Figure 4.63. Flexible PCBs sample (with silicone protection completely) analyses after 50 *Silk* washing cycles, a total of 32 samples were tested, (a) samples with SMDs mounted perpendicular to tracks, (b) samples with SMDs mounted parallel to tracks.

Damages provoked by the washing stresses at random points in the PCB samples are shown in Figure 4.64, Figure 4.65, and Figure 4.66. Cracks are visible in these pictures are highlighted with circles. They can be divided into three categories: the cracks in the track lines, at SMDs pasting point, and at the joining point of the track line with the measuring pad.

During the washing process, samples are undergone in various mechanical stresses, including bending, twisting, and shearing. These stresses impacted more intensively at the flexible mismatched surface joint [18]–[20]. Conductive paste along with rigid SMD increased the hardness of the flexible PCB at that specific point. A sharp decrease in the flexibility enhanced the probability of mismatch, and the resultant concentration of the stress caused the creation of cracks [21].

The mismatch is also possibly created between copper material used for the printing of tracks and base material. This possibility is further enhanced at the connection pad where copper printed width is reduced from 20 mm to 1 mm, or even 0.15 mm in some cases.

Figure 4.64. Damage analyses of washed PCBs with an optical microscope (cracks in the tracks of various widths)

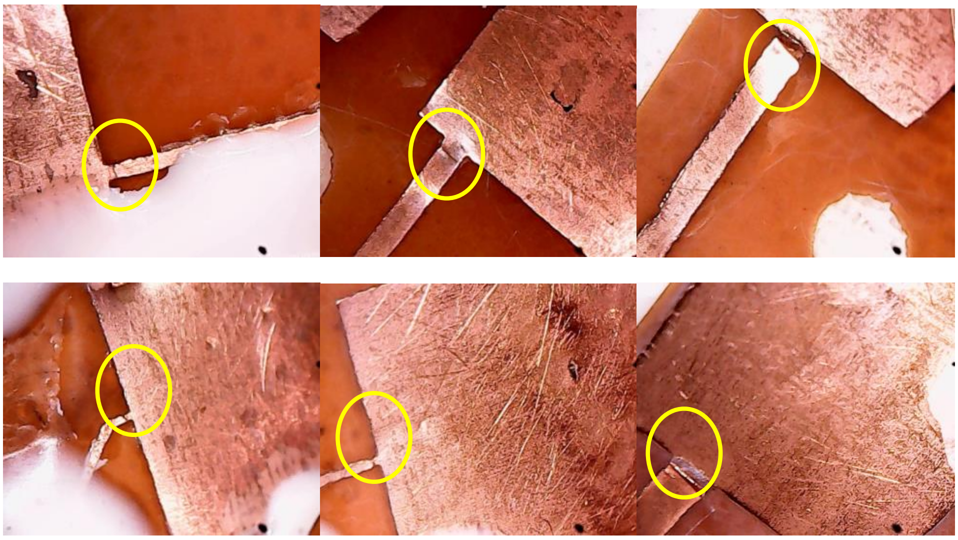

Figure 4.65. Damage analyses of washed PCBs with an optical microscope (cracks at surface mismatch point between measurement connection pad and tracks)

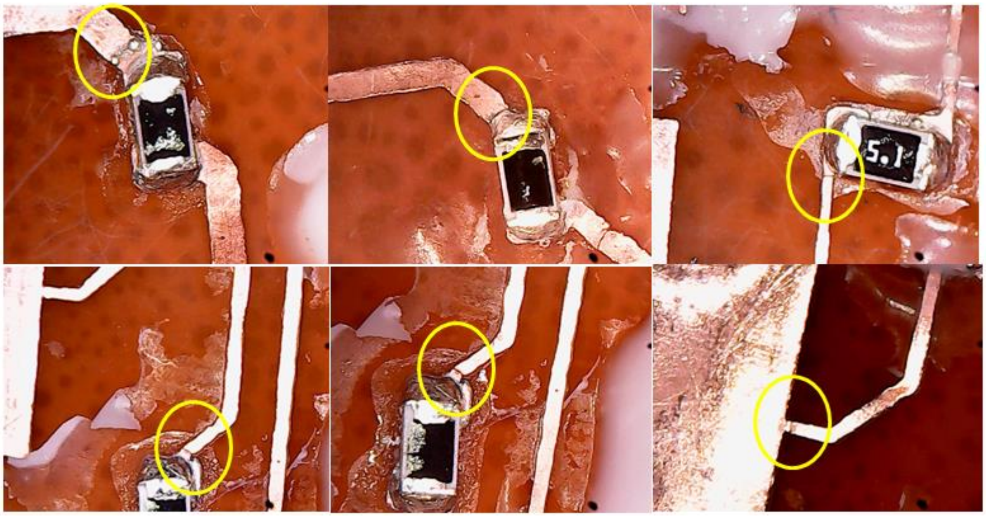

Figure 4.66. Damage analyses of washed PCBs with an optical microscope (cracks at surface mismatch point between SMD pad and tracks)

In the discussion of all results, samples with completely silicon coating protections showed the best results, which are pretty straightforward because silicon coating protected the samples from any possible mechanical damages during the washing process. The silicone coating also reduced the surface mismatch problem because the complete PCB circuit was covered with this coating. Hence, surface morphology and flexibility were the same for the whole sample. Among *Silk* and *Express* washing cycles, *Silk* washing cycles showed less impact on the samples due to their mild behavior during the process.

When we see samples without protections and with protections at SMD pasting point only, later showed worst results even it was protected to somehow when compared with other samples. The surface mismatch problem was highlighted again, and it was even amplified due to silicon coating at some random points in the flexible PCBs. The silicon coating was placed with the idea to protect the SMDs and their joints from possible damage. However, this silicon even enlarged the gap between flexible and semi-flexible surfaces, and hence resultant damages enhanced. That’s why these samples showed the minimum numbers of working pieces after 50 washing cycles.

Different track widths were investigated in these experiments. Tracks with thinner widths were more provoked to the damages and vice versa. Tracks usually above 0.45 mm were better in performance in all experiments compared to the thinner ones. Although, track width and spacing are designed based on the requirement and directly impact the manufacturing costs. However, for the flexible PCBs' reliability, it should be considered to have the appropriate track width that can withstand possible mechanical damages.

In these experiments, SMD resistance was placed parallel and perpendicular to the PCB tracks to investigate the impact of their positions in the washing damages. For the samples with complete silicon protections, SMD resistances' direction was not causing any difference in the results. However, for the examples without protections, SMD resistances placed parallel to the PCB tracks were relatively more damaged when compared to the perpendicularly placed resistance. Nevertheless, these samples were destroyed more than 50% in both cases, so we can't state that SMDs in one direction are better than the other one. However, for the reliability performance of e-textile systems, circuit designs and positions of installed SMDs should be considered.

4.4.2 Bending test

Martindale abrasion tests and Pilling tests are not performed because the PCBs are usually not directly exposed to mechanical stresses. PCBs in the e-textile systems are not designed to contact the skin directly, and they typically are used for electrical programming between various e-textile components. That's why they can be protected against washing and environmental stresses. However, flexibility is a vital property for better adoption in wearable e-textile systems. The PCBs should perform bending resistance to claim the required flexibility for e-textile systems.

The flexible PCBs with SMD mounted resistance were tested for bending tests. They were pasted on the plain cotton fabric with the help of silicon adhesive paste. One side of the fabric was attached with the to-and-fro moving arm of the machine. The other side of this fabric was placed over the circular rod and hanged with the known 1 kg of weight. Hence, samples were bent at 90° along the rod under a load of hanging weight during complete movement.

The samples were tested for 20,000 bending cycles, and resistance values were noted after every 4,000 cycles (Figure 4.67). The average R'/R value, up to 12,000 cycles, was approximately 1.5, and an overall 75% of samples have R'/R values less than 2. The samples start damaging after this point, and 62% of them increased their R'/R values above 2 after 20,000 bending cycles. Among them, 34% of samples increased their R'/R values above 5. The average R'/R value after 20,000 bending cycles was increased to 4.5. This value is relatively high when compared with washing tests analysis. In washing samples, the majority of samples were damaged entirely and hence removed from average values. But in the bending test case, no piece was wholly damaged, but they increased their electrical resistance values after specific bending cycles. Hence, a significant increase in the average R'/R value for these samples was observed.

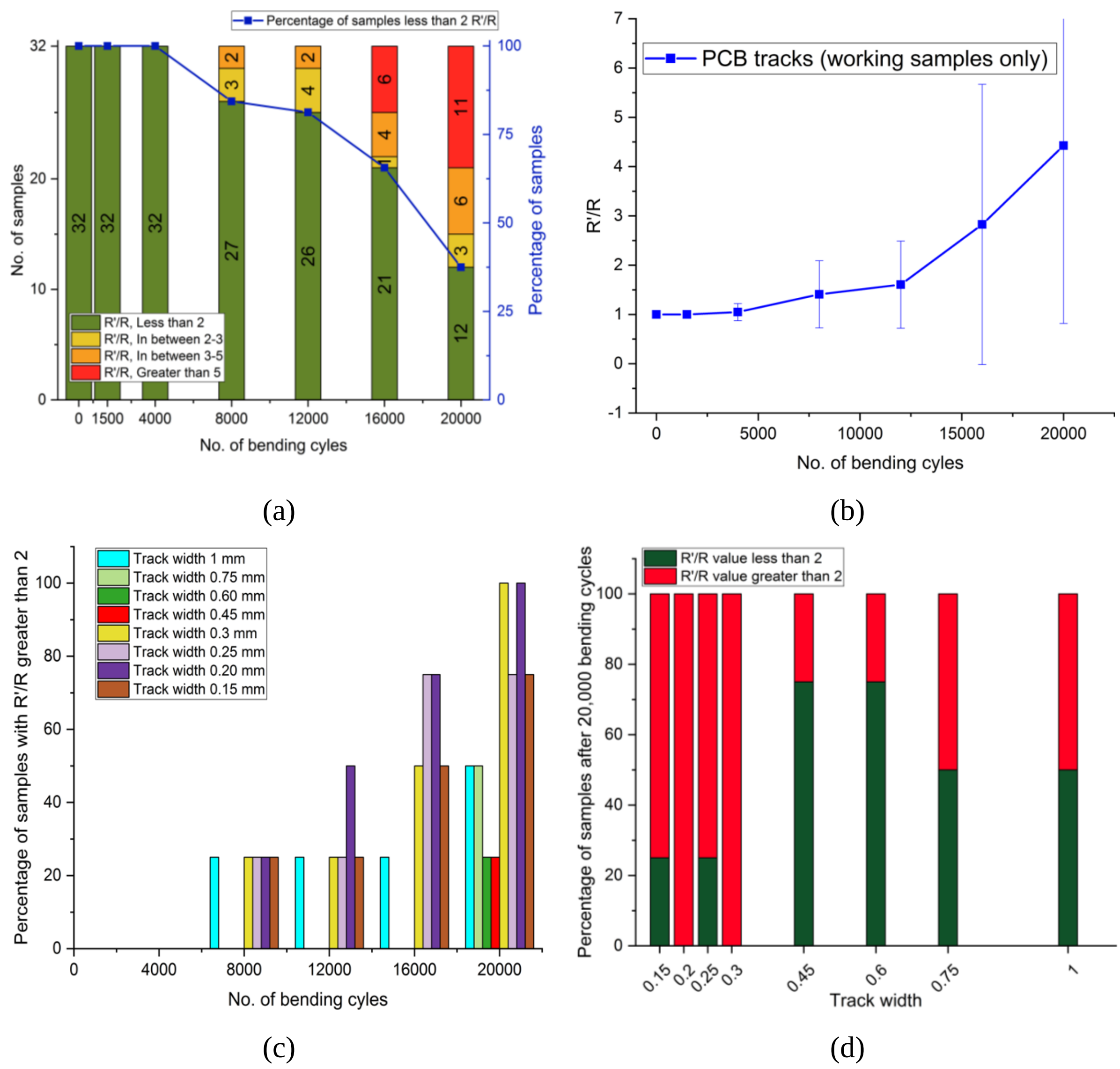

Figure 4.67. Flexible PCBs sample (without any protection) analyses after 20,000 bending cycles, a total of 32 samples were tested [22], (a) No. of samples with R'/R values increased above 2, 3, and 5 on the left y-axis and percentage of samples having R'/R value below 2 on the right y-axis, (b) average R'/R value of working samples only, (c) percentage of samples with R'/R value above 2 described based on track widths, (d) ratio of samples having R'/R values below and above 2 after complete washing cycles based on track widths

When we compare track widths for different samples, it was observed that models with thinner track widths were more impacted as compared to thicker ones, and their R'/R values were increased beyond the threshold level of 2. Samples with track width 0.45 mm and higher showed better resistance against bending cycles, and more than 50% of samples maintained their R'/R values below 2. Similarly, for SMD resistance positioning, both parallel and perpendicular pieces were equally damaged after 20,000 bending tests (Figure 4.68).

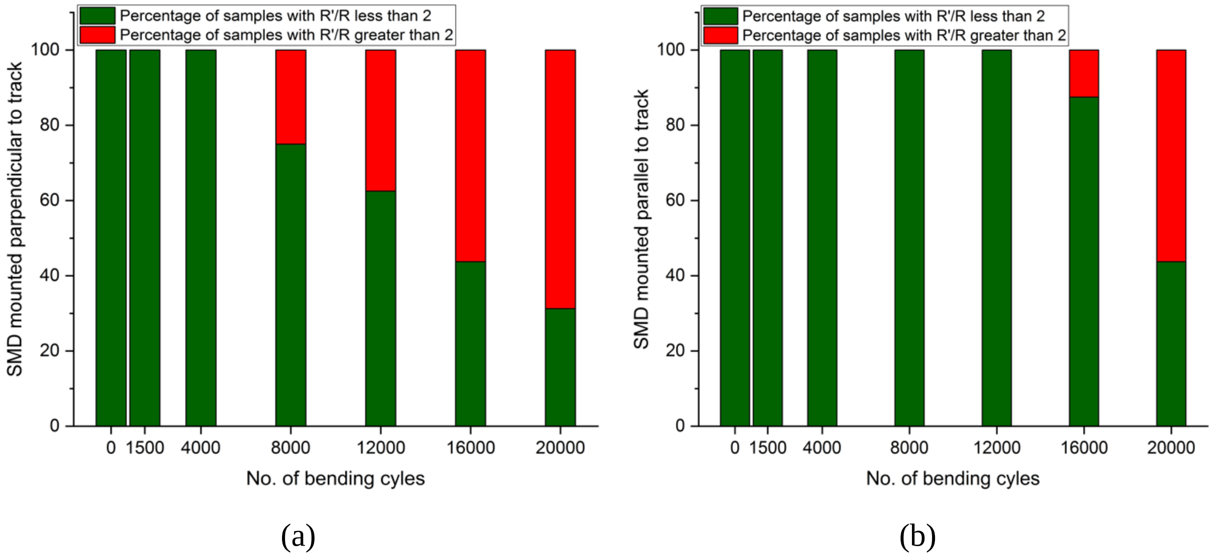

Figure 4.68. Flexible PCBs sample (without any protection) analyses after 20,000 bending cycles, a total of 32 samples were tested [22], (a) samples with SMDs mounted perpendicular to tracks, (b) samples with SMDs mounted parallel to tracks

As for totally silicone-protected samples, 94% of them showed R'/R values less than 2 after 16,000 bending cycles (Figure 4.69 (a)). After 16,000 cycles, samples start increasing their R'/R values and reached 5 after 20,000 bending cycles. However, only 25% of samples increased their R'/R values, and the remaining 75% of samples were in good condition with R'/R values less than 2. In comparison to track widths, samples with lesser track widths were more damaged, and it is understandable because smaller track widths have less conductive area, and only a small crack can destroy all the current passing paths (Figure 4.69 (b)). Here again, SMD position (parallel and perpendicular) did not impact, and both types of samples were equally damaged.

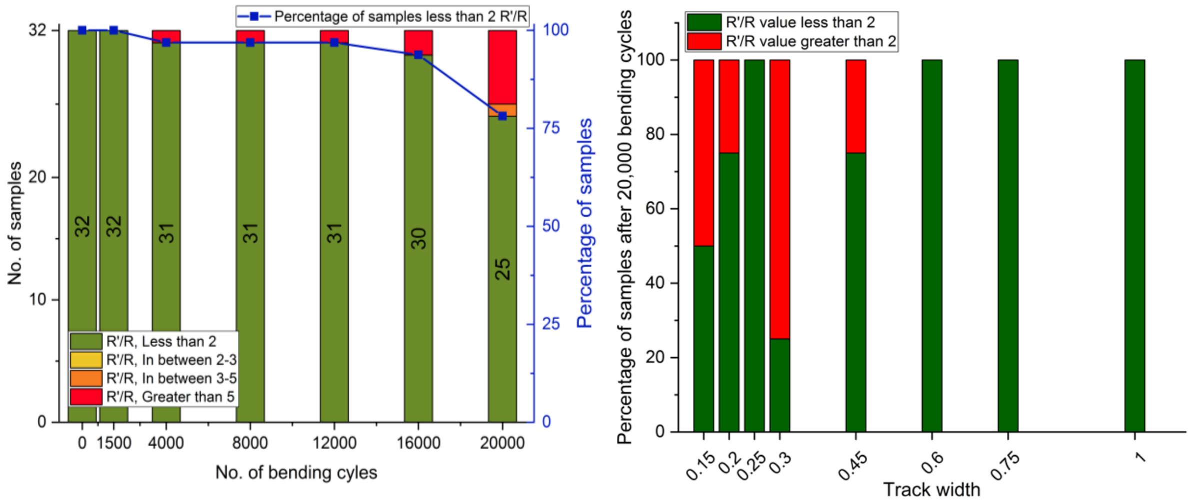

(a) (b)

Figure 4.69. Flexible PCBs sample (with silicone protection) analyses after 20,000 bending cycles, a total of 32 samples were tested [22], (a) No. of samples with R'/R values increased above 2, 3, and 5 on the left y-axis and percentage of samples having R'/R value below 2 on the right y-axis, (b) ratio of samples having R'/R values below and above 2 after complete washing cycles based on track widths.

Bending tests showed the same kind of trend as in the washing experiments. Here again, surface mismatch problems were highlighted, and bending force increased this phenomenon. Flexible PCBs are prepared with a polyamide sheet of 15 microns coppered with 35 microns. This surface mismatch is further enhanced at SMDs pasting points. In the bending test, no sample was utterly damaged, but their overall electrical resistance was increased. Most of the tracks were in good condition, but resistance was increased due to the damage at the SMD pasting point. The bending test was experimented with bending these samples at 90° around the circular rod, and under the known load. It impacted the soldering paste used for adhesion between the SMD and flexible PCBs because of the difference in their flexibility, as shown in Figure 4.70. This adhesion was weekend but was still in contact, causing increased electrical resistance instead of ultimately damage as rendered in the washing tests [18], [21].

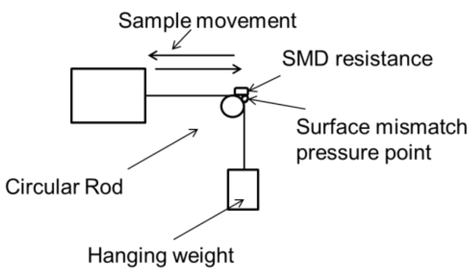

Figure 4.70. Schematic presentation of the sample movement in bending test [22]

A comparison graph to co-relate the damages among all samples is plotted in Figure 4.71. Washing samples protected with silicone coating presented the best results in all experiments following the examples without any protection. Prototypes with the *Silk* washing cycles were on the top of the graph due to mild washing forces acting during the process. Bending test results were between the range of silicon-coated and non-coated samples and may be used to co-relate the equaling damages as provoked in the washing process. For example, in these samples, we can predict that silicone-coated specimens washed with 50 *Express* washing cycles produced equivalent damages caused by 16,000 bending cycles. Of course, this analysis will be different for different types of products and will vary depending on the end-user requirements. However, these predictions will help the e-textile industry to reach a joint agreement between companies willing to develop the e-textile products adopted in the textile industry.

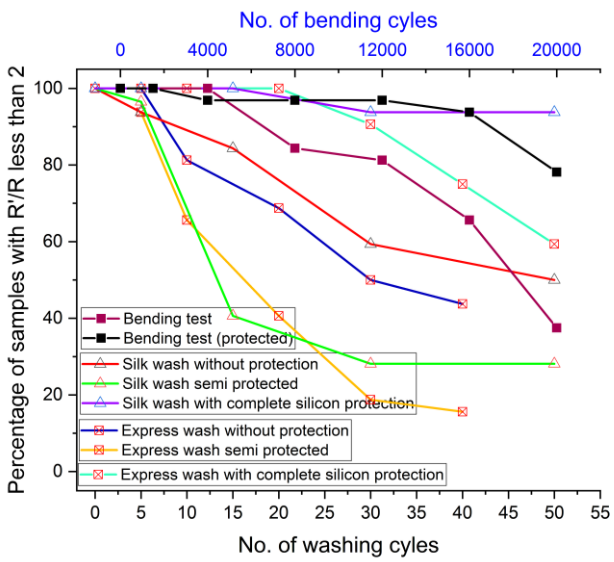

Figure 4.71. The comparison of all washed and bending test samples

4.5 Textile antennas

4.5.1 Washing tests

Textile antennas were washed up to 50 *Express* and *Silk* washing cycles. The resonance frequency and quality factor for these samples were measured using an Agilent 4964A RLC meter. These samples were tested after each washing cycle up to 5 washing and then after 8, 10, 15, 20, 25, 30, 40, and 50 washing cycles. A separate set of samples were used for each testing, and it was removed from the washing machine after completing the required number of washing cycles for those specific samples. And finally, the resonance frequency was measured together for all prototypes.

Figure 4.72 and Figure 4.73 show the resonance frequency (f_0) and quality factor (Q) of the samples for the complete 50 *Express* and *Silk* washing cycles. *Silk* washing is a gentle washing cycle, and it did not impact much on the textile antennas, even after 50 washing cycles. The resonance frequency for all the samples was in the range of 15-16 MHz. The average resonance frequency after 50 *Silk* washing cycles was 15.65 MHz. Among 10 cycles washed samples, a single piece increased its value to 21.28 MHz, which increased the average resonance frequency to 17.20 MHz. Overall, we can state that 50 *Silk* washing samples did not really damage the textile antennas. Quality factor (Q) for all pieces was nearly 40, considered the better range for textile antennas signals.

Samples washed with the *Express* washing cycles showed degradation after 20 washing cycles. This degradation is quite understandable, as it is a more intensive washing cycle when compared with *Silk* one. The resonance frequency was in the range of 15-16 MHz up to 20 washing cycles, and then it starts detonating. One sample each from 25, 30, and 50 cycles washed samples were damaged and did not give any results. All pieces from 40 cycles washed samples were destroyed, and no results were collected. Similarly, the quality factor is in the range of 40 for specimens up to 20 washing cycles, and then it dropped to 20, which indicates the damage of samples.

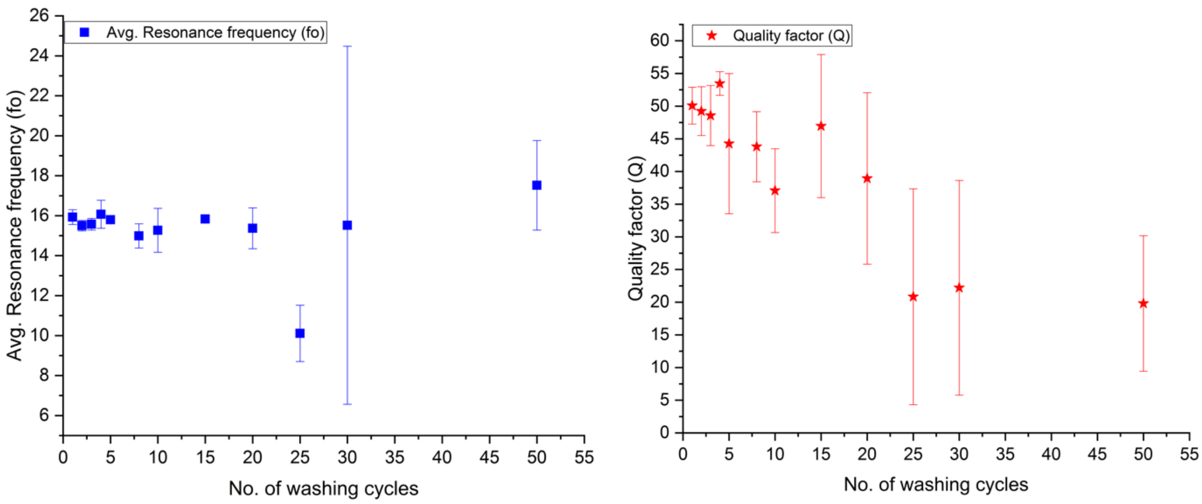

(a) (b)

Figure 4.72. Textile antennas after 50 *Express* washing cycles, (a) Average Resonance frequency (f_o), (b) Average Quality factor (Q)

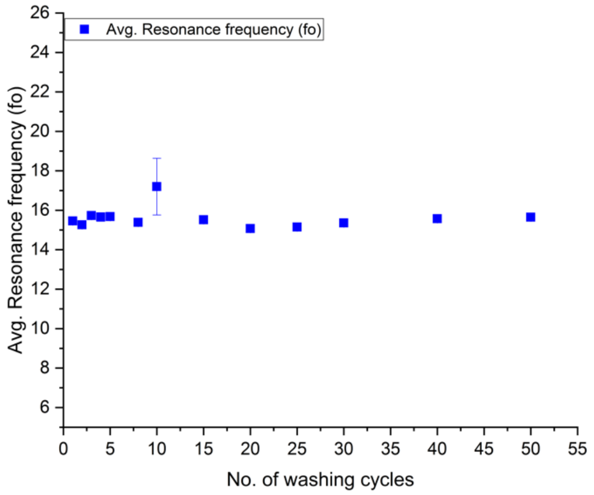

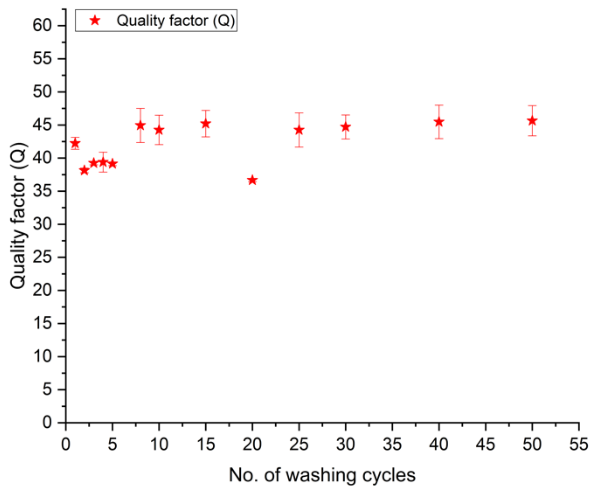

(a) (b)

Figure 4.73. Textile antennas after 50 *Silk* washing cycles, (a) Average Resonance frequency (f_o), (b) Average Quality factor (Q)

After the washing analysis, it is concluded that the *Silk* washing cycle did not damage the textile antennas of 13.56 MHz frequency prepared by conductive yarns. However, *Express* washing cycles were a nightmare for these antennas, and they start impacting after 20 washing cycles. It indicates that these antennas were good enough to bear the mild mechanical stresses in the washing process but got affected by the intensive ones.

4.5.2 Martindale abrasion tests

Martindale abrasion test was performed on these antennas. Total four samples were tested up to 10,000 Martindale abrasion cycles and resonance frequency and quality factor was calculated for these samples. The resonance frequency for all these samples was in the range of 15-16 MHz but quality factor for one sample decreased to 25. However, other three samples maintained their quality factor in the range of 38-40 (Table 4.2). This indicates that the conductive yarn in one sample was somehow damaged and increased its electrical resistance which decreased the quality factor for the antennas' impedance. But this increase in the electrical resistance is still in the acceptable range at it was good enough to transmit the resonance frequency at 15.00 MHz. Impedance evolution against the frequency is plotted for the sample M-2 and M-3 which indicates the both resonance frequencies in the good range (Figure 4.74). Hence, we can conclude that 10,000 abrasion cycles did not damaged the textile antennas and the resonance frequencies were in the good range after 10,000 abrasion cycles although electrical resistance was increased in one sample.

Table 4.2. Resonance frequency and quality factor for textile antennas after 10,000 Abrasion cycles

Samples id	Resonance frequency (f_o)	Quality factor (Q)
M-1	15.40	38.5
M-2	15.60	39.0
M-3	15.00	25.0
M-4	15.60	40.0

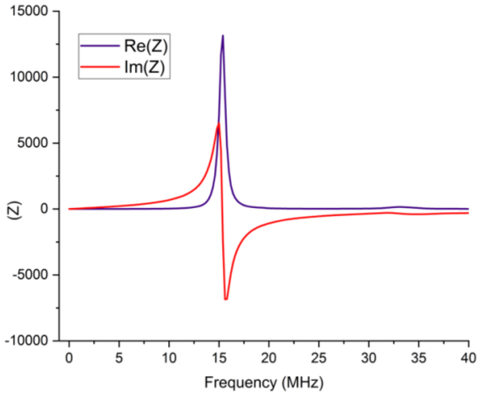

Figure 4.74. Impedance evolution for the real and imaginary part against the frequency after 10,000 abrasion cycles

4.5.3 Pilling Box test

The textile antennas were also investigated for the pilling box tests. Total four samples were tested up to 10,000 pilling box cycles and impedance (Z) values against frequency were recorded. However, all these samples were damaged and it was not possible to calculate the resonance frequency for these samples. It indicates that conductive yarns used to prepare the textile antennas were damaged caused by the continuous falling movements in the pilling box test.

4.5.4 Chemical tests

A separate set of samples for textile antennas were used for water and water-detergent solution tests. The samples were dipped in these solutions for 72 hours and impedance values against the frequency were recorded with the help of Agilent impedance analyzer.

Table 4.3 presents the resonance frequencies and quality factors for all these samples. One samples among samples immersed in the water was completely damaged and did not give any impedance values. One sample reduced the quality factor to 25.30, although resonance frequency was in good range (15.20). It means water impacted the conductive yarn and increased the linear resistance which ultimately reduced the quality factor (Figure 4.75).

On the other side, water-detergent solution was less damaging on the conductive yarn as compared to the water solution. Here only one sample reduced the quality factor to 25 and the resonance frequency for all samples was in the range of 15-16 MHz (Figure 4.76). This is the same trend which was observed when transmission lines were tested for water and water-detergent solutions. Different ingredients especially softeners present in the detergent help to reduce the damaging attack on the yarn surface. Due to the extraordinary combination of detergents, they serve an exceptional property as an interfacial activity. For example, water solvents with surfactants interfacial activity displaying as an amendment in the system properties and finally decreasing the interfacial tension between the water and the adjacent phase.

Table 4.3. Resonance frequency and quality factor for textile antennas after 72 hours immersion in water and water-detergent solution, W_i are samples with water solution, WD_i are samples with water-detergent solution

Samples id	Resonance frequency (f_o)	Quality factor (Q)
W-1	-	-
W-2	15.20	25.30
W-3	15.00	32.0
WD-1	15.40	38.0
WD-2	15.20	25.0
WD-3	15.20	38.5

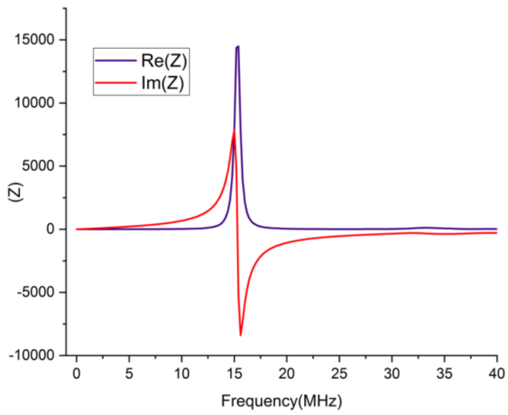

Figure 4.75. Impedance evolution for the real and imaginary part against the frequency after 72 hours immersion in the water solution

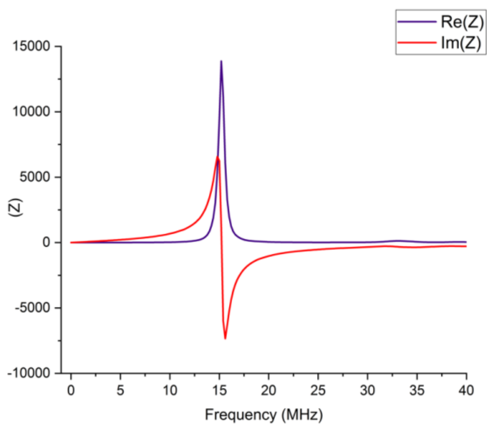

Figure 4.76. Impedance evolution for the real and imaginary part against the frequency after 72 hours immersion in the water-detergent solution

Textile antennas were tested for *Silk* and *Express* washing cycles. *Silk* washing cycle was mild cycle in term of the mechanical stresses working in it, whereas, *Express* cycle was harsher one. Textile antennas in *Silk* washing cycle maintained their properties after 50 washing cycles but they start damaging after 20 *Express* washing cycles. It revealed that higher mechanical stresses are damaging the conductive yarns which increased their electrical resistance. The antennas were also tested for mechanical and chemical tests to investigate their behavior against the proposed tests. The pilling box test was more damaging in term of textile antennas functionality; all samples were damaged after 10,000 pilling cycles. It seems that continuous falling movement in the pilling box damaged the conductive yarn surface. Same phenomenon was observed in the *Express* washing cycles, where number of revolutions in the washing drum is more than *Silk* washing and overall washing action time was also greater than *Silk* washing cycle. Chemical tests were also performed on textile antennas by immersing them in the water and water-detergent solution for 72 hours. The resultant resonance frequency was in the good range but quality factor for some samples reduced indicating the increase in the electrical resistance. Continuous immersion in the solutions attacked the conductive surface of the yarn and this phenomenon was further enhanced with intensive mechanical actions as the case in the *Express* washing cycles.

The experimental results revealed that available mechanical and chemical tests may be used to predict the damages provoked by the washing process. For example for these specific antennas, the pilling box tests with certain number of pilling cycles and water immersion tests with some fixed amount of time can give equivalent damages created by the certain numbers of the *Express* washing cycles.

References

[1] S. uz Zaman, X. Tao, C. Cochrane, and V. Koncar, “E-Textile Systems Reliability Assessment—A Miniaturized Accelerometer Used to Investigate Damage during Their Washing,” *Sensors*, vol. 21, no. 2, Art. no. 2, Jan. 2021, doi: 10.3390/s21020605.

[2] S. uz Zaman, X. Tao, C. Cochrane, and V. Koncar, “Launderability of Conductive Polymer Yarns Used for Connections of E-textile Modules: Mechanical Stresses,” *Fibers and Polymers*, vol. 20, no. 11, pp. 2355–2366, Nov. 2019, doi: 10.1007/s12221-019-9325-x.

[3] E. Ismar, S. uz Zaman, X. Tao, C. Cochrane, and V. Koncar, “Effect of Water and Chemical Stresses on the Silver Coated Polyamide Yarns,” *Fibers and Polymers*, vol. 20, no. 12, pp. 2604–2610, Dec. 2019, doi: 10.1007/s12221-019-9266-4.

[4] M. Wei *et al.*, “Manipulation of Nylon-6 Crystal Structures with Its α-Cyclodextrin Inclusion Complex,” *Macromolecules*, vol. 35, no. 21, pp. 8039–8044, Oct. 2002, doi: 10.1021/ma020765m.

[5] D. Garcia and H. W. Starkweather, “Hydrogen bonding in nylon 66 and model compounds,” *Journal of Polymer Science: Polymer Physics Edition*, vol. 23, no. 3, pp. 537–555, 1985, doi: https://doi.org/10.1002/pol.1985.180230310.

[6] S. Periyasamy, G. K. Prasad, S. K. Chattopadhyay, A. S. M. Raja, K. R. Kumar, and S. Jagadale, “Micro-roughening of polyamide fabric using protease enzyme for improving adhesion strength of rubber-polyamide composite,” *Journal of Polymer Engineering*, vol. 37, no. 3, pp. 297–306, Mar. 2017, doi: 10.1515/polyeng-2015-0541.

[7] N. Vasanthan and D. R. Salem, “FTIR spectroscopic characterization of structural changes in polyamide-6 fibers during annealing and drawing,” *Journal of Polymer Science Part B: Polymer Physics*, vol. 39, no. 5, pp. 536–547, 2001, doi: https://doi.org/10.1002/1099-0488(20010301)39:5<536::AID-POLB1027>3.0.CO;2-8.

[8] G. Rotter and H. Ishida, “FTIR separation of nylon-6 chain conformations: Clarification of the mesomorphous and γ-crystalline phases,” *Journal of Polymer Science Part B: Polymer Physics*, vol. 30, no. 5, pp. 489–495, 1992, doi: https://doi.org/10.1002/polb.1992.090300508.

[9] J. Falbe, *Surfactants in Consumer Products: Theory, Technology and Application*. Springer Science & Business Media, 2012.

[10] D. K. Bhui, H. Bar, P. Sarkar, G. P. Sahoo, S. P. De, and A. Misra, “Synthesis and UV–vis spectroscopic study of silver nanoparticles in aqueous SDS solution,” *Journal of*

Molecular Liquids, vol. 145, no. 1, pp. 33–37, Mar. 2009, doi: 10.1016/j.molliq.2008.11.014.

[11] N. Vigneshwaran, A. A. Kathe, P. V. Varadarajan, R. P. Nachane, and R. H. Balasubramanya, "Functional Finishing of Cotton Fabrics Using Silver Nanoparticles," *Journal of Nanoscience and Nanotechnology*, vol. 7, no. 6, pp. 1893–1897, Jun. 2007, doi: 10.1166/jnn.2007.737.

[12] D. D. Evanoff and G. Chumanov, "Synthesis and Optical Properties of Silver Nanoparticles and Arrays," *ChemPhysChem*, vol. 6, no. 7, pp. 1221–1231, 2005, doi: https://doi.org/10.1002/cphc.200500113.

[13] S. Pal, Y. K. Tak, and J. M. Song, "Does the Antibacterial Activity of Silver Nanoparticles Depend on the Shape of the Nanoparticle? A Study of the Gram-Negative Bacterium Escherichia coli," *Appl. Environ. Microbiol.*, vol. 73, no. 6, pp. 1712–1720, Mar. 2007, doi: 10.1128/AEM.02218-06.

[14] S. uz Zaman, X. Tao, C. Cochrane, and V. Koncar, "Understanding the Washing Damage to Textile ECG Dry Skin Electrodes, Embroidered and Fabric-Based; set up of Equivalent Laboratory Tests," *Sensors*, vol. 20, no. 5, p. 1272, Feb. 2020, doi: 10.3390/s20051272.

[15] P. Szakálos, G. Hultquist, and G. Wikmark, "Corrosion of Copper by Water," *Electrochem. Solid-State Lett.*, vol. 10, no. 11, p. C63, Aug. 2007, doi: 10.1149/1.2772085.

[16] Dils, Werft, Walter, Zwanzig, von Krshiwoblozki, and Schneider-Ramelow, "Investigation of the Mechanical and Electrical Properties of Elastic Textile/Polymer Composites for Stretchable Electronics at Quasi-Static or Cyclic Mechanical Loads," *Materials*, vol. 12, no. 21, p. 3599, Nov. 2019, doi: 10.3390/ma12213599.

[17] A. E. Broo, B. Berghult, and T. Hedberg, "Copper corrosion in drinking water distribution systems — the influence of water quality," *Corrosion Science*, vol. 39, no. 6, pp. 1119–1132, Jun. 1997, doi: 10.1016/S0010-938X(97)00026-7.

[18] L. Mao, Q. Meng, A. Ahmad, and Z. Wei, "Mechanical Analyses and Structural Design Requirements for Flexible Energy Storage Devices," *Advanced Energy Materials*, vol. 7, no. 23, p. 1700535, 2017, doi: https://doi.org/10.1002/aenm.201700535.

[19] N. Singh *et al.*, "Paintable Battery," *Scientific Reports*, vol. 2, no. 1, Art. no. 1, Jun. 2012, doi: 10.1038/srep00481.

[20] S.-R. Kim and J. A. Nairn, “Fracture mechanics analysis of coating/substrate systems: Part I: Analysis of tensile and bending experiments,” *Engineering Fracture Mechanics*, vol. 65, no. 5, pp. 573–593, Mar. 2000, doi: 10.1016/S0013-7944(99)00141-1.

[21] S.-I. Park, J.-H. Ahn, X. Feng, S. Wang, Y. Huang, and J. A. Rogers, “Theoretical and Experimental Studies of Bending of Inorganic Electronic Materials on Plastic Substrates,” *Advanced Functional Materials*, vol. 18, no. 18, pp. 2673–2684, 2008, doi: https://doi.org/10.1002/adfm.200800306.

[22] S. uz Zaman, X. Tao, C. Cochrane, and V. Koncar, “Wash analyses of flexible and wearable printed circuits for e-textiles and their prediction of damages,” *electronics*, vol. 10, pp. 1362, Jun. 2021, doi: https://doi.org/10.3390/electronics10111362.

5. General Conclusion

The research activities within my Ph.D. thesis were conducted with a focus on the washing reliability and standardization required for e-textile systems. This research was focused to create a clear picture regarding e-textile system reliability issues. The original intellectual contributions of this Ph.D. thesis are presented below:

- ❖ Understanding of the washing process and the contents of different programs including possible damages actions towards e-textile systems;
- ❖ Analyses of the damaging actions on different parts of e-textile systems (transmission lines, sensors/ actuators, electronic modules, textile antennas, etc.;
- ❖ Simulation of damages provoked by washing process using existing textile testing apparatuses such as chemical tests and mechanical tests (Martindale abrasion, pilling box, and bending tests, etc.);
- ❖ Proposal of the strategy to better protect e-textile systems against washing damages helping them to become acceptable by the market for industries;
- ❖ Definition of five categories for e-textile systems based on their fields of application including fashion, sports and leisure, PPE, medical, and military, and three classes based on their robustness and way of use. These categories include e-textile systems reliability related to the following characteristics (Figure 6.1, Figure 6.2, and Figure 6.3).

Different well-developed textile and electronic standards are available for guidelines. They should be modified for proper adoption with e-textile systems, or new norms should be developed based on these existing standards. The washing behavior of domestic washing machines was investigated to understand better the washing parameters and possible forces acting in the washing process. A novel technique of putting the waterproof sealed accelerometer in the washing drum was used to investigate the substrate behavior during the washing process carried out in the domestic washing machine. Based on these analyses, low- and high-speed movements and running and stop time for the washing substrate was highlighted for different washing programs. Diverse stresses involved in these washing processes were shortlisted in four primary categories: mechanical, chemical, temperature, and water stresses.

Different components of e-textile systems, including transmission lines/motherboards, sensors, flexible PCBs, and textile antennas, were investigated for the washing process, and their reliability against the washability was discussed. Several possible techniques that can be used to protect these e-textile components for the possible damages in the washing process were also presented in this study. Some e-textile system components can be covered entirely against environmental damages, e.g., transmission lines. However, others don't have these possibilities, e.g., ECG sensors that should contact the body and cannot be covered. Therefore, their washing reliability is an essential factor for market acceptance. These e-textile components were washed for 50 washing cycles for almost all types of samples. The 50 times washing threshold level was selected based on the idea that an e-textile system has at least one year of life and will be washed once a week.

A method for e-textile system reliability evaluation was presented in this study. Various available test methods can be used, based on the forces working in the washing process, to predict the washing damages without actually washing the product. For example, Martindale abrasion tests, Pilling box tests, and bending tests can simulate the washing machines' mechanical forces during the washing process. Similarly, water and detergent solution tests may be used as the alternative to the chemical stresses. Selected examples for e-textile components are tested with these alternate test methods, but it is not easy to cover all possible e-textile parts. These tests are performed to give the idea of how they may be adopted for e-textile reliability evaluation. Of course, the forces generated by test methods may react differently from the combined effect when performed separately. However, a general trend will be helpful to predict the overall behavior against the washing reliability. These alternate test methods can be used at different stages during the e-textile system development and on separate components before installing them in the final e-textile system.

These approaches can help the electronic industry, mainly because these industries are essential for e-textile system development, but they don’t have any standards for textile behavior. We all use electronics products in our life, but we don’t wash them in the washing machines. On the other side, products prepared for the e-textile systems should be washable because e-textiles will ultimately be washed in the washing machine. Hence, the electronic industry should have some guidelines to design e-textile components and test their reliability at each step during the manufacturing process. In this way, they can integrate their products into the textile without any fear of rejection in the market.

6. Proposed recommendations for e-textile wearable based on the experimental findings

Based on the research outcomes, some useful recommendations to develop testing methods and proceed with the e-textile system reliability assessment are presented below.

- Different e-textile system components will have different washing reliability requirements. Each component should be treated separately for washing reliability and the only e-textile system should be focused on reliability instead of the complete wearable product.
- Available washing test protocol may be adapted to the e-textile system after required modification in them. For example, washing and tumbling temperature for these systems should be reduced as compared to the normal textile clothing.
- The e-textile systems can be washed in the available washing machine but the washing program should be adjusted carefully. A short washing program does not always mean less damaging and there is the possibility that long washing programs have very little running time as compared to the short program. Similarly, it was observed that tumbling speed is not damaging much on the e-textile systems.
- It is possible to protect some components against washing damages with particular treatments or an extra layer of protective coatings. The treatments should be adopted separately for each component as there is the possibility that they can further damage the product instead of protecting it. For example, TPU film attached to the

transmission lines with the heated press may degrade the conductive coating from the surface due to higher temperature.

- E-textile reliability will depend on the product usage e.g., e-textile products being used in the medical, military, or PPE will need a high level of reliability and so norms for these products should according to their level. One possibility is to prepare the reliability standards with some sub-classes to differentiate the different levels of reliability. Maybe Class A reliability be reserved for military or medical standards and so on.
- Similarly, cheaper versions of these products can be developed with a lower reliability class for customers who want to use them but don't have the purchasing powers. These classes can be mentioned on the products and people can use a different level of reliability according to their requirements.
- The e-textile products should also be divided based on the user requirements. For example, maybe 50 washing cycles will be not enough for military-grade products but it can be more than enough for some other category products. In this case, Class A products for military usage will have a different level of reliability than Class A products for sports or any other category. So, either these classes should be divided into different sub-categories based on the usage or the required reliability level should be reduced in the general category classes.
- It is also possible that products used in the outer wearing need harsh washing cycles as compared to the inner wears where mild washing cycles will be enough. Hence, they will need a different level of reliability.
- When we talk about washing reliability, this definition may be different for different categories. This will directly be attached to the damage acceptance level. Products related to sensitive categories will have a narrow margin of damage acceptance and vice versa. For example, e-textile systems related to the medical fields may accept damage level 5%, which means they need 95% samples working in the good condition after approaching the required level of reliability. On the other side, if one product is designed for the fashion or leisure industry, maybe they will consider it reliable if 80% of samples are working after the required level of reliability.
- If we go further in detail, there should also be the definition of working samples. For example, if transmission lines are washed according to their reliability level, and resistance is increased to 2-3 times but still it is conductive. For one product category,

this increase can be acceptable and they can state it reliable but for the other category, maybe their requirement is a maximum 1.5-time increase from original values and hence they will not consider it reliable after certain washings.

- Another question was raised in the experiments, which characteristics should be considered important for reliability definitions.
- Overall, it is very complex to develop standards and divide them into multiple sub-categories. Some basic requirements should be included in the standards and others should be discussed on a product-to-product basis and mutual agreement should be prepared for stating the product reliability.

6.1 IPC-8981, Quality and reliability of e-textile wearable

IPC (International association of Printed Circuits), (*www.ipc.org*) is trade association working on the standards especially in the electronic industry. It is well developed standard association and currently standards covering almost all aspects of electronic industry is available under IPC umbrella.

E-textile systems have major role of electronics and many electronic industries are willing to take the opportunity for becoming the part of e-textile systems. However, lack of standards causing the problems because electronic industries don not have in depth knowledge for textiles and there should be some guideline for them to follow. IPC is leading this role to develop some basic standards and definitions for e-textile systems. The aim of their work is to give some pre-defined basic definitions related to e-textile systems and components related to it. IPC is working to develop reliability standards focused on e-textile components so that electronic industries can be integrated into e-textile systems without any hurdle.

The research outcomes are being applied for the development of the possibly first detailed draft of standard "*Quality and reliability of e-textile wearable*" *IPC-8981*, by the IPC Europe group (IPC D-75eu) chaired by Prof. Vladan Koncar (*https://www.ipc.org/ipc-e-textiles-initiative-join-effort*). IPC D-75eu is joint effort from various research laboratories and industries across the world to share their recommendations and expertise for the possible standard development.

Group is working since January 2020 and an initial draft is planned to be developed by December 2021. Some key details of this work are explained here. The discussion is divided into 5 different tasks that have to be discussed for the preparation of the initial draft. Some surveys based on the requirements to fulfill the tasks were also conducted from the industry for guidelines. Detailed explanations of the tasks along with current updates are presented here.

- **Task 1**

It is related to definitions of e-textile systems and different structures that could be part of these systems. Definitions related to conductive polymers, sensors, actuators, and conductive wires attached to the textiles are also covered in this task group.

- **Task 2**

Task 2 is concerned with the establishment of guidelines for the collection of the requirements from garment/wearable manufacturers concerning the data for electronic devices supposed to be integrated into e-textile structures. Requirements related to the protections, integration, and washability are also covered in this task group.

- **Task 3**

It is related to the definitions and categories based on several generic areas to account for the characteristics that should be included for their testing in terms of reliability. These categories include sports, medical, fashion, PPE (personal protective equipment), and military. A survey, based on these categories, was conducted by IPC and different experts from concerned industries participated in these surveys. Questions were asked that what characteristics should be imported and included for different generic categories. Percentages of peoples, who think that these characteristics are important, are plotted in the following plots. A threshold level of 60% was decided which means all characteristics above 60% were selected from these surveys (Figure 6.1 and Figure 6.2).

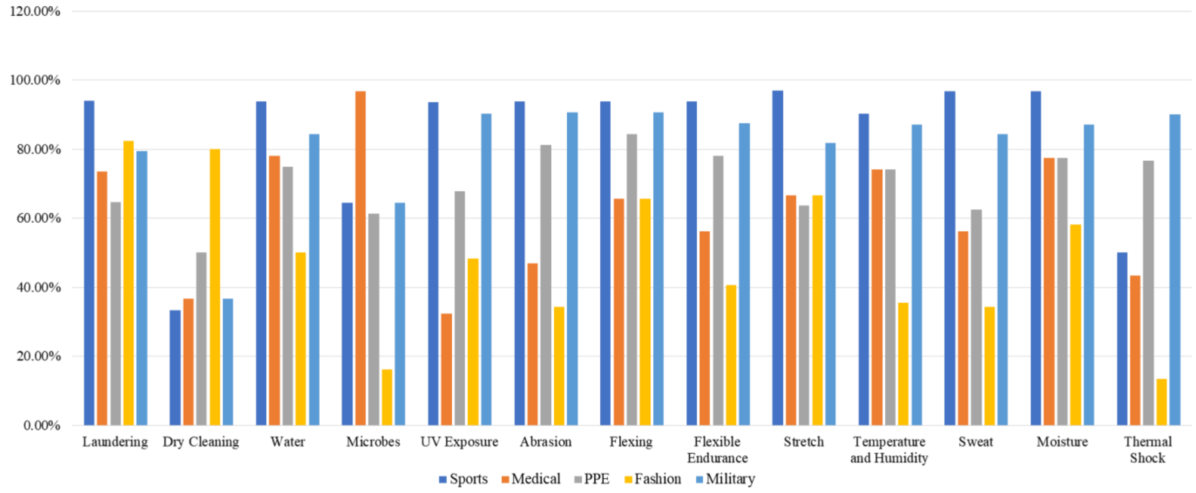

Figure 6.1. IPC Survey results for possible characteristics required by different categories for e-textile systems. Percentage of respondents who think these characteristics are important and should be included

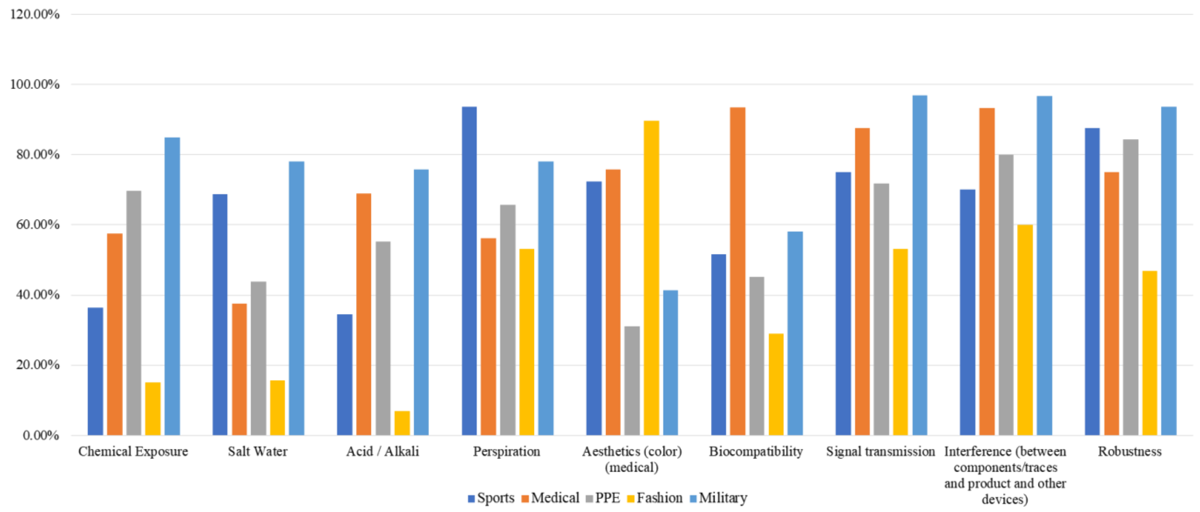

Figure 6.2. IPC Survey results for possible characteristics required by different categories for e-textile systems. Percentage of respondents who think these characteristics are important and should be included

- **Task 4**

In the next step, these products were classified into different classes by the intended end-item use. These include Class 1 (General e-textile wearable where functionality is the major requirement), Class 2 is specially purposed designed products where continued performance and extended life is important. This class is then further separated by Class 2A which covers the single-used or short-time used designed products. Class 3 discusses high-performance e-textile wearable where high performance and reliability cannot be tolerated. This class is further divided into 3A which covers single-/short time-used products.

Here again, industrial surveys were conducted by IPC to get a better understanding of the peoples related to these problems. A total of 30 respondents were included in this survey and there was the possibility to select more than one category where these classes can be included. The results obtained were according to the expectations where Class 1 was more concerned with the fashion industry and Class 3 was more concerned with the military, medical, and PPR products (Figure 6.3).

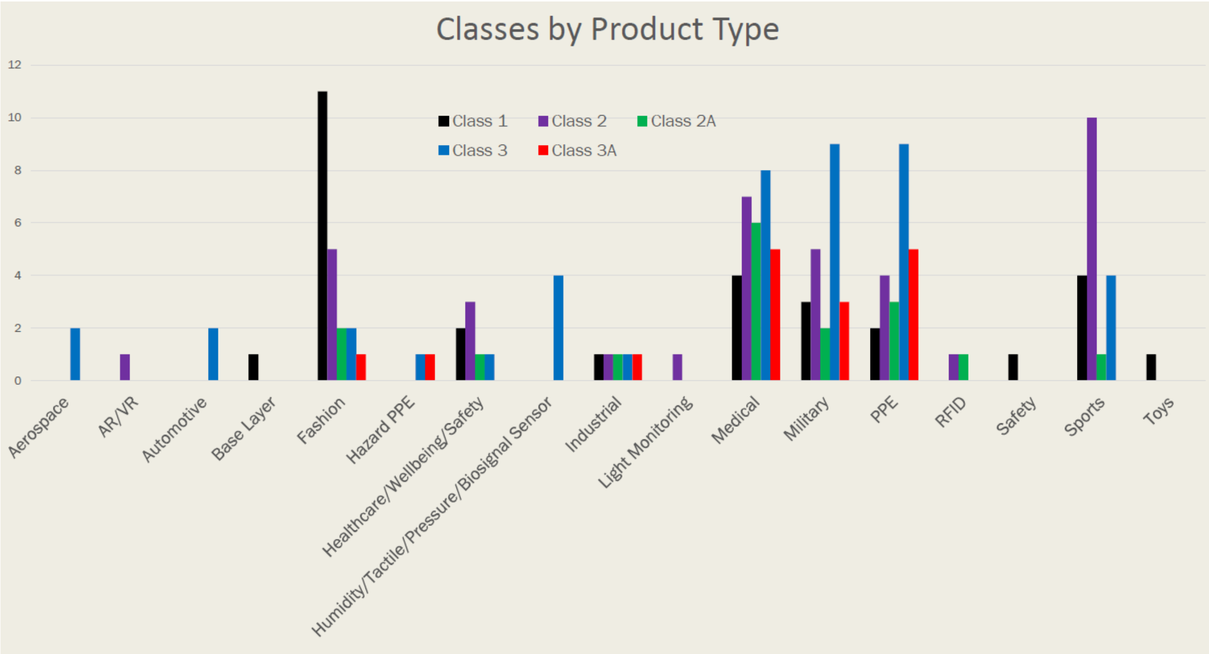

Figure 6.3. IPC Survey results for proposed Classes and their division in different categories

In the other question, it was asked which washing actions should be considered for these different Classes of e-textile systems (Figure 6.4). If we consider a 50% threshold level for these results, laundering, tumble drying, and dry cleaning should be included for all Class 1, 2, and 3 products. It means all products should be washing reliable if we want e-textile systems to be successful in the market.

Figure 6.4. IPC Surveys for cleaning of different Classes of e-textile systems. Percentage of respondent who thinks cleaning is important for these Classes

❖ **Task 5**

Based on these surveys, characteristics were combined in the sub-group for better understanding and easy to progress in standardization. In a separate sub-group, the general principle for these characteristics and quality requirements related to the different e-textile components including motherboards, sensors, actuators, electric modules, and power supply, are discussed. It is possible to use the available general principle standard with required modifications in it. One example is the use of ISO 105-A1. This standard is related to the colorfastness of general textiles but can be adapted to e-textile systems with some necessary modifications.

Sub-groups details along with proposed standardized numbering are presented below.

➢ **General principles (IPC-8981 A series)**

- *8981 A 01:* General principles of E-textile systems testing
- *8981 A 02:* Textile electronics board (textile motherboard): conductivity, contacts, and connections

- *8981 A 03:* Sensors (flexible, textile based, rigid): input vs. output for instance temperature vs. voltage, or humidity vs. resistance
- *8981 A 04:* Actuators (flexible, textile based, rigid): input vs. output response
- *8981 A 05:* Electronic modules (flexible PCB based, rigid PCB based, textile substrate based): complete functioning depending on the data book and the specifications given by the manufacturer
- *8981 A 06:* Power supply (rigid, flexible, energy harvesting): available power delivered, life time, charging capacity

Possible damaged stresses are combined in five different sub-groups.

- **Mechanical I (IPC 8981 B series):**
  - *8981 B 01:* Abrasion stresses
  - *8981 B 02:* Tensile stresses
  - *8981 B 03:* Shearing stresses
- **Mechanical II (IPC 8981 C series):**
  - *8981 C 01:* Flexing stresses
  - *8981 C 02:* Bending stresses
  - *8981 C 03:* Stretching stresses
  - *8981 C 04:*Torsion stresses
- **Exposure I (IPC 8981 D series):**
  - *8981 D 01:* Salt water
  - *8981 D 02:* Acid and Alkalis
  - *8981 D 03:* Sweat & Perspiration
  - *8981 D 04:*Microbes
- **Exposure II (IPC 8981 E series):**
  - *8981 E 01:* Water repellence
  - *8981 E 02:* Water hydrostatic
  - *8981 E 03:* UV
  - *8981 E 04:* Temperature
- **Cleaning (IPC 8981 F series):**
  - *8981 F 01:* Washing
  - *8981 F 02:* Drying

- *8981 F 03:* Dry cleaning

➢ **Wearability and comfort (IPC 8981 G series):**

- *8981 G 01:* Breathability
- *8981 G 02:* Air Flow
- *8981 G 03:* Weight of Components

I am currently working in sub-groups (General principles, Mechanical I, Exposure I, and Cleaning), for shortlisting and modifications of available standards.

All sub-groups have collected available standards related to these characteristics. The available standards, based on the needs, will either be modified to adapt them according to the e-textile requirements or new standards will be developed with the help of available standards. If no standard will be possible to adapt for some specific characteristic, the process of new standard writing with the help of available one will be started in that sub-group. For example, there is no standard available for anti-microbes' properties of e-textile systems. Norms are available for microbes' influences on the textile surfaces and its modifications. But in e-textile system, we need the microbe impact behavior on the e-textile system reliability. Hence, in this case a new standard need to be developed for microbe resistance properties in the e-textile systems.

Table 6.1 shows the complete matrix for the available standards shortlisted by sub-groups that can be modified and adopted for e-textile systems.

Table 6.1. Current progress of sub-groups and shortlisted standards

Group	Characteristic	Modifiable existing Standard(s)	Needs new standard / testing method
A) General	General principles	BS EN ISO 105-A01:2010	
	Textile motherboard	IPC-TM-650 Test methods Manual, 3.1 A, Contact resistance, Connectors 3.3 Crimp tensile strength, Connectors AATCC TM76 (surface el resistivity) AATCC TM84 (el. Resistance of yarns)	
	Sensors	Company Quality Control procedure if existing	
	Actuators	Company Quality Control procedure if existing	

Proposed recommendations for e-textile wearable based on the experimental findings

	Electronic Modules	Company Quality Control procedure if existing		
	Power Supply			Yes
		Flat	3D	
B) Mechanical I	Abrasion	ISO 12947 Textiles – Determination of abrasion resistance of fabrics by the Martindale method	EN ISO 12945-3 Textiles – Determination of the fabric propensity to surface pilling, fuzzing or matting –Part 3: Random tumble pilling method	
			AATCC TM93 Abrasion Resistance of Fabrics: Accelerotor Method	
	Tensile	ISO 13934-1 Textiles – Tensile properties of fabrics – Part 1: Determination of maximum force and elongation at maximum force using the strip method		
		ASTM D5035 – 11 Standard Test Method for Breaking Force and Elongation of Textile Fabrics (Strip Method)		
	Shearing	ASTM D 905 Standard Test Method for Strength Properties of Adhesive Bonds in Shear by Compression Loading		
	Peel Strength	ISO 11339 Adhesives – T-peel test for flexible-to-flexible bonded assemblies	ISO 8510-2 Peel test for a flexible-bonded-to-rigid test specimen assembly – Part 2: 180 degree peel	
		ASTM D1876-08 Standard Test Method for Peel Resistance of Adhesives (T-Peel Test)	ASTM D903 - 98 Standard Test Method for Peel or Stripping Strength of Adhesive Bonds	
C) Mechanical II	Flexing			
	Bending			
	Stretching			
	Torsion			

D) Exposure I	Salt Water	**ISO 105-E02:2013** specifies a method for determining the resistance of the colour of textiles of all kinds and in all forms to immersion in sea water.	
	Acid & Alkali	**ISO 105-**E05 Color fastness to spotting (acids) **ISO 105-E06:2006** Textiles — Tests for colour fastness — Part E06: Colour fastness to spotting: Alkali	
	Sweat & Perspiration	**ISO 105-E04:2013** Textiles — Tests for colour fastness — Part E04: Colour fastness to perspiration **AATCC 15-2002 (1994)** Colorfastness to Perspiration artificial sweet (acid, alkali)	
	Microbes *(this is focused on the anti-microbial properties of the e-textiles, not on the influence of microbes on the e-textiles)*	***AATCC 100*** *antimicrobial e-textiles* ***ISO 20743:2013*** *Textiles — Determination of antibacterial activity of textile products* ***ISO 20645:2004*** *Textile fabrics — Determination of antibacterial activity — Agar diffusion plate test* ***ASTM E3160 - 18*** *Standard test method for quantitative evaluation of the antibacterial properties of porous antibacterial treated articles*	Yes
E) Exposure II	Water repellence	IEC 60529 Test protocols water ingress seems applicable to E-textile systems - Need modifications to fixturing so item is positioned as it would be in use - Review that acceptance criteria is applicable to E-textiles systems and expand if necessary	
	Water: hydrostatic	Should be tested component level not in system level	
	UV	Instead of testing UV only test exposure to sunlight - AATCC TM169 - Standard allows filtering out IR to prevent overheating. Should	

		filtering IR be allowed in some cases or no? - Modification needed for fixture and positioning of the test sample - Test coupon/sample needs to be specified
	Temperature	This needs to be broken down to sub-categories - Storage & transportation - Operation in hot/cold - Temperature rise due to electrical current - Test coupon/sample needs to be specified
F) Cleaning	Washing	**AATCC TM135-2018t** The standards for Dimensional changes of fabrics after home laundering
		AATCC TM210-2019(2020) Test Method for Electrical Resistance **b**efore and After Various Exposure Conditions (for testing electrical resistance as well as modifications of established industry methods for laundering, dry cleaning, water, perspiration, acids and alkalis, ultraviolet (UV) radiation, and microbe exposure. Test exposures relevant to the expected end use of sample.)
		ISO 6330 Textiles – Domestic washing and drying procedures for textile testing
	Drying	ISO 6630 Textiles – Domestic washing and drying procedures for textile testing
	Dry Cleaning	
G) Wearability and Comfort	How to assess Breathability, Air Flow, and Weight of Components	

Currently, sub-groups are working for the modifications of available standards according to the requirements. After its completion, validation process will be initiated to perform the proposed tests on e-textile systems. Hopefully, when finished, we will be able to give the first draft of complete e-textile system standards.

Résumé

Nous vivons une époque où la modernisation et la numérisation se développent rapidement. Les entreprises attirent leurs clients grâce à des techniques nouvelles et des gammes de produits personnalisés. Cette concurrence a favorisé le développement de secteurs nouveaux et hybrides pour améliorer la satisfaction des clients. Au cours des dernières décennies, de nouveaux produits, impossibles à imaginer dans le passé, ont emargé. En même temps, l'utilisation des vêtements a suivi l'évolution de l'humanité, depuis son apparition. Le concept de vêtement a débuté par le remplacement des feuilles utilisées pour couvrir certaines parties du corps. Aujourd'hui, ces vêtements sont beaucoup mieux adaptés à l'utilisateur et sont utilisés dans divers domaines, tels que la médecine, le sport, l'armée et différents projets liés à la défense. Ces nouveaux vêtements, avec des fonctions additionnelles, ont complètement changé la façon d'utiliser et de développer des textiles et c'est la raison pour laquelle le textile n'est plus une industrie indépendante, mais un mélange de différentes industries travaillant ensemble sous réserve des fonctionnalités intégrées définies par l'utilisateur. Les textiles polyvalents et à fonctionnalités améliorées peuvent contenir un ou plusieurs composants intelligents, textiles ou non textiles, tissés, brodés, cousus, intégrés ou attachés à l'aide de différentes techniques disponibles. En fonction des besoins, ces composants sont des capteurs, des actionneurs et des antennes, des unités de traitement, des dispositifs de collecte d'énergie et de transmission de puissance. Ces textiles portables avancés sont appelés textiles intelligents, électronique portable, e-textiles, vêtements intelligents, textroniques, etc.

Pour progresser dans cette nouvelle partie immergée de l'industrie textile, il est important de comprendre les exigences et les problèmes liés à cette approche hybride. Les textiles intelligents sont constitués de composants provenant principalement des industries textile et électronique. Ces deux industries sont bien développées et disposent déjà de normes et de standards liés à chaque problème. Cependant, ces normes ne peuvent pas être appliquées aux systèmes e-textiles tels quels et une modification, ou le développement de nouvelles normes, est nécessaire pour rendre ces e-textiles fiables et acceptables pour les clients.

Cette thèse de doctorat est consacrée à l'étude et à la mise en évidence des difficultés auxquelles le marché des textiles électroniques est confronté en termes de fiabilité et de lavabilité. Les différentes options de lavage disponibles sont analysées avec la mise en évidence des différences entre elles, afin de mieux comprendre comment sélectionner l'option de lavage la plus appropriée pour les systèmes e-textiles. Un accéléromètre a également été utilisé pour des analyses de contraintes dans le tambour de machine à laver pour de mettre en évidence les protocoles de tests mécaniques standardisés disponibles qui peuvent être utilisés comme simulation de dommages équivalents, sans le processus de lavage. Différents composants des e-textiles, y compris les composants détachables et les composants fixes, sont étudiés séparément pour déterminer les contraintes de lavage sur chacun de ces composants en termes de fonctionnalité. Enfin, un modèle de simulation a été proposé pouvant être utilisé pour identifier les dommages causés par le lavage et les prévisions de fiabilité, sans avoir à laver les systèmes e-textiles. Les protocoles standards requis pour leur adaptabilité chez les clients sont discutés et la modification des normes actuelles ainsi que les modifications nécessaires sont présentés dans cette étude.

Mots clés : Textiles intelligents, Composants électroniques, Normalisation, Nettoyage, Fiabilité

Abstract

We live in an era where modernization and digitalization are increasing rapidly, and industries attract their customers with novel techniques and customized product ranges. This competition increased the development of new and hybrid fields for customers satisfactions. In recent decades we have a lot of modern innovative notations that ancient peoples can't even imagine. Similarly, textiles usage, especially as the wearing element, has a vast history in human evolution since ancient times. The wearing cloth concept started as the replacement of leaf used for covering body parts, but now day's textile wearable have multiple included options along with wearing requirements. Nowadays these user-defined textile wearable are being used in diverse fields ranging from medical, sports, military, and different defense-related projects. These new add-ons completely changed the way to use and develop wearable textiles. That's why now textile has not remained an independent industry but a mixture of different sectors working together subject to the integrated user-defined functionalities. Multipurpose and improved functionality textiles may comprise one or several textile or non-textile smart components that were weaved, embroidered, sewed, integrated, or attached using different available techniques. Based on requirements, these components can include sensors, actuators, and antennas, processing units, energy harvesting, and power transmitting devices. These advanced wearable textiles are usually named smart textiles, wearable electronics, e-textiles, smart clothing, textronic, etc.

It is essential to understand the requirements and problems related to this hybrid industry if we want to progress in this new immerging part of the textile industry. The electronic textile consists the components mainly from the textile and electronic industry. Both sectors are well-developed and already have norms and standards related to each problem. But these standards can't be applied to the e-textile systems as it is, and modification in these standards or development of new standards is required to make these e-textile products reliable and acceptable for customers.

This research is planned to investigate and highlight the difficulties the e-textile market faces in terms of reliability and washability. Different available washing options were studied to highlight the differences among them and understand the most suitable washing option for e-textile systems. The accelerometer device was used for stress analyses in the washing drum to highlight the available mechanical standardized test protocols that can be used as the simulation of equivalent damages without the washing process. Different e-textile components, including detachable and permanently fixed ones, are investigated for the washing stresses separately in terms of their functionality. Finally, a simulation model was proposed that can be exercised for wash damages and reliability predictions without actually washing the e-textile systems. Standard protocols required for their customers' adaptability are discussed, and necessary additions are presented in this study.

Keywords: Smart textiles, E-textile, Washing, Characterization, Standardization